“Activation of arene-heteroatom bonds by photoredox catalysis with visible light”

Dissertation

zur Erlangung des Doktorgrades der Naturwissenschaften
Dr. rer. nat.
an der Fakultät für Chemie und Pharmazie
der Universität Regensburg

vorgelegt von

Michal Májek

aus Bratislava (Slowakische Republik)

Regensburg 2015

The experimental part of this work was carried out between September 2012 and September 2015 at the University of Regensburg, Institute of Organic Chemistry under the supervision of Prof. Dr. Axel Jacobi von Wangelin.

The thesis was submitted on: 6.11.2015
Date of the defense: 10.12.2015

Board of examiners:
Prof. Dr. Olga García Mancheño (chairman)
Prof. Dr. Axel Jacobi von Wangelin (1st referee)
Prof. Dr. Burkhard König (2nd referee)
Prof. Dr. Frank-Michael Matysik (examiner)

Hey, now, baby, I'm beginning to see the light
Wine in the morning and some breakfast at night
Well, I'm beginning to see the light…

Velvet Underground: Beginning to see the light (1968)

Table of Contents:

Chapter 1:

Introduction

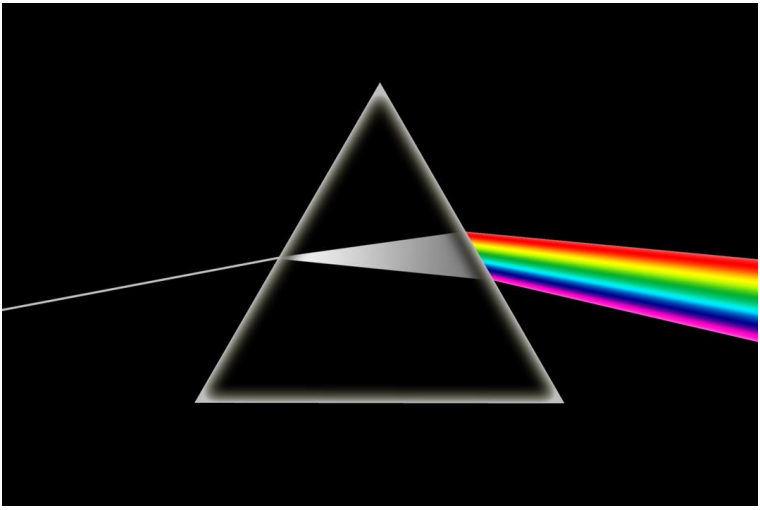

1.1: Chemistry and light

Light-induced reactions are as old as is the Earth itself, preceding life by hundreds of millions of years. As a matter of fact, the most probable source of the simplest organic molecules such as formaldehyde, which became the building for more complex molecules, starting with carbohydrates, were photochemical processes. Spectrum of the young Sun contained much more of the energetic UV light, and there was no ozone layer to protect the surface of the Earth, therefore photochemistry started immediately as the accretion processes finished and the stardust settled on the surface of the Earth.[1] Later on, living autotrophic organisms emerged on Earth, harnessing the light for the first time as an energy source for the living matter. Chlorophyll became integral for this process, as the first photocatalyst to use light energy for the separation of charges which is a hallmark of the modern, man-made photocatalysts as well.[2] Photosynthesizing organisms switched eventually to water splitting, generating oxygen as the by-product. Hard UV irradiation, which was still present on the surface of the Earth damaged biomacromolecules, endangering the living forms present. Thymine dimer formation by [2+2] cycloaddition was especially dangerous, as it presented a mechanism for long lasting DNA damage.[3] DNA repairing mechanisms were developed, but the rate of mutation was so high, that even if the organism survived, proper natural selection could not be operative. Increasing oxygen content in the atmosphere was the key to higher living forms, as it lead to the development of the ozone layer, which photochemicaly filters off the deadly, more energetic, part of UV spectrum.[4] Thus photochemistry was involved in all the key steps, which led to the existence of life itself, as well as for making the evolution possible, leading to the higher life forms, including the mankind.

Natural phenomena concerning light were intensively studied from the earliest days of science. Theoretical discoveries from optics came, driven by the demand from the more practical fields such as navigation, as well as from the transcendent but popular fields as astrology. While most of the laws of optics were discovered in earlier modern ages, it was not until the discovery of quantum physics, that the photochemical phenomena could be explained, as the wave-particle dichotomy is necessary for such explanations. Even though theory was not sufficient at the time to give any predictions in this field, experimental observations of photochemical phenomena were reported. Bleaching of textiles by sunlight was one of the first technologies developed by ancient Egyptians several thousand years before Christ. Later on, the poor light-fastness of dyes became a problem, as most of the natural dyes faded over time after exposure to sunlight. First scientific report of organic photochemical reaction comes from 1685 (just 20 years after the foundation of first

scientific journal) from England. The report concerns with the isolation of a light-labile dye, which gradually changed hue after the exposure to sunlight (it was an indigo-based dye isolated from a sea mollusk).[5] This report is worth mentioning, as it presents for the first time the use of photochemistry for production of an industrial chemical (purple textile dye), as well as the correlation between the intensity of irradiation and the rate of the photochemical reaction:

"The Letters, figures, or what else shall be made on the Linnen of Silk will presently appear of a pleasant light green colour, and, if placed in the Sun, will change into following colours… light green… deep green… Sea-green… Watchet-blew… Purplish-red… but the last and most beautifull colour, (after washing in scalding water and sope,) will be much a differing colour from all those mention'd i.e. of a fair bright Crimson, or neer to the Prince's colour… in the heat of the day, in Summer, the colours will come on so fast, that the sucession of each colour, will scarce be distinguisht. " (sic.)

The developments in inorganic and organic analysis led to the discovery of new photochemical reactions in the 19th century: Döbereiner has discovered the photoreduction of iron(III) by oxalate ligands in 1831, reporting for the first time an example of a photo-induced electron-transfer.[6] This reaction became later on the basis of the famous ferri-oxalate actinometer. Only a few years later, the photochemistry of a plant-derived organic compound santonin was discovered. The most important discovery that came from the investigation of the santonin chemistry was the discovery of the wavelength dependence of the photochemical transformations:[7]

"Das Santonin wird sowohl durch den unterlegten, als durch den blauen und violetten Strahl gefärbt (erster wirkt stärker als die gefärbten Strahlen); der gelbe, grüne und rote bringen nicht die mindeste Veränderung hervor…" (sic.)

Towards the end of the 19th century, most important classes of the organic photochemical reactions were discovered: [2+2] cycloadditions,[8] double bond cis-trans isomerizations[9] and radical halogenations,[10] reactions which are still mainly carried out by photochemistry in the laboratories of today. Photochemical discoveries until 1900, were by no means results of targeted research, but more of accidental "byproducts" of other lines of work, which the scientists of 19th century pursued. The change came with Giacomo Luigi Ciamician, a researcher from Bologna, who carried out an extensive screening of organic substrates for photochemistry. He dissolved different organic compounds in variety of solvents, let them expose to the strong Italian sunshine on the roof of his department, and analyzed the products by all the means available to him at the time. This lead to discovery of a large array of new reactions, and the

photochemistry seemed like a viable competitor to the coal tar-based organic chemistry of the early 20th century. Ciamician is probably most famous for his prophetic paper in Science, where he predicted a switchover of the human civilization from the fossil fuels to renewables as soon as 1912:[11]

"Where vegetation is rich, photochemistry may be left to the plants… On arid lands there will spring up industrial colonies without smoke and without smokestacks; forests of glass tubes will extend over plains and glass buildings will rise everywhere; inside of these will take place the photochemical processes that hitherto have been the guarded secret of the plants, but that will have been mastered by human industry…And if in a distant future the supply of coal becomes completely exhausted, civilization will not be checked for that, for life and civilization will continue as long as sun shines! If our black and nervous civilization, based on coal, shall be followed by a quieter civilization based on the utilization of solar energy, that will not be harmful to progress and to human happiness."

Figure 1. Giacomo Ciamician.

100 years after Ciamician's article, industry uses vast number of photochemical processes. Photochemistry is on one hand being used in water treatment as an ecologic process, but on the other hand the radical halogenations, once the biggest photochemical process, were used to produce products such as HCH with enormous environmental footprints. Chlorination of toluene to benzylchloride is one of the remaining industrial photochemical halogenations. Nowadays, the largest photochemical processes operated in industry are nitrosations, sulfochlorinations and sulfooxidations (Scheme 1).[12]

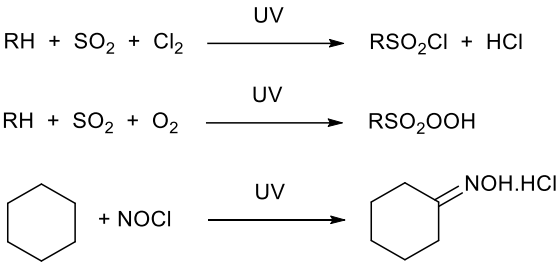

Scheme 1: Industrial photochemical processes.

There is one thing, which all these industrial processes have in common: they require ultraviolet irradiation. This stems from two factors: efficient UV sources were available relatively soon (mercury discharge lamp), and the transformations usually require the light to homolyticaly split strong σ-bonds. While the industrially used photochemical reactions are often efficient radical chain processes, therefore only relatively low light intensities are necessary, this becomes a problem when reactions with quantum yields below unity would be performed: high UV intensity would lead to unselective decomposition of reaction mixture, and would lead to poor economy of such process. Moreover, if we would like to realize the Ciamician's dream of using sunlight for chemistry, we would need to use visible part of the spectrum, as the intensity of UV irradiation on the surface of earth is relatively low (Figure 2, red color denotes intensity of solar irradiation on the surface of the Earth.).

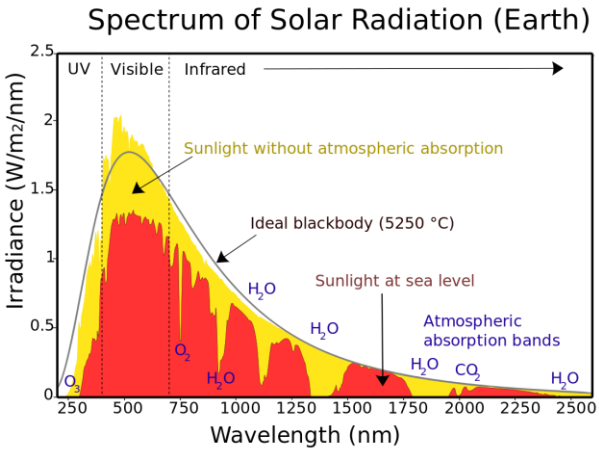

Figure 2. Spectral distribution of solar radiation.

Before moving on, we should shortly discuss the energetics of light-induced processes, and compare them with the conventional processes. Every chemist has an experience with the thermally-induced reactions. Such reactions use increased temperature, which translates to the increased vibrations of bonds, to overcome the activation energy. Activation energies of most organic reactions are in the 40-200 kJ/mol range.[13] Increased temperature increases the distribution of higher vibrational states for all of the vibrational modes. This gives rise to unwanted side-reactions. We can use the Arrhenius equation to calculate the activation energy difference, which is required to obtain certain selectivities. If we require selectivity 100:1, then the activation energy difference must be at least 10 kJ/mol at room temperature, and 20 kJ/mol at the maximal temperatures practically available in the laboratory with standard equipment (< 250 °C). It is straightforward, that this greatly limits the practicality of thermally-induced reactions: if there is a pathway with activation energy of 100 kJ/mol, probability of another pathway existing with activation energy of less than 120 kJ/mol is high. On the other hand, the light-induced reactions do not suffer from this drawback – they inject relatively high energies (Figure 3), selectively into the chromophore, exciting electrons into a single antibonding orbital.

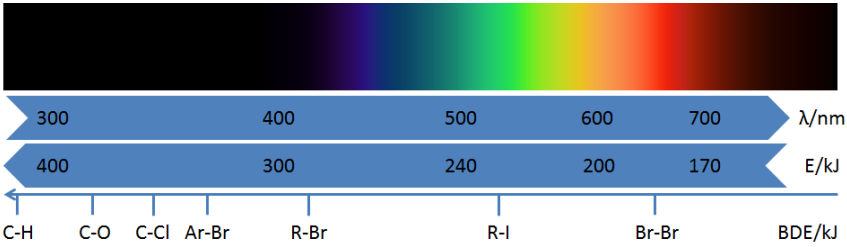

Figure 3. Bond dissociation energy (BDE) vs. photon energy.

Moreover, the thermally induced processes increase the energy of products as well, leading often to equilibration, while in case of photochemical processes, different absorption spectra usually allow selective activation of starting materials. Both of these features of photochemical processes are in a stark difference to the thermal reactions, and they allow to explore completely different reactivity patterns with orthogonal selectivities.[14] Due to the requirement of special equipment and know-how, photochemistry had the aura of a field reserved only to a handful of specialists. Development of cheap and easy to handle high intensity LED's (light emitting diodes) lead to the revival and broader acceptance or photochemistry in the synthetic community in the last years.[15]

1.2: Chemical photocatalysis: introduction

The term "photocatalysis" can have different meaning to different groups of specialists – differing from photosynthesis to water purification methods. We will use the following definition of chemical photocatalysis: *the use of chemical compounds - photocatalysts - to relay energy in some form from photons to other chemical compounds - substrates.* What are the reasons to use of chemical photocatalysis instead of direct excitation of a substrate compound? Basic law of photochemistry states, that in order to induce chemical change by irradiation at certain wavelength, light must be absorbed by the compound of interest at this wavelength. But if we look on an average organic molecule, it is most probably colorless, absorbing photons only in far UV. Therefore no chemical change occurs, when they are irradiated with visible/near-UV photons. This might come as a surprise, when comparing bond dissociation energies with energies of visible/near-UV photons (Figure 3) – they should have plenty of energy to induce reactions. Reason for this is, that the absorption spectrum of a compound depends on its HOMO-LUMO gap, which does not necessary correlate with the bond dissociation energy. In order to circumvent this problem, we can use photocatalyst, which absorbs the photon, and subsequently transfers energy to the reactant by radiationless processes. Before discussing concrete examples of photocatalysts used currently in synthesis, we will shortly look into the mechanism how these catalysts operate, and how can they be divided by this (Scheme 2).

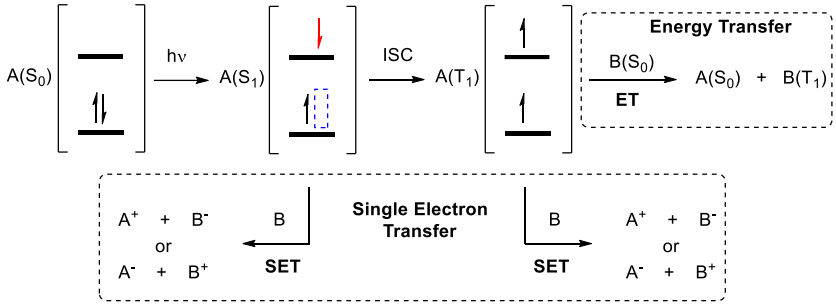

Scheme 2. Comparison of single electron transfer (SET) and energy transfer (ET).

Photocatalyst is first excited into its singlet excited state ($A(S_1)$) from its ground state ($A(S_0)$). If we compare the electronics of the excited state with the ground state, there is a hole in a low energy orbital (blue) and an electron in a high energy orbital (red). This translates into much higher oxidation as well as reduction power of the excited state in comparison to the ground state, and is able to perform single electron transfer. Limiting factor for this is the low lifetime of the singlet excited state

(1-100 ps).[14] In the case, that intersystem crossing (ISC) is possible, much longer lived triplet state of photocatalyst ($A(T_1)$) is formed. This can again induce single electron transfer, or energy transfer can occur. Energy transfer process is sometimes called sensitization and the photocatalysts, which operate via energy transfer, are called sensitizers.

1.2.1: Chemical photocatalysis: sensitizers

Discovery of photosensitization stemmed from the developments of the dye industry in the late 19th century. In this time, toxicity of proflavine was observed, and its toxic effects occurred only when the dye, light and oxygen were present in the system.[16] Using proflavine and leucomalachite dye as a model system, Kaunsky and de Brujin were able to prove in 1931, that proflavine "activates" the oxygen, and the "active" oxygen then reacts with leucomalachite dye, even when direct interaction of proflavine and leucomalachite is supressed (Scheme 3).[17] The exact form of the "active" oxygen became a topic of heated discussions, with the idea of singlet oxygen gaining mainstream acceptance in late 60's, when spectroscopic evidence became available.[18] Variety of photosensitizers suitable for generation of singlet oxygen was developed.[19] Nowadays singlet oxygen generated by sensitization is used for a broad variety of reactions such as Schenck-ene reactions,[20] [4+2] cycloadditions[21] and [2+2] cycloadditions.[22] In biological fields, photosensitization of oxygen is used in photodynamic therapy.[23]

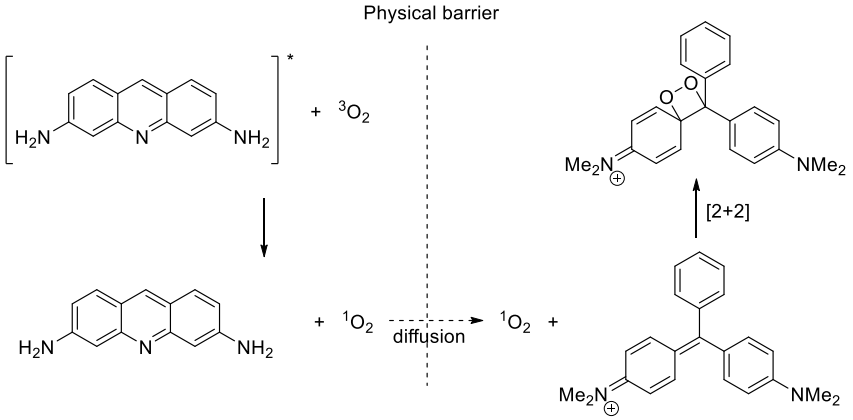

Scheme 3. Singlet oxygen generation by photosensitization with proflavine.

Most common singlet oxygen sensitizers operate in the visible range (Scheme 4). The same paradigm can be used to sensitize any compounds other than oxygen, as long

as the triplet energy of the sensitized compound is lower than the triplet energy of sensitizer.[14] The most successful group of sensitizers are ketones and aromatics, but virtually any compound can be used, as long they have efficient intersystem crossing, which generates long-lived triplet state.[24] In industrial scale, the most common application of triplet sensitizers is the field of photo-induced radical polymerizations.[15b,25] Most of them operate in the near UV and blue part of visible spectrum (Scheme 5).

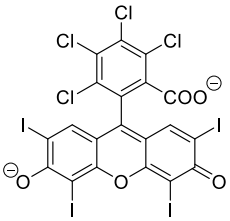

Rose Bengal
λ_{max} = 548
$\Phi(O_2)$ = 0.78

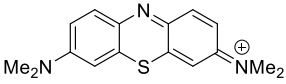

Methylene Blue
λ_{max} = 665
$\Phi(O_2)$ = 0.5

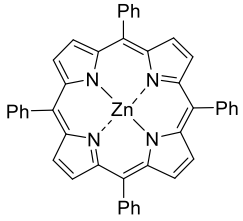

ZnTPP
λ_{max} = 585
$\Phi(O_2)$ = 0.83

Scheme 4. Common singlet oxygen sensitizers; λ_{max} stands for the wavelength of the absorption maximum, $\phi(O_2)$ for the quantum yield of singlet oxygen generation; measured in methanol for Rose Bengal, and Methylene Blue; measured in benzene for ZnTPP.[19a]

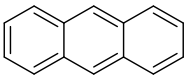

anthracene
λ_{max} = 372 nm
Φ(ISC) = 0.72
E_T = 1.8 eV

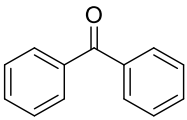

benzophenone
λ_{max} = 347 nm
Φ(ISC) = 1.00
E_T = 3.0 eV

biacetyl
λ_{max} = 416 nm
Φ(ISC) = 1.00
E_T = 2.4 eV

Scheme 5. Common triplet sensitizers; λ_{max} stands for the wavelength of the absorption maximum, ϕ(ISC) for the quantum yield of intersystem crossing; ET for the energy of the triplet excited state.[24]

1.2.2: Chemical photocatalysis: redox catalysis

Energy stored by the generation of charge-separated electron-hole pair within a molecule by excitation can be harnessed for reductive, as well as oxidative processes. In the older literature this process is often named as photoinduced electron transfer (PET).[26] First examples of photoinduced electron transfer come from the late 19th century, when charge transfer complexes of donor-acceptor pairs (e.g. hydroquinone-benzoquinone) were observed. Several decades ago, elementary steps of photosynthesis were discovered, and scientists started do make connection between the processes seen in the nature and the quenching of fluorescence by putative electron transfer.[27] Final proof of the photoinduced electron transfer came with the development of time-resolved spectroscopy and lead to the foundations of Rehm-Weller theory.[28] Rehm-Weller theory allows to predict the thermodynamic feasibility of photoinduced electron transfer processes (Figure 4).

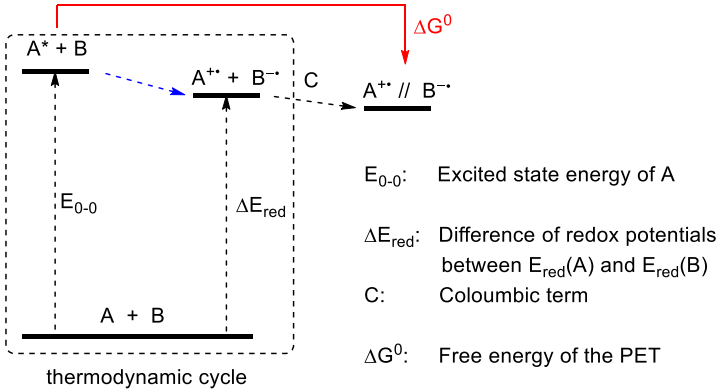

Figure 4. Thermodynamics of PET: Rehm-Weller theory.

We will demonstrate this on an example where A transfers electron to B upon excitation. By experimentation, we can obtain the energy of the excited state of A, and the redox potentials of A and B. By using a thermodynamic cycle, we can calculate the experimentally unavailable energy of electron transfer (blue arrow). In order to obtain the proper reaction free energy, Coulomb attraction between the generated charge-separated pair must be taken into consideration as well:

$$\Delta G^0 = \Delta E_{red} - E_{0-0} + C$$

Coulombic term is negligible in comparison with the other two terms, especially in polar solvents. It should be noted, that if only the hypothetical electrochemical half-reaction $A^{\bullet+}$ -> A* is considered, then there is explicitly no Coulombic interaction, and the modified Rehm-Weller equation can be used for the calculation of such (experimentally not available) redox potentials. This is of great use, when comparing the redox parameters of photocatalysts:

$$E_{red}(A^{\cdot+}/A^{*}) = E_{red}(A^{\cdot+}/A) - E_{0-0}$$

As was already noted, both oxidation as well as reduction capabilities of compounds are increased on excitation, therefore the PET can be both photo-induced oxidation as well as photo-induced reduction. In order to clarify this, terminology was borrowed from the fluorescent spectroscopy community, and we denote these two processes reductive and oxidative quenching (Scheme 6).

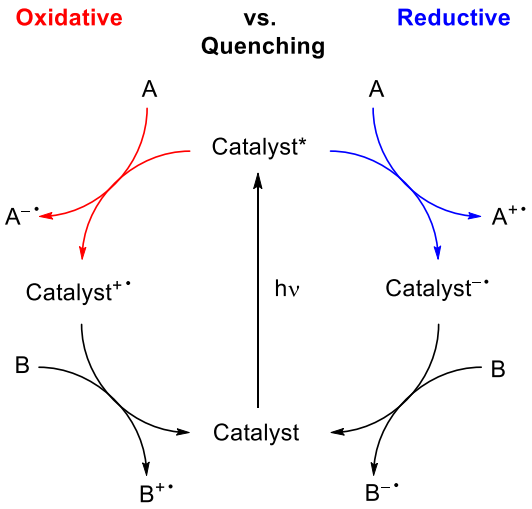

Scheme 6. Oxidative and reductive quenching mechanisms.

Photoredox catalysts are, as the name suggests, catalysts which only shuttle electrons by using the energy of the light. There are two different ways how this property can be implemented into a catalytic system. The more simple situation is, when we use the energy of light to overcome an energetic barrier of an otherwise thermodynamically forbidden reduction or oxidation (Scheme 7, A). This leaves the catalyst in its oxidized/reduced state, and in order to make the reaction catalytic, we

need to use sacrificial electron donor (SD) or acceptor (SA). In a simple way, we can view the role of the photocatalyst in such a process just as an electron transfer reagent between the sacrificial donor/acceptor and the substrate; in case of oxidative quenching, the terminal reductant is the sacrificial electron donor, and in case of reductive quenching, the sacrificial electron acceptor is the terminal electron sink. Common sacrificial electron donors used in photoredox catalysis are aliphatic amines (triethylamine, triethanolamine, EDTA),[29] hydrazine,[30] oxalate[31] and ascorbate.[32] As the sacrificial electron acceptor persulfate[33] diazonium salts,[34] viologens,[35] Co(III) salts[36] and carbon tetrahalides[37] are often used.

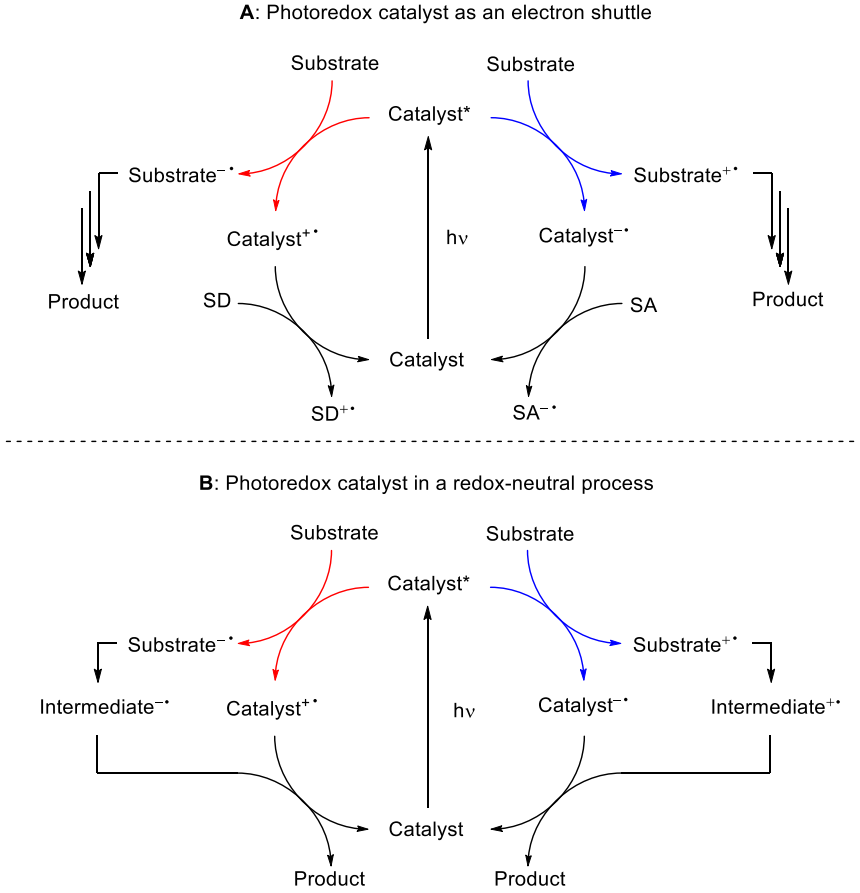

Scheme 7. Comparison of the mechanisms of photoredox catalysis.

It is possible to operate a photocatalytic system without the use of sacrificial electron acceptors or donors (Scheme 7, B). In this case, catalyst is used to generate reactive charged intermediates. These intermediates undergo chemical change and afterwards exchange the electron with the catalyst again by back electron transfer. Catalyst is thereby regenerated, and there is no waste from sacrificial donors/acceptors generated. It is interesting to note, that the most common photocatalytic process in the world, photosynthesis, incorporates both of these mechanisms: cyclic electron transport is a redox-neutral, cyclic process, while the non-cyclic electron transport uses a sacrificial electron donor: water.

Early attempts in the field of photoredox catalysis were aimed at the understanding of photosynthesis and design of man-made catalytic systems which would be able to emulate photosynthetic processes.[38] Nowadays, the main part of the effort is spent on the photocatalytic water splitting, a process which could provide us with a cheap source of renewable hydrogen for use as a fuel. Both heterogenous[39] and homogenous[33,40] systems for photocatalytic water splitting are being developed. Such photocatalytic systems use always transition metal complexes as the photocatalyticaly active site. In the use of photocatalysis for the carbon-carbon and carbon-heteroatom bond formation, organic compounds were used in the role of photocatalysts from the beginning. Discovery of the nature of charge-transfer complexes of 1,4-dicyanonaphthalene (DCN) lead first to the development of stoichiometric photo-induced oxidations with DCN.[41] This was followed by the pioneering work of Pandey in 1990, where he utilized DCN as the photocatalyst for oxidative deselenations (Scheme 8),[42] after which dozens of new organic photocatalysts were found.

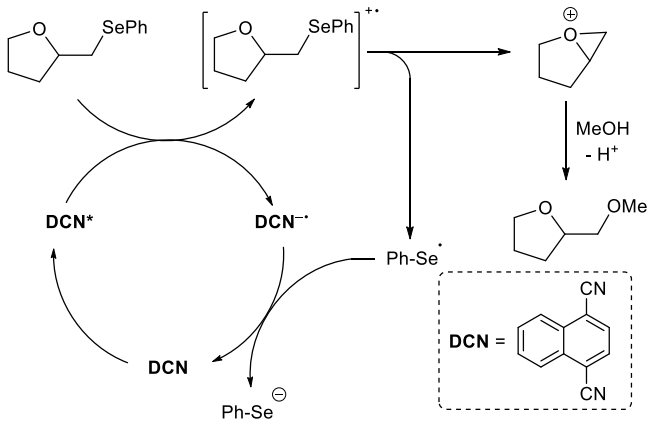

Scheme 8. Photocatalytic deleselenation by Pandey *et. al.*[42]

Majority of these catalysts operated usually via reductive quenching (Scheme 9).[43] The largest drawback of these catalysts is that they only absorb in the UV part of the spectrum.

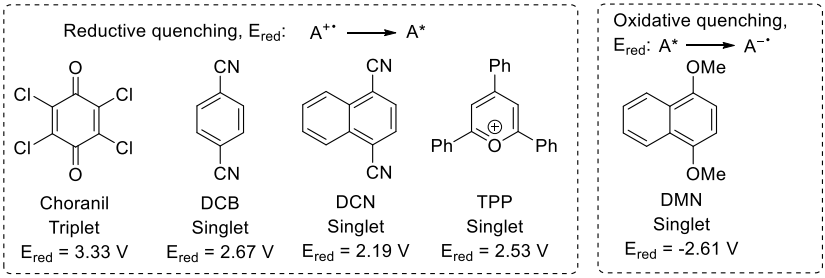

Scheme 9. Common early organic photoredox catalysts; Triplet/Singlet denotes which excited state is active in the PET, E_{red} stands for the redox potential as defined above, against standard calomel electrode (SCE).

In the same time as the organic photocatalysts were developed, new metallic-complex based catalysts, which were previously applied to the water splitting and optoelectronics, started to be used for catalytic C-C and C-X bond forming reactions. Their main advantage over the previously mentioned organic-based catalysts was, that they absorbed in visible part of the spectrum. The most important catalysts from these class are $Ru(bpy)_3^{2+}$, $Ir(ppy)_3$ and $Cu(dap)_2^+$ (bpy: 2,2'-bipyridine, ppy: 2-phenylpyridine, dap: 2,9-dianisylphenanthroline) (Scheme 10, right).

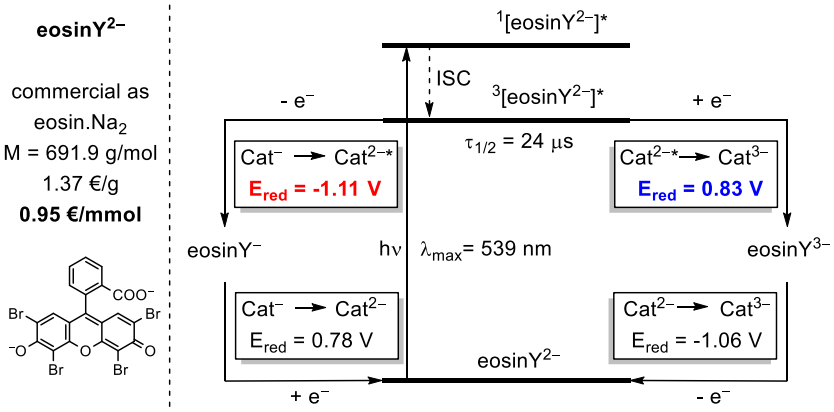

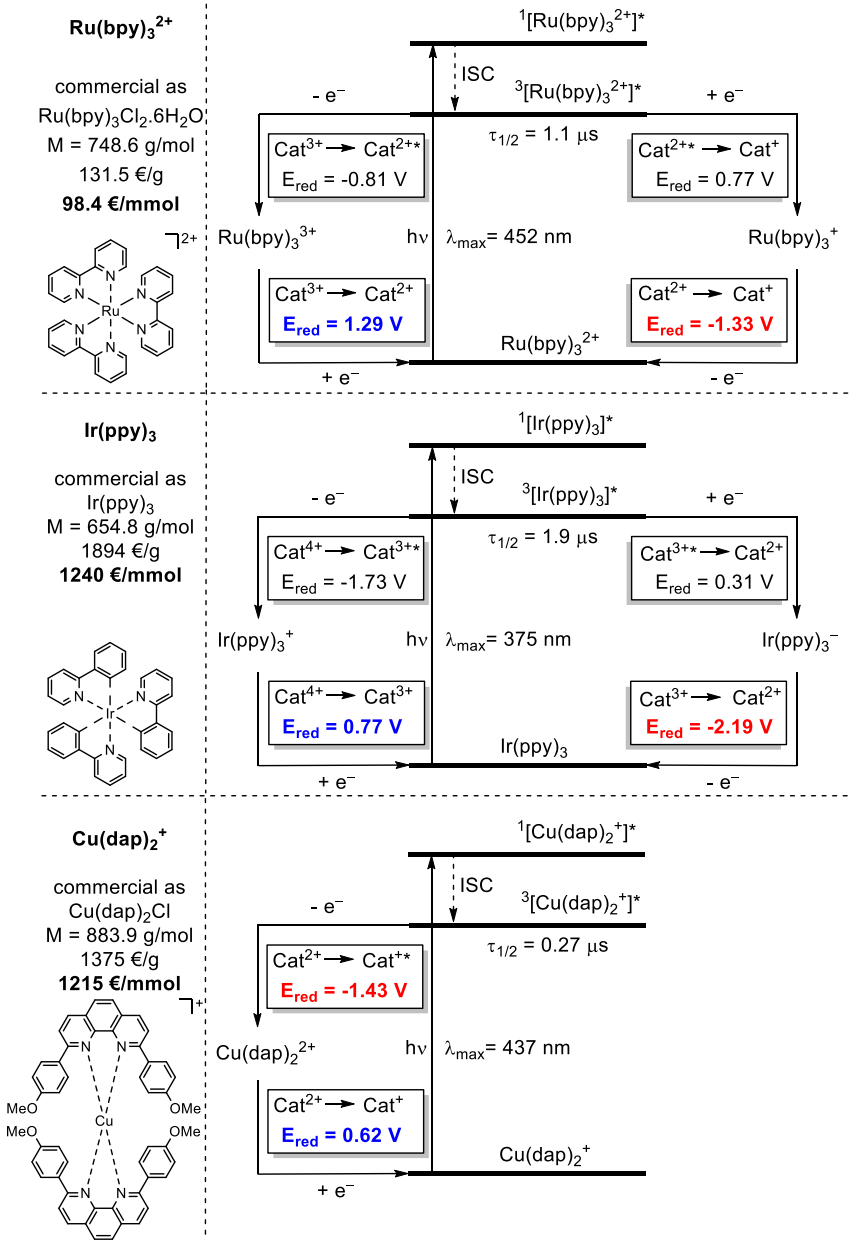

Scheme 10. Summary of the most commonly used photoredox catalysts. Redox potentials are against SCE.

In addition, after 2010, eosin Y had a comeback as a visible-light organic photocatalyst (Scheme 10, left). These four catalysts dominate the field of visible-light photocatalysis nowadays, with most of the new photocatalytic methods developed, utilize one of these catalysts.[44] If we compare the most common visible-light photocatalysts, they all have similar molecular weights. Their prices[45] differ substantially: with the non-metallic eosin Y being the cheapest, $Ru(bpy)_3^{2+}$ is in two orders of magnitude more expensive. $Ir(ppy)_3$ and $Cu(dap)_2^+$ are even tenfold more expensive than that, and while in the case of the copper catalyst is the main limiting factor the price of the ligand, which might drop significantly on scaling up, in case of the iridium catalysts it is the price of metal, which will always remain prohibitive for any larger scale applications. If we would just compare eosin Y and the ruthenium catalyst, $Ru(bpy)_3^{2+}$ has higher maximal oxidative power (1.29 V vs 0.83 V) as well as slightly higher maximal reductive power (-1.33 V vs. -1.11 V), but the price difference still makes eosin Y very competitive for larger scale applications.

1.2.3: Chemical photocatalysis: scope of photoredox catalysis

Scope of the reactions catalyzed by photoredox catalysis is very broad, counting hundreds of reactions (700 hits on the Web of Knowledge[46]), and reviewing all these reactions it beyond the scope of this thesis. We would therefore like to refer the reader to one of many reviews published on this matter.[44,47] Here, we will make a short introduction to the representative classes of photoredox-catalyzed reactions, which are encountered in the literature most frequently.

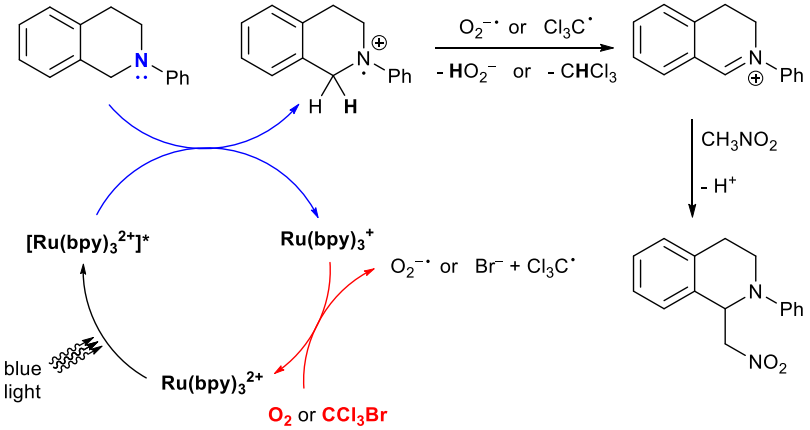

Scheme 11. Photocatalytic C-H activation of tetrahydroisoquinolines.

Probably the most frequently investigated reaction is the photoredox C-H activation of the tetrahydroisoquinolines (Scheme 11). Originally, Ru- and Ir- based catalysts were employed, and a large variety of nucleophiles other than nitromethane (cyanides, indoles, alkynes, phosphines, enamines, etc.) was successfully used.[48] König *et al.* has successfully used eosin Y for this reaction, starting the interest in the eosin Y chemistry.[49] Superoxide, which is produced in this reaction if oxygen is chosen as the sacrificial electron acceptor, can be used productively, for example for oxidative splitting of boronic acids to phenols.[50] In this case a simple amine (triethylamine) is used instead of the tetrahydroisoquinoline as the sacrificial electron donor. Major limit of this tetrahydroisoquinoline derivatization comes in the structure constraints of the starting material, as the nitrogen needs to be arylated in order for the reaction to proceed smoothly. Also, recently there has been a report of formation of charge transfer complexes between carbon tetrahalides and tetrahydroisoquinolines, which absorb in the visible range.[51] Therefore, some of the previous works, which reported photocatalytic reaction may instead be simple observations of the direct excitation of the charge transfer complex. This only underlines the necessity of control experiments in photocatalysis.

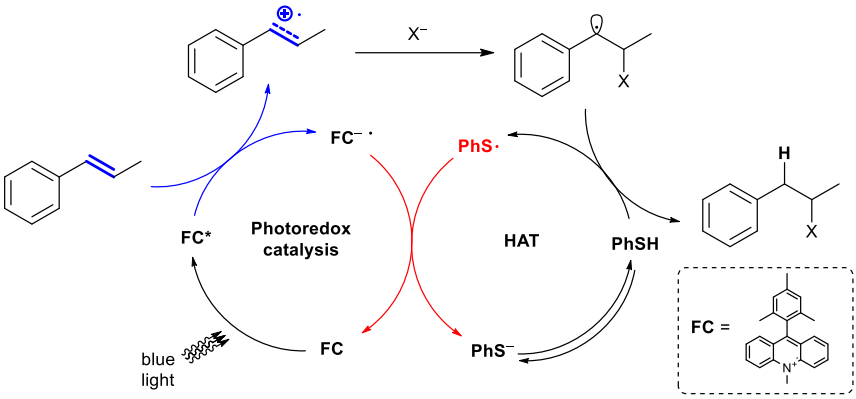

Scheme 12. Photoredox anti-Markovnikov addition to alkenes.

As we already mentioned, an important advantage of photoredox catalysis is, that it allows orthogonal selectivities to the conventional reactivity. A good example of this is the photoredox anti-Markovnikov addition of mineral acids to alkenes (Scheme 12).[52] This type of reactions combines electron transfer by photoredox catalysis with hydrogen atom transfer (HAT). As a photocatalyst, highly oxidizing 9-mesityl-10-methylacridinium perchlorate, which is also called Fukuzumi's catalyst (FC), was used.

Addition of a good hydrogen atom donor (*e.g.* thiophenol) ensures, that the intermediate benzyl radical does not dimerize, or reacts in some other side reaction, but is instead rapidly converted to product. Activation of styryl-systems by single electron oxidation is more universal strategy and can be successfully used to induce [2+2] cycloadditions,[53] or otherwise forbidden Diels-Alder reactions of two electron-rich systems.[54] If the redox potentials of the alkenes are low enough, Ru-based catalysis is also possible.[54]

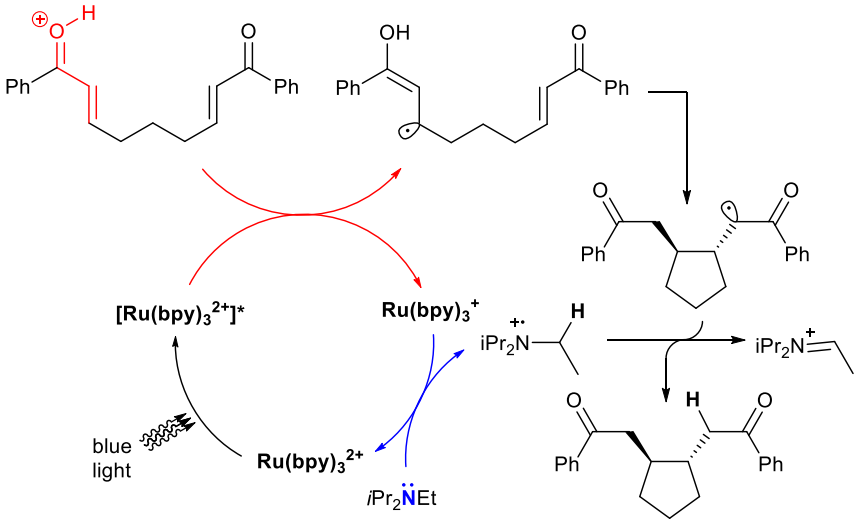

Scheme 13. Photoredox cyclization of enones.

Various cyclizations induced by polar crossover are another class of reactions, often encountered in the field of photoredox catalysis. As an example, using a reductive process, we have chosen cyclization of enones (Scheme 13).[55] This example also illustrates another strategy often used in the reductive activation of conjugated carbonyl compounds in photoredox catalysis: the reducible group is pre-activated by protonation in order to lower its reduction potential. Similarly, metal salts coordinating to the carbonyl group can be used in the same way.[56] [2+2] cycloadditions[57] or [3+2] electrocyclizations with photoredox-generated azomethine ylides[58] can be performed under similar conditions. Interestingly, if the redox potentials of alkenes do not allow electron transfer from photocatalyst, while their triplet energy is low enough, [2+2] cyclizations can also occur via triplet sensitization *via* the photocatalyst. This behavior was demonstrated both by metal-bearing (Ir)[59] as well as organic (flavine)[60] photocatalysts.

Another often used possibility of the photoredox catalysis is the reductive induction of heterolytic bond cleavage. This has been widely studied on diazonium salts.[61] Both organic and metal-complex catalysts were used for the catalysis of such arylations. Variety of π-electron donors can be coupled with the intermediate aryl radical (Scheme 14).

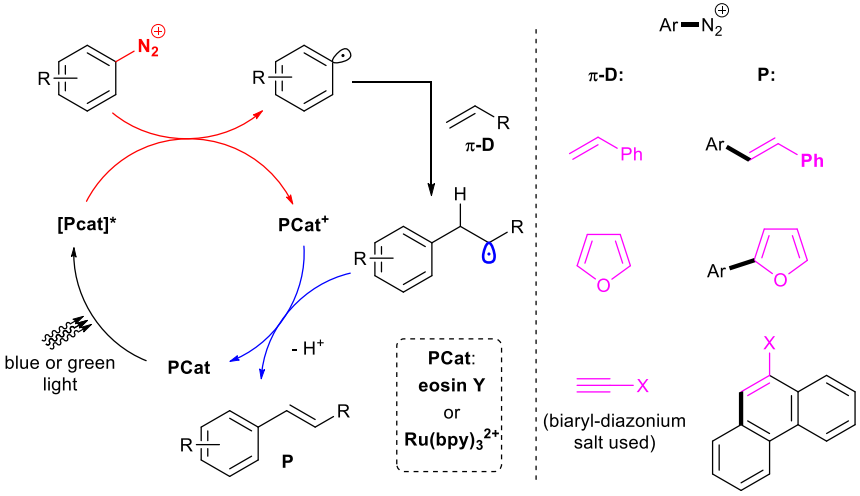

Scheme 14. Photoredox arylation of π- electron donors.

Intramolecular heterocyclizations,[62] photocatalytic Meerwein reaction,[63] or photoredox lithography[64] based on this approach were demonstrated. Major part of this thesis is dedicated to new methods using photoredox catalysis, therefore I would kindly ask the reader to consult respective chapters for more information on this topic. While arenediazonium salts are readily available, and even used in industry in larger scale,[65] people tend to shy away from them due to the anecdotic evidence of their explosive nature.[66] Obvious move to improve both the safety profile of the photocatalytic arylation reactions as well as to broaden the substrate scope would be use of aryl halides instead of arenediazonium salts. Main obstacle to this is the high redox potential of aryl halides in comparison to the arenediazonium salts. While Ru-based catalysts or eosin Y are not reducing enough, $Ir(ppy)_3$ has the necessary reducing power (up to -2.19 V, Scheme 10). Indeed, $Ir(ppy)_3$ was successfully employed for photocatalytic dehalogenation of aryl and alkyl halides,[67] even though more practical applications of this strategy have yet to come.

Alkyl halogen C-X bond cleavage is also required for the atom transfer radical polymerization (ATRP), and for its monomeric variant ATRA (atom transfer radical addition). While these reactions are mainly the domain of polymer chemists, and photoredox catalysis was also successfully applied for polymerizations of this type,[68] reactions useful for synthetic chemistry were also developed. Substrates such as perfluorinated alkyl iodides, benzyl halides or haloketones can be added across a double bond, using a Cu-based photocatalyst (Scheme 15).[69] Due to the more loose coordination sphere of $Cu(dap)_2^+$, different reactivities can be obtained with this catalyst by metal-coordination assistance, in comparison with the Ru- and Ir-based catalysts.[70]

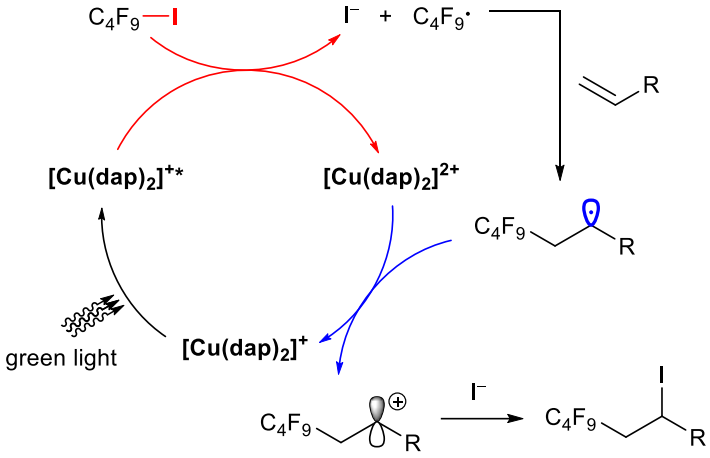

Scheme 15. Photoredox-ATRA reaction.

In the end, we will discuss several methods, where the photoredox catalysis was merged with other activation modes. Sanford *et al.* has presented a successful merger of palladium catalysis and photoredox catalysis (Scheme 16, A).[71] In this case, insertion of Pd(II) species into Ar-X bond was generally slow, and therefore reactions without photoredox catalysis required such high temperatures, that they were not compatible with diazonium salts. By inserting a photocatalytic step into the reaction, oxidative insertion needs not to occur, and the aryl radical, generated by photoredox step couples with the Pd(II) readily, so the reaction can occur at room temperature. Several other protocols operating in a similar merger of metal catalyzed C-H activation and photoredox catalysis have been reported: Pd(0)/Pd(II) systems,[72] Rh(I)/Rh(III) systems[73] and Cu(I) systems.[74] Ni(0)/Ni(II) catalysis merged with photoredox catalysis was used to enhance the rate of reaction with otherwise sluggish nickel catalyst.[75]

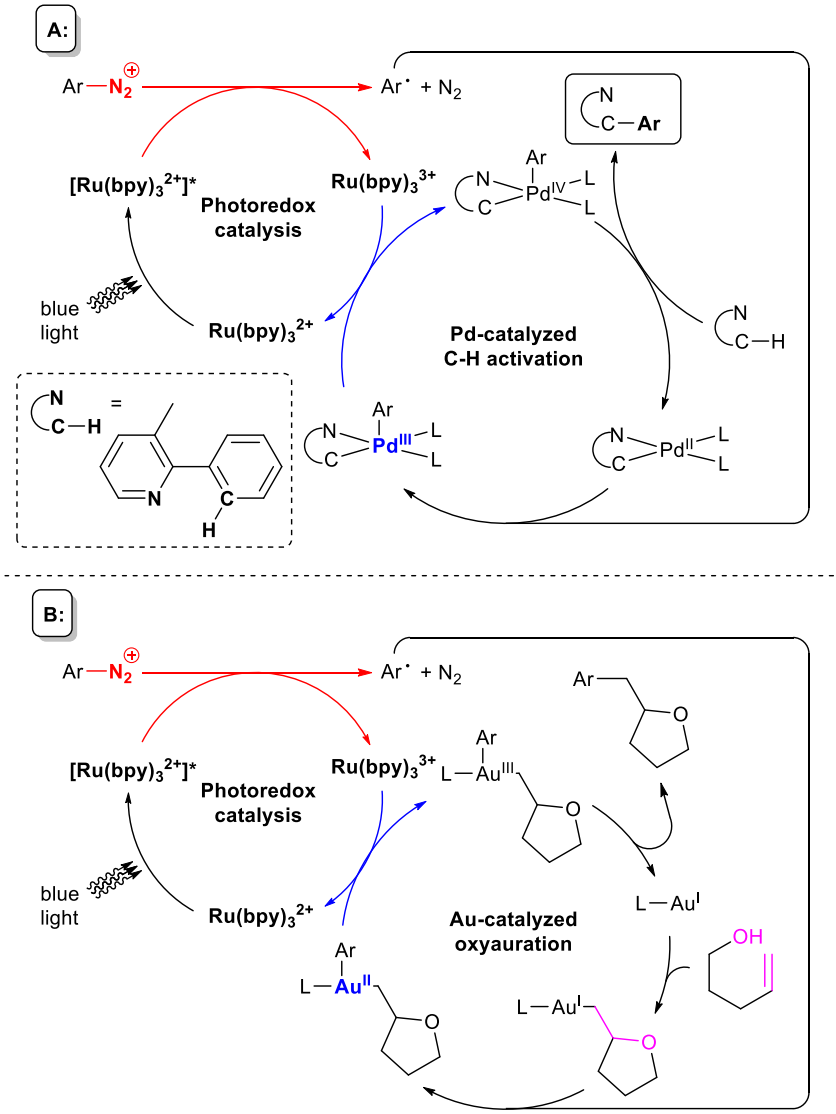

Scheme 16. Merger of photoredox catalysis and metal catalysis.

Gold-catalysed activation of multiple bonds can be also combined with photoredox catalysis (Scheme 16, B).[76] In this case, oxyauration step is followed by coupling of the Au(I) intermediate with aryl radical generated by the photoredox step – a step which

would have a prohibitive activation energy, if a conventional insertion of Au(I) into Ar-X bond was required. Other procedures based around this strategy were reported.[77] Recently, there were also reports of the use of gold complexes as the photoredox catalyst, albeit requiring UV irradiation.[78]

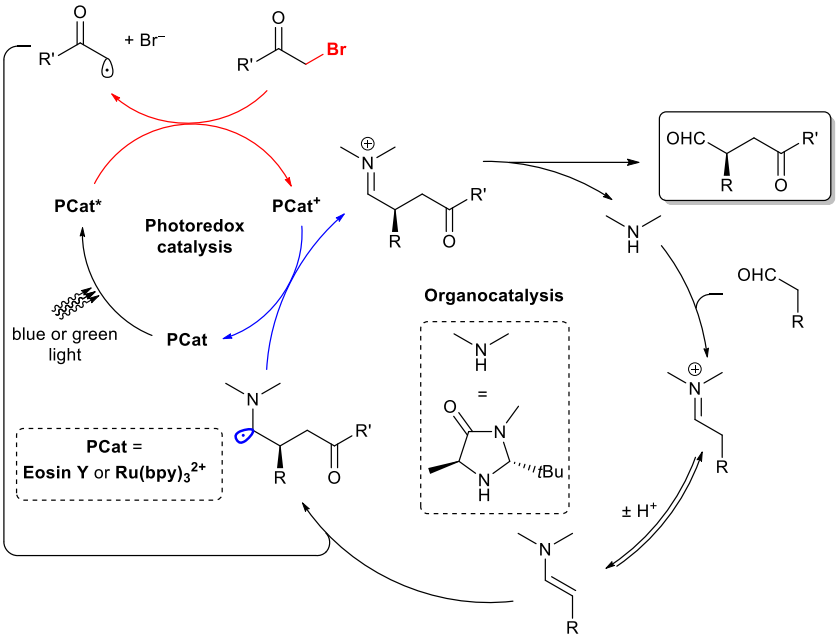

Scheme 17. Merger of photoredox catalysis and organocatalysis.

At last, we will discuss a combination of organocatalysis and photoredox catalysis. It is worth saying, that the early developments in this field started much of the revival of the photocatalysis in the second half of the 2000's. Idea of combining these two catalytic modes together came from the discovery of SOMO activation, independently by Simi and MacMillan in 2007.[79] Highlight of this discovery was in the fact, that high e.e.'s can be achieved with radical processes, which was unprecedented. Photocatalysis came on the scene soon after, as people realized, that redox steps required for the SOMO activation can be carried out by photoredox catalysts (Scheme 17).[80] This approach relies on the reaction of electrophilic, photoredox-generated, acyl radical with the electron rich enamine, generated in the organocatalytic step. Both Ru-based complexes and organic dyes, such as eosin Y can be used as the redox system. High enantioselectivities (e.e. > 98 %) are reached in most cases. Based on this approach,

many other procedures, e.g. enantioselective trifluoromethylations,[81] trichloromethylations[82] and amine functionalizations,[83] have been discovered, though the exhaustive review of these is beyond the scope of this thesis.

1.3: Conclusion and outlook

Photochemistry came a long way from the first observations of light-induced changes, through the heyday of UV-initiated processes in the middle of 20th century to its revival which came with the boom of photocatalysis that we are experiencing nowadays. Photocatalysts capable of carrying large amount of diverse transformations were already demonstrated, but a large part of scientific effort without doubt in the years to come, would be the design of new, more stable, cheaper and versatile photocatalysts. Photoredox catalysis already put several of the "dream" reactions into reality, with its capability to induce reactions orthogonal to the conventional, thermal chemistry. If the current trend is sustained, photoredox catalysis has the potential to change the thinking of chemists of this century in the same way, how the discovery of Pd-coupling chemistry changed the synthetic strategies of organic chemists in the last 40 years. Use of sunlight to carry out synthetic chemistry – the Ciamician's dream – is already being realized in pilot plants in sunny regions, using the energy of sun to make fine chemicals. In combination with electricity generation by photovoltaics, which is now producing more than 5 % of Europe's electricity in peak demand periods, utilization of sunlight reaches levels never reached before. In the 20th century, main hopes for the reduction of our dependence on exhaustible energy sources were put into nuclear fission, which is now eschewed, due to its safety profile, and nuclear fusion, which failed to materialize in applicable scale. Nowadays, the same hopes are put into the solar energy, and photochemistry can help to make these dreams true.

1.4: Thesis scope

This thesis is divided in the following 6 chapters, dealing with the application of photoredox catalysis for new transformations. Main emphasis is on the photoredox activation of aryl derivatives, to induce Ar-X bond cleavage.

Chapter 2 deals with a new organocatalytic visible light mediated synthesis of aryl sulfides. Variety of sulfides was synthesized from diazonium salts by the new photocatalytic method, which we have discovered. This method was also successfully implemented for the synthesis of seleno-derivatives and biologically relevant conjugates of cysteine. This chapter was published in the journal Chemical Communications: Májek M., Jacobi von Wangelin A., *Chem. Commun.* **2013**, *49*, 5507. Author of this thesis did all the synthetic work, and wrote the manuscript.

Chapter 3 deals with the mechanistic investigation of already reported reaction, which utilized eosin Y to generate aryl radicals from diazonium salts. pH dependence of the photocatalytic activity was investigated, and in combination with the evaluation of spectral distribution of irradiation sources used as the source of energy for the photocatalytic reactions, was used to explain discrepancies in the published data. Quantum yields of the reported reactions were measured, proving that some or the eosin Y-catalyzed reactions run by radical chain mechanism. This chapter was published in the Beilstein Journal of Organic Chemistry: Májek M. Filace F., Jacobi von Wangelin A., *Beilstein J. Org. Chem.* **2014**, *10*, 981. Fabiana Filace did quantum yield determination for photocatalytic arylation and for photocatalytic methylthiolation. Author of this rest of the synthetic work, and wrote the manuscript.

Chapter 4 introduces new photoredox carbonylation protocol for diazonium salts. Scope of the reaction includes products not easily available by conventional methods, such as *t*-butyl esters. Reaction runs through an unprecedented single-electron reduction-oxidation carbonylation. Proposed mechanism was proven by a combination of DFT calculations and physico-chemical methods. This chapter was published in the journal Angewandte Chemie International Edition: Májek M., Jacobi von Wangelin A., *Angew. Chem. Int. Ed.* **2015**, *54*, 2270. Author of this thesis did all the synthetic and theoretical work, and wrote the manuscript.

Chapter 5 concerns with the new visible light-driven hydro/deutero defunctionalization of anilines. Defunctionalization of diazonium salts can be carried out efficiently using this method, with DMF as the hydrogen atom donor. If deuterated DMF is used, this method turns into a selective deuteration tool. Proposed mechanism was proven by a combination of DFT calculations and physico-chemical methods including isotopic labeling. This chapter was published in the Chemistry: European Journal: Májek M., Filace F., Jacobi von Wangelin A., *Chem. Eur. J.* **2015**, *21*, 4518. Fabiana Filace did synthesis of the starting materials and carried out the photocatalytic defunctionalizations. Author of this thesis did the selective deuteration experiments, and all the mechanistic and theoretical work, and wrote the manuscript.

Chapter 6 prenents our efforts towards the photocatalytic synthesis of β-arylated ketones. Synthesis of starting materials – cyclopropanols – based on Kulinkovich synthesis, was optimized, and a small library of starting materials was synthesized. Instead of the awaited β-arylated ketones, 5-aryl-N-arylpyrazoles were obtained by the photocatalytic reaction. We have optimized the photocatalytic method, and investigated the substrate scope of this reaction. Mechanistic studies of the unexpected reaction are still ongoing. This chapter was not published yet.

Chapter 7 introduces a new strategy for photocatalytic activation of unreactive bonds: the visible-to-UV photon upconversion for photoredox catalysis. Energy harvested from two consecutive photons is stored by photon upconversion into one catalyst, which activates unreactive Ar-Br bonds. DFT calculations were used to calculate activation energies of electron transfer by Marcus theory, explaining the selectivity of this reaction. Results from this chapter were published in the Chemistry: European Journal: Májek M., Feltmeier U., Dick B., Ruiz-Perez R., Jacobi von Wangelin A., *Chem. Eur. J.* **2015**, in press; DOI: 10.1002/chem.201502698. Experimental work was carried out by Raul Ruiz-Perez and Uwe Faltmeier. Author of this thesis did the DFT calculations and their implementation to Marcus theory framework. Only selected figures and tables from this joint publication are used in this thesis.

1.5: References

1. Canuto V. M., Levine J. S., Augustsson T. R., Imhoff C. L., Giampapa M. S., *Nature* **1983**, *305*, 281.
2. Hohmann-Marriott M. F., Blankenship R. E., *Annu. Rev. Plant Biol.* **2011**, *62*, 515.
3. Setlow R. B., Swenson P. A., Carrier W. L., *Science* **1963**, *142*, 1464.
4. Berkner L. V., Marshall L. C., *J. Atmos. Sci.* **1965**, *22*, 225.
5. Cole W., *Phil. Trans.* **1685**, *15*, 1278.
6. Döbereiner J. F., *Pharm. Centralbl*. **1831**, *2*, 383.
7. Trommsdorff H., *Ann. Pharm.* **1834**, *11*, 190.
8. Liebermann. C., *Ber. Dtsch. Chem. Ges.***1877**, *10*, 2177.
9. Perkin W. H., *J. Chem. Soc.* **1881**, *39*, 409.
10. Schramm J., *Ber. Dtsch. Chem. Ges.* **1884**, *17*, 2922.
11. Ciamician G., *Science* **1912**, *36*, 385.
12. Fisher M., *Angew. Chem. Int. Ed.* **1978**, *17*, 16.
13. Kalsi P. S., *Organic Reactions and their Mechanisms*, New Age International, New Delhi, **2005**, pp. 123.
14. Klán P., Wirtz J., *Photochemistry of Organic Compounds*, John Wiley and Sons, Chichester, **2009**.
15. a) Bach T., Hehn J. P., *Angew. Chem. Int. Ed.* **2011**, *50*, 1000; b) Hoffmann N., *Chem. Rev.* **2008**, *108*, 1052; c) Knowles J. P., Elliott L. D., Booker-Milburn K. I., *Beilstein J. Org. Chem.* **2012**, *8*, 2025; d) Yagci Y., Jockusch S., Turro N. J., *Macromolecules* **2010**, *43*, 6245.

16. a) Raab O., *Z. Biol.* **1904**, *39*, 524; von Tappeiner H., Jodlbauer A., *Dtsch. Arch. Klin. Med.* **1904**, *80*, 427.
17. Kautsky H., de Brujin H., *Naturwissenchaften* **1931**, *19*, 1043.
18. a) Foote C. S., *Acc. Chem. Res.* **1968**, *1*, 104; b) Greer A., *Acc. Chem. Res.* **2006**, *39*, 797.
19. a) DeRosa M. C., Crutchley R. J., *Coord. Chem. Rev.* **2002**, *233-234*, 351; b) Ogilby P. R., *Chem. Soc. Rev.* **2010**, *39*, 3181; c) Schweitzer C., Schmidt R., *Chem. Rev.* **2003**, *103*, 1685.
20. a) Orfanopoulos M., *Tetrahedron* **2000**, 56, 1595; b) Clennan E. L., *Tetrahedron* **2000**, *56*, 9151.
21. a) Schenck G. O., Gollnick K., In: *1,4-Cycloaddition Reactions* (Ed: Hamer, J.), Academic Press, Orlando, **1967**, p. 255; b) Bloodworth A. J., Eggelte H. J., In: *Singlet Oxygen* (Ed: Frimer, A. A.), CRC Press, Boca Raton, **1985**, Vol. 2, p. 93.
22. Schaap A. P., Zaklika K. A., In: *Singlet Oxygen* (Eds.: Wasserman H. H., Murray R. W.) Academic Press, New York, **1979**, p. 173.
23. a) Huang Z., *Technol. Cancer Res. Treat.* **2005**, *4*, 283; b) MacDonald I. J., Dougherty T. J., *J. Porphyrins Phthalocyanines* **2001**, *5*, 105; c) Dolmans D. E. J. G. J., Fukumura D., Jain R. K., *Nat. Rev. Cancer* **2003**, *3*, 380.
24. Zhao J., Wu W., Sun J., Guo S., *Chem. Soc. Rev.* **2013**, *42*, 5323.
25. Gruber H. F., *Prog. Polym. Sci.* **1992**, *17*, 953.
26. Roth H. D., In: *Topics in Current Chemistry 156: Photoinduced Electron Transfer I* (Ed.: Mattay J.), Springer, Berlin, **1990**, 1.
27. Rabinowitch E., *Photosynthesis and Related Processes*, Interscience, New York, **1945**.
28. Knibbe H., Rehm D., Wetler A., *Ber. Bunsenges. Phys. Chem.* **1968**, *72*, 257.
29. Prasad D. R., Hoffman M. Z., *J. Phys. Chem.* **1984**, *88*, 5660.
30. Hirao T., Shiori J., Okahata N., *Bull. Chem. Soc. Jpn.* **2004**, *77*, 1763.
31. Hoffman M. Z., Prasad D. R., *J. Photochem. Photobiol. A* **1990**, *54*, 197.
32. Maji T., Karmakar A., Reiser O., *J. Org. Chem.* **2011**, *76*, 736.
33. Hansen M., Li F., Sun L., König B., *Chem. Sci.* **2014**, *5*, 2683.
34. Lombard J., Jose D. A., Castillo C. E., Pansu R., Chauvin J., Deronzier A., Collomb M.-N., *J. Mater. Chem. C* **2014**, *2*, 9824.
35. Bard A. J., Fox M. A., *Acc. Chem. Res.* **1995**, *28*, 141.
36. Hamada T., Ishida H., Usui S., Watanabe Y., Tsumura K., Ohkubo K., *J. Chem. Soc., Chem. Commun.* **1993**, 909.
37. Condie A. G., Stephenson C. R. J., *Org. Lett.* **2012**, *14*, 94.
38. Gust D., Moore T. A., Moore A. L., *Acc. Chem. Res.* **2001**, *34*, 40.
39. a) Maeda K., Teramura K., Lu D., Takata T., Saito N., Inoue Y., Domen K., *Nature* **2006**, *440*, 295; b) McCormick T. M., Calitree B. D., Orchard A., Kraut

N. D., Bright F. V., Detty M. R., Eisenberg R., *J. Am. Chem. Soc.* **2010**, *134*, 15480.
40. Kudo A., Miseki Y., *Chem. Soc. Rev.* **2009**, *38*, 253.
41. Albini A., Fasani E., Mella M., *J. Am. Chem. Soc.* **1986**, *108*, 4119.
42. Pandey G., Sekhar B. B. V. S., Bhalerao U. T., *J. Am. Chem. Soc.* **1990**, *112*, 5650.
43. Fagnoni M., Dondi D., Ravelli D., Albini A., *Chem. Rev.* **2007**, *107*, 2725.
44. a) Tucker J. W., Stephenson C. R. J., J. Org. Chem. 2012, 77, 1617; b) Prier C. K., Rankic D. A., MacMillan D. W. C., Chem. Rev. 2013, 113, 5322; c) Teplý F., *Collect. Czech. Chem. Commun.* **2011**, *76*, 859; d) Paria S., Reiser O., *ChemCatChem* **2014**, *6*, 2477; e) Hari D. P., König B., *Chem. Commun.* **2014**, *50*, 6688.
45. Prices from Sigma-Aldrich as of 10/2015.
46. Obtained by searching for "photoredox" in the title of the papers by Web of Knowledge, as of 10/2015
47. a) Angnes R. A., Li Z., Correia C. R. D., Hammond G. B., *Org. Biomol. Chem.* **2015**, *13*, 9152; b) Schultz D. M., Yoon T. P., *Science* **2014**, *343*, 1239176; c) Zi Y., Yi H., Lei A., *Org. Biomol. Chem.* **2013**, *11*, 2387; d) Xuan J., Xiao W.-J., *Angew. Chem. Int. Ed.* **2012**, *51*, 6828; e) Zeitler K., *Angew. Chem. Int. Ed.* **2009**, *48*, 9785.
48. a) Condie A. G., Gonzalez-Gomez J. C., Stephenson C. R. J., *J. Am. Chem. Soc.* **2010**, *132*, 1464; b) Freeman D. B., Furst L., Condie A. G., Stephenson C. R. J., *Org. Lett.* **2012**, *14*, 94
49. Hari D. P., König B., *Org. Lett.* **2011**, *13*, 3852.
50. Pitre S. P., McTiernan C. D., Ismaili H., Scaiano J. C., *J. Am. Chem. Soc.* **2013**, *135*, 13286.
51. Franz J. F., Kraus W. B., Zeitler K., *Chem. Commun*. **2015**, *51*, 8280.
52. a) Wilger D. J., Grandjean J. M., Lammert T., Nicewicz D. A., *Nature Chem.* **2014**, *6*, 720; b) Perkowski A. J., Nicewicz D. A., *J. Am. Chem. Soc.* **2013**, *135*, 10334,
53. Riener M., Niicewicz D. A., Chem. Sci. 2013, 4, 2625.
54. Lin S., Padilla C. E., Ischay M. A., Yoon T. P., *J. Am. Chem. Soc.* **2011**, *133*, 19350.
55. Du J., Espelt L. R., Guzei I. A., Yoon T. P., *Chem. Sci.* **2011**, *2*, 2115.
56. Tyson E. L., Farney E. P., Yoon T. P., *Org. Lett.* **2012**, *14*, 1110.
57. Ischay M. A., Anzovino M. E., Du J., Yoon T. P., *J. Am. Chem. Soc.* **2008**, *130*, 12886.
58. Rueping M., Leonori D., Poisson T., *Chem. Commun*. **2011**, *47*, 9615.
59. Lu Z., Yoon T. P., *Angew. Chem., Int. Ed.* **2012**, *51*, 10329.

60. Mojr V., Svobodová E., Straková K., Neveselý T., Chudoba J., Dvořáková H., Cibulka R., *Chem. Commun.* **2015**, *51*, 12036.
61. a) Hari D. P., Schroll P., König B., *J. Am. Chem. Soc.* **2012**, *134*, 2958; b) Schroll P., Hari D. P., ., König B., *ChemistryOpen* **2012**, *1*, 130; c) Xiao T., Dong X., Tang Y., Zhou L., *Adv. Synth. Catal.* **2012**, *354*, 3195.
62. Hari D. P., Hering T., König B., *Org. Lett.* **2012**, *14*, 5334.
63. Hari D. P., Hering T., König B., *Angew. Chem., Int. Ed.* **2014**, *53*, 725.
64. Schroll P., Fehl C., Dankesreiter S., König B., *Org. Biomol. Chem.* **2013**, *11*, 6510.
65. Siegrist U., Rapold T., Blaser H.-U., *Org. Process Res. Dev.* **2003**, *7*, 429.
66. Sullivan J. M., *J. Chem. Educ.* **1971**, *48*, 419.
67. Nguyen J. D., D'Amato E. M., Narayanam J. M. R., Stephenson C. R. J., *Nature Chem.* **2012**, *4*, 854.
68. a) Xu J., Atme A., Martins A. F. M., Jung K., Boyer C., *Polym. Chem.* **2014**, *5*, 3321; b) Yamago S., Nakamura Y., *Polymer* **2013**, *54*, 981; c) Fors B. P., Hawker C. J., *Angew. Chem. Int. Ed.* **2012**, *51*, 8850.
69. a) Pirtsch M., Paria S., Matsuno T., Isobe H., Reiser O., *Chem. Eur. J.* **2012**, *18*, 7336; b) Paria S., Pirtsch M., Kais V., Reiser O., *Synthesis* **2013**, *45*, 2689.
70. Bagal D. B., Kachkovskyi G., Knorn M., Rawner T., Bhanage B. M., Reiser O., *Angew. Chem. Int. Ed.* **2015**, *54*, 6999.
71. Kalyani D., McMurtrey K. B., Neufeld S. R., Sanford M. S., *J. Am. Chem. Soc.* **2011**, *133*, 18566.
72. Zoller J., Fabry D. C., Ronge M. A., Rueping M., *Angew. Chem. Int. Ed.* **2014**, *53*, 13264.
73. Fabry D. C., Zoller J., Raja S., Rueping M., *Angew. Chem. Int. Ed.* **2014**, *53*, 10228.
74. Perepichka I., Kundu S., Hearne Z., Li C.-J., *Org. Biomol. Chem.* **2015**, *13*, 447.
75. Zuo Z., Ahneman D. T., Chu L., Terrett J. A., Doyle A. G., MacMillan D. W. C., *Science* **2014**, *345*, 437.
76. Sahoo B., Hopkinson M. N., Glorius F., *J. Am. Chem. Soc.* **2013**, *135*, 5505.
77. a) Shu X.-Z., Zhang M., He Y., Frei H., Toste F. D., *J. Am. Chem. Soc.* **2014**, *139*, 5844; b) Hopkinson M. N., Sahoo B., Glorius F., *Adv. Synth. Catal.* **2014**, *356*, 2794.
78. a) Kaldas S. J., Cannillo A., McCallum T., Barriault L., *Org. Lett.* **2015**, *17*, **2864**; b) Xie J., Shi S., Zhang T., Mehrkens N., Rudolph M., Hashmi S. K., *Angew. Chem. Int. Ed.* **2015**, *54*, 6046.
79. a) Sibi M. P., Hasegawa M., *J. Am. Chem. Soc.* **2007**, *129,* 4124; b) Beeson T. D., Mastracchio A., Hong J.-B., Ashton, K., MacMillan, D. W. C., *Science* **2007**, *316,* 582.

80. a) Nicewicz D. A., MacMillan D. W. C., *Science* **2008**, *322*, 77; b) Neumann M., Füldner S., König B., Zeitler K., *Angew. Chem. Int. Ed.* **2011**, *50*, 951.
81. Nagib D. A., Scott M. E., MacMillan D. W. C., *J. Am. Chem. Soc.* **2009**, *131*, 10875.
82. Huo H., Wang C., Harms K., Meggers E., *J. Am. Chem. Soc.* **2015**, *137*, 9551.
83. DiRocco D. A., Rovis T., *J. Am. Chem. Soc.* **2012**, *134*, 8094.

Chapter 2:

Organocatalytic visible light mediated synthesis of aryl sulfides

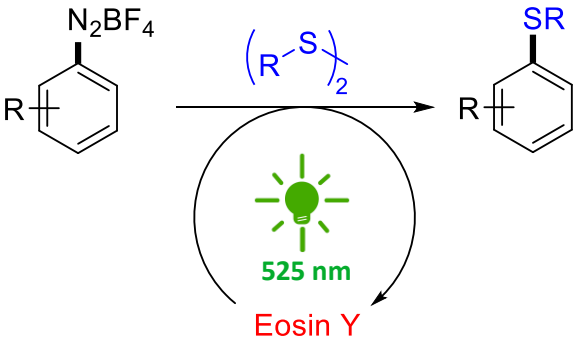

This chapter has been published:
Májek M., Jacobi von Wangelin A., *Chem. Commun.* **2013**, *49*, 5507.

Author contributions:
MM synthesized starting materials, did photochemical reactions, and wrote the manuscript.

2.1: Introduction

The development of mild and sustainable protocols for aromatic substitutions is of utmost importance to the synthesis of fine chemicals, agrochemicals, pharmaceuticals, materials, and natural products.[1] Numerous thermal, Lewis acid-mediated, and metal-catalyzed protocols are currently available to the organic chemist in order to access a large variety of substitution patterns. The re-discovery of visible light as abundant energy source for the activation of chemical reactants has prompted renewed interest in light-mediated aromatic substitutions as powerful alternative to metal-catalyzed "dark" reactions.[2] Such catalytic reactions in the presence of suitable photo-sensitizers mostly involve single electron transfer (SET) processes that bear a close conceptual relationship to Sandmeyer-type reactions.[3] The merit of the photo-catalytic synthesis is the mild generation of aryl radicals by a photo-sensitized electron transfer which avoids the direct photolysis of bonds requiring UV light[4] and the employment of stoichiometric copper(I) salts.

Early studies of photoredox catalysis utilized arene-diazonium salts as precursors for aryl radicals, whose choice is not deliberate: Diazonium salts are easily prepared and undergo facile and irreversible oxidation due to the release of dinitrogen. $Ru(bpy)_3Cl_2$-sensitized intramolecular Pschorr-type arylations were first reported by Deronzier in 1984.[5] Modern developments include intermolecular arylations of electron-rich π-donors for the synthesis of biaryls, stilbenes, α-arylketones, and thiophenes (Scheme 1).[6]

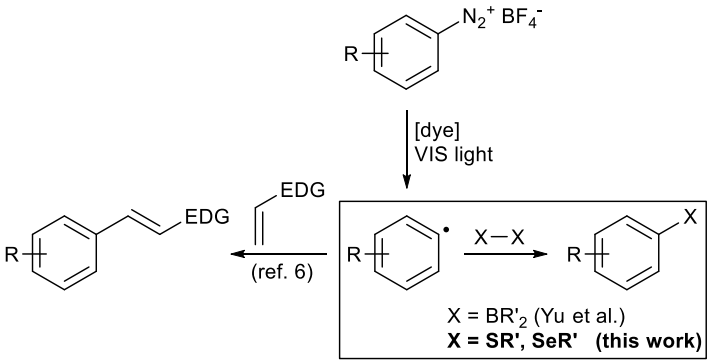

Scheme 1. Formal nucleophilic substitutions at arenediazonium salts via visible light mediated SET reductions.

However, the prevalent use of ruthenium and iridium photo-catalysts is still a severe limitation of many photo-redox protocols in terms of sustainability and

scalability. The persistent quest to introduce cheaper metal-free dyes has been addressed with the successful use of eosin dyes.[7] While these reports clearly demonstrate the viability of aryl radical trapping by π-donors (i.e. alkenes, arenes), examples utilizing σ-donors have remained scarce. To the best of our knowledge, there is only one report where diboranes have been oxidatively cleaved to give arylboronates (Scheme 1).[8] In an effort to extend this general concept to the synthesis of thioethers, we have developed a visible light-mediated thiolation of diazonium salts in the presence of eosin Y. Arylsulfides are key structural motifs in synthetic and natural molecules.[9] Their synthesis is usually performed by treatment of readily available arenediazonium salts with thiols under neutral or basic conditions.[10] However, the intermediate diazosulfide species is a potent explosive even in wet conditions and has already caused violent detonations in many instances.[11]

We envisioned the oxidative cleavage of disulfides by aryl radicals to be a promising catalytic strategy for the synthesis of aryl sulfides.[11,12] The high nucleophilicity of sulfur should entail rapid trapping of the radical and avoid the accumulation of potentially hazardous intermediates, while the neighboring sulphur atom can stabilize partial unsaturation or charges. In combination with the mild visible light-mediated generation of aryl radicals from arenediazonium salts, this would provide an attractive alternative to thermal reactions involving explosive intermediates (Scheme 2). The presence of free aryl radicals in the related "dark" process with stoichiometric copper salts was proven by EPR spectroscopy.[13]

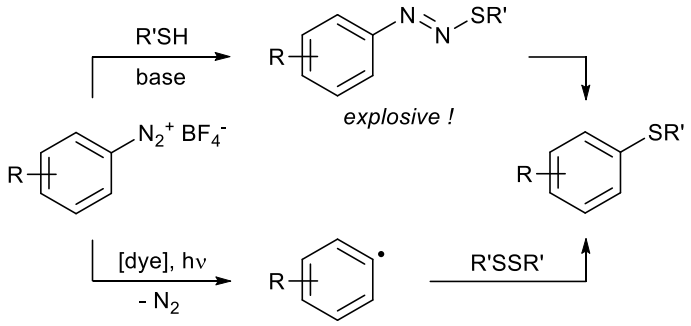

Scheme 2. Azo coupling vs. disulfide route to aromatic sulfides.

2.2: Results and discussion

Initial experiments with 4-bromobenzenediazonium tetrafluoroborate (**1**) and dimethyldisulfide (DMDS), a commercial food additive and sulfiding agent, supported our assumption (Table 1). The optimized set of conditions includes irradiation (green LED, λ_{max} = 525 nm, 3.8 W) of a solution of **1**, 1.5 equiv. DMDS, and eosin Y (2 mol%) in dimethylsulfoxide (DMSO) at 18 °C for 6 h. *N*-Methyl pyrrolidinone (NMP) showed low solubilization of **1**, while *N*,*N*-dimethylformamide also effected reductive dediazotation.[14] Fluorescein, neutral red, and $Ru(bpy)_3Cl_2$ gave lower yields.

Table 1. Selected optimization experiments.[a]

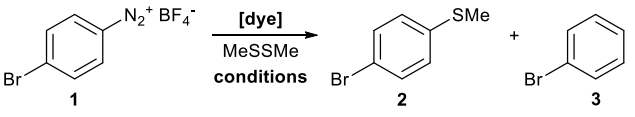

Entry	Solvent	Dye (mol%)	equiv. DMDS	2 / 3 [%]
1 [b]	DMSO	Eosin Y (5)	5	49 / -
2	DMSO	Eosin Y (5)	5	73 / -
3 [c]	DMSO	Eosin Y (5)	5	71 / -
4	NMP	Eosin Y (5)	5	29 / -
5 [d]	MeCN	Eosin Y (5)	5	65 / -
6	DMF	Eosin Y (5)	5	25 / 27
7 [e]	DMF	Eosin Y (5)	-	- / 81
8	DMSO	Fluorescein (5)	5	25 / -
9	DMSO	Neutral Red (5)	5	29 / -
10	DMSO	$Ru(bpy)_3Cl_2$ (5)	5	69 / -
11	DMSO	Eosin Y (2)	5	72 / -
12	DMSO	Eosin Y (1)	5	63 / -
13	**DMSO**	**Eosin Y (2)**	**1.5**	**73 / -**
14	DMSO	Eosin Y (2)	1	42 / -
15 [g]	DMSO	-	1.5	- / -
16	DMSO	-	0.5	3 / -
17 [g]	DMSO	Eosin Y (2)	0.5	3 / -

[a] Standard conditions: 0.5 mmol 4-bromobenzenediazonium tetrafluoroborate, 0.025 mmol eosin Y, 2.5 mmol dimethyldisulfide (DMDS), 2 mL solvent, 18°C, 6 h irradiation with green LED (λ_{max}= 525 nm, 3.8 W); [b] 2 h; [c] 20 h; [d] 7 mL MeCN; [e] no DMDS; [f] without eosin Y; [g] in the dark.

A catalyst-free dark reaction gave no product. When irradiating this mixture, very low yields were observed possibly due to a charge transfer complex between **1** and

DMSO which exhibits absorbance in the visible region.[15] The scope of the protocol was evaluated by employment of various arenediazonium salts (Table 2).

Table 2. Substrate scope.

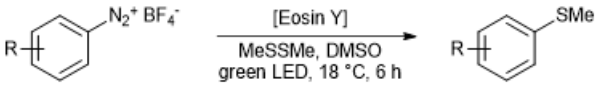

Entry	R	Aryl methyl sulfide	Yield [%]
1	2-Me	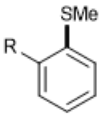	80
2	2-CO_2Me		77
3	2-CF_3		68
4	2-NO_2		48
5	3-Cl	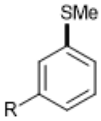	89
6	3-NO_2		60
7	4-OH		57
8	4-OMe		87
9	4-Me	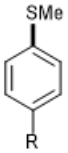	77
10	4-Cl		85
11	4-Br		73
12	4-I		51 [a]
13	4-F		69
14	4-CF_3		67
15	4-NO_2		39
16	-C_4H_4-	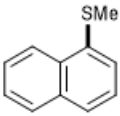	31 [b]

[a] Polymer formation observed; [b] 12% 1,4-di(methylsulfanyl)naphthalene.

The reaction conditions tolerated the presence of esters, nitro groups, and halides (F, Cl, Br), while concomitant substitution of iodide and resultant polymer formation was observed (entry 12). Iodoarene moieties are subject to iodine transfer to aryl radicals.[16] Consistently, addition of iodobenzene to the reaction of 4-iodobenzenediazonium tetrafluoroborate also afforded 1,4-diiodobenzene.

Conversion of 1-naphthalenediazonium salt was unselective giving a mixture of mono- and disubstituted products (entry 16). Similar selectivity was observed in the presence of diphenyldiselenide to give an unsymmetrical diarylselenide (Scheme 3).[17] The synthesis of an arylsulfide bioconjugate bearing an amino acid residue was realized by reaction with dimethyl *L*-cystinate.[18]

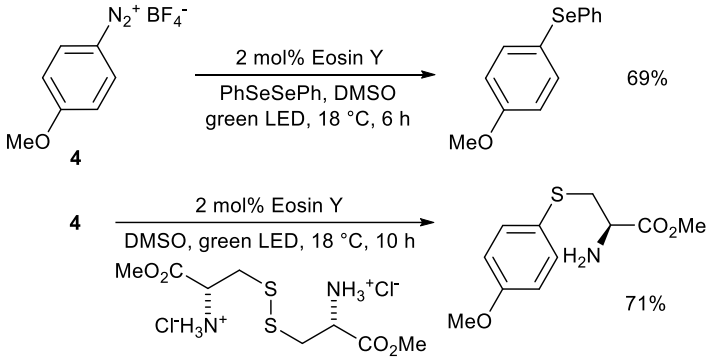

Scheme 3. Synthesis of cysteine and selenide derivatives.

On the basis of previous reports,[5,6] we propose a mechanism for the photocatalytic thiolation (Scheme 4).

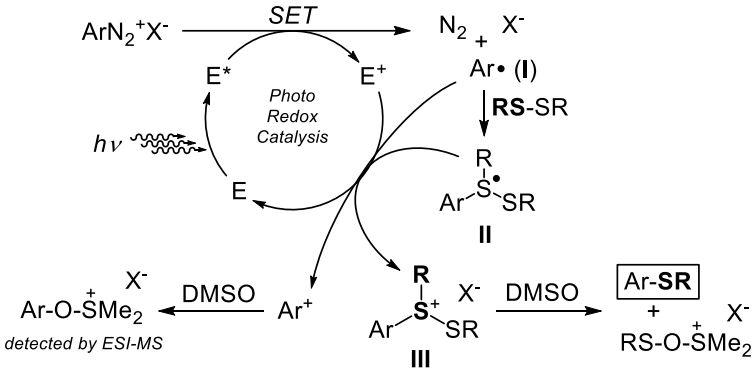

Scheme 4. Proposed reaction mechanism.

The arene-diazonium salt (**I**) is susceptible to SET reduction by the excited photocatalyst. The resulting aryl radical **II** is attacked by the nucleophilic disulfide to give a trivalent sulfur radical **III**, which is stabilized by the neighboring aryl and sulfur

substituents.[19] One-electron oxidation of **III** by the eosin Y radical cation furnishes an electrophilic species which undergoes substitution in the presence of a large excess of DMSO (solvent).[20] A long radical chain mechanism is unlikely, as ^{1}H NMR monitoring showed that product formation stopped when the light source was removed.[21] We have investigated the nature of by-products. Thermal heterolytic cleavage of arenediazonium salts occurs at elevated temperatures (>40°C) to give an aryl cation which is rapidly trapped by the nucleophilic solvent DMSO.[22] The resultant $[ArOSMe_2]^+$ was detected by ESI-MS.[21]

2.3: Conclusion

In summary, we have developed a new photocatalytic thiolation protocol in the presence of only 2 mol% eosin Y which allows the facile synthesis of arylsulfides in good yields at room temperature. The mild reaction conditions (green light, r.t.) tolerate various functional groups and can be applied to the conjugation with thiol-containing amino acids as well as introduction of arylselenide moiety. Presented method is a viable alternative to the traditional process, which involves unstable intermediates, dangerous at larger scales. We have done further investigations into the mechanism of this reaction to support our proposed mechanism.[23] In the meantime a similar photocatalytic process was introduced, using flow technology.[24]

2.4: Experimental part

General

Commercial chemicals were used as obtained from Sigma-Aldrich or Fisher. Solvents were used without further purification. DMSO was dried over molecular sieves (certified <0.005% water content, Sigma-Aldrich). TLC was performed using commercial silica gel coated aluminium plates (DC60 F254, Merck). Visualization was done by UV light. Product yields were determined as isolated by column chromatography using silica gel (Acros Organics, mesh 35-70). Purity and structure confirmation was done by ^{1}H NMR, ^{13}C NMR, GC-MS, and ^{19}F NMR (where appropriate). NMR spectral data were collected on a Bruker Avance 300 (300 MHz for ^{1}H spectra; 75 MHz for ^{13}C spectra) spectrometer and a Bruker Avance 400 (400 MHz for ^{1}H spectra; 100 MHz for ^{13}C spectra; 376 MHz for ^{19}F spectra) spectrometer at 25 °C. Chemical shifts are reported in δ/ppm, and coupling constant *J* given in Hertz. Solvent residual peak were used as internal reference for all NMR measurements. The number of protons was obtained by integration of appropriate signals. Abbreviations used in NMR spectra: s – singlet, d – doublet, t – triplet, q – quartet, m – multiplet, bs – broad singlet, dd – doublet of doublet, ddd – doublet of doublet of doublet.

General Procedure for the Synthesis of Arenediazonium salts

The parent aniline (4.5 mmol) was dissolved in glacial acetic acid (3 mL) and 48 % aqueous solution of tetrafluoroboric acid (1.3 mL). Then, an isoamylnitrite (1 mL) solution in glacial acetic acid (2 mL) was slowly added at room temperature during 5 min. Diethylether (15 mL) was added, and reaction mixture was cooled down to -30 °C in order to induce crystallization of the product. Crystals were filtered off *in vacuo*, washed with diethylether (2 x 10 mL) and dried on air to furnish the corresponding diazonium salts.

General Procedure for Photo-Catalytic Thiolation

A 10 mL Schlenk flask was charged with the arenediazonium salt (0.5 mmol) and eosin Y (0.01 mmol). Dry DMSO (2 mL) was added under a stream of nitrogen. Then, nitrogen was bubbled through the solution during vigorous stirring for 15 min. Dimethyldisulfide (67 µL, 0.75 mmol) was added and the reaction vessel was sealed with a rubber septum. The reaction mixture was irradiated with green light (LED, λ_{max} = 525 nm, 3.8 W) for 6 h at 18°C (= r.t.). Deionized water (3 mL) was added to the reaction mixture, and the resulting emulsion was extracted with diethylether (2 x 5 mL). The combined organic extracts were washed with brine (5 mL) and dried over $MgSO_4$. The solvent was evaporated *in vacuo*, and the residue was purified by flash column chromatography (silica gel) using pentane/diethylether mixtures (from 100/0 to 80/20) as eluent to obtain pure product.

4-Chlorothioanisole

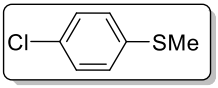

^{1}H NMR (400 MHz, $CDCl_3$, ppm) δ 7.26 (d, *J* = 8.7 Hz, 2H), 7.18 (d, *J* = 8.7 Hz, 2H), 2.47 (s, 3H). ^{13}C NMR (100 MHz, $CDCl_3$, ppm) δ 137.3 (C), 131.0 (C), 128.9 (CH), 128.0 (CH), 16.2 (CH_3). GC-MS (EI) *m/z* (relative intensity): 160.0 (35) [M^+], 158.0 (100), 145.0 (22), 143.0 (55),), spectral data were consistent with literature.[25]

4-(Methylthio)anisole

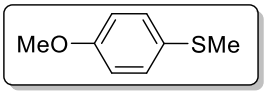

^{1}H NMR (400 MHz, $CDCl_3$, ppm) δ 7.28 (d, *J* = 8.8 Hz, 2H), 6.86 (d, *J* = 8.8 Hz, 2H),

3.79 (s, 3H), 2.45 (s, 3H). ^{13}C NMR (100 MHz, $CDCl_3$, ppm) δ 157.3 (C), 129.2 (CH), 128.0 (C), 113.7 (CH), 54.3 (CH_3), 17.2 (CH_3). GC-MS (EI) *m/z* (relative intensity): 154.0 (94) [M^+], 139.0 (100), 111.0 (23), 96.0 (19), spectral data were consistent with literature.[25]

3-Chlorothioanisole

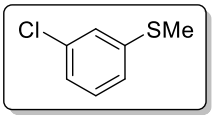

^{1}H NMR (400 MHz, $CDCl_3$, ppm) δ 7.21 (t, *J* = 1.9 Hz, 1H), 7.19 (d, *J* = 7.8 Hz, 1H), 7.13 – 7.08 (m, 2H), 2.48 (s, 3H). ^{13}C NMR (100 MHz, $CDCl_3$, ppm) 140.7 (C), 134.8 (C), 129.8 (CH), 125.8 (CH), 125.1 (CH), 124.5 (CH), 15.6 (CH_3). GC-MS (EI) *m/z* (relative intensity): 160.0 (36) [M^+], 158.0 (100), 127.0 (18), 125.0 (27), spectral data were consistent with literature.[26]

4-Bromothioanisole

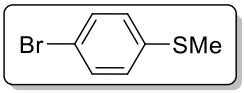

^{1}H NMR (400 MHz, $CDCl_3$, ppm) δ 7.39 (d, *J* = 8.6 Hz, 2H), 7.11 (d, *J* = 8.6 Hz, 2H), 2.46 (s, 3H). ^{13}C NMR (100 MHz, $CDCl_3$, ppm) δ 137.8 (C), 131.8 (CH), 128.2 (CH), 118.7 (C), 19.9 (CH_3), 16.0 (CH_3). GC-MS (EI) *m/z* (relative intensity): 204.0 (100) [M^+], 202.0 (98), 188.9 (34), 186.9 (34), 108.0 (99), spectral data were consistent with literature.[27]

3-Nitrothioanisole

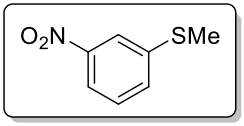

^{1}H NMR (400 MHz, $CDCl_3$, ppm) δ 8.00 (t, *J* = 2.0 Hz, 1H), 7.91 (ddd, *J* = 8.1 Hz, *J* = 2.0 Hz, *J* = 1.0 Hz, 1H), 7.48 (ddd, *J* = 7.9 Hz, *J* = 1.8 Hz, *J* = 1.0 Hz, 1H), 7.39 (t, *J* = 8.0Hz 1H), 2.51 (s, 3H). ^{13}C NMR (100 MHz, $CDCl_3$, ppm) δ 147.8 (C), 140.6 (C), 130.9 (CH), 128.4 (CH), 119.2 (CH), 118.7 (CH), 14.4 (CH_3). GC-MS (EI) *m/z* (relative intensity): 169.0 (100) [M^+], 123.0 (36), 108.0 (41) , spectral data were consistent with literature.[26]

Methyl *S*-methylthiosalicylate

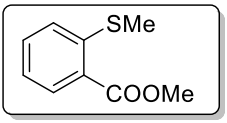

^{1}H NMR (400 MHz, $CDCl_3$, ppm) δ 8.00 (dd, *J* = 7.8 Hz, *J* = 1.5 Hz, 1H), 7.91 (ddd, *J* = 8.2 Hz, *J* = 7.4 Hz, *J* = 1.5 Hz, 1H), 7.27 (d, *J* = 8.2 Hz, 1H), 7.15 (ddd, *J* = 8.0 Hz, *J* = 7.8 Hz, *J* = 1.0 Hz, 1H), 3.92 (s, 3H), 2.46 (s, 3H). ^{13}C NMR (100 MHz, $CDCl_3$, ppm) δ 167.0 (C), 143.5 (C), 132.5 (CH), 131.4 (CH), 126.9 (C), 124.3 (CH), 123.6 (CH), 52.1 (CH_3), 15.6 (CH_3). GC-MS (EI) *m/z* (relative intensity): 182.0 (89) [M^+], 167.0 (32), 151.0 (100), spectral data were consistent with literature.[25]

4-Hydroxythioanisole

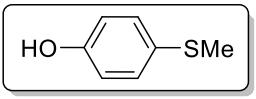

^{1}H NMR (400 MHz, $CDCl_3$, ppm) δ 7.23 (d, *J* = 8.8 Hz, 2H), 6.79 (d, *J* = 8.8 Hz, 2H), 4.88 (bs, 1H), 2.44 (s, 3H). ^{13}C NMR (100 MHz, $CDCl_3$, ppm) δ 153.1 (C), 129.4 (CH), 128.0 (C), 115.1 (CH), 17.1 (CH_3). GC-MS (EI) *m/z* (relative intensity): 140.0 (97) [M^+], 125.0 (100), 97.0 (33), spectral data were consistent with literature.[31]

2-Nitrothioanisole

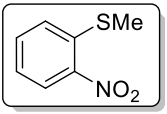

^{1}H NMR (400 MHz, $CDCl_3$, ppm) δ 8.26 (dd, *J* = 8.3 Hz, *J* = 1.5 Hz, 1H), 7.59 (ddd, *J* = 8.6 Hz, *J* = 7.3 Hz, *J* = 1.5 Hz, 1H), 7.37 (d, *J* = 8.0 Hz, 1H), 7.26 (ddd, *J* = 8.0 Hz, *J* = 7.3 Hz, *J* = 1.3 Hz, 1H), 2.50 (s, 3H). ^{13}C NMR (100 MHz, $CDCl_3$, ppm) δ 145.4 (C), 139.4 (C), 133.7 (CH), 126.3 (CH), 125.7 (CH), 124.2 (CH), 16.1 (CH_3). GC-MS (EI) *m/z* (relative intensity): 169.0 (39) [M^+], 108.0 (35), 96.0 (33), 78.0 (100), spectral data were consistent with literature.[29]

2-Methylthioanisole

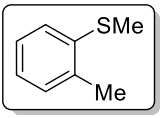

^{1}H NMR (400 MHz, $CDCl_3$, ppm) δ 7.23 – 7.13 (m, 3H), 7.09 – 7.04 (m, 1H), 2.47 (s, 3H), 2.34 (s, 3H). ^{13}C NMR (100 MHz, $CDCl_3$, ppm) δ 137.6 (C), 135.8 (C), 129.8 (CH), 126.3 (CH), 124.6 (2x CH), 20.0 (CH_3), 15.3 (CH_3). GC-MS (EI) *m/z* (relative intensity): 138.1 (100) [M^+], 123.0 (65), 91.0 (70), spectral data were consistent with literature.[25]

4-Nitrothioanisole

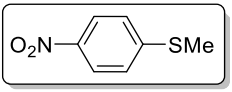

^{1}H NMR (400 MHz, $CDCl_3$, ppm) δ 8.08 (d, *J* = 9.0 Hz, 2H), 7.24 (d, *J* = 9.0 Hz, 2H), 2.51 (s, 3H). ^{13}C NMR (100 MHz, $CDCl_3$, ppm) δ 147.9 (C), 143.8 (C), 124.0 (CH), 122.9 (CH), 13.9 (CH_3). GC-MS (EI) *m/z* (relative intensity): 169.0 (100) [M^+], 139.0 (72), 123.0 (14), 108.0 (38), spectral data were consistent with literature.[25]

Thioanisole

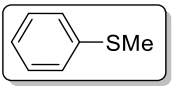

^{1}H NMR (400 MHz, $CDCl_3$, ppm) δ 7.32 – 7.25 (m, 4H), 7.17 – 7.11 (m, 1H), 2.49 (s, 3H). ^{13}C NMR (100 MHz, $CDCl_3$, ppm) δ 138.4 (C), 128.9 (CH), 126.7 (CH), 125.1 (CH), 15.9 (CH_3). GC-MS (EI) *m/z* (relative intensity): 124.0 (100) [M^+], 109.0 (56), 91.0 (40), 78.0 (48), spectral data were consistent with literature.[32]

4-Iodothioanisole

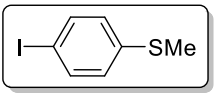

^{1}H NMR (400 MHz, $CDCl_3$, ppm) δ 7.58 (d, *J* = 8.6 Hz, 2H), 6.99 (d, *J* = 8.6 Hz, 2H), 2.46 (s, 3H). ^{13}C NMR (100 MHz, $CDCl_3$, ppm) δ 138.7 (C), 137.7 (CH), 128.3 (CH), 89.3 (C), 15.7 (CH_3). GC-MS (EI) *m/z* (relative intensity): 249.9 (100) [M^+], 234.9 (22), 126.9 (20), 108.0 (41) , spectral data were consistent with literature.[28]

4-Methylthioanisole

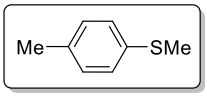

^{1}H NMR (400 MHz, $CDCl_3$, ppm) δ 7.19 (d, *J* = 8.2 Hz, 2H), 7.10 (d, *J* = 8.2 Hz, 2H), 2.47 (s, 3H), 2.32 (s, 3H). ^{13}C NMR (100 MHz, $CDCl_3$, ppm) δ 134.1 (C), 133.7 (C), 128.6 (CH), 126.3 (CH), 19.9 (CH_3), 15.6 (CH_3). GC-MS (EI) *m/z* (relative intensity): 138.0 (100) [M^+], 123.0 (37), 91.0 (85), spectral data were consistent with literature.[25]

4-(Trifluoromethyl)thioanisole

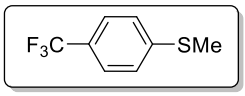

^{1}H NMR (400 MHz, $CDCl_3$, ppm) δ 7.52 (d, *J* = 8.2 Hz, 2H), 7.30 (d, *J* = 8.2 Hz, 2H), 2.51 (s, 3H). ^{13}C NMR (100 MHz, $CDCl_3$, ppm) δ 143.9 (C), 126.8 (q, *J* = 32.7 Hz, C), 125.6 (CH), 125.5 (q, *J* = 3.8 Hz, C), 124.4 (q, *J* = 271.6 Hz, CF_3), 15.1 (CH_3). ^{19}F NMR (376 MHz, $CDCl_3$, ppm) δ -62.3 (s, CF_3). GC-MS (EI) *m/z* (relative intensity): 192.0 (100) [M^+], 173.0 (16), 159.1 (36), spectral data were consistent with literature.[29]

2-(Trifluoromethyl)thioanisole

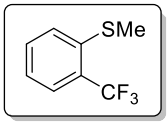

^{1}H NMR (400 MHz, $CDCl_3$, ppm) δ 7.63 (d, *J* = 7.8 Hz, 1H), 7.48 (t, *J* = 7.3 Hz, 1H), 7.38 (d, *J* = 7.9 Hz, 1H), 7.23 (t, *J* = 6.7 Hz, 1H), 2.52 (s, 3H).^{13}C NMR (100 MHz, $CDCl_3$, ppm) δ 137.3 (C), 130.1 (CH), 127.2 (q, *J* = 30.3 Hz, C), 126.5 (CH), 125.6 (q, *J* = 5.7 Hz, CH), 123.0 (q, *J* = 273.8 Hz, CF_3), 123.7 (CH), 15.4 (CH_3). ^{19}F NMR (376 MHz, $CDCl_3$, ppm) δ -61.5 (s, CF_3). GC-MS (EI) *m/z* (relative intensity): 192.0 (100) [M^+], 177.0 (14), 171.0 (15), 159.1 (33), spectral data were consistent with literature.[30]

4-Fluorothioanisole

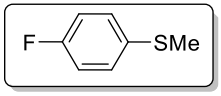

^{1}H NMR (400 MHz, $CDCl_3$, ppm) δ 7.29 – 7.22 (m, 2H), 7.04 – 6.98 (m, 2H), 2.47 (s, 3H).

^{13}C NMR (100 MHz, $CDCl_3$, ppm) δ 160.1 (d, *J* = 246.6 Hz, C), 132.3 (C), 128.2 (d, *J* = 7.9 Hz, CH), 114.9 (d, *J* = 21.9 Hz, CH), 16.2 (CH_3). ^{19}F NMR (376 MHz, $CDCl_3$, ppm) δ -117.3 (s, F). GC-MS (EI) *m/z* (relative intensity): 142.0 (100) [M^+], 127.0 (19), 109.0 (18), 96.0 (21), 83.0 (37), spectral data were consistent with literature.[25]

1-Methylthionaphthalene

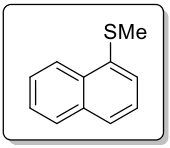

^{1}H NMR (400 MHz, $CDCl_3$, ppm) δ 8.28 (d, *J* = 8.3 Hz, 1H), 7.84 (d, *J* = 7.6 Hz, 1H), 7.67 (d, *J* = 7.8 Hz, 1H), 7.57 – 7.49 (m, 2H), 7.45 – 7.37 (m, 2H), 2.58 (s, 3H).^{13}C NMR (100 MHz, $CDCl_3$, ppm) δ 135.8 (C), 133.7 (C), 131.7 (C), 128.6 (CH), 126.2 (CH), 126.1 (CH), 125.9 (CH), 125.7 (CH), 124.3 (CH), 123.7 (CH), 16.3 (CH_3). GC-MS (EI) *m/z* (relative intensity): 174.1 (100) [M^+], 159.0 (53), 128.1 (25), 115.1 (92), spectral data were consistent with literature.[25]

1,4-Bis(methylthio)naphthalene

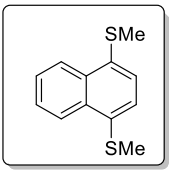

^{1}H NMR (400 MHz, $CDCl_3$, ppm) δ 8.36 – 8.31 (m, 2H), 7.61 – 7.56 (m, 2H), 7.38 (s, 2H), 2.55 (s, 6H).^{13}C NMR (100 MHz, $CDCl_3$, ppm) δ 133.8 (2 x C), 132.1 (2 x C), 126.6 (2 x CH), 125.1 (2 x CH), 124.5 (2 x CH), 16.8 (2 x CH_3). GC-MS (EI) *m/z* (relative intensity): 220.0 (100) [M^+], 205.0 (95), 190.0 (21), 171.1 (23), 158.0 (35), spectral data were consistent with literature.[33]

(4-Methoxyphenyl)(phenyl)selane

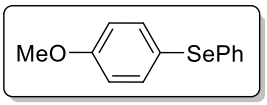

^{1}H NMR (400 MHz, $CDCl_3$, ppm) δ 7.51 (d, *J* = 8.8 Hz, 2H), 7.37 – 7.19 (m, 5H), 6.86 (d, *J* = 8.8 Hz, 2H), 3.81 (s, 3H). ^{13}C NMR (100 MHz, $CDCl_3$, ppm) δ 158.9 (C), 135.5 (CH), 132.2 (C), 129.9 (CH), 128.0 (CH), 125.4 (CH), 118.9 (C), 114.2 (CH), 54.2 (CH_3).

GC-MS (EI) *m/z* (relative intensity): 263.9 (44) [M^+], 184.0 (100), 169.0 (46), 141.0 (38) , spectral data were consistent with literature.[34]

Cystine dimethylester dihydrochloride

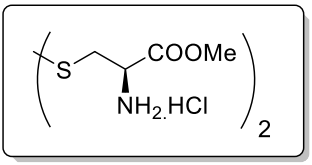

To a suspension of cystine (0.8 g, 3.33 mmol) in dry methanol (20 mL), thionyl chloride (0.6 mL, 8.27 mmol) was added slowly at room temperature. The temperature was increased to 80 °C over a period of 15 min, and the reaction mixture was stirred at this temperature for 3 h, then left to cool down and stirred overnight at room temperature. The volatiles were evaporated *in vacuo*, and the residue was dissolved in a minimal amount of methanol. Crystals of crude product crashed out from the solution by addition of diethylether. The product was filtered *in vacuo*, washed two times with diethylether and dried on air to obtain white crystals of cystine dimethylester dihydrochloride (1.04 g, 3.05 mmol, 92 %).

^{1}H NMR (400 MHz, $CDCl_3$, ppm) δ 8.98 (bs, 6H), 4.34 (t, *J* = 5.7 Hz, 2H), 3.75 (s, 6H), 3.43 – 3.26 (m, 4H). ^{13}C NMR (100 MHz, $CDCl_3$, ppm) δ 172.0 (C), 56.8 (CH_3), 54.2 (CH), 38.5 (CH_2), spectral data were consistent with literature.[35]

(*R*)-Methyl 2-amino-3-((4-methoxyphenyl)thio)propa-noate hydrochloride

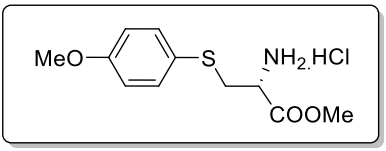

A dry Schlenk flask was charged with *p*-methoxyphenyldiazonium tetrafluoroborate (111 mg, 0.5 mmol), eosin Y (6 mg, 0.01 mmol) and cystine dimethylester dihydrochloride (205 mg, 0.6 mmol). Dry DMSO (4 mL) was added under a stream of nitrogen, and nitrogen was bubbled through reaction solution during vigorous stirring for 15 min, after which the reaction vessel was sealed. The mixture was irradiated with green light for 10 h at r.t. Then, water (5 mL) was added to the reaction mixture, and aqueous NaOH solution was added until pH 12. The mixture was extracted with ethyl acetate (2 x 7 mL), the combined organic extracts were washed with brine (5 mL) and dried over $MgSO_4$. The solvent was evaporated *in vacuo*, and the residue was dissolved

in a minimal amount of diethyl ether. A stream of dry HCl gas was introduced into solution. The crystals that have crashed out were filtered *in vacuo*, washed with diethyl ether and dried in high vacuum to obtain (*R*)-methyl 2-amino-3-((4-methoxyphenyl)thio)propanoate hydrochloride (98 mg, 0.35 mmol, 71 %) as tan crystals, that turn blue on prolonged exposure on air. Freebase (R)-methyl 2-amino-3-((4-methoxyphenyl)thio)propanoate for analytical purposes was liberated from methanol solution of the hydrochloride salt by addition of NaOH.

^{1}H NMR (400 MHz, $CDCl_3$, ppm) δ 8.99 (bs, 3H), 7.53 (d, *J* = 8.8 Hz, 2H), 6.81 (d, *J* = 8.8 Hz, 2H), 4.37 – 4.25 (m, 1H), 3.86 – 3.76 (m, 2H), 3.75 (s, 3H), 3.48 (s, 3H). ^{13}C NMR (100 MHz, $CDCl_3$, ppm) δ 168.2 (C), 159.9 (C), 135.5 (CH), 122.9 (C), 114.8 (CH), 55.4 (CH_3), 53.2 (CH), 52.3 (CH_3), 36.4 (CH_2). GC-MS (EI) (after neutralization of HCl salt with Na_2CO_3) *m/z* (relative intensity): 241.0 (51) [M^+], 193.9 (15), 153.0 (50), 139.0 (81), 124.9 (60), 108.0 (100).

NMR Monitoring of Reaction Progress: Irradiation vs. Dark reaction

A dry Schlenk flask was charged with *p*-methoxyphenyldiazonium tetrafluoroborate (0.1 mmol) and eosin Y (0.005 mmol). Dry DMSO-d_6 (0.7 mL) was added under a stream of nitrogen. Then, nitrogen was bubbled through the solution during vigorous stirring for 15 min. Dimethyldisulfide (16 µL, 0.18 mmol) was added and the reaction mixture was transferred to a dry, argon-purged NMR tube and sealed. The NMR tube was irradiated with green light for 30 sec, and a ^{1}H NMR spectrum was immediately recorded. This routine was repeated another 10 times, after which the irradiation was stopped. Then, another five ^{1}H NMR spectra were measured over 12 minutes. The amount of product formed was determined by comparing integral intensities of protons of product vs. the parent diazonium salt (Figure 1). After the irradiation of sample was discontinued, rate of product formation dropped to zero. While such a simple experiment can prove, that no long-lived radical chain process is involved,[36] it is not suitable to prove non-existence of shorter radical chains.[37] Results from quantum yield determination for this reaction strongly suggest, that no radical chain process is involved in this case.[23]

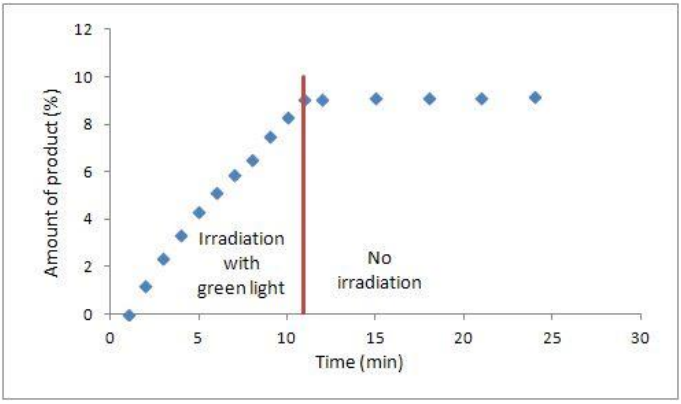

Figure 1. Light ON-OFF NMR experiment

By-Product from Thermal Decomposition of Arenediazonium Salt

A reaction was performed under standard reaction conditions, using *p*-methoxyphenyldiazonium tetrafluoroborate and dimethyl disulfide. After the termination of irradiation, a high vacuum was applied to the flask, and all volatiles were distilled off at 130 °C. The residue was dissolved in methanol and subjected to MS analysis. The major by-product detected by MS was $[Ar\text{-}OSMe]^+$ with Ar = 4-MeOPh and could have formed via the following mechanism (Figure 2):

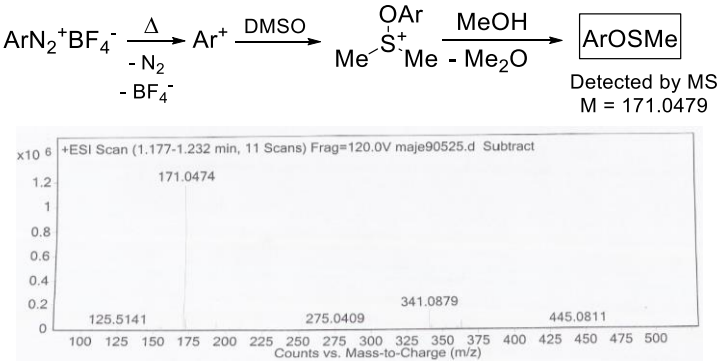

Figure 2. Mechanism of the thermal by-product formation

H and ^{13}C NMR spectra of selected compounds

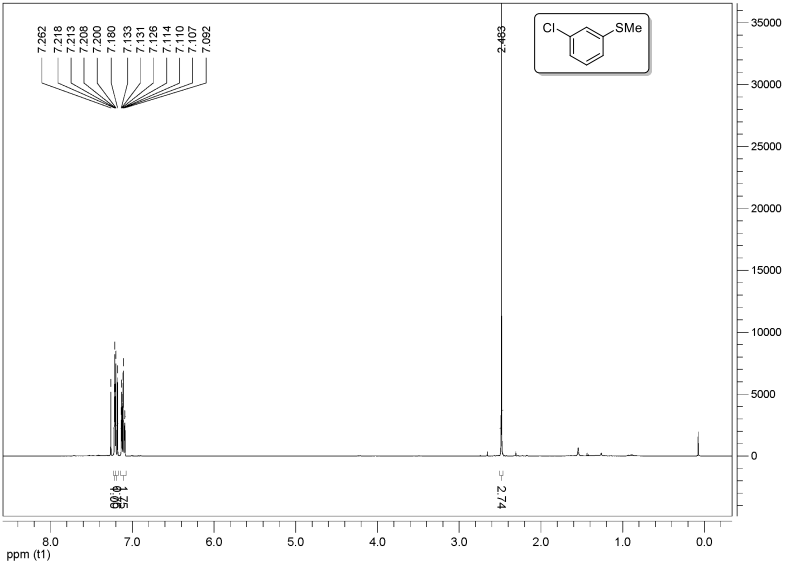

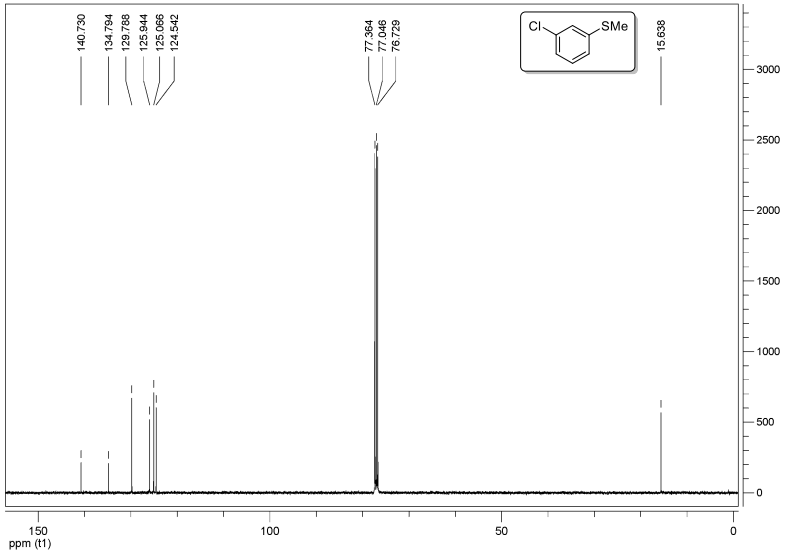

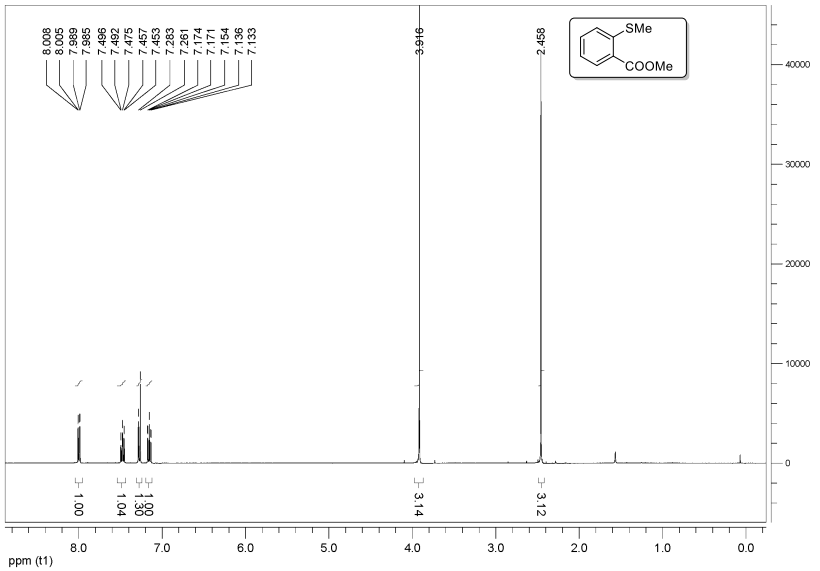
8.008
8.005
7.989
7.985
7.496
7.492
7.475
7.457
7.453
7.283
7.261
7.174
7.171
7.154
7.136
7.133
3.916
2.459
SMe
COOMe
1.00
1.04
1.00
1.00
3.14
3.12
ppm (t1)

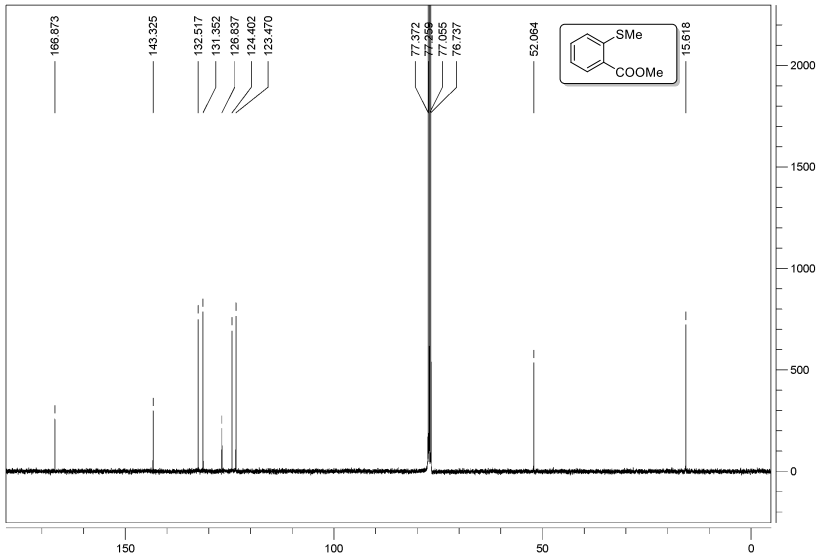
166.873
143.325
132.517
131.352
126.837
124.402
123.470
77.372
77.055
76.737
52.064
15.618
SMe
COOMe

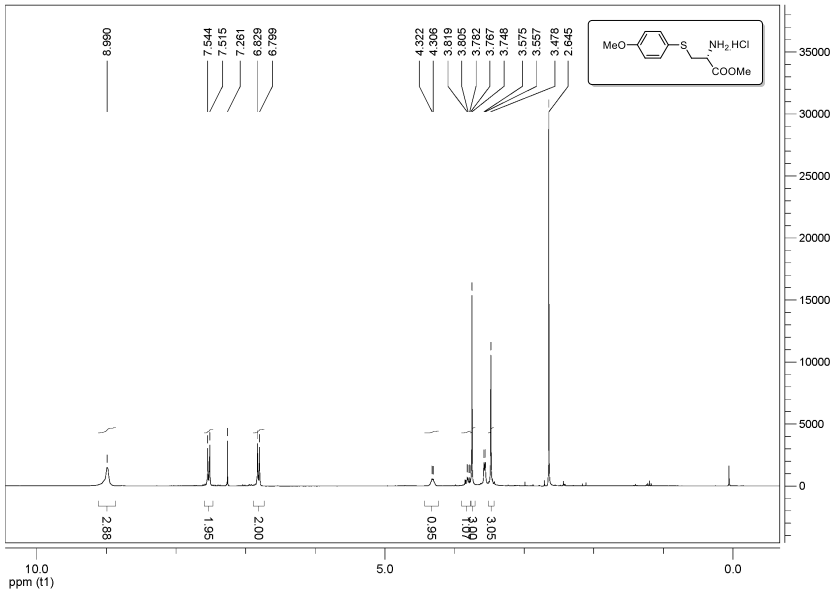
8.990
7.544
7.515
7.261
6.829
6.799
4.322
4.306
3.819
3.805
3.782
3.767
3.748
3.575
3.557
3.478
2.645
MeO
S
NH2 HCl
COOMe
2.88
1.95
2.00
0.95
1.00
3.05
10.0
5.0
0.0
ppm (t1)

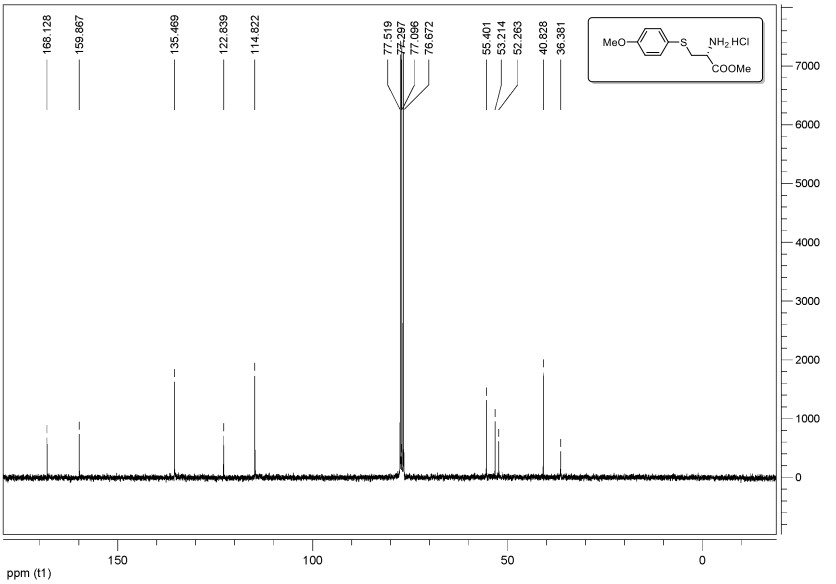
168.128
159.867
135.469
122.839
114.822
77.519
77.297
77.096
76.672
55.401
53.214
52.263
40.828
36.381
MeO
S
NH2 HCl
COOMe
150
100
50
0
ppm (t1)

2.5: References

1: a) Smith M. B., March J., *March's Advanced Organic Chemistry: Reactions, Mechanisms, and Structure*, 6th ed., Wiley, Hoboken, **2007**, Ch. 11 & 13; b) Rueping M., Nachtsheim B. J., *Beilstein J. Org. Chem.* **2010**, *6*, No. 6. DOI:10.3762/bjoc.6.6 c) Torborg C., Beller M., *Adv. Synth. Catal.* **2009**, *351*, 3027.

2: a) Xi Y., Yi H., Lei A., *Org. Biomol. Chem.* **2013**, *11*, 2387; b) Xuan J., Xiao W.-J., *Angew. Chem. Int. Ed.* **2012**, *51*, 6828; b) Teplý F., *Collect. Czech. Chem. Commun.* **2011**, *76*, 859; c) Zeitler K., *Angew. Chem. Int. Ed.* **2009**, *48*, 9785; d) Fagnoni M., Dondi D., Ravelli D., Albini A., *Chem. Rev.* **2007**, *107*, 2725; e) Lewis N. S., *Science* **2007**, *315*, 798; f) Oelgemöller M., Jung C., Mattay J., *Pure Appl. Chem.* **2007**, *79*, 1939.

3: a) Sandmeyer T., *Ber. Dtsch. Chem. Ges.* **1884**, *17*, 2650; b) Beletskaya I. P, Cheprakov A. V., *Coord. Chem. Rev.* **2004**, *248*, 2337.

4: Fagnoni M., Albini A., *Acc. Chem. Res.* **2005**, *38*, 713.

5: Cano-Yelo H., Deronzier A., *J. Chem. Soc., Perkin Trans. 2* **1984**, 1093.

6: a) Hari D. P., Schroll P., König B., *J. Am. Chem. Soc.* **2012**, *134*, 2958; b) Schroll P., Hari D. P., König B., *ChemistryOpen* **2012**, *1*, 130; c) Hering T., Hari D. P., König B., *J. Org. Chem.* **2012**, *77*, 10347; d) Hari D. P., Hering T., König B., *Org. Lett.* **2012**, *14*, 5334; e) Kalyani D., McMurtrey K. B., Neufeldt S. R., Sanford M. S., *J. Am. Chem. Soc.* **2011**, *133*, 18566. f) For a timely review of arenediazonium salt chemistry, see: Mo F., Dong G., Zhang Y., Wang J., *Org. Biomol. Chem.* **2013**, *11*, 1582.

7: a) Neumann M., Füldner S., König B., Zeitler K., *Angew. Chem. Int. Ed.* **2011**, *50*, 951; b) Wang X., Maeda K., Thomas A., Takanabe K., Xin G., Carlsson J. M., Domen K., Antonietti M., *Nature Materials* **2009**, *8*, 76; c) LiuJ. , Wen S., Hou Y., Zuo F., Beran G. J. O., Feng P., *Angew. Chem. Int. Ed.* **2013**, *52*, 3241.

8: Yu J., Zhang L., Yan G., *Adv. Synth. Catal.* **2012**, *354*, 2625.

9: Selected recent examples: a) Johannesson P., Lindeberg G., Johannesson A., Nikiforovich G. V., Gogoli A., Synergren B., Le Greves M., Nyberg F., Karlen A., Hallberg A., *J. Med. Chem.* **2002**, *45*, 1767; b) Llauger L., He H. Z., Kim J., Aguirre J., Rosen N., Peters U., Davies P., Chiosis G., *J. Med. Chem.* **2005**, *48*, 2892; c) De Martino G., Edler M. C., La Regina G., Coluccia A., Barbera M. C., Barrow D., Nicholson R. I., Chiosis G., Brancale A., Hamel E., Artico M., Silvestri R., *J. Med. Chem.* **2006**, *49*, 947; d) Gangjee A., Zheng Y. B., Talreja T., Mc Guire J. J., Kisliuk R. L., Queener S. F., *J. Med. Chem.* **2007**, *50*, 2046.

10: Page P. C. B., Wilkes R. D., Reynolds D. In: *Comprehensive Organic Functional Group Transformations, Vol. 2* (Katritzky A. R., Meth-Cohn O., Rees C. W., eds.), Elsevier, Oxford, **1995**, Chapter 2.03, 113.

11: a) Laquidara J., *Chem. Eng. News* **2001**, *79*, 6; b) Spencer H., *Chem. Brit.* **1977**, *13*, 240.

12: a) Witt D., *Synthesis* **2008**, *16*, 2491; b) Zincke T., *Chem. Ber.* **1911**, *44*, 769; c) Hogg P. J., *Trends Biochem. Sci.* **2003**, *28*, 210; d) Burns J. A., Butler J. C., Moran J. Whitesides G. M., *J. Org. Chem.* **1991**, *56*, 2648; e) Dmitrenko O., Thorpe C., Bach R. D., *J. Org. Chem.* **2007**, *72*, 8298; f) Erlandsson M., Hällbrink M., *Int. J. Pept. Res. Ther.* **2005**, *11*, 261; g) Kundu D., Ahammed S., Brindabad C. R., *Green Chem.* **2012**, *14*, 2024; h) Effenberger F., Isak H., *Chem. Ber.* **1989**, *122*, 545; i) Luxen A., Christiaens L., *Tetrahedron Lett.* **1982**, *23*, 3905.

13: Kopylova B. V., Yashkina L. V., Kandror I. I., Freidlina R. Kh., *Izv. Akad. Nauk SSSR, Ser. Khim.* **1972**, 947.

14: a) Doyle M. P., Dellaria J. F., Siegfried B., Bishop S. W., *J. Org. Chem.* **1977**, *42*, 3494; b) Wassmundt F. W., Kiesman W. F., *J. Org. Chem.* **1995**, *60*, 1713.

15: a) Kosynkin D., Bockman T. M., Kochi J. K., *J. Am. Chem. Soc.* **1997**, *119*, 4846; b) Hirose Y., Wahl Jr. G. H., Zollinger H., *Helv. Chim. Acta* **1976**, *59*, 1427; c) Pazo Llorente R., Bravo-Díaz C., Gonzalez-Romero E., *Eur. J. Org. Chem.* **2004**, 3221.

16: a) Zard S. Z., *Radical Reactions in Organic Synthesis*, University Press, Oxford, **2003**, Chapter 6; b) Matyjaszewski K., *Macromolecules* **2012**, *45*, 4015; c) Balczewski P., Szadowiak A., Bialas T., *Heteroatom Chem.* **2006**, *17*, 22; d) Tanner D. D., Reed D. W., Setiloane B. P., *J. Am. Chem. Soc.* **1982**, *104*, 3917; e) Hart D. J., *Science* **1984**, *223*, 883.

17: a) Mugesh G., du Mont W. W., Sies H., *Chem. Rev.* **2001**, *101*, 2125; b) Nogueira C. W., Zeni G., Rocha J. B. T., *Chem. Rev.* **2004**, *104*, 6255.

18: Selected examples of *S*-aryl cystinates: a) Drysdale M. J., Reinhard J. F., *Bioorg. Med. Chem. Lett.* **1998**, *8*, 133; b) Brown J. D., Khatri H. N., Harrington P. J., Johnston D. A., Topping R. J., Dauer R. R., Rowe G. K., *US Patent* 2000, 6765109; c) Dua R. K., Taylor E. W., Phillips R. S., *J. Am. Chem. Soc.* **1993**, *115*, 1264; d) Kaldor S. W., Kalish V. J., Davies II J. F., Shetty B. V., Fritz J. E., Appelt K., Burgess J. A., Campanale K. M., Chirgadze N. Y., Clawson D. K., Dressman B. A., Hatch S. D., Khalil D. A., Kosa M. B., Lubbehusen P. P., Muesing M. A., Patick A. K., Reich S. H., Su K. S., Tatlock J. H., *J. Med. Chem.* **1997**, *40*, 3979; e) Herradura P. S., Pendola K. A., Guy R. K., *Org. Lett.* **2000**, *2*, 2019.

19: a) Glass R. S., *Top. Curr. Chem.* **1999**, *205*, 1; b) Fontecave M., Ollagnier-de-Choudens S., Mulliez E., *Chem. Rev.* **2003**, *103*, 2149.

20: Kingsbury C. A., *J. Org. Chem.* **1964**, *29*, 3262.

21: a) However, this NMR experiment does not exclude the operation of rapid short-chain mechanisms. For further details, see experimental part; b) Miyake Y., Nakajima K., Nishibayashi Y., *J. Am. Chem. Soc.* **2012**, *134*, 3338; Zhu S., Das A., Bui

L., Zhou H., Curran D. P., Rueping M., *J. Am. Chem. Soc.* **2013**, *135*, 1823; c) Zhao J., Wu W., Sun J., Guo S., *Chem. Soc. Rev.* **2013**, *42*, 5323.
22: a) Szele I., Zollinger H., *Helv. Chim. Acta* **1978**, *61*, 1721; b) Canning P. S. J., McCrudden K., Maskill H., Sexton B., *J. Chem. Soc., Perkin Trans. 2* **1999**, 2735.
23: Májek M., Filace F., Jacobi von Wangelin A., *Beilstein J. Org. Chem.* **2014**, *10*, 981.
24: Wang X., Cuny D. G., Noël T., *Angew. Chem. Int. Ed.* **2013**, *52*, 7860.
25: Luo F., Pan C., Li F., Chen F., Cheng J., *Chem. Commun.* **2011**, *47*, 5304.
26: Hanson P., Hendrickx R. A. A. J., Smith J. R. L., *Org. Biomol. Chem.* **2008**, *6*, 745.
27: Altman R. A., Anderson K. W., Buchwald S. L., *J. Org. Chem.* **2008**, *73*, 5167.
28: Sevez G., Pozzo J.-L., *Dyes Pigmemnts* **2011**, *89*, 246.
29: Qiao Q., Dominique R., Sidduri A., Lou J., Goodnow R. A., *Synth. Commun.* **2009**, *40*, 3691.
30: Knauber T., Arikan F., Röschensthaler G.-V., Gossen L. J., *Chem. Eur. J.* **2011**, *17*, 2689.
31: Samant S. B.., Sukhthankar G. M., *Bioorg. Med. Chem. Lett.* **2011**, *21*, 1051.
32: Perumal S., Chandrasekarn R., Selvraj S., Ganesan M., Wilson D. A., *Mag. Reson. Chem.* **2000**, *38*, 55.
33: Clark P. D., Mesher S. T. E., Primak A., Yao H., *Catal. Lett.* **1997**, *48*, 79.
34: Reddy V. P., Kumar A. V., Swapna K., Rao K. R., *Org. Lett.* **2009**, *11*, 951.
35: Holzwarth M. S., Frey W., Plietker B., *Chem. Commun.* **2011**, *47*, 11113.
36: Fors B. P., Hawker C. J., *Angew. Chem. Int. Ed.* **2012**, *51*, 8850.
37: Cismesia M. A., Yoon T. P., *Chem. Sci.* **2015**, DOI:10.1039/C5SC02185E

Chapter 3:

On the Mechanism of Photocatalytic Reactions with Eosin Y

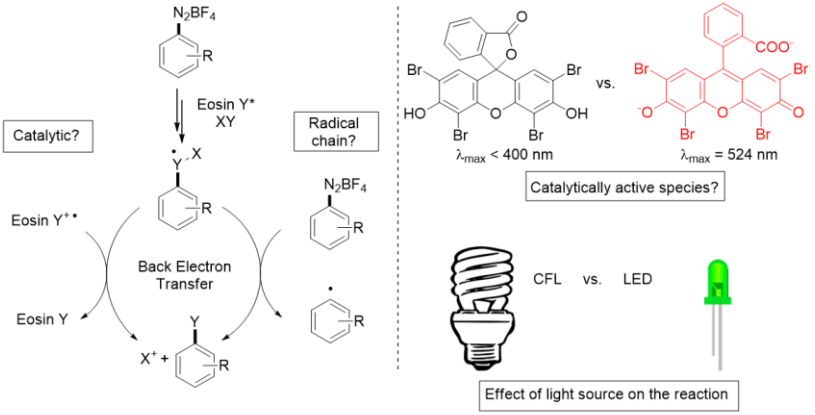

This chapter has been published:
Májek M. Filace F., Jacobi von Wangelin A., *Beilstein J. Org. Chem.* **2014**, *10*, 981; Figure 3 was not present in the publication, additional informations have been added.

Author contributions:
FF did quantum yield determination for photocatalytic arylation and for photocatalytic methylthiolation. MM did rest of the synthetic and analytical work, and wrote the manuscript

3.1: Introduction

The ability of natural systems to harness solar energy for the genesis of matter has been fascinating mankind since time immemorial and has stimulated numerous reproduction attempts in the context of chemical synthesis over the last two centuries. The vast majority of photochemical reactions known until the 1980s exploited stoichiometric amounts of a photoactive molecular entity to drive a chemical transformation.[1] Only recently, a steadily growing number of homogeneous transition metal complexes which are redox-active and show absorption in the visible range of the solar spectrum have been demonstrated to catalyze light-driven organic reactions. The use of the pyridyl-based complexes $[Ru(bpy)_3]^{2+}$, $[Ir(ppy)_3]$ and $[Ir(ppy_2)(dtbbpy)]^+$ for the mediation of redox processes has certainly attracted the most interest, incipiently in photocatalytic reactions of activated organic electrophiles.[2-8]

Despite the numerous examples of efficient catalytic photo-redox transformations with organometallic dyes known to date, their high price, toxicity profile, and problematic recyclability might limit their more general use especially on larger scales. However, the recent pursuit of environmentally more benign photoactive catalysts has focused on much cheaper metal-free dyes. Several commercially available fluorescein and xanthene dyes have been successfully applied to photo-redox reactions, including radical substitutions at α-amino, β-carbonyl, and aryl moieties.[9,10] Among them, eosin Y, the 2',4',5',7'-tetrabromo derivative of fluorescein, has been most widely employed. The redox potential of the EY^+/EY^* pair of 1.1 V (vs. SCE) is experimentally not available as both of the compounds are short-lived intermediates. However, the redox potential can be obtained indirectly via analysis of the thermodynamic cycle involving the energy of the triplet state eosin Y* (T_1) (derived from fluorescence measurements) and the energy of the radical cation eosin $Y^{+\bullet}$ (derived from cyclovoltammetric experiments, for more details see experimental and computational part). Much effort has been directed at the oxidative quenching of eosin Y* (T_1) with suitable electrophiles in order to generate aryl radicals by a light-driven single electron transfer (SET) process (*i.e.* one-electron reduction of Ar-X, see Scheme 1). Due to their easy reducibility, arenediazonium salts are especially attractive precursors which constitute versatile alternatives to haloarene-based strategies. They are readily available by diazotation of anilines, no toxic metals are required, the bond cleavage generates gaseous N_2 which escapes the reaction mixture. Photo-redox reactions with arenediazonium salts are often more selective than traditional methods such as copper(II)-mediated Meerwein arylations[11] or protocols employing stoichiometric iron(II) or titanium(III) reductants in aqueous media.[12-14] This renaissance of arenediazonium chemistry has recently led to various applications of eosin Y to visible

light-driven syntheses of biaryls,[15] stilbenes,[16] benzothiophenes,[17] α-phenylketones,[18] phenanthrenes,[19] arylsulfides,[20] and arylboron pinacolates[21] (Scheme 1).

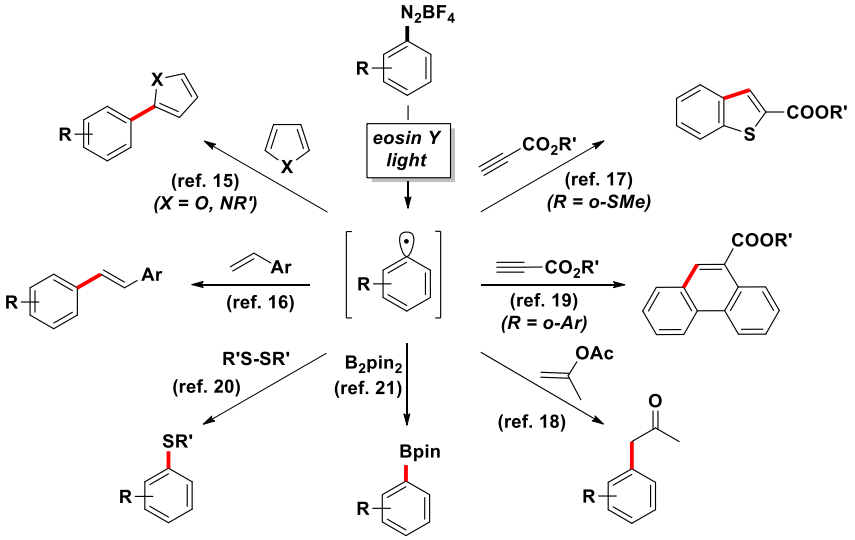

Scheme 1. Oxidative quenching of eosin Y with aryldiazonium salts and reactions of the resultant aryl radicals.

Numerous mechanistic studies have been performed at reactions with organometallic photocatalysts,[3-8] whereas much less attention has been directed at eosin Y-catalyzed reactions. The reductive quenching pathway of eosin Y, which operates in the photooxidation of isoquinolines,[9] has been studied in a single report.[22] To the best of our knowledge, related data have not been collected for the much more widely used oxidative quenching. Most literature protocols were interpreted in analogy to the related $[Ru(bpy)_3Cl_2]$-catalyzed reactions and similar mechanisms were proposed (Scheme 2).[15-21] These generally commence with the SET between excited eosin Y and the arenediazonium salt (**I**) to give aryl radical **II**. Nucleophilic attack onto reactive **II** generates the more stable complex **III** which is prone to back-electron transfer upon oxidative formation of the cationic species **IV**. Terminal elimination of X^+ (mostly a proton) gives the substitution product **V**. Two general pathways of back-electron transfer can be followed: Path A involves one-electron reduction of the radical cation state of the catalyst. Radical chain propagation (B) can occur when the SET occurs with another molecule of the starting material **I**. Some attempts have been made to differentiate between radical chain and photocatalysis mechanisms by monitoring the reaction progress after the light sources have been switched off.[20] Clearly, such

experiments neglect the existence of short radical chains and thus provide no conclusive evidence of the mechanism.

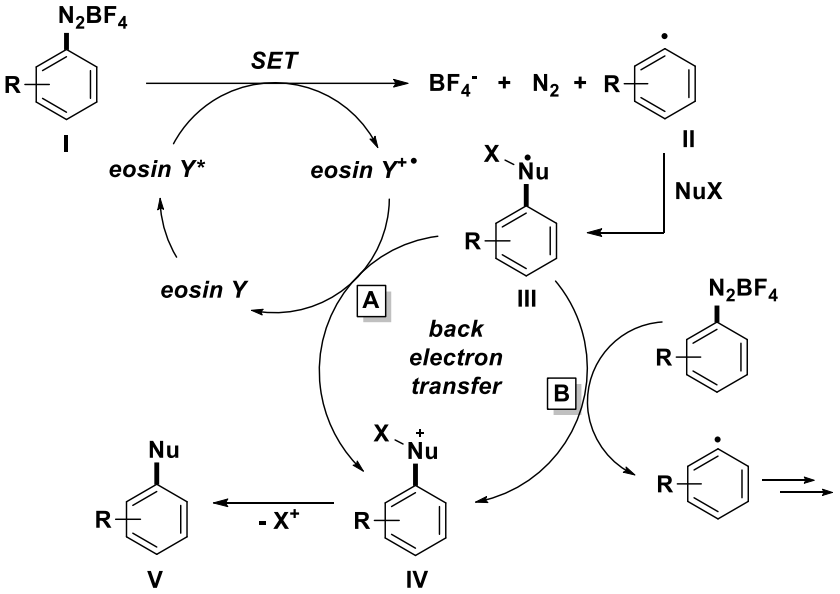

Scheme 2. Proposed general reaction mechanism of eosin Y-catalyzed substitutions with aryldiazonium salts.

In general, the thermodynamic feasibility of a redox process is determined by the difference of redox potentials of the two half reactions. The redox potential of most arenediazonium salts (redox pair **I/II**, Scheme 2) is close to 0 V vs. SCE.[23,24] The redox potentials of the short lived adducts **III/IV** are unknown and experimentally not (easily) available. However, it is likely that their potential is greater than 0 V in many cases which makes the radical species **III** a sufficiently strong reductant for arenediazonium salts of type **I**. After all, the unambiguous determination of the underlying reaction mechanisms is not possible without further spectroscopic, kinetic, and theoretical experiments. The studied systems are mostly too complex for transient absorption spectroscopy. We have so far failed to obtain any insight from photo-CIDNP NMR experiments. Therefore, we have decided to evaluate the efficiency of the radiation events of several recent literature protocols by recording the quantum yields Φ.[15-17,19-21] Furthermore, we have learned along the way that the reactions appear to be strongly dependent on the pH of the solution and the type of lamp used for irradiation. Here, we present a detailed study on the direct consequences of these

three major factors for the outcome and mechanism of several recently reported eosin Y-catalyzed aromatic substitution protocols starting from arenediazonium salts.[15-21]

3.2: Results and discussion

Effect of pH on the efficiency of Eosin Y-mediated photocatalysis

For better comparison, we have employed identical reagent concentrations and reaction conditions (solvents) as reported in the original papers.[15-21] Dry DMSO was mostly used as solvent, with the exception of the phenanthrene[19] and arylboron pinacolate[21] syntheses which were run in acetonitrile. Much to our surprise, the solutions of eosin Y and arenediazonium salts in acetonitrile were yellow (instead of the usual red color; see Figure 1, conditions as in the borylation paper[21]) and did not exhibit intense fluorescence (Figure 2, conditions as in the borylation paper[21]). We have suspected this to be a consequence of facile acid-base reactions of the catalyst eosin Y. Indeed, immediate color change was effected by addition of base (tetra-*n*-butylammonium hydroxide, TBAOH), and strong fluorescence occurred in the green spectrum. This dramatic pH effect on the spectroscopic properties of eosin Y solutions prompted us to further investigate this behavior.

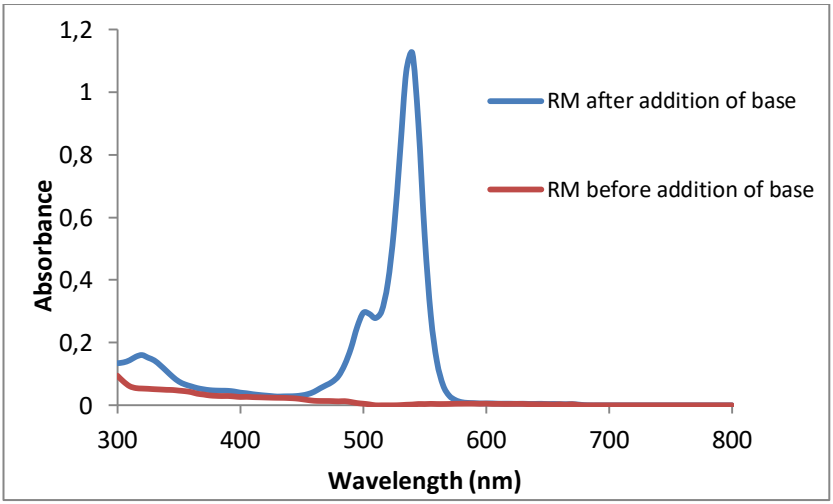

Figure 1. UV-VIS spectra of the photoborylation reaction mixture (RM).

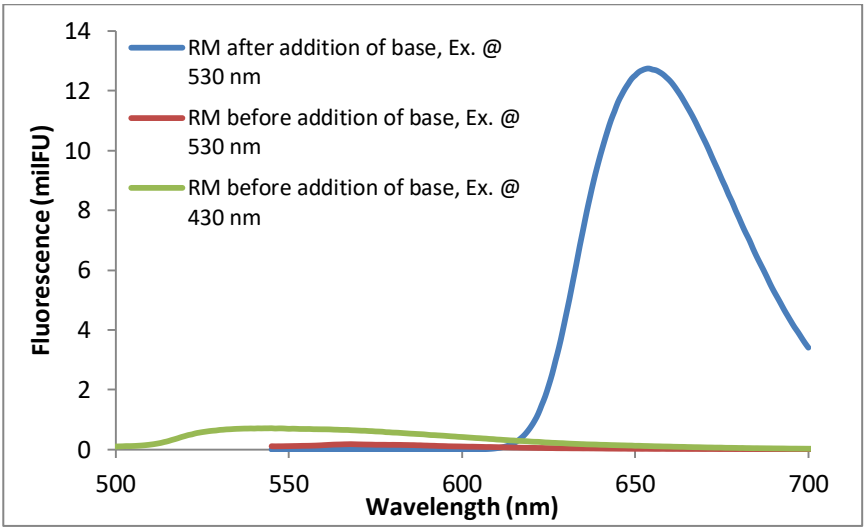

Figure 2. Fluorescence spectra of the photoborylation reaction mixture (RM).

The organic dye eosin Y can exist in four different structures in solution: the spirocyclic form EY1, the neutral EY2, the monoanionic EY3, and the dianionic form EY4 (Scheme 3). Eosin Y contains two relatively acidic protons (pK_a 2.0, 3.8 in water)[25] which can be easily abstracted to give dianionic EY4. Lack of clarity exists in many publications on photoredox catalysis with regard to the nature of the employed dye. The authors either report the use of "eosin Y, spirit soluble" – which can be EY1 or EY2 according to the Sigma-Aldrich catalogue,[26] or claim the use of the free acid EY2. The presence of stoichiometric amounts of bases, e.g. in eosin Y-catalyzed photo-oxidative transformations with amines,[9] results in the quantitative generation of the dianionic form EY4 under the reaction conditions. On the other hand, the SET-generation of aryl radicals from arenediazonium salts by photocatalysis proceeds in the absence of base. The non-aqueous conditions should not provide a significant buffering capacity. Here, the presence of only minute amount of impurities in the solvents or starting materials is sufficient to push the acid-base equilibria of the catalytic amounts of eosin Y in either direction. The spirocyclic form EY1 contains an interrupted conjugation of the fluorone ring system and thus would be photocatalyticaly inactive under visible light irradiation. The neutral form EY2 exhibits only weak fluorescence when irradiated with visible light (Figure 2). Studies on related alkylated eosin derivatives suggest that this fluorescent state is very short lived and is therefore also not appropriate for photo-redox catalysis.[27] The charged forms EY3 and EY4 are catalytically active, which in turn

also means that solutions containing commercial "eosin Y, spirit soluble" would *per se* not trigger efficient photo-redox catalysis. In such cases, catalytic activity as observed in recent publications by König *et al.* is dependent on the operation of acid-base equilibration (e.g. in DMSO solution) so that the employed eosin Y is converted *in situ* to the active species EY3 or EY4.[15-18]

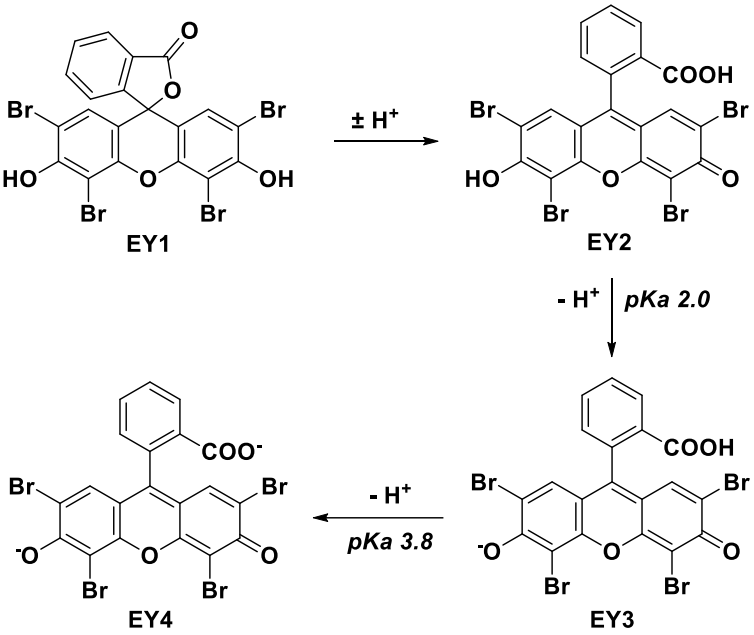

Scheme 3. Acid-base behaviour of eosin Y.

Efforts to reproduce the photo-redox synthesis of arylboron pinacolates in acetonitrile have so far failed in our hands when irradiating at 525 nm.[21] No product formation was observed, and UV-VIS spectra showed no appreciable absorption at this wavelength. However, the addition of minor quantities of base (TBAOH) to the reaction mixture resulted in strong absorption at 525 nm and good photocatalytic activity under irradiation. The substitution of acetonitrile with DMSO in the same reaction gave strong absorption at 525 nm and allowed photocatalytic synthesis of the desired arylboronic ester in good yields in the absence of extra base. This discrepancy is most likely associated with the different properties of DMSO and acetonitrile as bases. DMSO is a stronger base than acetonitrile which enhances the acidity of most Brønsted acids in DMSO.[28] These observations lead to the conclusion that photo-redox reactions

catalyzed by eosin Y (or similar organic dyes) cannot be discussed without strict specification of the employed form of the dye and the reaction conditions. Conclusive mechanistic proposals of visible light driven reactions with these dyes also need to address the operation of acid-base equilibria and the pH dependence of absorption properties.

Effect of the light source on the eosin Y-mediated photocatalysis

Another reaction parameter which lacks clarity and consistency among the literature reports is the source of irradiation. Several groups including ourselves have used commercial narrow-band LEDs with a maximum intensity at 525 nm (green light).[15-18,20] Other reactions were irradiated with white light from broad-band compact fluorescent lamps (CFL).[19,21] The determination of quantum yields requires the use of narrow-band light sources due to the variation of the optical density of the samples with the wavelength. Therefore, we have studied the impact of different irradiation types on the course of the photocatalytic reaction. Although the type of CFLs was not specified in the literature,[19,21] the majority of commercial CFLs cover similar spectral ranges with the individual UV edge being significantly below 400 nm and with substantial radiation power in the region of 400-500 nm (Figure 3).

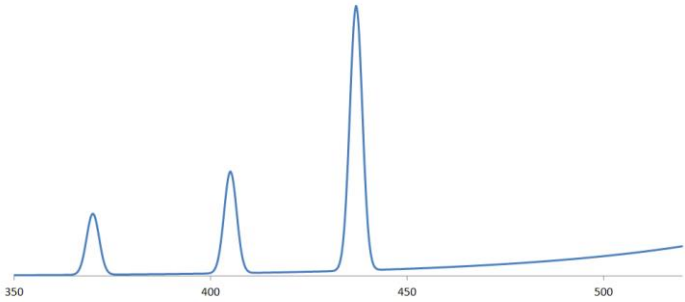

Figure 3. Sylvania CFL (deluxe warm white) spectral power distribution. According to technical information bulletin of Osram Sylvania.

A similar wavelength distribution is seen in the spectrum of commercial white-colored LEDs (see Supporting Information for spectrum). The activation energy of thermal heterolysis of arenediazonium ions is appr. 115 kJ/mol (1.19 eV).[29] The energy of a photon at the edge of the visible spectrum (400 nm) is 3.1 eV so that such photons carry sufficient energy to heterolyze diazonium ions to give highly electrophilic aryl

cations. Moreover, arenediazonium salts are known to form weak charge transfer complexes with solvent molecules whose absorption tails into the visible range.[30]

These observations support the notion that the use of broad-band visible irradiation indeed can indeed have a profound effect on the outcome of a photocatalytic reaction. We have therefore examined if direct absorption of the arene diazonium ions can trigger a productive pathway under irradiation with broad-band light sources even in the absence of the photocatalyst. As representative examples we chose the recently reported syntheses of arylboronic esters[21] and phenanthrenes.[19] The absorption spectrum of a mixture of *p*-bromobenzenediazonium tetrafluoroborate (*p*-$BrC_6H_4N_2BF_4$) and bispinacolato diboron (B_2pin_2) in acetonitrile shows a significant shoulder of a UV absorption band tailing into the visible part of the spectrum (Figure 4).[30] At the UV/VIS edge (400 nm), the absorbance of the system is still more than 0.1 which translates into 21% of all light being absorbed at this wavelength. When we performed the borylation reaction according to the literature report[21] but without the addition of the photocatalyst eosin Y, 54% yield of the borylation product were obtained by direct photolysis (Scheme 4). These observations are in full accord with a report of direct reaction of thermally generated aryl cations (from arenediazonium salts) with bispinacolato diboron to give the corresponding arylboronic esters.[31] It is thus very likely that direct light-triggered heterolysis of the starting material accounts for substantial amounts of product formation under conditions which were believed to proceed through photocatalytic SET.

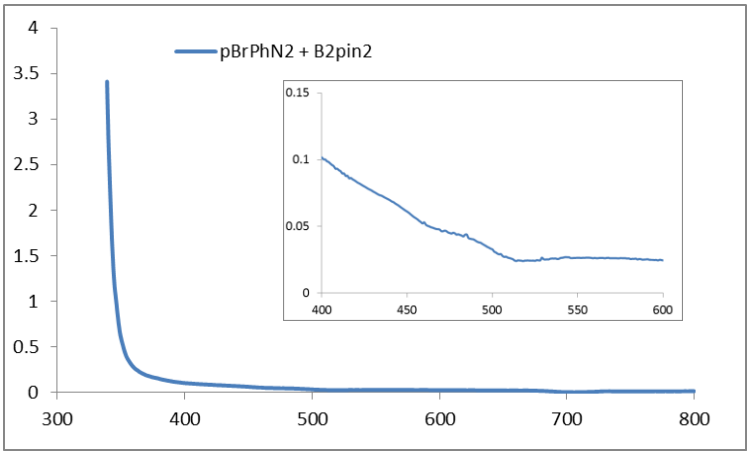

Figure 4. UV-VIS spectrum of *p*-bromobenzenediazonium tetrafluoroborate ($pBrPhN_2$) and bispinacolato diboron (B_2pin_2) in acetonitrile.

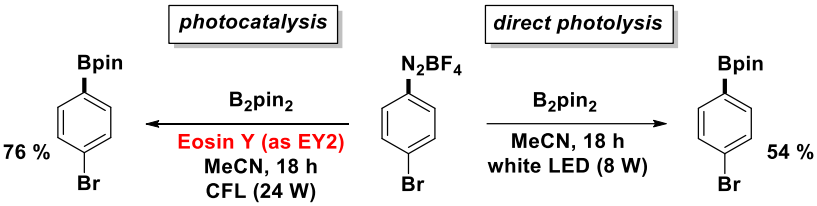

Scheme 4. Eosin Y-catalyzed and dye-free photolytic borylation.

A similar behavior was found in our study of the phenanthrene synthesis.[19] A solution of *o*-biphenyldiazonium tetrafluoroborate in acetonitrile showed strong absorption between 400-500 nm with all light at the UV/VIS edge at 400 nm being completely absorbed (Figure 5). This again indicates that direct photocleavage of the C-N bond might be operating. The cyclization reaction with ethyl propiolate according to the literature protocol[19] but in the absence of eosin Y did not afford any phenanthrene product (Scheme 5). Instead, Ritter-type reaction proceeded to give the corresponding acetanilide after aqueous work-up which is consistent with the original report by Deronzier from 1984.[32] The significant overlap of the absorption spectra of the arenediazonium salt recorded before and after the addition of eosin Y (Figure 5) suggests that direct photolysis of the C-N bond could account for the erosion of product yield in the catalytic process due to competitive heterolysis of the substrate and subsequent ionic Ritter reaction. This notion was supported by our experiments performed in DMSO where a higher portion of the photocatalyst resides in the active EY3 and EY4 states. Following an otherwise identical protocol, irradiation at 525 nm resulted in the formation of the phenanthrene in 71% yield (*cf.* literature yield of 53%).[19]

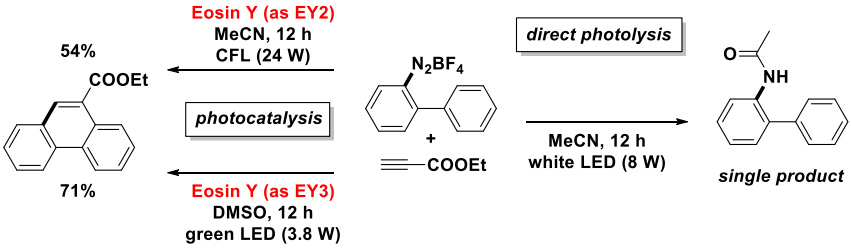

Scheme 5. Eosin Y-catalyzed and dye-free reactions with ethyl propiolate.

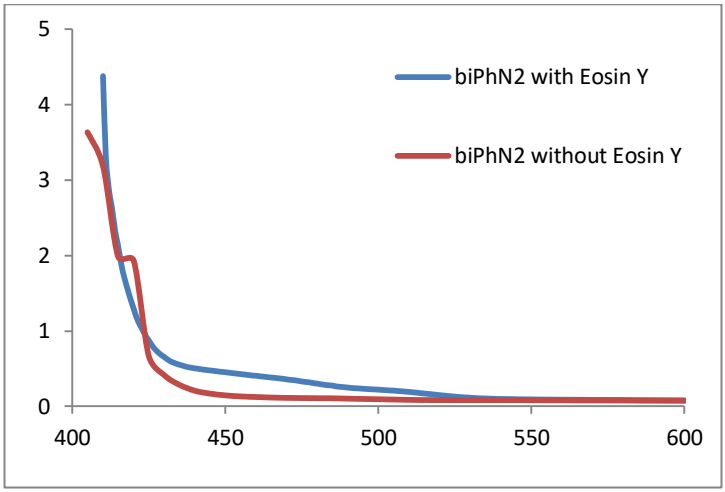

Figure 5. UV-VIS spectra of *o*-biphenyldiazonium tetrafluoroborate ($biPhN_2$) in acetonitrile

Quantum yields of eosin Y-catalyzed reactions

The determination of quantum yields of light-driven reactions provides valuable insight into the efficiency of the radiative processes and thus can be used for the mechanistic understanding of such processes. The magnitude of quantum yields ϕ also describes how much energy is wasted into thermal dissipation in such systems, which is an especially critical parameter for the evaluation of sustainability of a photocatalytic process. The quantum yield is defined as the efficiency of a photochemical reaction in the studied system:

ϕ = (rate of substrate conversion) / (absorbed photon flux)

Theoretically, if a simple photocatalytic process is considered, the quantum yield would be in the range $0 < \phi \leq 1$. It approaches unity as the efficiency of the photocatalytic step increases. In reality, quantum yields can exceed unity in cases where the products of the photocatalytic reaction induce (radical) chain reactions. Therefore, the determination of quantum yields ϕ provides a meaningful answer to mechanistic ambiguities. For the eosin Y-catalyzed reactions with arenediazonium salts, conclusive answers to the distinction between photocatalytic and radical chain mechanisms can be derived directly from ϕ.

A quantification of the photon flux is rather problematic. Recently, devices became available which use solar cells for the direct measurement of photon fluxes.[33] However, chemical actinometry constitutes a prevalent indirect method of photon flux measurement.[34] Several effective chemical actinometers are known for UV spectral studies whereas similar experiments in the visible range are much more limited by the availability of chemical actinometers. Even more challenging are photon flux determinations above 500 nm which marks the spectral cut-off of the commonly used Hatchard-Parker ferrioxalate. None of the chemical actinometers that operate in this region are commercially available. We therefore decided to prepare potassium Reineckate, a robust actinometer for the >500 nm region, according to a literature method.[34,35]

Quantum yields ϕ were measured for all aforementioned visible light driven reactions in the same solvent, DMSO. Irradiation was performed with a green LED (3.8 W) at 525 nm. All other reaction conditions were adopted from the individual literature reports.[15-21] For more details on the actinometry experiments and quantum yield determinations, see the experimental part. The observed quantum yields ϕ of the studied reactions varied by almost two orders of magnitude, between 4.7 and 0.075. This already indicates the operation of different mechanisms in these aromatic substitution reactions with arenediazonium salts. The redox potentials of most substituted arenediazonium salts cluster with very little deviation around 0.0 V vs. SCE (± 0.2 V)[23,24] so that the observed differences in ϕ can be largely attributed to different mechanistic pathways. Our experiments (Scheme 6) afforded quantum yields of $\phi > 1$ for the hetero-biaryl coupling[15] and the Heck-type olefination with styrene,[16] respectively. This indicates that in addition to a photocatalytic path (Scheme 2, A) radical chain propagation is operating under the reaction conditions (Scheme 2, B). This contrasts with the other reactions where the quantum yields range between 0.6 and 0.075. In the original paper from Deronzier,[32] where similar reactions under catalysis of $Ru(bpy)_3^{2+}$ were studied, ϕ values of 0.46-0.78 were reported. Our actinometric experiments of the eosin Y-catalyzed phenanthrene synthesis[19] and photoborylation[21] gave similar quantum yields of 0.35 and 0.60, respectively. This suggests that the photocatalytic pathway is indeed populated (Scheme 2, A). Finally, the benzothiophene synthesis[17] and photothiolation[19] exhibited relatively low quantum yields which could be a consequence of non-productive processes that are responsible for the significant loss of energy. The presence of electron-rich alkylthiolate moieties in both systems could in principle effect reversible redox processes with the catalyst eosin Y which might account for the erosion of ϕ.

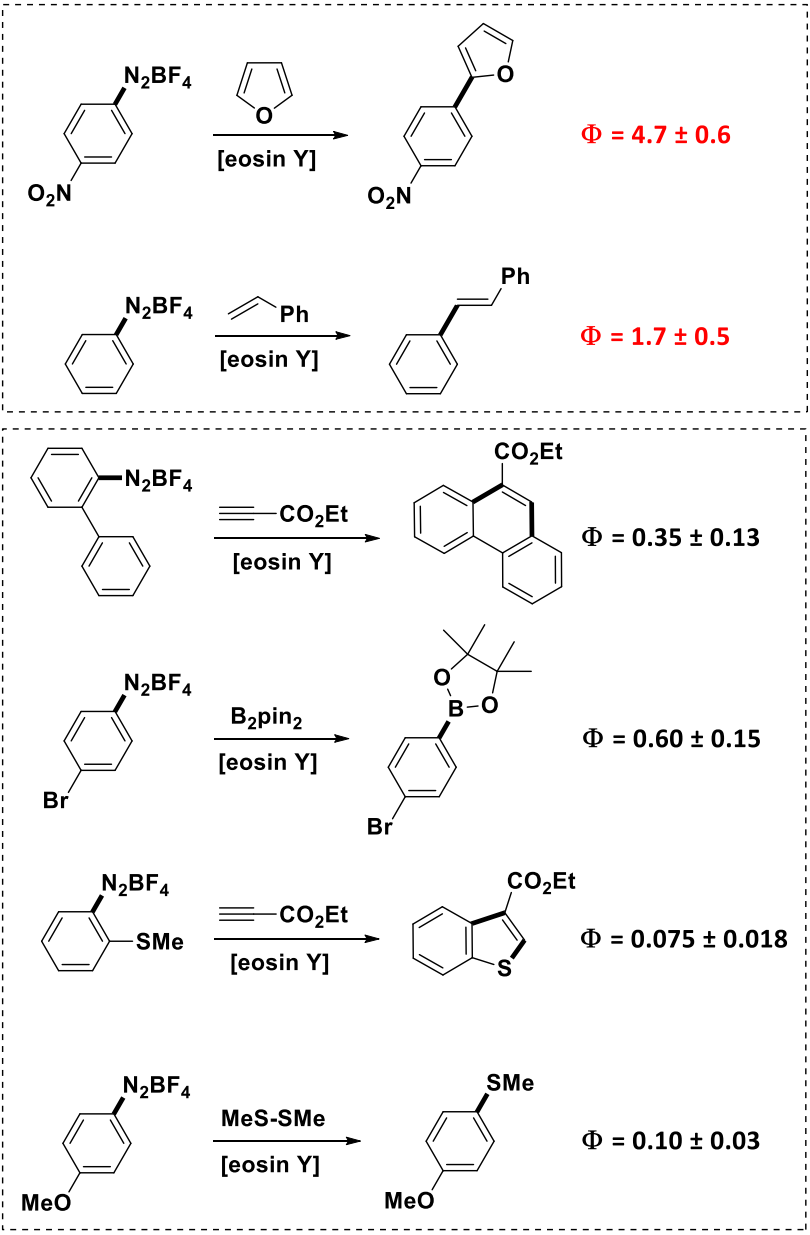

Scheme 6: Quantum yield determinations of selected visible light-driven aromatic substitutions.

It is important to point out, that the photon flux used to calculate the aforementioned quantum yields were determined by chemical actinometry, using light induced potassium Reineckate ligand exchange – a monomolecular process, while the probed reactions are all bimolecular reactions. A question might arise if such approach is valid, and if one can use results from these quantum yield measurements to characterize these reactions on global level, not only in the given reaction conditions. If the determined quantum yields are higher than one in the given reaction conditions, there is certainty, that one photon produced more than one molecule of product, and that radical chain process must be present to allow this. In the case, when the quantum yield is lower than one, situation is more difficult: If the vast majority of the photocatalyst gets deactivated by other mechanisms than quenching with reactant (in this case diazonium salt), quantum yield may be lower than one even though an efficient radical chain process is present in the system.[36] In such instance, it is important to take into account the ratio of quenching *Q* caused by substrate to the other deactivation processes, which are in the given conditions characterized by the fluorescence lifetime $\tau_{1/2}$ of the excited dye in the absence of quencher (Stern-Volmer relation):

$$Q = \frac{k_{DA}[A]}{\tau_{1/2}^{-1} + k_{DA}[A]}$$

where k_{DA} represents the Stern-Volmer quenching rate constant, and [A] is the concentration of the quencher.[37] It is known, that most diazonium salts are very efficient quenchers of eosin Y, having k_{DA} rate constants at the diffusion limit.[38] In such case, the diffusion limit rate constants k_{DIF} can be derived from Stokes-Einstein equation:

$$k_{DIF} = \frac{8RT}{3\eta}$$

where the *R* represents the universal gas constant, *T* the thermodynamic temperature, and η stands for the dynamic viscosity of the solvent. This translates to $k_{DIF} \approx 10^{10}$ $Lmol^{-1}s^{-1}$ for acetonitrile and $k_{DIF} \approx 10^{9}$ $Lmol^{-1}s^{-1}$ for DMSO. Concentrations of diazonium salts in the investigated reactions had lower limit at 0.1 M. Fluorescence lifetime of eosin Y in reaction conditions can be estimated at 10 μs.[39] Given all these values, one can calculate the lower limit of the quenching efficiency to be $Q > 99\%$ in the systems, which we had investigated in this work. Errors made by quantum yield determination are in one order of magnitude higher than the error coming from the photocatalyst deactivation, obtained numbers therefore give a valid picture of operative mechanism, and they can be used to asset the viability of radical chain processes.

3.3: Conclusion

In summary, we have investigated the impact of several reaction parameters on the outcome and mechanism of photocatalytic aromatic substitution reactions of arenediazonium salts in the presence of eosin Y. However, the significance of these data certainly extends to other light-driven reactions that lie beyond the focus of this study. Eosin Y (and many other organic photocatalysts) undergo rapid acid/base equilibria which significantly alter the photophysical properties. It is therefore of pivotal importance to ascertain the actual nature of the employed dye under the reaction conditions. Experimental details should always be given to specify the employed dye, the presence of acids and bases as well as the purity of the reagents, solvents, and additives. The use of broad-spectrum lamps in photocatalytic reactions with arenediazonium salts is strongly discouraged as they promote heterolytic C-N bond cleavage towards highly reactive aryl cation species. The standard reaction conditions of many literature reports involve concentrations which are orders of magnitude higher than those suitable for absorption spectroscopy studies. This means that even very inefficient transitions (at tailings of absorption maxima) can indeed trigger productive processes and therefore need to be addressed in mechanistic rationalizations. Quantum yield determinations with potassium Reineckate have now allowed the distinction between photocatalytic and radical chain mechanisms. However, the operation of the prevalent pathway is likely dictated by the stability of the relevant catalytic intermediates. Recently a similar study was attempted on the [2+2] photocatalyzed reactions that were explored previously by Yoon et al.[40] Results from this study strongly hints, that radical chain pathways may be prevalent in a large array of previously reported photoredox reactions, and therefore more attention should be given to this factor, when proposing reaction mechanisms.[36] Research community has started to be more interested in this topic, with very recent paper in appearing in Science, summarizing the determination of quantum yields in photocatalysis, that were done so far.[41]

3.4: Experimental and computational part

General methods

Commercial chemicals were used as obtained from Sigma-Aldrich or Fisher. Solvents were used without further purification. For most reactions, DMSO dried over molecular sieves (certified <0.005% water content, Sigma-Aldrich) was used. TLC was performed on commercial silica gel coated aluminum plates (DC60 F254, Merck). Visualization was done with UV light. Product yields were determined by quantitative GC-FID. Authentic product samples were synthesized according to the cited literature

reports.[15-21] Purity and structure were confirmed based on ^{1}H NMR, ^{13}C NMR and GC-MS. NMR spectral data were collected on a Bruker Avance 400 (400 MHz for ^{1}H; 100 MHz for ^{13}C) spectrometer at 25 °C. Chemical shifts are reported in δ/ppm, and coupling constants *J* are given in Hertz. Solvent residual peaks were used as internal reference for all NMR measurements. Abbreviations: s – singlet, d – doublet, t – triplet, q – quartet, m – multiplet, dd – doublet of doublet.

Synthesis of the chemical actinometer

Potassium Reineckate: Attempts to reproduce the one-step synthesis by Szychlinski *et al.*[42] were not successful (operation was discontinued after formation of copious almond-smelling gases was observed during synthesis). Therefore, the synthesis was performed via a two-step procedure:

A: Synthesis of ammonium Reineckate by a modified protocol according to Dakin:[43] Ammonium thiocyanate (100 g, 1.3 mol) was heated in a beaker in an oil bath (oil bath temperature 150 °C), until a homogenous molten mass was formed. Then, a finely powdered mixture of ammonium dichromate (20 g, 68 mmol), and ammonium thiocyanate (20 g, 0.26 mol) was added in small portions during which the mixture was rapidly stirred with a glass rod. Vigorous evolution of gas was observed when approx. 1/10 of the dichromate-thiocyanate mixture has been added. After the completion of addition (approx. 20 min), the reaction was agitated with a glass rod for another 30 min, after which the heating was stopped. The mixture was further vigorously stirred and solidified on cooling. (Stirring prevents the formation of an indivisible solid!) The cooled solids were finely powdered in a mortar and added to an ice-water mixture (80 mL). The resultant mixture was stirred for 10 min, and then the insoluble portion was filtered off. The collected precipitates were dissolved in hot water (60 °C, 200 mL), and the resultant mixture quickly filtered to remove any residual precipitate. The filtrate was placed in a refrigerator (6°C) for 12 h. The formed crystals were filtered and washed on the filter with copious amounts of cold water until the filtrate was free of SCN^- ions (checked by reaction with Fe(III)). After drying on air, ammonium Reineckate monohydrate (ammonium tetrathiocyanato-diamminechromate(III) monohydrate) was obtained as deep violet crystals (34.7 g, 72 % yield). The dried product obtained by this method can be stored at room temperature under ambient light conditions for several months without decomposition. Attempts to further purify the crystals by crystallization from water-ethanol mixtures were unsuccessful but formed toxic HCN gas.

B: Synthesis of potassium Reineckate:
All operations were carried under red light (11 W, Osram, Slovak Republic) in a dark room with exclusion of other forms of irradiation. An aqueous solution of KNO_3 (50 mL, saturated at ambient temperature) was heated up to 50°C. Then, ammonium Reineckate monohydrate (2.0 g, 5.6 mmol) was added in one portion and the mixture was stirred for 5 min. The resultant solution was cooled to 6°C in a refrigerator upon which crystals formed. The crystals were filtered and washed with a minimal amount of cold water. After drying on air, potassium Reineckate (potassium tetrathiocyanatodiamminechromate(III) monohydrate) was obtained as deep violet crystals (1.7 g, 84 % yield). Potassium Reineckate readily decomposes upon exposure to ambient light, even in solid phase.

Chemical actinometry and quantum yield measurements:
Actinometry measurements were performed using a method according to Wegner and Adamson with potassium Reineckate.[44,45] Quantum yield measurements were performed in the regime of total absorption of the incoming light by the dye. Irradiation was performed with a green high-power LED (Luxeon Rebel, Canada, P = 3.8 W, λ_{max} = 450 nm). Apparatus for the quantum yield measurement consisted of a stationary optical table, onto which light source and the reaction sample were fixed at a defined distance, with the face of cuvette facing the intercepting light beam at right angle. Rapid stirring of sample was required to keep the mixture homogenous as well as to help the removal of the evolved gas. All the samples were thoroughly degassed by passing nitrogen through them for a period of 5 minutes under red light. The photon flux interacting with the sample was determined to be $1.5 \cdot 10^8$ photons per second (corresponding to irradiance of 0.55 µW/m^2 at the point of intercept of radiation with cuvette wall) which did not drift over the time of the measurements as confirmed by repetitive experiments. The individual reaction times were chosen so that conversion was kept below 10% as required by the used protocol.[44,45] The substrate conversions were determined by quantitative GC-FID analysis with *n*-pentadecane as internal standard. All quantum yields were determined as an average of at least three subsequent measurements.

Redox potential of Eosin Y:
Knowledge of the exact redox potential of the pair Eosin Y$^{+\cdot}$ / Eosin Y* (T_1) is central to the discussion of reaction mechanisms involving redox steps. This value is experimentally not available as both of the compounds are short-lived intermediates. However, the redox potential can be obtained indirectly via analysis of the following thermodynamic cycle:

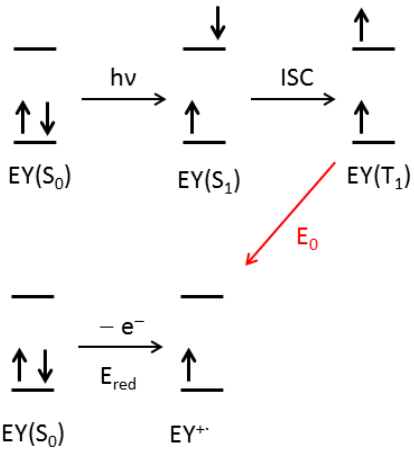

Figure 6. Thermodynamic cycle of eosin Y.

The energy of the triplet state eosin Y* (T_1) is derived from fluorescence measurements:[46] $\Delta E(\text{triplet}) = E(\text{Eosin Y}(T_1)) - E(\text{Eosin Y}(S_0)) = 1.89$ eV.

The energy of the radical cation eosin $Y^{+\cdot}$ is derived from cyclovoltammetric experiments:[47] $\Delta E_{red} = E(\text{Eosin Y}^{+\cdot}) - E(\text{Eosin Y}(S_0)) = 0.78$ eV.

The combination of both values according to the aforementioned thermodynamic cycle allows the calculation of E_0:

$\Delta E_0 = \Delta E(\text{triplet}) - \Delta E_{red}$ so that **$E_0 = 1.11$ eV**, therefore the redox potential of the Eosin $Y^{+\cdot}$ / Eosin Y* (T_1) couple is -1.11 V**.**

Light sources used in the experiments

In the vast majority of experiments, where the irradiation was performed selectively with green light to excite eosin Y dye, 525 nm high power LED was used as the energy source (Luxeon Rebel, Canada, P = 3.8 W, λ_{max} = 525 nm). Experiments, which required protection from photolysis of unstable compounds, were performed using a low powered conventional red filament bulb (11 W, Osram, Slovak Republic). No evolution of gas from the reaction mixtures containing diazonium salts was observed, when working under such light source, even after prolonged exposure times. For experiments with white light, broad spectrum LED was used (Cree XM-L, Hong Kong, P = 9.9 W) (Figure 7, measured by irradiance meter).

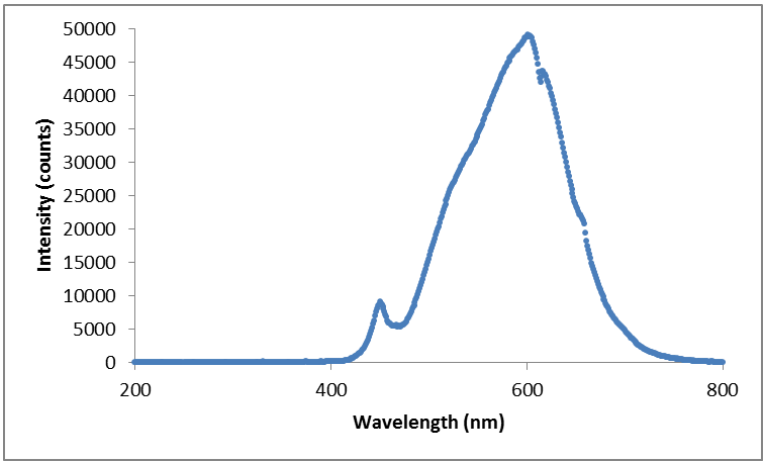

Figure 7. Spectrum of white LED used in experiments with white light.

Spectral data of the synthesized compounds

All products used as calibration standards for GC-FID quantification were synthesized by literature methods.[15-21] Stilbene was used as internal reference (Sigma-Aldrich).

2-(4-Nitrophenyl)furan

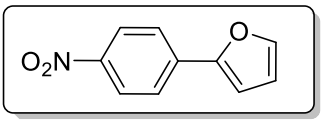

^{1}H NMR (400 MHz, $CDCl_3$, ppm) δ 8.25 (d, *J* = 9.0 Hz, 2H), 7.79 (d, *J* = 9.0 Hz, 2H), 7.58 (dd, *J* = 1.7 Hz, *J* = 0.5 Hz, 1H), 6.88 (dd, *J* = 3.5 Hz, *J* = 0.5 Hz, 1H), 6.56 (dd, *J* = 3.5 Hz, *J* = 1.7 Hz, 1H).^{13}C NMR (100 MHz, $CDCl_3$, ppm) δ 151.8 (C), 146.5 (C), 144.2 (CH), 136.5 (C), 124.4 (CH), 124.0 (CH), 112.5 (CH), 109.0 (CH). GC-MS (EI) *m/z* (relative intensity): 189 (100) [M^+], 159 (68), 131 (36), 115 (68), 89 (23), spectral data were consistent with literature.[15]

2-(4-Bromophenyl)-4,4,5,5-tetramethyl-1,3,2-dioxaborolane:

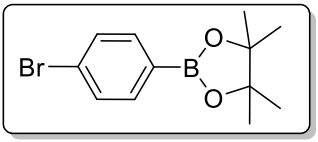

^{1}H NMR (400 MHz, $CDCl_3$, ppm) δ 7.66 (d, *J* = 8.3 Hz, 2H), 7.51 (d, *J* = 8.3 Hz, 2H), 1.34 (s, 12H).^{13}C NMR (100 MHz, $CDCl_3$, ppm) δ 136.4 (CH), 131.0 (C), 131.0 (CH), 126.3 (C), 84.1 (C), 24.9 (CH_3). GC-MS (EI) *m/z* (relative intensity): 284 (56) [M^+], 282 (56), 269 (100), 267 (100), 198 (73), 196 (74), 185 (84), 186 (95), 103 (33), spectral data were consistent with literature.[21]

Ethyl benzo[*b*]thiophene-3-carboxylate:

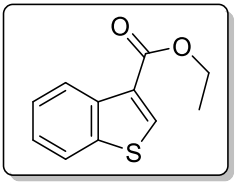

^{1}H NMR (400 MHz, $CDCl_3$, ppm) δ 8.06 (s, 1H), 7.88 – 7.83 (m, 2H), 7.47 – 7.38 (m, 2H), 4.41 (q, *J* = 7.1 Hz, 2H), 1.42 (t, *J* = 7.1 Hz, 3H).^{13}C NMR (100 MHz, $CDCl_3$, ppm) δ 162.9 (CO), 142.2 (C), 138.8 (C), 133.9 (C), 130.4 (CH), 126.9 (CH), 125.5 (CH), 124.9 (CH), 122.8 (CH), 61.6 (CH_2), 14.4 (CH_3). GC-MS (EI) *m/z* (relative intensity): 206 (57) [M^+], 177 (50), 161 (100), 133 (24), 89 (40), spectral data were consistent with literature.[19]

Ethyl phenanthrene-9-carboxylate:

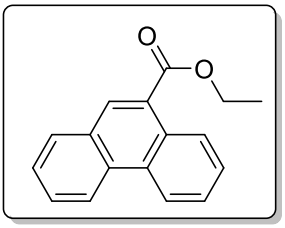

^{1}H NMR (400 MHz, $CDCl_3$, ppm) δ 8.94 – 8.90 (m, 1H), 8.76 –8.72 (m, 1H), 8.70 (d, *J* = 8.3 Hz, 1H), 8.47 (s, 1H), 7.98 (d, *J* = 8.0 Hz, 1H), 7.78 – 7.62 (m, 4H), 4.53 (q,

J = 7.1 Hz, 2H), 1.51 (t, *J* = 7.1 Hz, 3H).^{13}C NMR (100 MHz, $CDCl_3$, ppm) δ 167.7 (CO), 132.1 (C), 132.1 (CH), 130.8 (C), 130.2 (C), 130.0 (CH), 129.1 (C), 128.9 (CH), 127.4 (CH), 127.0 (CH), 126.9 (CH), 126.7 (C), 126.7 (CH) 122.9 (CH), 122.7 (CH), 61.3 (CH_2), 14.5 (CH_3). GC-MS (EI) *m/z* (relative intensity): 250 (100) [M^+], 205 (87), 177 (71), 151 (16), spectral data were consistent with literature.[17]

(4-Methoxy)thioanisole:

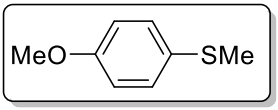

^{1}H NMR (400 MHz, $CDCl_3$, ppm) δ 7.28 (d, *J* = 8.8 Hz, 2H), 6.86 (d, *J* = 8.8 Hz, 2H), 3.79 (s, 3H), 2.45 (s, 3H).^{13}C NMR (100 MHz, $CDCl_3$, ppm) δ 157.2 (C), 129.2 (CH), 127.8 (C), 113.6 (CH), 54.3 (CH_3), 17.1 (CH_3). GC-MS (EI) *m/z* (relative intensity): 154 (81) [M^+], 139 (100), 124 (7), 111 (18), spectral data were consistent with literature.[20]

Phenanthrene synthesis with white LED as the energy source

We have performed the formal [4+2] cyclization reaction as proposed in the original procedure, with broad-spectrum light source, in the absence of photocatalyst. *ortho*-Biphenyldiazonium tetrafluoroborate in acetonitrile was irradiated in the presence of excess of ethyl propiolate in acetonitrile with broad spectrum LED irradiation source (Scheme 7). Only the product of direct photolysis was observed: Aryl cation generated by heterolysis of Ar-N bond has been trapped by acetonitrile in a Ritter-fashion, giving acetamide derivative on workup. No other products could be observed by GC-MS in a significant amount (Figure 8).

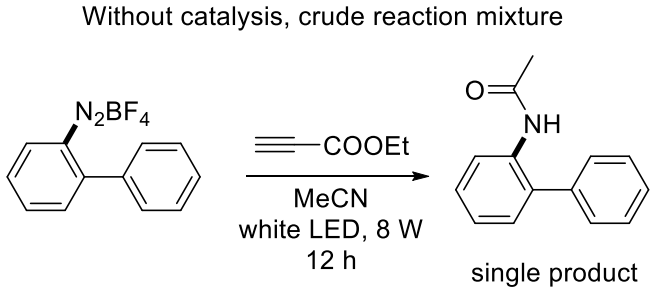

Scheme 7. Direct photolysis of biphenyldiazonium salt.

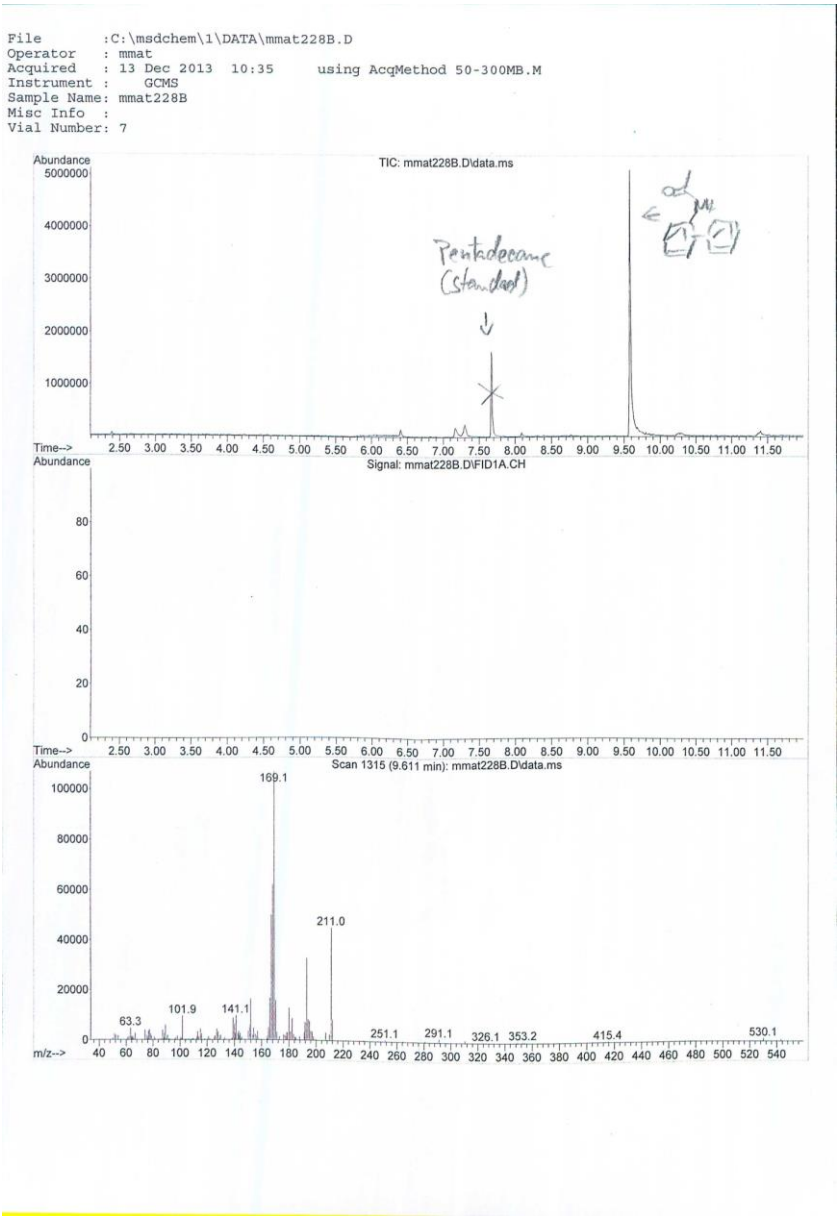

Figure 8. GC-MS chromatogram of direct photolysis mixture.

^{1}H and ^{13}C NMR spectra of selected compounds

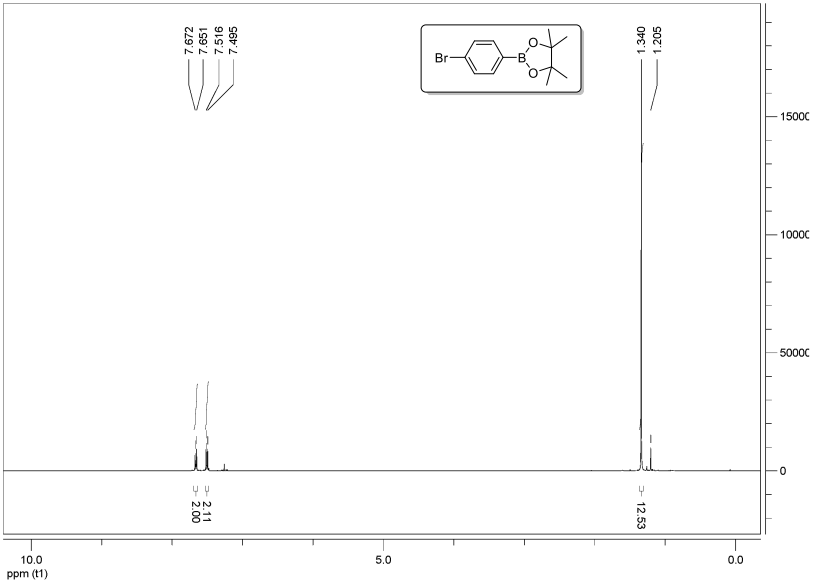

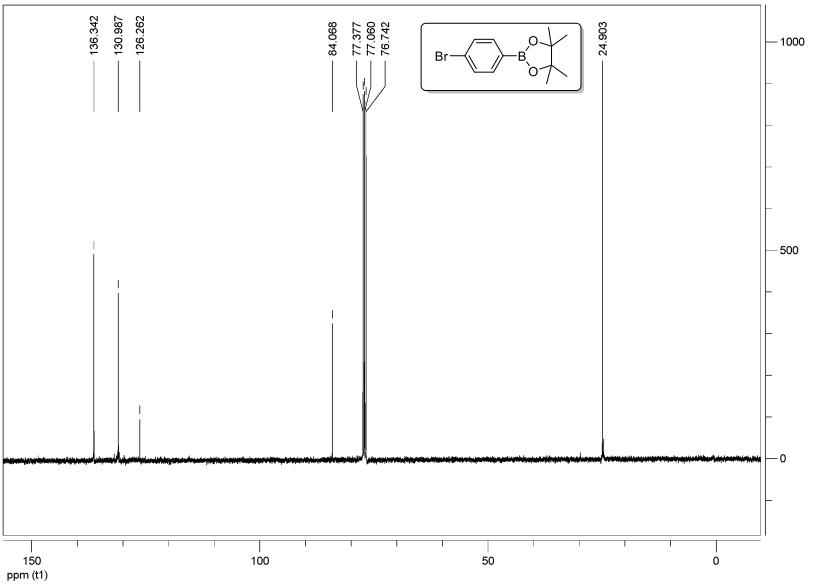

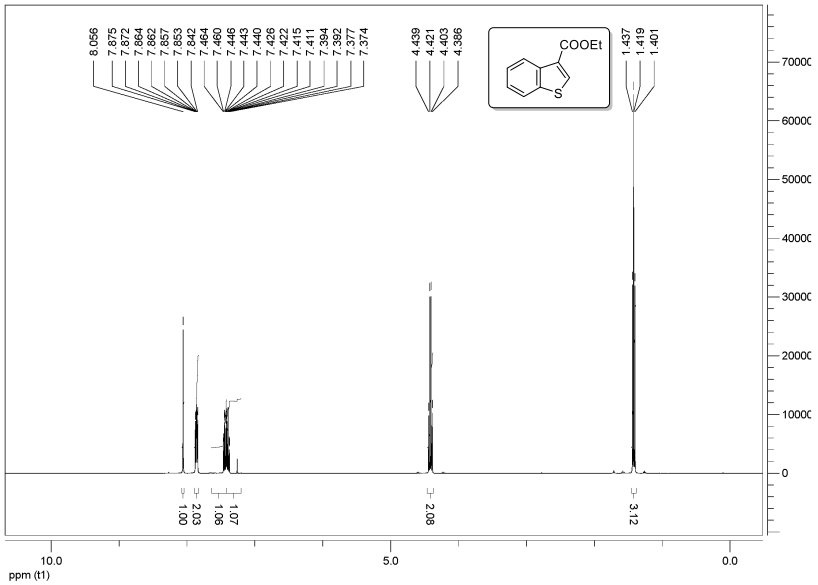
8.056
7.875
7.872
7.864
7.862
7.857
7.853
7.842
7.464
7.460
7.446
7.443
7.440
7.426
7.422
7.415
7.411
7.394
7.392
7.377
7.374
4.439
4.421
4.403
4.386
1.437
1.419
1.401
COOEt
S
1.00
2.03
1.06
1.07
2.08
3.12
10.0
5.0
0.0
ppm (t1)

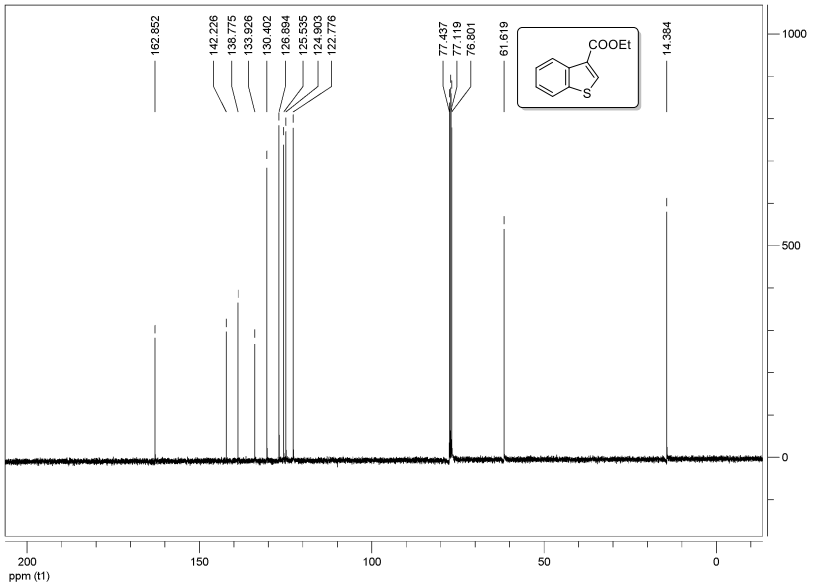
162.852
142.226
138.775
133.926
130.402
126.894
125.535
124.903
122.776
77.437
77.119
76.801
61.619
14.384
COOEt
S
200
150
100
50
0
ppm (t1)

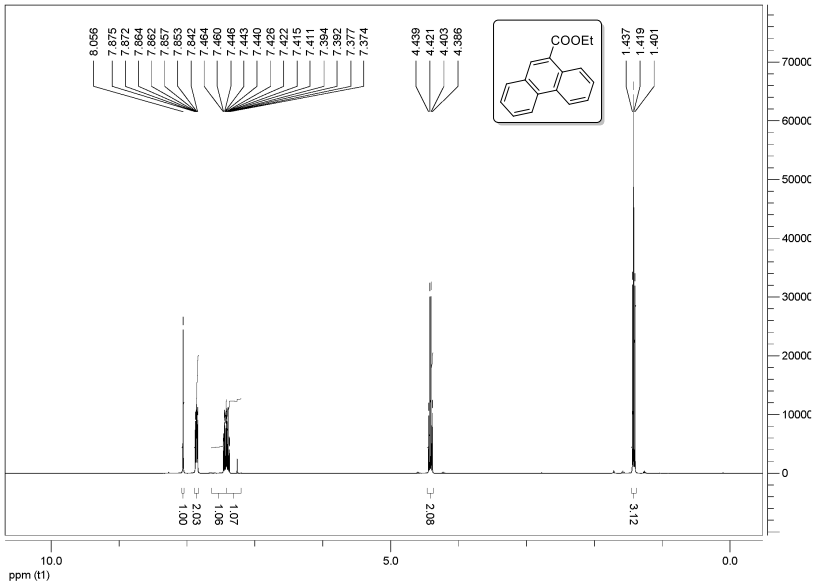
8.056
7.875
7.872
7.864
7.862
7.857
7.853
7.842
7.464
7.460
7.446
7.443
7.440
7.426
7.422
7.415
7.411
7.394
7.392
7.377
7.374
4.439
4.421
4.403
4.386
1.437
1.419
1.401
COOEt
1.00
2.03
1.06
1.07
2.08
3.12
10.0
5.0
0.0
ppm (t1)

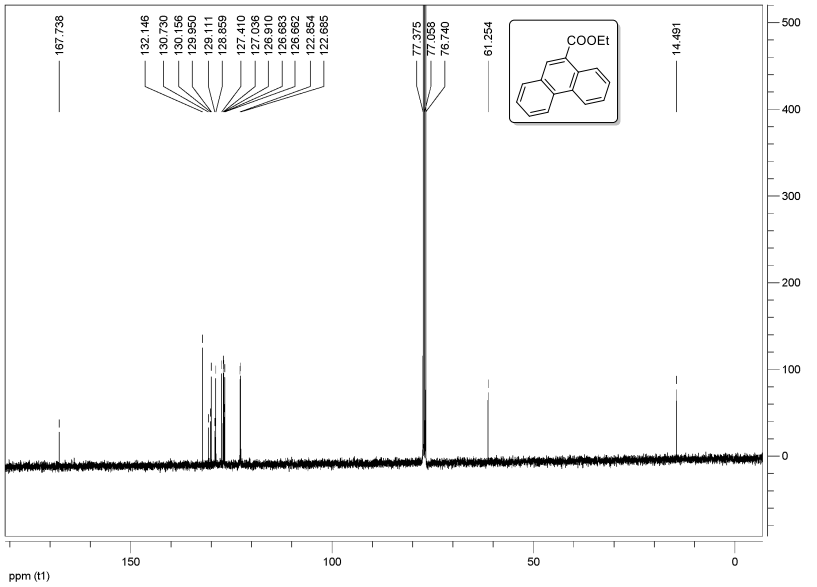
167.738
132.146
130.730
130.156
129.950
129.111
128.859
127.410
127.096
126.910
126.683
126.662
122.854
122.685
77.375
77.058
76.740
61.254
14.491
COOEt
150
100
50
0
ppm (t1)

3.5: References

1: *CRC Handbook of Organic Photochemistry and Photobiology*, 3rd ed., Griesbeck A. G., Oelgemöller M., Ghetti F., eds., CRC Press, Boca Raton, **2012**.
2: Nguyen J. D., D'Amato E. M., Narayanam J. M. R., Stephenson C. R. J., *Nat Chem.* **2012**, *4*, 854.
3: Teplý F., *Collect. Czech. Chem. Commun*. **2011**, *76*, 859.
4: Narayanam J. M. R., Stephenson C. R. J., *Chem. Soc. Rev*. **2011**, 40, 102.
5: Zeitler K., *Angew. Chem. Int. Ed.* **2009**, *48*, 9785.
6: Xuan J., Xiao W.-J., *Angew. Chem. Int. Ed.* **2012**, *51*, 6828.
7: Májek M., Jacobi von Wangelin A., *Angew. Chem. Int. Ed.* **2013**, *52*, 5919.
8: Reckenthäler M., Griesbeck A. G., *Adv. Synth. Catal.* **2013**, *355*, 2727.
9: Hari D. P., König B., *Org. Lett*. **2011**, *13*, 3852.
10: Condie A. G., Gonzalez-Gomez J. C., Stephenson C. R. J., *J. Am. Chem. Soc.* **2010**, *132*, 1464.
11: Rondestvedt C. S., in *Organic Reactions* (Baldwin J. E., Bittman R., Boswell G. A., Heck R. F., Hirschmann R. F., Kende A. S., Leimgruber W., Marshall J. A., McKusick B. C., Meinwald J., Trost B. M., Weinstein, B., eds.) Wiley, New York, **1976**, 225.
12: Wetzel A., Ehrhardt V., Heinrich M. R., *Angew. Chem. Int. Ed.* **2008**, *47*, 9130.
13: Heinrich M. R., Wetzel A., Kirschstein M., *Org. Lett.* **2007**, *9*, 3833.
14: Heinrich M. R., *Chem. Eur. J.* **2009**, *15*, 820.
15: Hari D. P., Schroll P., König B., *J. Am. Chem. Soc.* **2012**, *134*, 2958.
16: Schroll P., Hari D. P., König B., *ChemistryOpen* **2012**, *1*, 130.
17: Hari D. P., Hering T., König B., *Org. Lett.* **2012**, *14*, 5334.
18: Hering T., Hari D. P., König B., *J. Org. Chem.* **2012**, *77*, 10347.
19: Xiao T., Dong X., Tang Y., Zhou L., *Adv. Synth. Catal.* **2012**, *354*, 3195.
20: Májek M., Jacobi von Wangelin A., *Chem. Commun.* **2013**, *49*, 5507.
21: Yu J., Zhang L., Yan G., *Adv. Synth. Catal.* **2012**, *354*, 2625.
22: Liu Q., Li Y.-N., Zhang H.-H., Chen B., Tung C.-H., Wu L.-Z., *Chem. Eur. J.* **2012**, *18*, 620.
23: Allongue P., Delamar M., Desbat B., Fagebaume O., Hitmi R., Pinson J., Saveant J.-M., *J. Am. Chem. Soc.* **1997**, *119*, 201.
24: Combellas C., Jiang D.-E., Kanoufi F., Pinson J., Podvorica F. I., *Langmuir* **2009**, *25*, 286.
25: Baristela V. R., Pellosi D. S., de Souza F. D., da Costa W. F., Santin S. M. O., de Souza V. R., Caetano W., de Oliveira H. P. M., Scarminio I. S., Hioka N., *Spectrochim. Acta. A* **2011**, *79*, 889.

26: http://www.sigmaaldrich.com/catalog/product/sial/230251? (accessed Jan. 24th, 2014)
27: del Valle J. C., Catalan J., Amant-Guerri F., *J. Photochem. Photobiol. A* **1993**, *72*, 49.
28: Himmel D., Goll S. K., Leito I., Krossing I., *Angew. Chem. Int. Ed.* **2010**, *49*, 6885.
29: Crossley M. L., Kienle R. H., Benbrook C. H., *J. Am. Chem. Soc.* **1940**, *62*, 1400.
30: Hirose Y., Wahl G. H., Zollinger H., *Helv. Chim. Acta* **1976**, *59*, 1427.
31: Zhu C., Yamane M., *Org. Lett.* **2012**, *14*, 4560.
32: Cano-Yelo H., Deronzier A., *J. Chem. Soc., Perkin Trans. 2* **1984**, 1093.
33: Megerle, U., Lechner, R., König, B., Riedle, E., *Photochem. Photobiol. Sci.* **2010**, *9*, 1400.
34: Kuhn H. J., Braslavsky S. E., Schmidt R., *Pure Appl. Chem*. **2004**, *76*, 2105.
35: Wegner E. E., Adamson A. W., *J. Am Chem. Soc.* **1966**, *88*, 394.
36: Cismesia M. A., Yoon T. P., *Chem. Sci.* **2015**, DOI:10.1039/C5SC02185E.
37: Verhoeven J. W., *Pure Appl. Chem.* **1996**, *68*, 2223.
38: Macrae P. E., Wright T. R., *J. Chem. Soc., Chem. Commun.*, **1974**, 898.
39: Penzkofer A., Beidoun A., *Chem. Phys.* **1993**, *177*, 203.
40: Lin S., Ischay M. A., Fry C. G., Yoon T. P., *J. Am. Chem. Soc.* **2011**, *133*, 19350.
41: Käräs M. D., Matsuura B. S., Stephenson C. R. J., *Science* **2015**, *349*, 1285.
42: Szychlinski J., Bilski P., Martuszewski K., Blazejowski J., *Analyst* **1989**, *114*, 739.
43: Dakin H. D., *Org. Synth.* **1935**, *15*, 74.
44: Kuhn H. J., Braslavsky S. E., Schmidt R., *Pure Appl. Chem*. **2004**, *76*, 2105.
45: Wegner E. E., Adamson A. W., *J. Am Chem. Soc.* **1966**, *88*, 394.
46: Mau A. W.-H., Johansen O., Sasse H. F., *Photochem. Photobiol.* **1985**, *41*, 503.
47: Lazarides T., McCormick T., Du P., Luo G., Lindley B., Eisenberg R., *J. Am. Chem. Soc.* **2009**, *131*, 9192.

Chapter 4:

Visible Photo-Redox Catalysis Enables Metal-Free Carbonylations

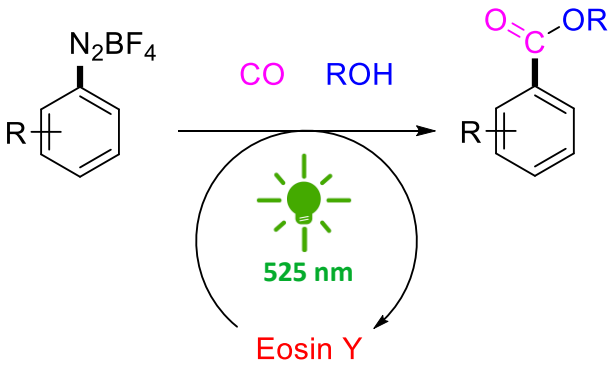

This chapter has been published:
Májek M., Jacobi von Wangelin A., *Angew. Chem. Int. Ed*. **2015**, *54*, 2270. Schemes 1,3,4,6,13 and figures 6,7 were not present in the publication. Further information has been added with respect to the aforementioned publication.

Author contributions:
MM synthesized starting materials, did photochemical reactions, and wrote the manuscript.

4.1: Introduction

Aromatic esters are key building blocks in the synthesis of fine chemicals, agrochemicals, pharmaceuticals, and materials[1] They can be prepared by various methods;[2] most importantly by the esterification of benzoic acids with alcohols under Brønsted or Lewis acid catalysis at elevated temperatures or alternatively by the trimodular reaction of an aromatic electrophile bearing a suitable leaving group, gaseous carbon monoxide, and the alcohol in the presence of transition metal catalysts, mostly combinations of Pd or Ni complexes with phosphine ligands.[3] Several metal-catalyzed carbonylation reactions are being applied in industrial and academic syntheses of carbonyl compounds.[4] Carbon monoxide (CO) is abundantly available as primary product from the gasification of all carbon-based raw materials (oil, natural gas, coal, biomass). The reaction mechanism of metal-catalyzed carbonylations bears a close relationship to cross-coupling reactions.[3] While aryl halides are the most prominent class of electrophilic reagents in such reactions, arenediazonium salts offer specific advantages due to their ionic character, halogen-free preparation from anilines, and incorporation of a most potent leaving group, dinitrogen (N_2). Arenediazonium salts have been used in numerous cross-coupling protocols[5] while there are only isolated reports on carbonylations to benzoates (Scheme 1).[6] Earlier report used nickel tetracarbonyl as both catalyst as well as source of CO and offered low yields, whereas the more recent examples relied on the use of expensive palladium salts as the catalyst.

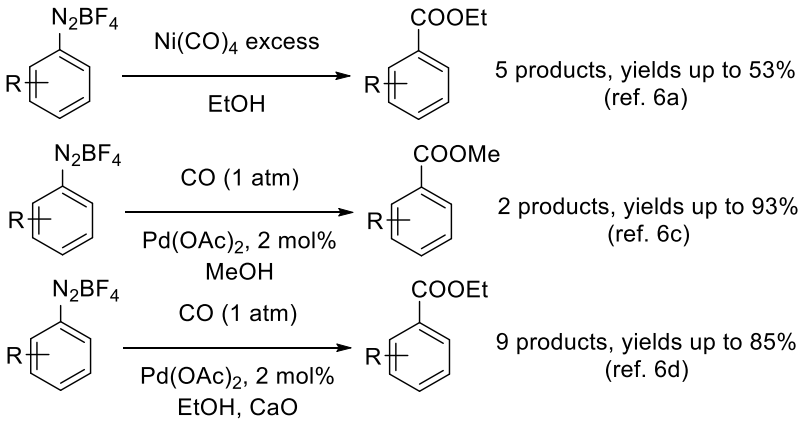

Scheme 1. Metal catalyzed carbonylative esterifications of diazonium salts

The generally accepted mechanism of metal-catalyzed carbonylations involves reductive activation of the electrophilic aryl-X followed by CO insertion and nucleophilic displacement with the alcohol in the presence of stoichiometric amounts of base.[7] The first and last step can be viewed as formal metal-centered two-electron redox reactions which result in an overall redox-neutral process (Scheme 2, top).[3] Here, we wish to report on an alternative metal-free and base-free process which involves a hitherto unknown one-electron redox mechanism that is driven by visible light in the presence of an organic dye (Scheme 2, bottom). The following criteria provided further stimuli for our explorations of such redox carbonylations: Reductive single electron transfer (SET) processes with arene diazonium salts proceed even with mild, non-metallic, reducing agents due to their low redox potentials (≈ 0 V vs. SCE).[8,9] Secondly, the availability of low lying σ- and π-orbitals makes CO a good radical trap. The intermediate aryl radical can react with CO while being unreactive toward the alcohol.

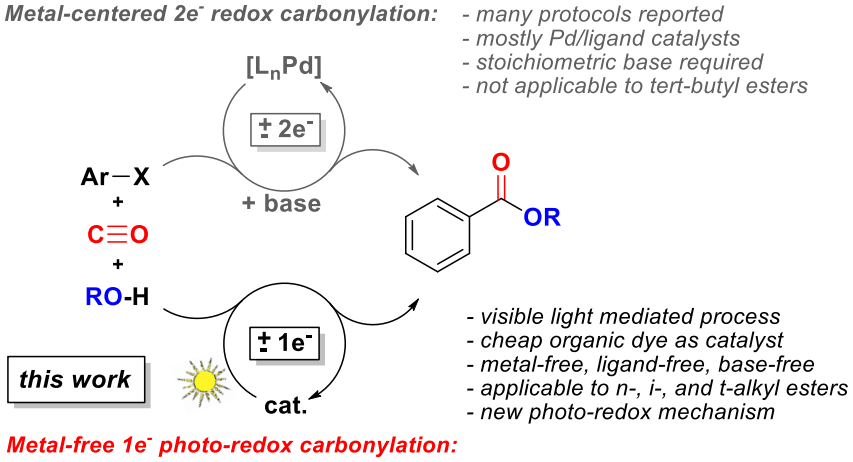

Scheme 2. Pd-catalyzed redox carbonylation vs. novel photo-redox catalysis.

Concept of the generation of aryl- or alkyl- radical, their trapping with CO molecule, and subsequent coupling with third component to obtain products with incorporated carbonyl moiety is not new. Alkyl- and aryl- radical intermediates can be obtained either by homolysis of R-X bond, or by a hydrogen abstraction from unfunctionalized comounds.[10] From the point of view of this thesis a very interesting method of preparing alkyl radicals for carbonylations is the photocatalytic method, based on hydrogen atom abstraction from nonsubstituted hydrocarbons, by the tungsten-based photocatalyst.[11] Acyl radicals that are obtained from the intermediate radicals by reaction with carbon monoxide can then abstract hydrogen from good hydrogen atom

donors such as tributyltin hydride.[12] This reaction can be used to introduce formyl or hydroxymethylene moiety into the molecule. Other option is a recombination with other radical, which is present in the system in higher concentrations, and this case is particularly interesting if the alkyl-/aryl- halides are used to generate the intermediate alkyl radical (Scheme 3). In this case, the acyl radical formed by the carbonylation step recombines with halide, generating reactive acyl halide, which gets readily alcoholised in the reaction conditions to give esters.[13] The drawback of this method lies in the high energy, which is needed to split the R-X bond, translating to the necessity to utilize photons of the UV part of the spectrum for this transformation.

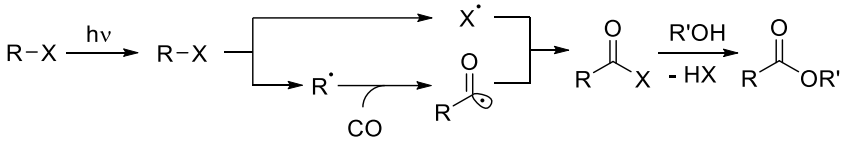

Scheme 3. Radical carbonylation based on cleavage-recombination mechanism

If one looks for the radical carbonylation methods that can be used to produce carboxylic acid derivatives from the point of mechanisms, there is another group, which we have not examined so far: the coupling of the intermediate electron-poor acyl radicals with non-radical O- or N- nucelophiles. Two recent works fall into this category: radical carbonylation of aryl iodides using potassium *t*-butoxide as the reductant from Lei *et al*.[14] The other one of them is the light-induced amidocarbonylation from Ryu *et al*.[15] Both of these reactions involve transfer of an electron pair to the electron-poor acyl radical – but as the sp^2 hybridized orbital is already occupied by one electron, attack occurs on the π-bond (Scheme 4).

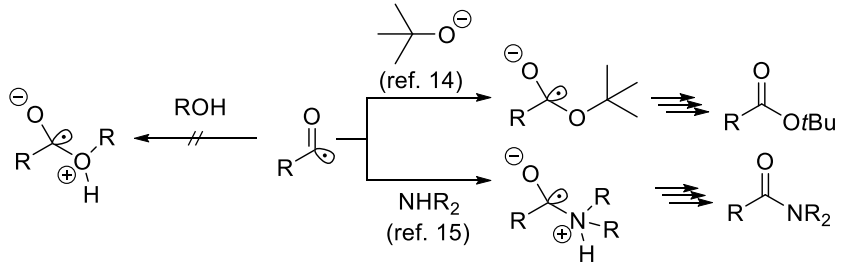

Scheme 4. Formation of carboxylic acid derivatives by reaction with nucleophile

Driving force for this bond formation is probably better stabilization of half full sp^3 orbital by the neighboring heteroatoms. As the carbonyl center on the acyl radical is not particularly electrophilic, only good nucleophiles such as alcoholates and amines

react in such fashion – alcohol itself is not nucleophilic enough. In contrast, we sought to develop a process, where the reactivity of carbonyl center would be increased by oxidation to acylium intermediate prior to the reaction with nucleophile, which should smoothly react even with less activated nucleophiles such as alcohols. Moreover, all the already mentioned processes require high energy investments – either in the form of UV irradiation used for homolytic bond cleavage, or in elevated temperatures needed to promote electron transfer from relatively poor reductant such as *t*-butoxide.

Our aim was to utilize visible light in order to overcome the activation energy. The utilization of visible light as the most abundant source of energy to enable chemical transformations has recently experienced a renaissance which is largely driven by new developments in the field of photo-redox catalysis.[16] Significant effort has been devoted to visible light-driven aromatic substitutions of arenediazonium salts in the presence of various photosensitizers.[17] tris(bipyridine)Ru(II) and other metal complexes (Ir, Cu) have emerged as most powerful photocatalysts.[18] However, the good coordination ability of CO ligands and the existence of numerous stable carbonyl complexes of Ru (and other metals) discourage the use of such organometallic catalysts for the proposed aromatic carbonylation process.[19] Organic dyes, *e.g.* the cheap fluoresceins, display similar photo-catalytic activity in some reactions[20] and seemed more appropriate as no interference with the presence of carbon monoxide is known.[21] Furthermore, CO only exhibits absorptions in the vacuum UV range below 180 nm.[22]

4.2: Results and discussion

Our initial studies of the proposed photocatalytic carbonylation with 4-ethoxybenzenediazonium tetrafluoroborate (**1a**) in methanol used reaction conditions that were reported for related photo-redox Meerwein reactions.[23] Under irradiation with green light (LED, λ_{max} = 525 nm, 3.8 W), solutions of **1a** in methanol were reacted under an atmosphere of CO at room temperature to give methyl 4-methoxybenzoate (**2a**, Table 1, further experimental data can be found in the experimental and computational part). Following setup was used to allow both irradiation as well as the reaction with gaseous CO at the same time: High-power LED was mounted to a cooling block, and placed in such fashion that the incoming light was intercepting the bottom of the autoclave at right angle. Small window from quartz glass on the bottom of autoclave allowed the light to be transmitted on the bottom of the magnetically stirred sample vials placed directly on the window.

Table 1. Selected optimization experiments.

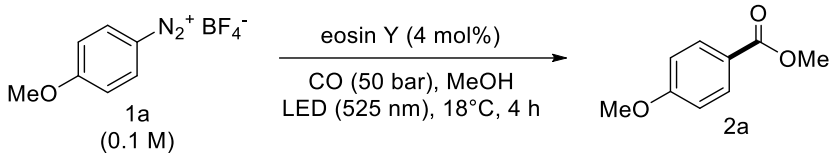

Entry	Deviation from the optimized conditions	Yield of 2a [%]
1	-	**83**
2 [a]	Rose bengal	8
3 [a]	Eosin B	29
4 [a]	Fluorescein	24
5 [a]	$[Ru(bpy)_3]Cl_2$	30
6	without dye	2
7	dark reaction at 60°C	<1

Conditions: **1a** (0.1 mmol), eosin Y (0.04 mmol), methanol (1 mL), CO (50 bar), irradiation(LEDs, λ_{max} = 525 nm, 3.8 W), 18°C, 4 h. [a] in methanol/acetonitrile (1/1)

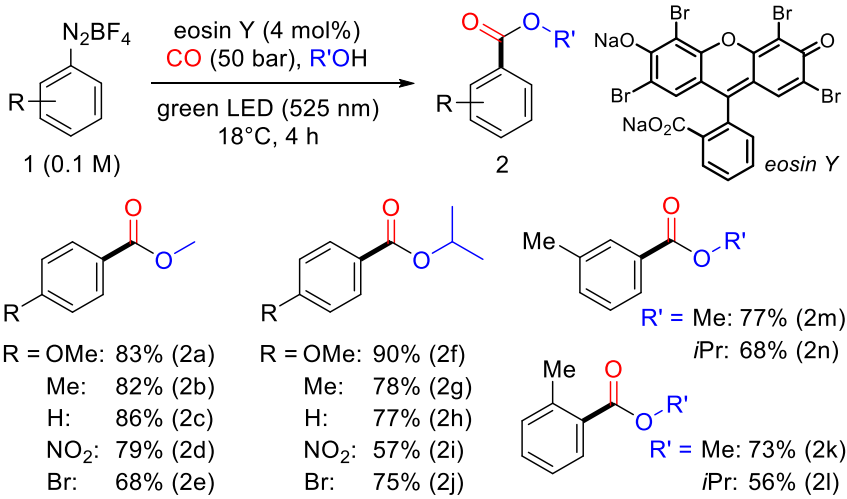

Scheme 5. General conditions and scope of photo-redox carbonylation.

Commercial eosin Y (4 mol%, employed as disodium salt) was used as metal-free photoredox catalyst. Unwanted dimerization (Ar_2) and reduction (Ar-H) was suppressed at higher dilutions due to the higher relative concentration of CO and the alcohol.

Other dyes fared poor (entries 2-5). Lower pressures of CO resulted in low conversion and competing hydrodediazonation (10-25 %) and biaryl coupling (≈ 5 %). Eosin-free (entry 6), dark and thermal reactions (entry 7) produced only minimal amounts of **2a**. The optimized conditions were applied to the synthesis of various alkyl benzoates (Scheme 5). Several functional groups and electron-poor and -rich substituents within the substrates (nitro, chloro, bromo, esters, benzylic protons) were tolerated. The main by-products of these reactions, which were identified by GC-MS analysis, were the hydrodediazonation products, which are formed from the intermediate aryl radicals by the hydrogen abstraction from the alcohol component. Both methanol as well as *iso*-propanol is prone to such reactions, giving volatile formaldehyde and acetone, respectively, which are lost on the workup (Scheme 6). All alcohols, bearing α- hydrogens with respect to hydroxyl group will be prone to this side reaction in our reaction conditions.

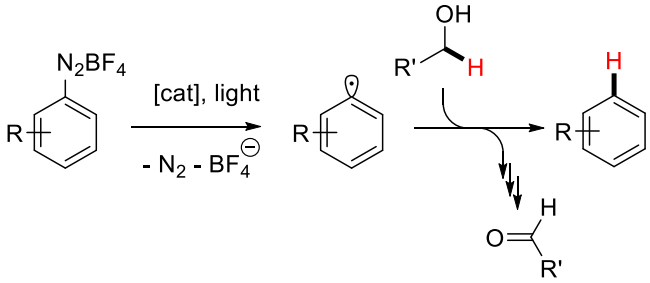

Scheme 6. Mechanism of the by-product formation

In order to probe the robustness of the radical carbonylation protocol in presence of various functional groups, we have employed a high-throughput additive testing strategy similar to one recently proposed by Glorius *et al.*[24] A screening of various additives (Scheme 7) exhibited significant tolerance of halogen-containing electrophiles, acidic protons, π-nucleophiles and electron-deficient arenes without erosion of ester yield or additive consumption (for further information, see experimental and computational part). The presence of 1 eq. of phenol (pK_a ≈ 9) was well tolerated which is in contrast to the employment of phenol (in large excess) as reaction partner under otherwise identical conditions, where complex product mixtures were formed. It is important to point out, that phenols are, when used in large excess, prone to react in an azo-coupling fashion, depleting not only the phenol, but more importantly also the diazonium salt, hampering the reaction progress. Methylthio-bearing compounds did not affect the ester formation in agreement with a previous report,[25] where *S*-alkylated compounds were produced under similar

conditions. Interestingly, *t*-butylisonitrile - a competent radical trap in some reactions[26] - was tolerated. There was only little interference with iodobenzene, presumably by radical cleavage of the weak Ar-I bond. The addition of thiophenol led to large yield decrease, which is known from reports of diazosulfide formation/ photocatalytic cleavage at similar conditions.[27] Biarylsulfide (Ar-S-Ar) coupling was observed in this case. The presence of aniline or *N*,*N*-dimethylaniline resulted in the quenching of the excited state of the dye. Azobenzenes were detected in small amounts. Addition of triphenylphosphine led to inhibition due to quenching of the excited dye. Accordingly, triphenylphosphine oxide was formed (further details about additive screening can be found in the experimental and computational part). Result of this additive screening show, that most functional groups are tolerated, because given enough pressure of CO, the aryl radical coupling with carbon monoxide would precede the coupling with additives. On the other hand, the extremely electron-rich additives are not tolerated, as they tend to suspend the catalytic effect of eosin Y* by efficient quenching, as well as they tend to directly react with electron poor diazonium salts.

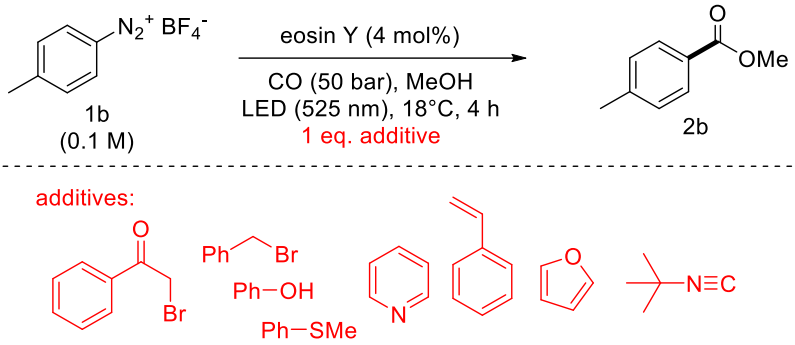

Scheme 7. Compatibility with various functionalized additives that resulted in unaffected ester formation without competing conversion of the additive.

t-Butyl esters are notoriously difficult to obtain by conventional esterification protocols due to their steric bulk.[1,2,28] Palladium-catalyzed carbonylation protocols also fail to provide access to *t*-butyl esters. The photocatalytic carbonylation, however, produced *t*-butyl benzoates in very good yields which exceed those of the less hindered methyl and *i*-propyl esters. This is due to the lack of α-hydrogens within *t*-butanol which excludes undesired radical H-abstraction and subsequent reductive reactions (Scheme 8).

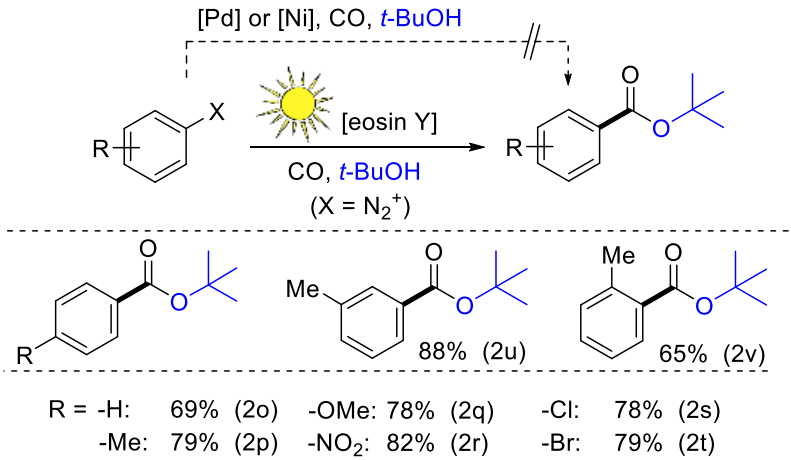

Scheme 8. Carbonylations with t-butanol as esterification partner

We have probed the effectiveness of the metal-free photo-carbonylation in the context of the synthesis of **2w**, a low-odor, low-volatility, and low-viscosity ester produced on multi-ton scales for applications as coalescent in the formulation of latex paints (Velate® 368), plasticizer in the manufacture of key polymers, as sunscreen and antiperspirant ingredient in cosmetics (Finsolv® EB), as textile dye carrier for the treatment of synthetic fibers, and as solvent for cellulose ethers.[29]

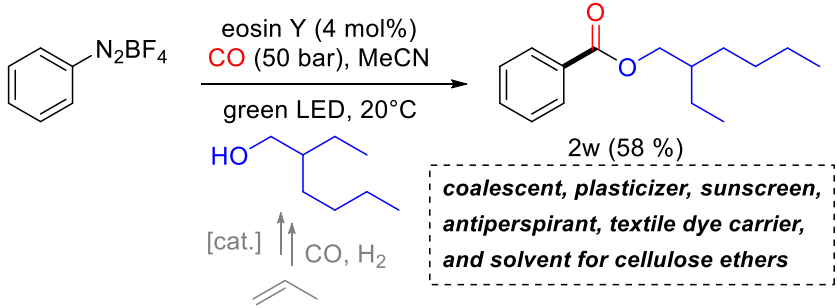

Scheme 9. Synthesis of the technical ester **2w**.

Under standard conditions, 2-ethylhexyl benzoate (**2w**) was obtained in 58 % yield from the reaction of PhN_2BF_4 with 2-ethylhexanol and CO under green light irradiation (Scheme 9). Acetonitrile was used as co-solvent to solubilize the diazonium salt in the fatty alcohol. Methyl 4-anisate (**2a**) is another technical product with applications as

food and flavor ingredient. Technical applications of catalytic reactions are always associated with the search for an effective catalyst separation technique. The intensely colored eosin Y ($\varepsilon \approx 10^5$ $M^{-1}cm^{-1}$, 530 nm, ethanol)[30] was removed from the reaction mixture by adsorption on basic alumina.[31] UV/VIS spectra documented complete removal of the dye while < 1 % of product was lost in this operation (Figure 1).

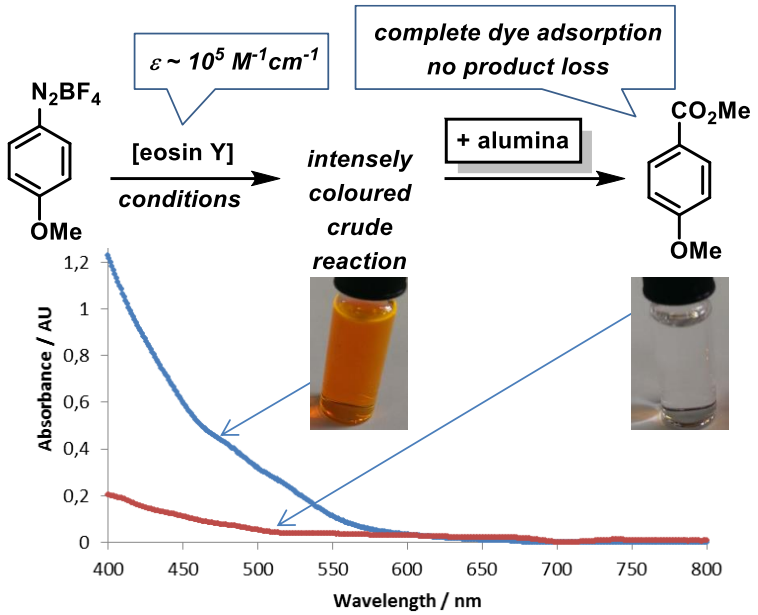

Figure 1. Dye removal with basic alumina. Bottom: corresponding absorption spectra before (blue) and after (red) work-up.

The mechanistic proposal of a visible light-driven dye-catalyzed process was supported by the following experiments: The product yields severely dropped when no photocatalyst was present in the reaction and/or under dark conditions. Reactions in the dark and at increased temperature (up to 70 °C) gave no carbonylation product which excludes homolytic bond cleavage of the starting material to an aryl radical under these conditions. Instead, the thermal dark reaction of **1a** in methanol at 70°C produced small amounts of the corresponding methylether and aryl fluoride (Scheme 10).

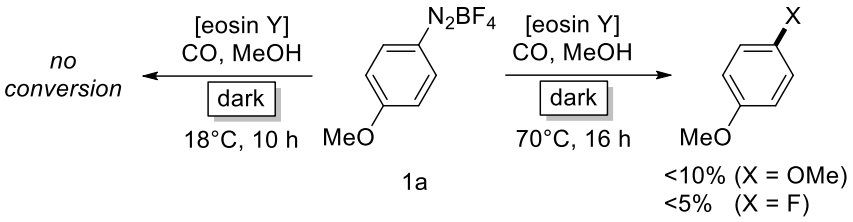

Scheme 10. Dark reactions of 4-anisyldiazonium salt (**1a**).

Observation of such by-products is consistent with the reactivity of diazonium salts, if one takes into account the reactivity of the aryl cations – which are the species generated by the thermal decomposition of arenediazonium cation. Aryl cations are very electrophilic and will react with the closest nucleophile present, given that the rate of this reaction is likely to be at diffusion limit. This nucleophile is either methanol – which is in the reaction mixture present in great excess, or it is fluoride from tetrafluoroborate, which forms ion pairs with arenediazonium cations in the solution. The observation, that fluorinated product is formed in a Schiemann-fashion even more underlines the extreme electrophilicity of the intermediate species, as it reacts even with such poor nucleophile as tetrafluoroborate. This observation is consistent with previous reports of unsuccessful attempts on thermolytic carbonylations of diazonium salts.[32] Plausible explanation of this reactivity pattern is in the high electrophilicity of the aryl cation intermediate. While Koch-Haaf carbonylation is quite efficient for the substrates where the intermediate cationic species is stabilized, or when the structure of present nucleophile allows reversibility of the direct nucleophile attack on the carbon center, this is not the case with aryl cations. Addition of nucleophile is fast and irreversible in this case – and therefore no reaction with CO occurs, unless unrealistically concentrations of CO would be applied. In practical sense, such approach is impossible, given the finite solubility of CO in organic solvents as well as physical limits for the reaction vessel. We have performed detailed mechanistic studies to prove the postulate of a light-driven reduction-oxidation cascade which is devoid of any sacrificial redox partner. On the basis of related literature reports[17,23,33] and our own findings we propose the following operating mechanism (Scheme 11).

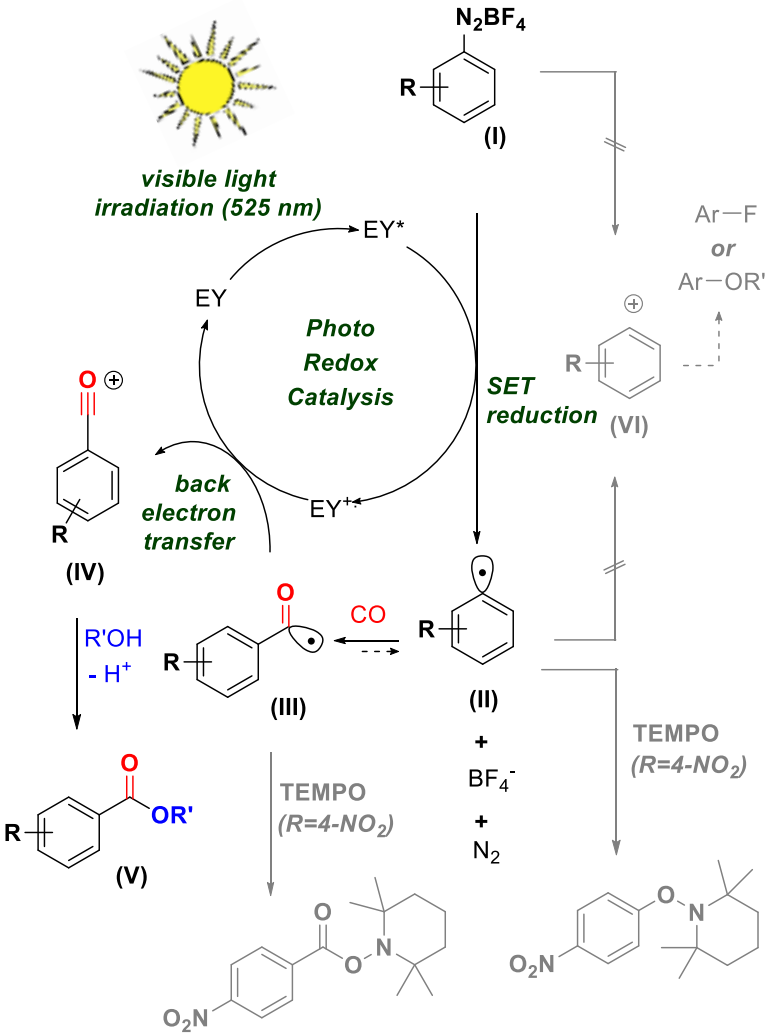

Scheme 11. Mechanism of the visible light-driven eosin-catalyzed carbonylation of arene diazonium salts.

The electron-deficient arenediazonium salt (**I**) accepts one electron from the electron-rich, dianionic, photo-excited state of eosin Y (EY*). This single electron transfer (SET) results in the release of dinitrogen N_2 and generation of aryl radical **II**. This initiation step is thermodynamically favored due to the more positive redox potential of the **I**→**II** reduction (≈ 0 V vs. SCE)[9] compared with the $EY^{+\bullet}$→EY* reduction

(-1.1 V vs. SCE). The aryl radical **II** then rapidly reacts with CO to acyl radical **III**.[34] Upon addition of the radical trap TEMPO (2,2,6,6-tetramethylpiperidinyloxyl), the formation of adducts with both radical species (**II**, **III**) were observed (for further information see experimental and computational part). We further propose that **III** is subject to rapid one-electron oxidation to give the highly electrophilic acylium ion **IV**. Reaction thereof with the alcohol affords the benzoate ester **V**. The back electron transfer (BET) is supposed to be fast as no adduct of acyl radical **III** with electron-rich π-donors (i.e. anisole, furan, styrene) was detected. This assumption can be instructively substantiated by thermodynamic data: The redox potential of the $EY^{+\bullet} \rightarrow EY$ reduction is –0.8 V (vs. SCE). The potential of the **III**→**IV** redox couple is experimentally not available since both of species are short lived. However, an estimation of this redox potential could be derived from DFT calculations which provided values of –0.14 V to 0.82 V (vs. SCE) depending on the substitution pattern at the aromatic ring (Scheme 12, details on the calculations ate in the experimental and computational part). Therefore, the BET step is thermodynamically feasible.

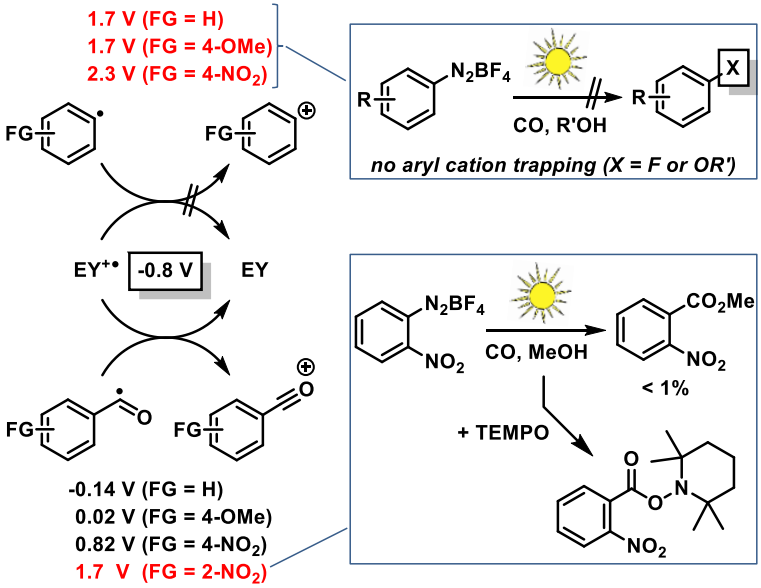

Scheme 12. The back electron transfer (BET): DFT calculations on the prohibitive redox process to aryl cations (top left), the operating BET to give acylium ions (bottom left), and supportive preparative experiments (right).

Solely for the 2-nitroaroyl radical species, calculation of the redox potential of the back electron transfer gave a prohibitive value of 1.7 V (vs. SCE). Indeed,

2-nitrobenzenediazonium tetrafluoroborate did not afford the desired ester under carbonylation conditions. On the other hand we can conclusively prove, that both reductive formation of acyl radical **III** in addition to aryl radical **II** are formed for 2-nitrobenzenediazonium tetrafluoroborate, as we can detect the corresponding intermediates. Addition of TEMPO to the reaction resulted in the formation of the aryl-TEMPO as well as benzoyl-TEMPO adduct. Both experiments provide further evidence of the postulated mechanism as the carbonylation of the intermediate 2-nitroaryl radical is operative but the BET to $EY^{+\bullet}$ is thermodynamically prohibited.[27] The operation of a reaction between the aryl cation and CO as known from acid-catalyzed Gatterman-Koch carbonylations[35] was also excluded based on DFT calculations. The carbonylation of aryl cations (**VI**, from thermal heterolysis of arenediazonium) was already disproven (Scheme 10). A potential back electron transfer with $EY^{+\bullet}$ already at the aryl radical stage (**II**) can likewise be refuted. The DFT-derived reduction potentials of the **VI**/**II** couples of our substrates are 1.7-2.3 V (vs. SCE, details on calculation are in the experimental and computational part). These values are prohibitively high in comparison with the oxidizing power of $EY^{+\bullet}$ (-0.8 V vs. SCE) and thus exclude the intermediacy of aryl cations.

At last, we have attempted to apply the here presented carbonylation strategy to the radical carbonylative cross-coupling of aromatic compounds. The idea behind this was to trap the intermediate acyl radicals with electron rich aromates, which would be followed up by SET oxidation and deprotonation in order to restore aromaticity (Scheme 13).

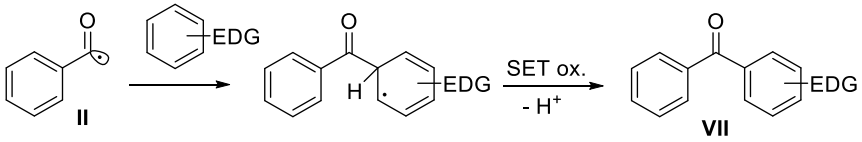

Scheme 13. Proposed radical carbonylative cross-coupling.

We have unsuccessfully screened series of electron donor bearing benzenes as well as electron rich heterocycles as the coupling partners for this reaction, without any success. We propose, that this is due to very fast oxidation of acyl radical **II** to acylium ion **III**. While attack of **III** on electron rich aromatics in a Friedel-Crafts fashion can technically produce the desired coupling products **VII**, it is well known, that such reactions have rate constants in several orders of magnitude lower than the attack of radicals.[36] In order to make such a reaction efficient one would need to employ a very nucleophilic coupling partner, such as indole. But this presents an issue with respect to

the electrophilicity of the diazonium cations, which will directly couple with such electron rich compounds. Indeed, when we tried to perform a carbonylative cross-coupling with *p*-nitrobenzenediaznoium tetrafluoroborate, *N*-methylindole, and CO under photocatalytic conditions, we have observed the formation of azocoupling product already after 15 minutes, but no carbonylation product could be detected by GC-MS. This is in agreement with previously published data, where the same azocoupling is reported to be finished after 20 minutes.[37] Interestingly, recent publication from Gu *et al.* shows such carbonylation to be efficient, and to give large yield of carbonylation product after 16 h, while no formation of azocoupling product is mentioned.[38]

4.3: Conclusion

This new protocol enables metal-free and base-free carbonylations via an organic dye catalyzed photo-redox mechanism. Alkyl benzoates can be prepared from arenediazonium salts, CO, and alcohols at room temperature under irradiation with visible light. The reaction uses catalytic eosin Y as cheap photosensitizer. Mechanistic studies support the sequential operation of SET reduction, carbonylation, and back electron transfer to give aryl cations which undergo rapid addition to alcohols. Unlike in metal-catalyzed carbonylations, *t*-butyl esters can be prepared in good yields. The general method has been applied to the synthesis of industrial cosmetics/food ingredients and a paint coalescent.

4.4: Experimental and computational part

Materials and methods

Commercial chemicals (≥98% purity) were used as obtained from Sigma-Aldrich or Fisher. Solvents (anhydrous, ≥99%) were used without further purification. Acetonitrile was stored over molecular sieves (Sigma-Aldrich). Carbon monoxide (4.7) was used. TLC was performed on commercial SiO_2-coated aluminium plates (DC60 F254, Merck). Visualization was done by UV light. Product yields were determined from isolated materials after flash column chromatography on silica gel (Acros Organics, mesh 35-70) or for optimization and screening purposes by quantitative GC-FID measurements. *n*-Pentadecane was used as internal standard; the yield-% was calculated from a linear calibration curve that was set up from at least five data points of various concentrations of authentic product material. Purity and structure confirmation of literature-known compounds was performed by 1H NMR, 13C NMR, and MS. NMR spectral data were collected on a Bruker Avance 300 (300 MHz for ^{1}H; 75 MHz for ^{13}C) spectrometer and a Bruker Avance 400 (400 MHz for ^{1}H; 100 MHz for ^{13}C)

spectrometer at 20 °C. Chemical shifts are reported in δ/ppm, coupling constants J are given in Hertz. Solvent residual peaks were used as internal standard for all NMR measurements. The quantification of ^{1}H cores was obtained from integrations of appropriate resonance signals. Abbreviations used in NMR spectra: s – singlet, d – doublet, t – triplet, q – quartet, m – multiplet, bs – broad singlet, dd – doublet of doublet, ddd – doublet of doublet of doublet.

General procedure for the synthesis of arenediazonium salts

The parent aniline (4.5 mmol) was dissolved in glacial acetic acid (3 mL) and 48% aqueous tetrafluoroboric acid (1.3 mL) at room temperature. Then, a solution of *iso*-amyl nitrite (1 mL) in glacial acetic acid (2 mL) was slowly added at room temperature over 5 min. Diethylether (15 mL) was added, and the reaction mixture was cooled to -30 °C in order to induce crystallization of the ionic product. The crystals were filtered off, washed with cold diethylether (2 x 10 mL) and dried on air to give analytically pure arenediazonium tetrafluoroborates.

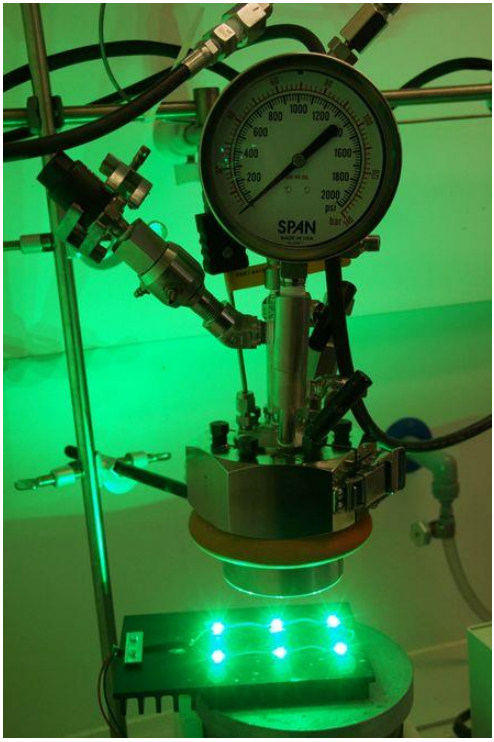

Figure 2. Reaction setup

General procedure for carbonylation

A vial (3 mL) was charged with a magnetic stirbar, the arenediazonium salt (0.1 mmol), and eosin Y (0.004 mmol) under N_2 and capped with a rubber septum. Dry solvent (1 mL, alcohol or mixture with MeCN if poor solubility of diazonium salt) was added. The vial was purged with N_2 (5 min) in the dark and transferred to a reactor containing a quartz window bottom (Parr Instr.). The septum was punctured with a needle. The reactor was sealed, placed on a magnetic stirrer, and slowly filled with CO (50 bar). The reaction was irradiated with external LEDs (λ_{max} = 525 nm, 3.8 W). After 4 h at 18 °C, the gas was released and the vial retrieved. Water (5 mL) was added to give an emulsion that was extracted with ethyl acetate (2 x 5 mL). The organic phases were washed (5 mL brine) and dried (Na_2SO_4). Volatiles were evaporated and the residues purified by SiO_2 gel chromatography.

Table 2. Selected optimization experiments.

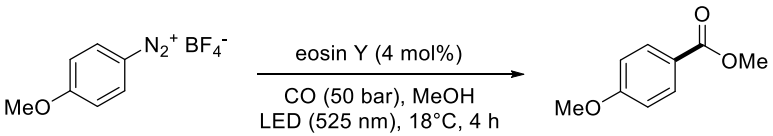

1a (0.1 M) 2a

Entry	Deviation from the optimized conditions	Yield of 2a [%]
1	-	**83**
2	0.5 M **1a** in MeOH/MeCN (1/1)	27
3	0.25 M **1a** in MeOH/MeCN (1/1)	30
4	MeOH/MeCN (1/1)	57
5	0.05 M **1a** in MeOH/MeCN (1/1)	43
6	MeOH/MeCN (1/1), 2 mol% eosin Y	49
7	MeOH/MeCN (1/1), rose bengal	8
8	MeOH/MeCN (1/1), eosin B	29
9	MeOH/MeCN (1/1), fluorescein	24
10	$[Ru(bpy)_3]Cl_2$	30
11	40 atm CO	62
12	20 atm CO	<5
13	without dye	2
14	addition of 1 equiv. KOAc	49
15	dark reaction	2
16	dark reaction at 60°C	<1

Opt. conditions: 4-anisyldiazonium salt (**1a**, 0.1 mmol), eosin Y (0.04 mmol), alcohol (1 mL), CO (50 atm), irradiation with LEDs (λ_{max} = 525 nm, 3.8 W), 18°C, 4 h.

Optimization of reaction conditions

General procedure was altered as defined in the Table 2. Most important parameter, which was optimized, is the concentration of diazonium salt. High concentrations are problematic, as the relative concentration of carbon monoxide to diazonium salt is lowered. Overly dilute reaction mixtures lead to lowered probability of catalyst coming in contact with diazonium salt, and this leads also to decreased yields. Lowering pressure of CO also negatively affects the relative concentration of carbon monoxide in solution and leads to decreased yields. Control experiments were performed in order to prove that photocatalysis is needed for the reaction to proceed. Indeed, without photocatalysis, carbonylation reaction does not occur at all.

Table 3. Compatibility with functionalized additives.

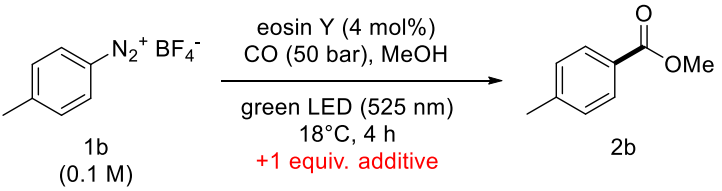

Exp.	Additive	Yield	Additive conversion >20%
1	None	82 %	-
2	Benzyl bromide	81 %	-
3	Iodobenzene	60 %	+
4	Thiophenol	27 %	+
5	*t*ert-Butyl isonitrile	78 %	-
6	Furan	72 %	-
7	Aniline	21 %	+
8	N,N-Dimethylaniline	9 %	+
9	Phenol	70 %	-
10	Triphenylphosphine	0 %	+
11	Thioanisole	77 %	-
12	α-Bromobenzophenone	82 %	-
13	Pyridine	72 %	-

Additive screening

General procedure was altered by adding 1 equivalent of additive as specified by Table 3. Variety of compounds that are known to be reactive under photocatalytic conditions were employed to probe the robustness of carbonylation protocol. Amount of product formation as well as the additive conversion was determined from GC-FID measurements. Structures of by-products obtained from conversion of additives were determined by GC-MS. Iodobenzene got partially dehalogenated to benzene. Thiophenol got converted to Ar-S-Ph species. Both aniline and N,N-dimethylaniline reacted to higher mass product, which were presumably the products of azo-coupling. Triphenylphosphine was oxidized to triphenylphosphine oxide.

Synthesis of industrial emollient Velate™ 368

An optimization of the alcohol/acetonitrile ratio was performed (acetonitrile is needed as co-solvent due to the poor solubility of the benzenediazonium salt in 2-ethylhexanol) (Table 4). Other than that, standard conditions were applied (0.1 M solution of diazonium salt, 50 bar CO, 20°C). At dilutions lower than 1:6, a complex and inseparable products mixture was formed.

Table 4. Optimization of 2-ethylhexyl benzoate synthesis

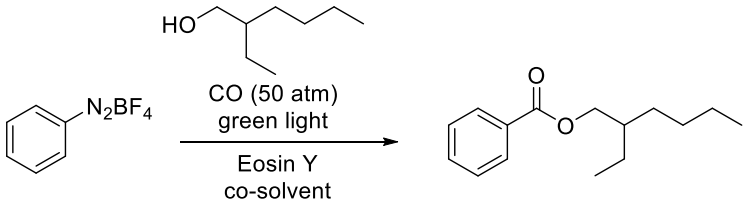

Exp.	ROH/MeCN (*v*/*v*)	Yield [%]
1	1:1	40
2	1:2	46
3	1:3	49
4	1:4	58

Removal of eosin Y from crude product

For technical applications, the complete removal of the organic dye from the product is desirable. Treatment of the crude reaction with basic alumina, filtration (or decantation), and subsequent washing of the alumina with methanol led to quantitative adsorption of the dye. UV/VIS absorption spectra documented the disappearance of the characteristic absorption bands while less than 1% of product material was lost.

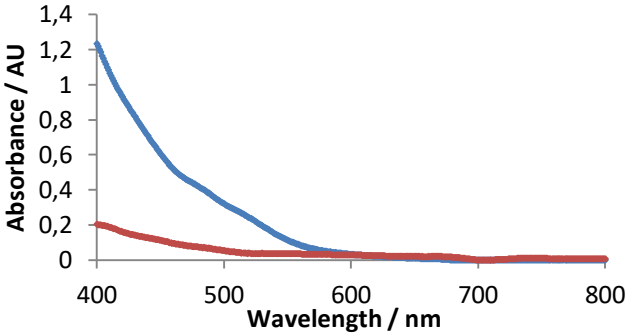

Figure 3. Absorption spectra of reaction mixture before (blue), and after (red) treatment with alumina.

Mechanistic experiments with TEMPO-trapping

See standard procedure above, but with addition of TEMPO (1 equiv., 0.1 mmol). Crude solution obtained by extraction with ethyl acetate was subjected to MS analysis. Experiment was repeated for two different diazonium salts: *p*-methoxyphenyldiazonium tetrafluoroborate and *o*-nitrophenyldiazonium tetrafluoroborate (Scheme 14, 15; Figure 4, 5).

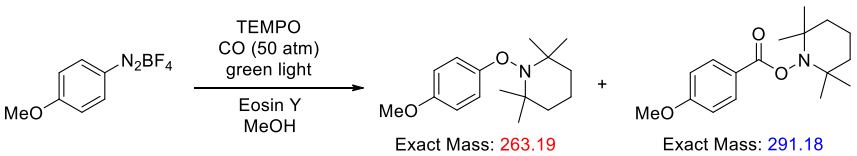

Scheme 14. TEMPO-trapping of intermediates with *p*-methoxyphenyldiaznoium tetrafluoroborate

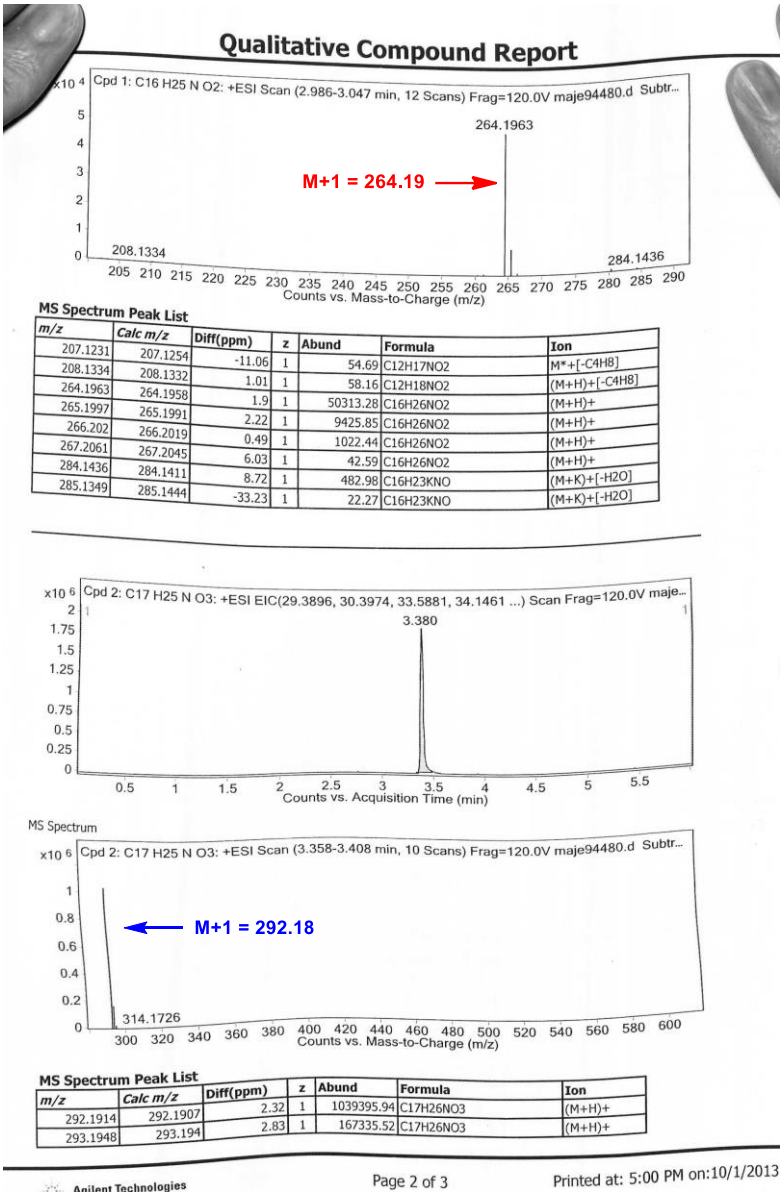

Figure 4. Mass spectrum of TEMPO-adducts of intermediates with *p*-methoxyphenyldiaznoium tetrafluoroborate

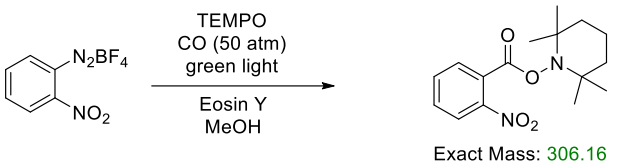

Scheme 15. TEMPO-trapping of intermediates with *o*-nitrophenyldiaznoium tetrafluoroborate

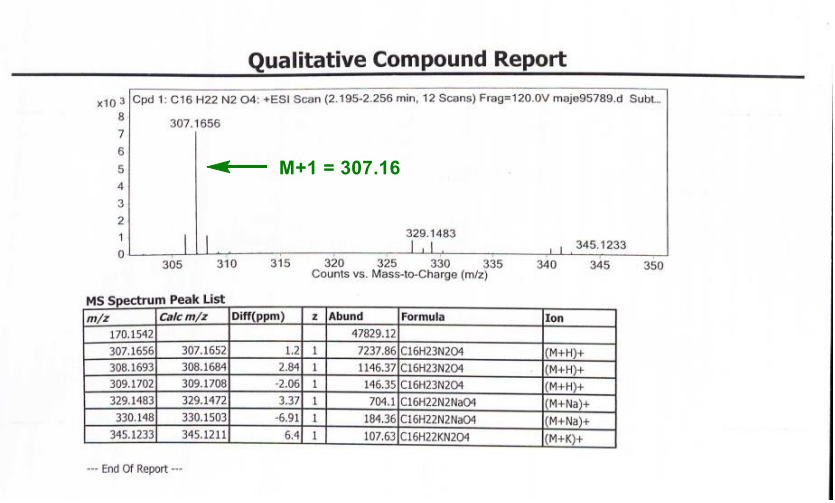

m/z	Calc m/z	Diff(ppm)	z	Abund	Formula	Ion
170.1542				47829.12		
307.1656	307.1652	1.2	1	7237.86	C16H23N2O4	(M+H)+
308.1693	308.1684	2.84	1	1146.37	C16H23N2O4	(M+H)+
309.1702	309.1708	-2.06	1	146.35	C16H23N2O4	(M+H)+
329.1483	329.1472	3.37	1	704.1	C16H22N2NaO4	(M+Na)+
330.148	330.1503	-6.91	1	184.36	C16H22N2NaO4	(M+Na)+
345.1233	345.1211	6.4	1	107.63	C16H22KN2O4	(M+K)+

Figure 5. Mass spectrum of TEMPO-adducts of intermediates with *o*-nitrophenyldiaznoium tetrafluoroborate

Calculation of redox potentials

Redox properties of the proposed intermediate cation/radical pairs were calculated according to Friesner:[39] Optimization of geometries was performed *in vacuo* using the B3LYP functional and 6-311G(d,p) basis set. Single point calculations were performed using the PCM solvation model (in methanol), the B3LYP functional, and aug-cc-pVTZ basis set. All calculations were done with the Gaussian G03W program package.[40] Zero point energies were included in the calculations. The results are summarized in the following table (Table 4). Redox potentials are obtained by subtracting 4.19 V from energy difference ΔE(cation->radical).[39]

Table 4. DFT calculations for redox potential determination.

Structure	E	ZPE	E+ZPE	ΔE(eV)	ΔE(eV) vs. SCE
R1	-345.040	0.095205	-344.945		
K1	-344.894	0.098386	-344.796	4.051	-0.138
R2	-459.609	0.126608	-459.482		
K2	-459.457	0.129474	-459.328	4.212	0.024
R3	-549.646	0.098667	-549.547		
K3	-549.463	0.100414	-549.363	5.013	0.825
R4	-549.689	0.099846	-549.59		
K4	-549.472	0.100915	-549.371	5.937	1.749
R5	-231.651	0.08647	-231.564		
K5	-231.43	0.083344	-231.346	5.930	1.742
R6	-346.215	0.118116	-346.097		
K6	-345.995	0.115613	-345.879	5.923	1.735
R7	-436.237	0.088814	-436.148		
K7	-435.995	0.085587	-435.91	6.484	2.296

Electronic energies and zero point energies are in Hartree

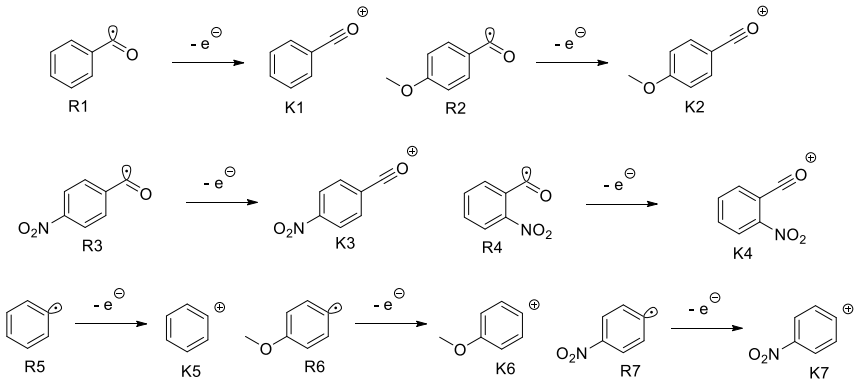

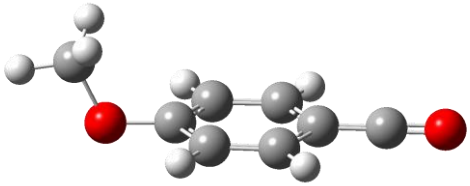

Figure 6. Optimized geometry of *p*-methoxybenzoyl radical

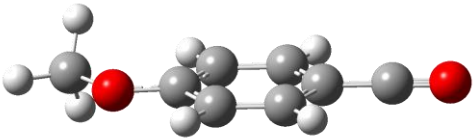

Figure 7. Optimized geometry of *p*-methoxybenzoylium

Representative optimized geometries of intermediates **II** and **III** derived from *p*-methoxyphenyldiazonium tetrafluoroborate are given on figures 6 and 7. Two important features can be seen from the pictures. Firstly, the positive charge in type **III** intermediate is stabilized by conjugation of methoxy substituent with the rest of the molecule, but this is not the case with the radical **II**. Secondly, steric crowding in the acylium intermediate is virtually non-existent, allowing reactions with bulky nucleophiles such as *t*-butanol.

Analytical data of synthesized compounds:

Methyl 4-bromobenzoate

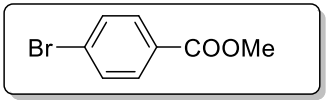

^{1}H NMR (400 MHz, $CDCl_3$, ppm) δ 7.85 (d, *J* = 8.6 Hz, 2H), 7.53 (d, *J* = 8.6 Hz, 2H), 3.87 (s, 3H). ^{13}C NMR (100 MHz, $CDCl_3$, ppm) δ 166.4 (C), 131.7 (CH), 131.1 (CH), 129.1 (C), 128.0 (C), 52.3 (CH_3). GC-MS (EI) *m/z* (relative intensity): 216 (40) [M^+], 214 (39), 185 (99), 183 (100), 157 (34), 155 (35), 135 (6), spectral data were consistent with literature.[41]

_t_-Butyl 4-bromobenzoate

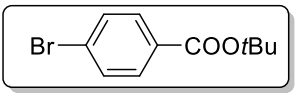

^{1}H NMR (400 MHz, $CDCl_3$, ppm) δ 7.95 (d, *J* = 9.0 Hz, 2H), 6.89 (d, *J* = 9.0 Hz, 2H), 3.85 (s, 3H), 1.58 (s, 9H). ^{13}C NMR (100 MHz, $CDCl_3$, ppm) δ 165.0 (C), 131.5 (CH), 131.0 (CH), 130.9 (C), 127.5 (C), 81.5 (C), 28.2 (CH_3). GC-MS (EI) *m/z* (relative intensity): 258 (2) [M^+], 256 (2), 203 (46), 202 (44), 201 (48), 200 (43), 157 (32), 155 (32), 57 (100), spectral data were consistent with literature.[41]

_i_-Propyl 4-bromobenzoate

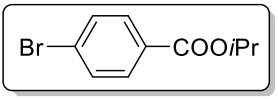

^{1}H NMR (400 MHz, $CDCl_3$, ppm) δ 7.89 (d, *J* = 8.6 Hz, 2H), 7.57 (d, *J* = 8.6 Hz, 2H), 5.24 (sept, *J* = 6.2 Hz 1H), 1.36 (d, *J* = 6.2 Hz, 6H). ^{13}C NMR (100 MHz, $CDCl_3$, ppm) δ 165.4 (C), 131.6 (CH), 131.1 (CH), 129.8 (C), 127.7 (C), 68.8 (CH), 21.9 (CH_3). GC-MS (EI) *m/z* (relative intensity):244 (13) [M^+], 242 (13), 202 (55), 200 (55), 185 (98), 183 (100), 163 (24), spectral data were consistent with literature.[42]

Methyl 4-methylbenzoate

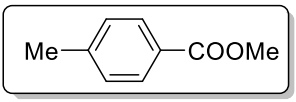

^{1}H NMR (400 MHz, $CDCl_3$, ppm) δ 7.88 (d, *J* = 8.1 Hz, 2H), 7.19 (d, *J* = 8.1 Hz, 2H), 3.85 (s, 3H), 2.36 (s, 3H). ^{13}C NMR (100 MHz, $CDCl_3$, ppm) δ 167.2 (C), 143.6 (C), 129.6 (CH), 129.1 (CH), 127.5 (C), 52.0 (CH_3), 21.7 (CH_3). GC-MS (EI) *m/z* (relative intensity): 150 (34) [M^+], 119 (100), 91 (51), 65 (23), spectral data were consistent with literature.[43]

_i_-Propyl 4-methylbenzoate

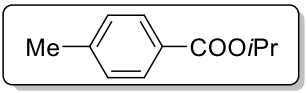

^{1}H NMR (400 MHz, $CDCl_3$, ppm) δ 7.88 (d, *J* = 8.2 Hz, 2H), 7.19 (d, *J* = 8.2 Hz, 2H), 5.19 (sept, *J* = 6.2 Hz, 1H), 2.36 (s, 3H), 1.31 (d, *J* = 6.2 Hz, 6H). ^{13}C NMR (100 MHz,

$CDCl_3$, ppm) δ 166.3 (C), 143.3 (C), 129.6 (CH), 129.0 (CH), 128.2 (C), 68.2 (CH), 22.0 (CH_3), 21.7 (CH_3). GC-MS (EI) *m/z* (relative intensity): 178 (19) [M^+], 136 (52), 119 (100), 91 (41), spectral data were consistent with literature.[43]

_t_-Butyl 4-methylbenzoate

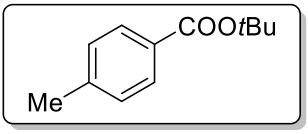

^1H NMR (400 MHz, $CDCl_3$, ppm) δ 7.83 (d, *J* = 8.1 Hz, 2H), 7.16 (d, *J* = 8.1 Hz, 2H), 2.35 (s, 3H), 1.54 (s, 9H). ^{13}C NMR (100 MHz, $CDCl_3$, ppm) δ 165.9 (C), 143.0 (C), 129.5 (CH), 129.3 (C), 128.9 (CH), 80.7 (C), 28.3 (CH_3), 21.7 (CH_3). GC-MS (EI) *m/z* (relative intensity): 192 (1) [M^+], 137 (83), 119 (100), 91 (89), spectral data were consistent with literature.[44]

Methyl 4-nitrobenzoate

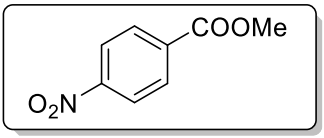

^1H NMR (400 MHz, $CDCl_3$, ppm) δ 8.29 (d, *J* = 8.9 Hz, 2H), 8.21 (d, *J* = 8.1 Hz, 2H), 3.98 (s, 3H). ^{13}C NMR (100 MHz, $CDCl_3$, ppm) δ 164.2 (C), 149.6 (C), 134.5 (C), 129.7 (CH), 122.6 (CH), 51.8 (CH_3). GC-MS (EI) *m/z* (relative intensity): 181 (27) [M^+], 164 (23), 150 (100), 135 (8), 120 (44), spectral data were consistent with literature.[43]

***i*-Propyl 4-nitrobenzoate**

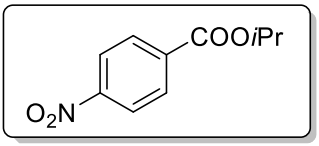

^1H NMR (400 MHz, $CDCl_3$, ppm) δ 8.29 (d, *J* = 9.1 Hz, 2H), 8.20 (d, *J* = 9.1 Hz, 2H), 5.29 (sept, *J* = 6.2 Hz, 1H), 1.40 (d, *J* = 6.2 Hz, 6H). ^{13}C NMR (100 MHz, $CDCl_3$, ppm) δ 164.2 (C), 150.4 (C), 136.3 (C), 130.6 (CH), 123.5 (CH), 69.8 (CH), 21.9 (CH_3). GC-MS (EI) *m/z* (relative intensity): 209 (2) [M^+], 193 (4), 179 (11), 168 (74), 150 (100), 137 (24), 120 (48), spectral data were consistent with literature.[43]

_t_-Butyl 4-nitrobenzoate

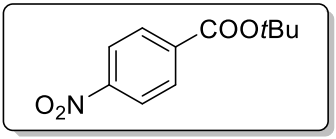

^{1}H NMR (400 MHz, $CDCl_3$, ppm) δ 8.21 (d, *J* = 9.0 Hz, 2H), 8.10 (d, *J* = 9.0 Hz, 2H), 1.57 (s, 9H). ^{13}C NMR (100 MHz, $CDCl_3$, ppm) δ 164.2 (C), 149.6 (C), 134.5 (C), 129.7 (CH), 122.6 (CH), 51.8 (CH_3). GC-MS (EI) *m/z* (relative intensity): 223 (0.3) [M^+], 208 (1), 168 (3), 150 (72), 137 (8), 121 (11), 57 (100), spectral data were consistent with literature.[45]

Methyl 3-methylbenzoate

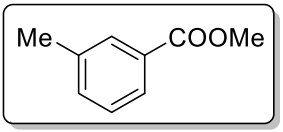

^{1}H NMR (400 MHz, $CDCl_3$, ppm) δ 7.89 – 7.80 (m, 2H), 7.39 – 7.29 (m, 2H), 3.91 (s, 3H), 2.40 (s, 3H). ^{13}C NMR (100 MHz, $CDCl_3$, ppm) δ 167.2 (C), 143.6 (C), 138.1 (C), 133.7 (CH), 130.1 (CH), 130.1 (C), 128.3 (CH), 126.7 (CH), 52.0 (CH_3), 21.3 (CH_3). GC-MS (EI) *m/z* (relative intensity): 150 (49) [M^+], 119 (100), 91 (61), spectral data were consistent with literature.[46]

_i_-Propyl 3-methylbenzoate

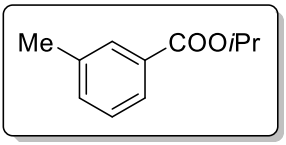

^{1}H NMR (400 MHz, $CDCl_3$, ppm) δ 7.82 – 7.77 (m, 2H), 7.34 – 7.24 (m, 2H), 5.20 (sept, *J* = 6.3 Hz, 1H), 2.36 (s, 3H), 1.32 (d, *J* = 6.3 Hz, 6H). ^{13}C NMR (100 MHz, $CDCl_3$, ppm) δ 166.3 (C), 138.1 (C), 133.5 (CH), 130.9 (C), 130.1 (CH), 128.2 (CH), 126.7 (CH), 68.3 (CH), 22.0 (CH_3), 21.3 (CH_3). GC-MS (EI) *m/z* (relative intensity): 178 (23) [M^+], 136 (45), 119 (100), 91 (79), spectral data were consistent with literature.[47]

_t_-Butyl 3-methylbenzoate

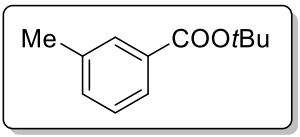

^{1}H NMR (400 MHz, $CDCl_3$, ppm) δ 7.81 – 7.77 (m, 2H), 7.36 – 7.26 (m, 2H), 2.39 (s, 3H), 1.59 (s, 9H). ^{13}C NMR (100 MHz, $CDCl_3$, ppm) δ 166.0 (C), 138.0 (C), 133.2 (CH), 132.0 (C), 130.0 (CH), 128.1 (CH), 126.6 (CH), 80.9 (C), 28.3 (CH_3), 21.4 (CH_3). GC-MS (EI) *m/z* (relative intensity): 192 (3) [M^+], 137 (75), 136 (79), 119 (100), 91 (77), spectral data were consistent with literature.[44]

Methyl 4-methoxybenzoate

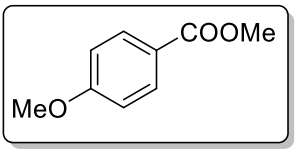

^{1}H NMR (400 MHz, $CDCl_3$, ppm) δ 7.99 (d, *J* = 8.9 Hz, 2H), 6.91 (d, *J* = 8.9 Hz, 2H), 3.88 (s, 3H), 3.85 (s, 3H). ^{13}C NMR (100 MHz, $CDCl_3$, ppm) δ 166.9 (C), 163.4 (C), 131.6 (CH), 122.6 (C), 113.6 (CH), 55.4 (CH_3), 51.9 (CH_3). GC-MS (EI) *m/z* (relative intensity): 166 (42) [M^+], 135 (100), 107 (14), 92 (17), spectral data were consistent with literature.[41]

_i_-Propyl 4-methoxybenzoate

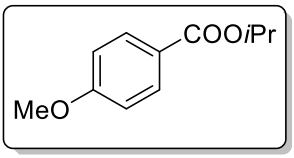

^{1}H NMR (400 MHz, $CDCl_3$, ppm) δ 7.99 (d, *J* = 9.0 Hz, 2H), 6.91 (d, *J* = 9.0 Hz, 2H), 5.22 (sept, *J* = 6.3 Hz, 1H), 3.86 (s, 3H), 1.35 (d, *J* = 6.3 Hz, 6H). ^{13}C NMR (100 MHz, $CDCl_3$, ppm) δ 165.9 (CO), 163.2 (C), 131.5 (CH), 123.4 (C), 113.5 (CH), 68.0 (CH), 55.4 (CH_3), 22.0 (CH_3). GC-MS (EI) *m/z* (relative intensity): 194 (21) [M^+], 179 (7), 152 (48), 135 (100), spectral data were consistent with literature.[43]

_t_-Butyl 4-methoxybenzoate

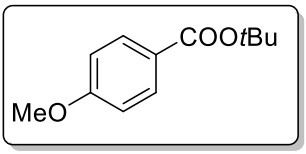

^{1}H NMR (400 MHz, $CDCl_3$, ppm) δ 7.94 (d, *J* = 8.9 Hz, 2H), 6.90 (d, *J* = 8.9 Hz, 2H), 3.85 (s, 3H), 1.58 (s, 9H). ^{13}C NMR (100 MHz, $CDCl_3$, ppm) δ 165.7 (C), 163.0 (C), 131.4 (CH), 124.5 (C), 113.4 (CH), 80.6 (C), 55.5 (CH_3), 28.3 (CH_3). GC-MS (EI) *m/z* (relative intensity): 192 (2) [M^+], 137 (75), 119 (100), 91 (84), spectral data were consistent with literature.[44]

_i_-Propyl 2-methylbenzoate

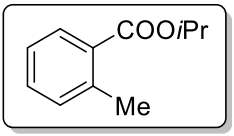

^{1}H NMR (400 MHz, $CDCl_3$, ppm) 7.88 (dd, *J* = 8.1 Hz, *J* = 1.4 Hz, 1H), 7.38 (dt, *J* = 7.6 Hz, *J* = 1.4 Hz, 1H), 7.26 – 7.21 (m, 2H), 5.25 (sept, *J* = 7.3 Hz, 1H), 2.60 (s, 3H), 1.37 (d, J = 7.3 Hz, 6H). ^{13}C NMR (100 MHz, $CDCl_3$, ppm) 167.4 (C), 139.8 (C), 131.7 (CH), 131.6 (CH), 130.5 (C), 130.4 (CH), 125.7 (CH), 68.8 (CH), 22.0 (CH_3), 21.7 (CH_3). GC-MS (EI) *m/z* (relative intensity): 178 (26) [M^+], 136 (60), 119 (84), 118 (100), 91 (65), spectral data were identical were consistent with literature.[43]

Methyl 2-methylbenzoate

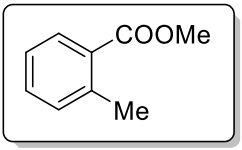

^{1}H NMR (400 MHz, $CDCl_3$, ppm) δ 7.91 (dd, *J* = 8.2 Hz, *J* = 1.4 Hz, 1H), 7.40 (dt, *J* = 7.5 Hz, *J* = 1.4 Hz, 1H), 7.26 – 7.23 (m, 2H), 3.89 (s, 3H), 2.60 (s, 3H). ^{13}C NMR (100 MHz, $CDCl_3$, ppm) δ 168.1 (C), 140.2 (C), 132.0 (CH), 131.7 (CH), 130.6 (CH), 129.6 (C), 125.7 (C), 51.8 (CH_3), 21.7 (CH_3). GC-MS (EI) *m/z* (relative intensity): 150 (62) [M^+], 135 (11), 119 (100), 118 (67), 91 (66), spectral data were consistent with literature.[43]

Methyl benzoate

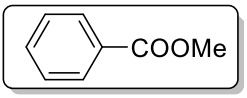

^{1}H NMR (400 MHz, $CDCl_3$, ppm) δ 8.04 (d, *J* = 8.5 Hz, 2H), 7.56 – 7.51 (m, 1H), 7.43 (t, *J* = 7.6 Hz, 2H), 3.91 (s, 3H). ^{13}C NMR (100 MHz, $CDCl_3$, ppm) δ 167.1 (C), 132.9 (CH), 130.2 (C), 129.6 (CH), 128.4 (CH), 52.1 (CH_3). GC-MS (EI) *m/z* (relative intensity): 136 (42) [M^+], 105 (100), 77 (66), 51 (29), spectral data were consistent with literature.[43]

***i*-Propyl benzoate**

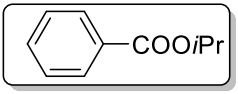

^{1}H NMR (400 MHz, $CDCl_3$, ppm) δ 8.04 (d, *J* = 8.4 Hz, 2H), 7.57 – 7.52 (m, 1H), 7.43 (t, *J* = 7.6 Hz, 2H), 5.26 (sept, *J* = 6.3 Hz, 1H), 1.37 (d, *J* = 6.3 Hz, 6H). ^{13}C NMR (100 MHz, $CDCl_3$, ppm) δ 166.1 (C), 132.7 (CH), 131.0 (C), 129.6 (CH), 128.3 (CH), 68.4 (CH), 22.0 (CH_3). GC-MS (EI) *m/z* (relative intensity): 164 (14) [M^+], 123 (34), 105 (100), 77 (55), spectral data were consistent with literature.[48]

***t*-Butyl benzoate**

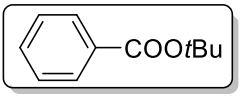

^{1}H NMR (400 MHz, $CDCl_3$, ppm) δ 8.00 (d, *J* = 8.5 Hz, 2H), 7.55 – 7.50 (m, 1H), 7.44 – 7.39 (m, 2H), 1.60 (s, 9H). ^{13}C NMR (100 MHz, $CDCl_3$, ppm) δ 165.8 (C), 132.2 (CH), 132.1 (C), 129.4 (CH), 128.2 (CH), 81.0 (C), 28.2 (CH_3). GC-MS (EI) *m/z* (relative intensity): 178 (0.4) [M^+], 163 (0.7), 123 (90), 105 (100), 77 (91), spectral data were consistent with literature.[44]

***t*-Butyl 4-chlorobenzoate**

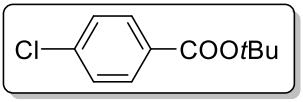

^{1}H NMR (400 MHz, $CDCl_3$, ppm) δ 7.92 (d, *J* = 8.7 Hz, 2H), 7.38 (d, *J* = 8.7 Hz, 2H), 3.85 (s, 3H), 1.59 (s, 9H). ^{13}C NMR (100 MHz, $CDCl_3$, ppm) δ 164.9 (C), 138.8 (C),

130.9 (CH), 130.5 (C), 128.5 (CH), 81.5 (C), 28.2 (CH_3). GC-MS (EI) *m/z* (relative intensity): 159 (13) [M^+], 158 (14), 157 (41), 156 (39), 141 (31), 139 (100), 111 (47), spectral data were consistent with literature.[44]

_t_-Butyl 2-methylbenzoate

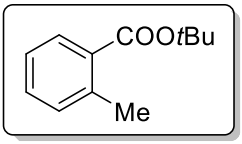

^{1}H NMR (400 MHz, $CDCl_3$, ppm) δ 7.82 (d, *J* = 7.2 Hz, 1H), 7.34 (dt, *J* = 7.4 Hz, *J* = 1.4 Hz, 1H), 7.25 – 7.20 (m, 2H), 2.58 (s, 3H), 1.60 (s, 9H). ^{13}C NMR (100 MHz, $CDCl_3$, ppm) δ 167.3 (C), 139.3 (C), 131.8 (C), 131.5 (CH), 131.3 (CH), 130.3 (CH), 125.6 (CH), 81.0 (C), 28.3 (CH_3), 21.7 (CH_3). GC-MS (EI) *m/z* (relative intensity): 192 (6) [M^+], 136 (83), 119 (100), 118 (86), 91 (71), spectral data were consistent with literature.[44]

2-Ethylhexyl benzoate

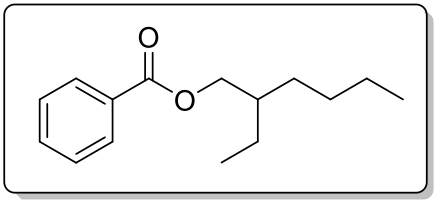

^{1}H NMR (400 MHz, $CDCl_3$, ppm) δ 8.04 (dd, *J* = 8.4, *J* = 1.3 Hz, 2H), 7.58 – 7.53 (m, 1H), 7.47 – 7.42 (m, 2H), 4.29 – 4.20 (m, 2H), 1.73 (sept, J = 6.1 Hz, 1H), 1.51 – 1.26 (m, 8H), 0.95 (t, *J* = 7.5 Hz, 3H), 0.91 (t, *J* = 7.1 Hz, 3H). ^{13}C NMR (100 MHz, $CDCl_3$, ppm) δ 166.8 (C), 132.8 (CH), 130.6 (C), 129.6 (CH), 128.4 (CH), 67.4 (CH_2), 39.0 (CH), 30.6 (CH_2), 29.0 (CH_2), 24.1 (CH_2), 23.0 (CH_2), 14.1 (CH_3), 11.1 (CH_3). GC-MS (EI) *m/z* (relative intensity): 234 (0.2) [M^+], 156 (12), 123 (15), 112 (24), 105 (100), 77 (60), spectral data were consistent with literature.[49]

^{1}H and ^{13}C NMR spectra of selected compounds

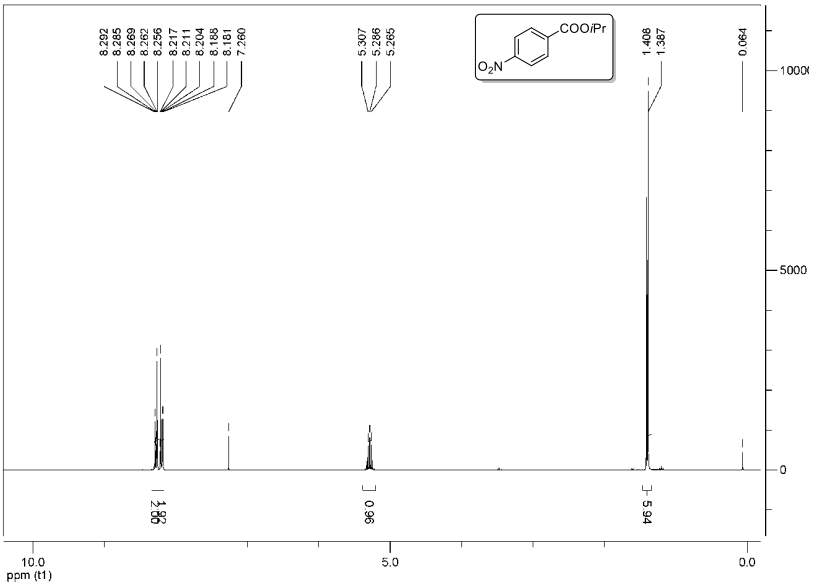

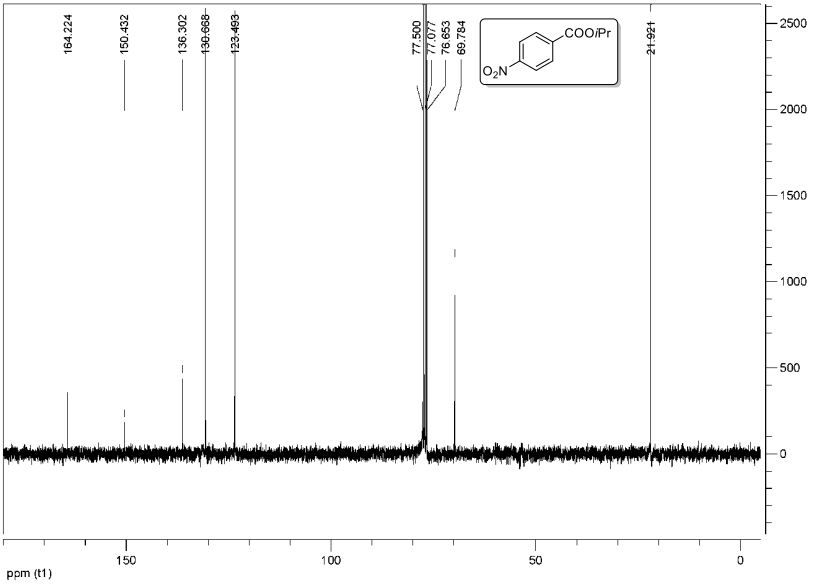

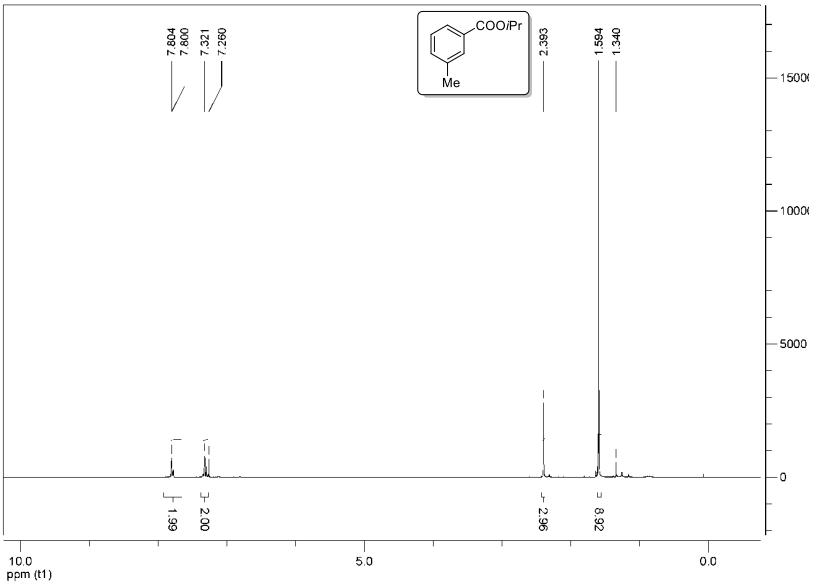
7.804
7.800
7.321
7.260
COO/Pr
Me
2.393
1.584
1.340
1.99
2.00
2.96
8.92
10.0
5.0
0.0
ppm (t1)

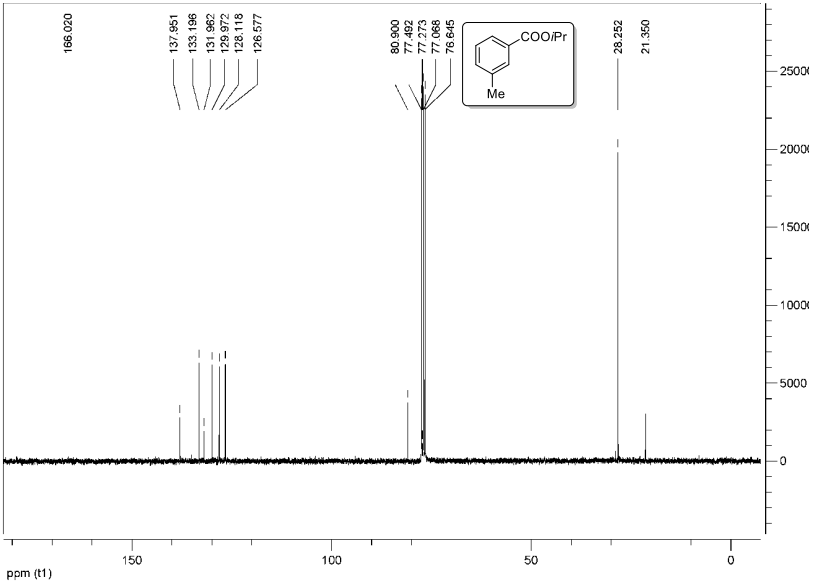
166.020
137.951
133.196
131.962
129.972
128.118
126.577
80.900
77.492
77.273
77.068
76.645
COO/Pr
Me
28.252
21.350
150
100
50
0
ppm (t1)

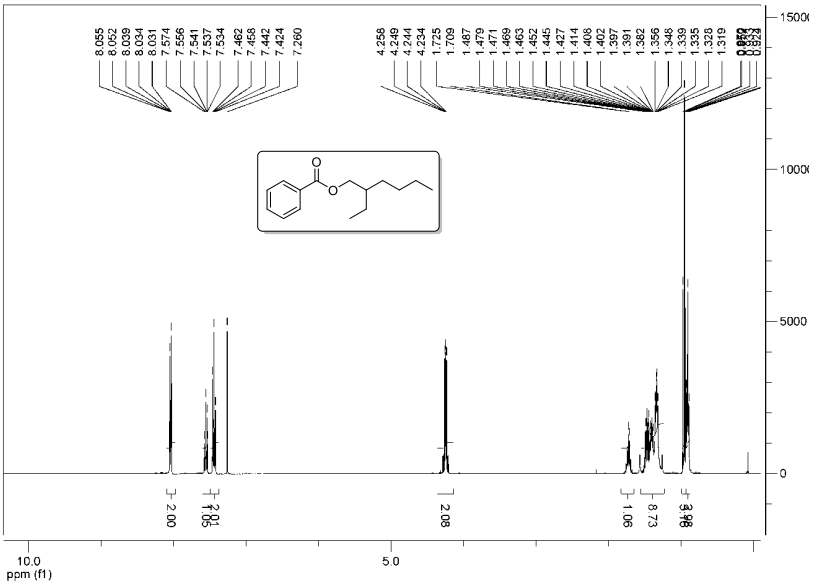
8.055
8.052
8.039
8.034
8.031
7.574
7.556
7.541
7.537
7.534
7.462
7.458
7.442
7.424
7.260
4.258
4.249
4.244
4.234
1.725
1.709
1.487
1.479
1.471
1.469
1.463
1.452
1.445
1.427
1.414
1.408
1.402
1.397
1.391
1.382
1.356
1.348
1.339
1.335
1.328
1.319
2.00
2.01
2.05
2.08
1.06
8.73
3.18
10.0
ppm (f1)
5.0

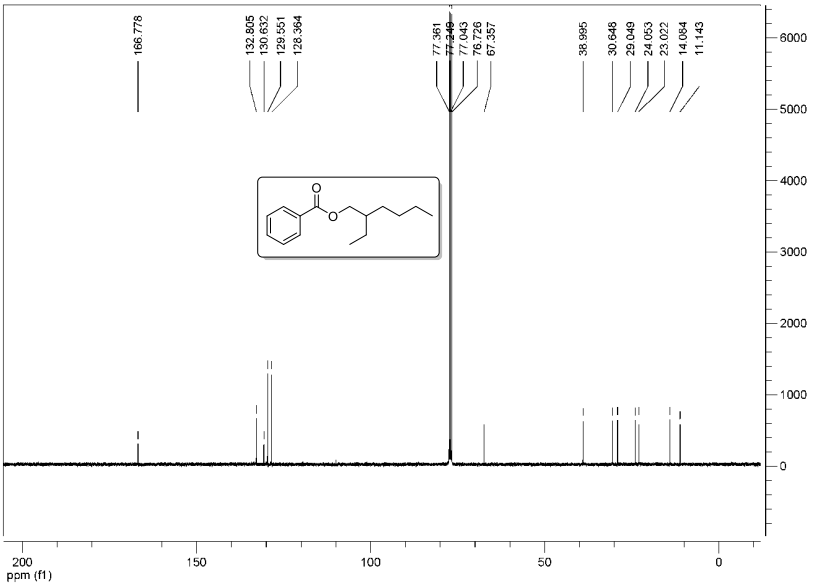
166.778
132.805
130.632
129.551
128.364
77.361
77.043
76.726
67.357
38.995
30.648
29.049
24.053
23.022
14.084
11.143
200
ppm (f1)
150
100
50
0

4.5: References

1: Riemenschneider W., Bolt H. M., In *Ullmann's Encyclopedia of Industrial Chemistry*; Vol. 13, Wiley-VCH, Weinheim, **2005**, 245.

2: Otera J., Nishikido J., *Esterification: Methods, Reactions, and Applications*; 2nd ed., Wiley-VCH, Weinheim, **2010**.

3: Brennführer A., Neumann H., Beller M., *Angew. Chem. Int. Ed.* **2009**, *48*, 4114.

4: a) Magano J., Dunetz J. R., *Chem. Rev.* **2011**, *111*, 2177; b) Colquhoun H. M., Thompson D. J., Twigg M. V., *Carbonylation. Direct Synthesis of Carbonyl Compounds*; Plenum Press, New York, **1991**.

5: Roglans A., Pla-Quintana A., Moreno-Manas M., *Chem. Rev.* **2006**, *106*, 4622.

6: a) Clark J. C., Cookson R. C., *J. Chem. Soc.* **1962**, 686; b) Kikukawa K., Kono K., Nagira K., Wada F., Matsuda T., *J. Org. Chem.* **1981**, *46*, 4413; c) Sengupta S., Sadhukhan S. K., Bhattacharyya S., Guha J., *J. Chem. Soc., Perkin Trans. 1* **1998**, 407. d) Cai M.-Z., Hu R.-H., *Chin. J. Appl. Chem.* **2001**, *18*, 924.

7: Barnard C. F. J., *Organometallics* **2008**, *27*, 5402.

8: Abeywickrema A. N., Beckwith A. L. J., *J. Org. Chem.* **1987**, *52*, 2568.

9: a) Allongue P., Delamar M., Desbat B., Fagebaume O., Hitmi R., Pinson J., Saveant J.-M., *J. Am. Chem. Soc.* **1997**, *119*, 201; b) Combellas C., Jiang D.-E., Kanoufi F., Pinson J., Podvorica F. I., *Langmuir* **2009**, *25*, 286.

10: Chatgilialoglu C., Crich D., Komatsu M., Ryu I., *Chem. Rev.* **1999**, *99*, 1992, 1991.

11: a) Jaynes B. S., Hill C. L., J. Am. Chem. Soc. 1995., 117, 4704; b) Ryu I., Tani A., Fukuyama T., Ravelli D., Montanaro S., Fagnoni M., *Org. Lett.* **2013**, *15*, 2554.

12: Ryu I., Kusano K., Ogawa A., Kambe N., Sonoda N., *J. Am. Chem. Soc.* **1990**, *112*, 452.

13: Nagahara K., Ryu I., Komatsu M., Sonoda N., *J. Am. Chem. Soc.* **1997**, *119*, 5465.

14: Zhang H., Shi R., Ding A., Lu L., Chen B., Lei A., *Angew. Chem. Int. Ed.* **2012**, *51*, 12542.

15: Kawamoto T., Sato A., Ryu I., *Chem. Eur. J.* **2015**, DOI:10.1002/chem.201503164

16: a) Narayanam J. M. R., Stephenson C. R. J., *Chem. Soc. Rev.* **2011**, *40*, 102; b) Zeitler K., *Angew. Chem. Int. Ed.* **2009**, *48*, 9785; c) Schultz D. M., Yoon T. P., *Science* **2014**, *343*, 985; d) Ravelli D., Protti S., Fagnoni M., Albini A., *Curr. Org. Chem.* **2013**, *17*, 2366.

17: Selected examples: a) Kalyani D., McMurtrey K. B., Neufeldt S. R., Sanford M. S., *J. Am. Chem. Soc.* **2011**, *133*, 18566; b) Hari D. P., Schroll P.,

König B., *J. Am. Chem. Soc.* **2012**, *134*, 2958; c) Sahoo B., Hopkinson M. N., Glorius F., *J. Am. Chem. Soc.* **2013**, *135*, 5505.

18: Selected examples: Ru: a) Prier C. K., Rankic D. A., MacMillan D. W. C., *Chem. Rev.* **2013**, *113*, 5322; Ir: b) Noble A., MacMillan D. W. C., *J. Am. Chem. Soc.* **2014**, *136*, 11602; c) Pirnot M. T., Rankic D. A., Martin D. B. C., MacMillan D. W. C., *Science* **2013**, *339*, 1593; d) Zhu S., Das A., Bui L., Zhou H., Curran D. P., Rueping M., *J. Am. Chem. Soc.* **2013**, *135*, 1823; Cu: e) Majek M., Jacobi von Wangelin A., *Angew. Chem. Int. Ed.* **2013**, *52*, 5919; f) Pirtsch M., Paria S., Matsuno T., Isobe H., Reiser O., *Chem. Eur. J.* **2012**, *18*, 7336.

19: Deacon G. B., Patrick J. M., Skelton B. W., Thomas N. C., White A. H., *Aust. J. Chem.* **1984**, *37*, 929.

20: a) Nicewicz D. A., Nguyen T. M., *ACS Catal.* **2014**, *4*, 355; b) Hari D. P., König B., *Chem. Commun.* **2014**, *50*, 6688; c) Ravelli D., Fagnoni M., Albini A., *Chem. Soc. Rev.* **2013**, *42*, 97.

21: a) Okada M., Fukuyama T., Yamada K., Ryu I., Ravelli D., Fagnoni M., *Chem. Sci.* **2014**, *5*, 2893; b) Ryu I., Tani A., Fukuyama T., Ravelli D., Fagnoni M., Albini A., *Angew. Chem. Int. Ed.* **2011**, *50*, 1869.

22: Lu H.-C., Chen H.-K., Cheng B.-M., Kuo Y.-P., Ogilvie J. F., *J. Phys. B: At. Mol. Opt. Phys.* **2005**, *38*, 3693.

23: Hari D. P., König B., *Angew. Chem. Int. Ed.* **2013**, *52*, 4734.

24: K. D. Collins, A. Rühling, F. Glorius, *Nat. Protoc.* **2014**, *9*, 1348.

25: Májek M., Jacobi von Wangelin A., *Chem. Commun.* **2013**, *49*, 5507.

26: Benati L., Leardini R., Minozzi M., Nanni D., Scialpi R., Spagnolo P., Strazzari S., Zanardi G., *Angew. Chem. Int. Ed.* **2004**, *43*, 3598.

27: Wang X., Cuny G. D., Noël T., *Angew. Chem. Int. Ed.* **2013**, *52*, 7860.

28: a) Greene T. W., Wuts P. G. M., *Protective Groups in Organic Synthesis*, Wiley, New York, **1999**

29: Stanley R., *Paint & Coatings Industry* **2001**, *17*, 68.

30: Zipfel E., Grezes J.-R., Seiffert W., Zimmermann H. W., *Histochemistry* **1982**, *75*, 539.

31: Forgacs E., Cserhati T., Oros G., *Environ. Int.* **2004**, *30*, 953.

32: Lewis E. S., Insole J. M., *J. Am. Chem. Soc.* **1964**, *86*, 32.

33: Majek M., Filace F., Jacobi von Wangelin A., *Beilstein J. Org. Chem.* **2014**, *10*, 981.

34: For acyl radicals in different mechanisms, see refs. 10, 21, 28b, and: a) Ryu I., *Chem. Soc. Rev.* **2001**, 30, 16; b) Sumino S., Fusano A., Okai H., Fukuyama T., Ryu I., *Beilstein J. Org. Chem.* **2014**, *10*, 150; c) Kawamoto T., Okada T., Curran

D. P., Ryu I., *Org. Lett.* **2013**, *15*, 2144; d) Fusano A., Sumino S., Nishitani S., Inoue T., Morimoto K., Fukuyama T., Ryu I., *Chem. Eur. J.* **2012**, *18*, 9415.

35: Tanaka M., Fujiwara M., Xu Q., Souma Y., Ando H., Laali K. K., *J. Am. Chem. Soc.* **1997**, *119*, 5100.

36: McClelland R. A., Cozens F. L., Li J., Steenken S., *J. Chem. Soc., Perkin Trans. 2*, **1996**, 1531.

37: Jackson A. H., Lynch P. P., *J. Chem. Soc., Perkin Trans. 2*, **1987**, 1483.

38: Gu L., Jin C., Liu J., *Green Chem.* **2015**, *17*, 3733.

39: a) Baik M.-H., Friesner R. A., *J. Phys. Chem. A* **2002**, *106*, 7407; b) Fu Y., Liu L., Yu H.-Z., Wang Y.-M., Guo Q.-X., *J. Am. Chem. Soc.* **2005**, *127*, 7227.

40: Frisch M. J., Trucks G. W., Schlegel H. B., Scuseria G. E., Robb M. A., Cheeseman J. R., Montgomery Jr. J. A., Vreven T., Kudin K. N., Burant J. C., Millam J. M., Iyengar S. S., Tomasi J., Barone V., Mennucci B., Cossi M., Scalmani G., Rega N., Petersson G. A., Nakatsuji H., Hada M., Ehara M., Toyota K., Fukuda R., Hasegawa J., Ishida M., Nakajima T., Honda Y., Kitao O., Nakai H., Klene M., Li X., Knox J. E., Hratchian H. P., Cross J. B., Adamo C., Jaramillo J., Gomperts R., Stratmann R. E., Yazyev O., Austin A. J., Cammi R., Pomelli C., Ochterski J. W., Ayala P. Y., Morokuma K., Voth G. A., Salvador P., Dannenberg J. J., Zakrzewski V. G., Dapprich S., Daniels A. D., Strain M. C., Farkas O., Malick D. K., Rabuck A. D., Raghavachari K., Foresman J. B., Ortiz J. V., Cui Q., Baboul A. G., Clifford S., Cioslowski J., Stefanov B. B., Liu G., Liashenko A., Piskorz P., Komaromi I., Martin R. L., Fox D. J., Keith T., Al-Laham M. A., Peng C. Y., Nanayakkara A., Challacombe M., Gill P. M. W., Johnson B., Chen W., Wong M. W., Gonzalez C., Pople J. A., *Gaussian 03, Revision A.1*, Gaussian Inc., Pittsburgh, **2003**.

41: Zhang N., Yang R., Zhang-Negrerie D., Du Y., Zhao K., *J. Org. Chem.* **2013**, *78*, 8705.

42: Parham W. E., Jones L. D., *J. Org. Chem.* **1976,** *41*, 2704.

43: Tschaen B. A., Schmink J. R., Molander G. A., *Org. Lett.* **2013**, *15*, 500.

44: Zhang H., Shi R., Ding A., Lu L., Chem B., Lei A., *Angew. Chem. Int. Ed.* **2012***, 51*, 12542.

45: McNulty J., Nair J. J., Robertson A., *Org. Lett.* **2007**, *9*, 4575.

46: Koos P., Polyzos A., O'Brien M., Baxendale I., Ley S. V., *Org. Biomol. Chem.* **2011**, *9*, 6903.

47: Nagaki A., Kim H., Moriwaki Y., Matsuo C., Yoshida J., *Chem. Eur. J.* **2010**, *16*, 11167.

48: Twibanire J. K., Grindley T. B., *Org. Lett.* **2011**, *13*, 2988.

49: Kim B. R., Sung G. H., Ryu K. E., Kim J.-J., Yoon Y.-J., *Bull. Korean Chem. Soc.* **2013**, *34*, 3410.

Chapter 5:

Visible light-driven hydro/deutero defunctionalization of anilines

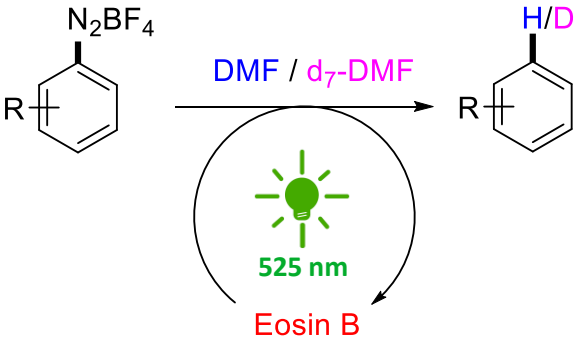

This chapter has been published:
Májek M., Filace F., Jacobi von Wangelin A., *Chem. Eur. J.* **2015**, *21*, 4518. Table 4 and figure 1 were not present in the publication. Further information was added with respect to the aforementioned publication.

Author contributions:
FF did synthesis of the starting materials and carried out the photocatalytic defunctionalizations with DMF. MM did selective deuterations, mechanistic studies, and wrote the manuscript.

5.1: Introduction

Anilines are readily accessible starting materials which constitute key intermediates within numerous organic syntheses. Moreover, the strongly electron-donating amino group can facilitate the introduction of further substituents at the arene.[1] The stereoelectronic directing effect of amino substituents can also be exploited as a temporary tactical tool (Scheme 1). This strategy might require the removal of the amine after the desired amine-directed transformation. The condensation of anilines with nitrosonium salts (to arenediazonium salts) and subsequent reductive substitution of dinitrogen is the most prominent method of aromatic deamination. Such strategy was successfully employed in total syntheses of natural products[2] and many preparations of polyfunctional aromatic building blocks[3] and supramolecular entities.[4] Furthermore, the replacement of the formal hydride reagent in the latter step, the hydrodediazonation, with a deuteride equivalent would provide a straight-forward access to deuterium labelled arenes.[5,6]

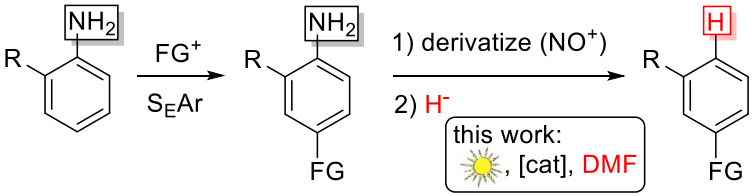

Scheme 1. Synthesis tactic with amine as auxiliary: Use as directing group in arene functionalizations and subsequent removal.

Defunctionalizations of arenediazonium salts were already reported more than 100 years ago within azobenzene dyes research programs. Today, a large variety of dediazonation protocols are available in the literature of which the vast majority of transformations operate by a reductive single-electron transfer mechanism (Scheme 2). The arenediazonium salt accepts one electron (e^-) from a suitable donor which results in the cleavage of the C-N bond and release of the most potent leaving group, dinitrogen (N_2). The formed aryl radical is trapped by the hydrogen atom donor (H· donor) to give the defunctionalized compound. In most cases, the formal electron donor and hydrogen donor moieties are within the same reduction reagent. Traditionally, hypovalent inorganic phosphorus compounds were used as both e^- and $H^\bullet$ donors.[7] Alternative reducing agents include bisulfite,[8] hydrogen peroxide,[9] and alcohols or ethers under basic conditions.[10,11] Tertiary amines can serve as e^- and $H^\bullet$ donors[12] but can also be employed in combination with a more reactive H donor.[13] Organic hydrogen atom and electron donors containing radical-stabilizing heteroatoms

such as hexa-methylphosphoramide (HMPA),[14] formamide,[15] and *N*,*N*-dimethylformamide (DMF)[16,17] have been shown to be especially competent. For the latter, effective combinations with Fe(II) salts as single-electron reductants were also reported.[18]

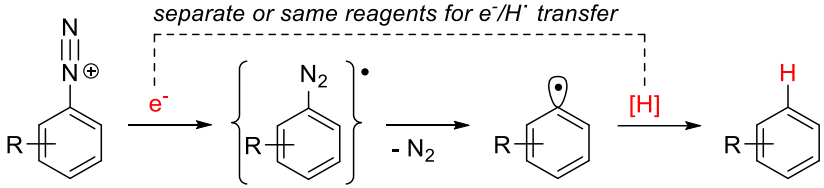

Scheme 2. General mechanism of the hydrodediazonation of arenes.

However, the aforementioned methods suffer from severe drawbacks. The presence of good nucleophiles such as water and alcohols promotes ionic reactions of the electrophilic diazonium salts which result in the formation of unwanted phenols and ethers, respectively. Inorganic reductants mostly exhibit low solubility in organic solvents and often require the employment of super-stoichiometric amounts. From the viewpoint of price, availability, scale-up, substrate solubility, and general handling, the use of DMF appears to be especially attractive. DMF contains seven potential H donor atoms. The major drawbacks of DMF-mediated hydrodediazonation are the incompatibility of the commonly employed Fe(II) co-reductant with several functional groups and the elevated temperatures which also promote C-N bond heterolysis and competitive nucleophilic substitution.[18] The commercial availability of deuterated DMF derivatives (d_1, d_6, and d_7) is an advantage over many alternative methods where the synthesis of deutero-benzenes is limited by the accessibility of a suitable D donor.

Here, we wish to report on an optimized protocol for the reductive dediazonation of arenediazonium salts with DMF which operates under ambient conditions and in the absence of additional reductants. Our strategy utilizes visible light as the most abundant source of energy on the surface of our plant to drive a chemical redox reaction of arenediazonium salts in the presence of a catalytic sensitizer. In recent years, this photocatalytic[19] approach has led to the development of several efficient procedures which involved the generation of aryl radical intermediates and their subsequent reaction with π-electron donors,[20] σ- or n-electron donors.[21] Organometallic sensitizers (mostly Ru, Ir, Cu complexes with pyridine-based ligands) and organic dyes (mostly fluoresceins) have been reported to achieve high synthetic efficacy in various photo-redox catalytic reactions with arenediazonium salts.

5.2: Results and discussion

Initial experiments were performed with 4-methoxybenzene-diazonium tetrafluoroborate in DMF with 2 mol% eosin Y (disodium salt) at room temperature. Gratifyingly, the reaction proceeded smoothly to give the desired product anisole in 90% yield after 3 h (Table 1, entry 1). Shorter reaction times led to low conversion (entries 2-3).

Table 1. Selected catalyst optimization experiments.

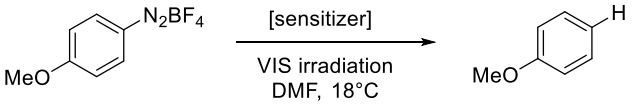

Entry	Sensitizer (mol%)	Time [h]	Yield [%] [a]
1	Eosin Y (2)	3	90
2	Eosin Y (2)	2	89
3	Eosin Y (2)	1	70
4	Rose Bengal (2)	1	37
5	Erythrosin B (2)	1	48
6	Fluorescein (2)	1	51
7	Bromocresol Green (2)	1	11
8 [b]	$[Ru(bpy)_3Cl_2]$ (2)	1	95
9 [b]	$[Ir(ppy)_3]$ (2)	1	30
10	**Eosin B (2)**	**1**	**96**
11	Eosin B (2)	0.5	87
12	Eosin B (2)	0.25	80
13	Eosin B (1.5)	0.5	89
14	**Eosin B (1)**	**0.5**	**91**

Standard conditions: 0.25 mmol 4-anisyldiazonium tetrafluoroborate, sensitizer, 2 mL DMF, 18°C, irradiation with green LED (λ_{max} 525 nm, 3.8 W).
[a] GC yields (vs. internal reference *n*-pentadecane). [b] Irradiation with blue LED (λ_{max} 450 nm, 3.8 W); ppy = 2-phenylpyridine

Among several sensitizers tested, $Ru(bpy)_3Cl_2$ (bpy = 2,2'-bipyridine) and eosin B (2-(4,5-tetrabromo-2,7-dibromo-6-oxido-3-oxo-3*H*-xanthen-9-yl)benzoate) afforded the highest selectivities and allowed for shorter reaction times. In an effort to devise an operationally simple, safe, and low-cost protocol, we proceeded with eosin B as photocatalyst which could be employed in 1 mol% loading. A brief survey of alternative

solvents and additives containing potential H donor motifs vicinal to heteroatoms resulted in no superior hydro-dediazonation system (Table 2). Hydrogen atom donors as trimethylamine and HMPA could be employed as sources of the hydrogen atom, but DMF is superior to them, with concern to its safety profile and price. Concentration of the starting material is also important, as too high concentrations lead to increased amount of radical recombination, generating biaryls.

Table 2. Screening of hydrogen atom donors.

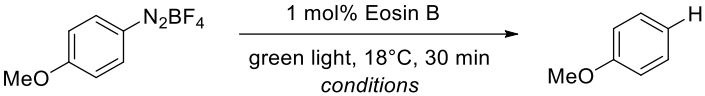

Entry	Solvent	Additive (eq.)	c[ArN_2BF_4] (M)	Yield[%] [a]
1	MeCN	-	0.13	10
2	MeOH	-	0.13	8
3	MeCN	NEt_3 (10)	0.13	39
4	MeCN	DMF (10)	0.13	6
5	MeCN	DMF (20)	0.13	6
6	MeCN	DMF (30)	0.13	8
7	MeCN	HMPA (10)	0.13	81
8	MeCN/DMF (1/1)	-	0.13	27
9	NMP	-	0.13	53
10	**DMF**	**-**	**0.13**	**91**
11	DMF	-	0.25	46
12	DMF	-	0.5	25
13 [b]	DMF	-	0.13	4
14 [c]	DMF	-	0.13	2

Standard conditions: 0.25 mmol 4-anisyldiazonium tetrafluoroborate, 1 mol% eosin B, 2 mL solvent, additive, 18°C, 30 min, irradiation with green LED (λ_{max} = 525 nm, 3.8 W). [a] GC yields (vs. internal reference *n*-pentadecane). [b] No catalyst added. [c] Dark reaction.

Table 3. Substrate scope.

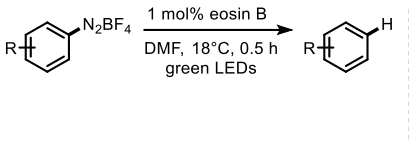

Product	R	Yield [%] [a]	R	Yield [%] [a]
	Cl	87	N_3	99
	Br	98	CO_2Me	88
	Me	95	NO_2	85
	CF_3	97	SH	0
	CN	87	Ph	78
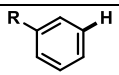	Br	97	Me	78
	Cl	77	NO_2	69
	I	49	OH	0
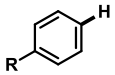	F	90	NO_2	69
	Cl	99	CHO	37
	Br	97	COMe	88
	I	68	SMe	13
	Me	90	OMe	88

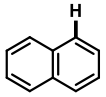
77%

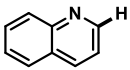
0%


76%

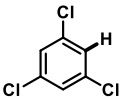
88%

25 mmol arenediazonium tetrafluoroborate, 1 mol% eosin B, 2 mL DMF, 18°C, 30 min, irradiation with green LED (λ_{max} 525 nm, 3.8 W). [a] GC yields (vs. internal reference *n*-pentadecane).

The optimized set of reaction conditions was applied to various substrates (Table 3). The reaction tolerated esters, ketones, ethers, nitriles, halogens, and trifluoromethyl substituents at the arene. Iodine-bearing arenediazonium salts gave somewhat lower yields, presumably due to radical C-I cleavage. Interestingly, the reaction was compatible with an azide substituent. Unprotected OH and SH moieties inhibited conversion, most likely as a consequence of their high nucleophilicity which leads to azo coupling (or other nucleophilic side reactions) and reductive quenching of the excited catalyst. A less pronounced erosion of activity was observed

for thioanisole. The highly electrophilic 2-quinolyldiazonium tetra-fluoroborate underwent rapid decomposition.

Table 4. Comparison to state-of-art procedures. Reported yields are compared to yields obtained by our photocatalytic process (in brackets). PGi = prostaglandin.

	radical initiator	H-donor	time		
(ref. 7)	H_3PO_2 200 eq.	H_3PO_2 200 eq.	~day	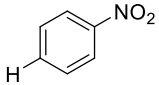 65 (69)	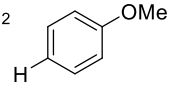 80 (88)
(ref. 10)	$RO^{\ominus}$ 2 eq.	ROH solvent	10 min	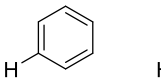 60 (91)	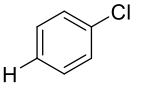 91 (87)
(ref. 16)	65 °C	DMF solvent	10 min	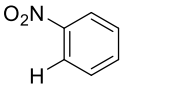 72 (85)	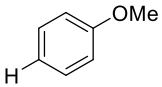 75 (88)
(ref. 18)	$FeSO_4$ 1 eq.	DMF solvent	~minutes	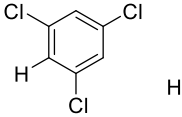 66 (88)	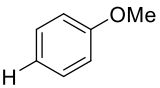 61 (88)
(ref. 12)	NEt_3 slight excess	NEt_3 slight excess	~minutes	only one product ~70%	
(ref. 8)	$NaHSO_3$ 10 eq.	$NaHSO_3$ 10 eq.	~hours	PGi derivatives ~60-80%	

We can compare of our photocatalytic method to the state-of-art reactions for hydrodediazonations (Table 4). Photocatalytic variant is superior in many aspects to the traditional systems - only catalytic amount of radical initiator is used, and cheap and easy to handle hydrogen atom donor is used. Photocatalytic method is more selective, giving often higher yields, than the conventional ones.

We have further probed the feasibility of related deutero-dediazonations in the presence of commercially available d_7-DMF as solvent. Low yields of the monodeutero derivatives were obtained after 30 min (<40% at standard conditions), whereas good

conversions were observed after 8 h (Scheme 3). For all cases, complete deuteration (100% D) at the former ArN_2^+ moiety was determined (NMR, MS) as no other competent H atom source was present in the reaction mixture. This is in stark contrast to previous protocols for arene deuterations which often suffered from poor isotope incorporation due to competitive H atom transfer from other sources.[5,6,22]

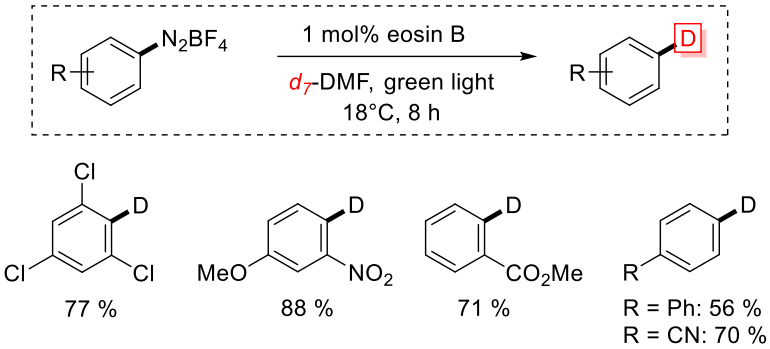

Scheme 3. Deutero dediazonations with d_7-DMF.

The observation of slow conversion of the deuterations prompted us to further investigate the mechanism of H/D atom abstraction and the degree of the kinetic isotope effect (KIE). On the basis of previous studies,[20,21,23] we have proposed the following reaction mechanism (Scheme 4): The photo-excited eosin B (**EB**) effects one-electron reduction of the arene-diazonium salt to give the aryl radical. Hydrogen atom transfer from DMF (**DMF-H**) furnishes the defunctionalized arene **III** and the DMF radical (**DMF$^\bullet$**). Then, bifurcation into two pathways is possible: a) **DMF$^\bullet$** can regenerate the photocatalyst by back electron transfer (photocatalysis), or b) reduce another substrate to the aryl radical (radical chain propagation). It has been shown for related light-mediated reactions that both pathways can be operative, depending on the employed substrates.[23] The **DMF$^+$** ion resulting from both pathways undergoes hydrolysis to volatile products upon work-up.

In order to clarify the operating mechanism, we have determined the quantum yield of the hydrodediazonation reaction. Chemical actinometry with potassium Reineckate (Scheme 4) according to a recently reported procedure[23] gave a quantum yield $\Phi = 2.5 \pm 0.4$ for the hydrodediazonation of 4-anisyl tetrafluoroborate under standard conditions. This value documents significant participation of a radical chain process, even though the average chain lengths are rather short. Further support of the

proposed mechanism was derived from a thermodynamic analysis of the relevant single electron transfer steps.

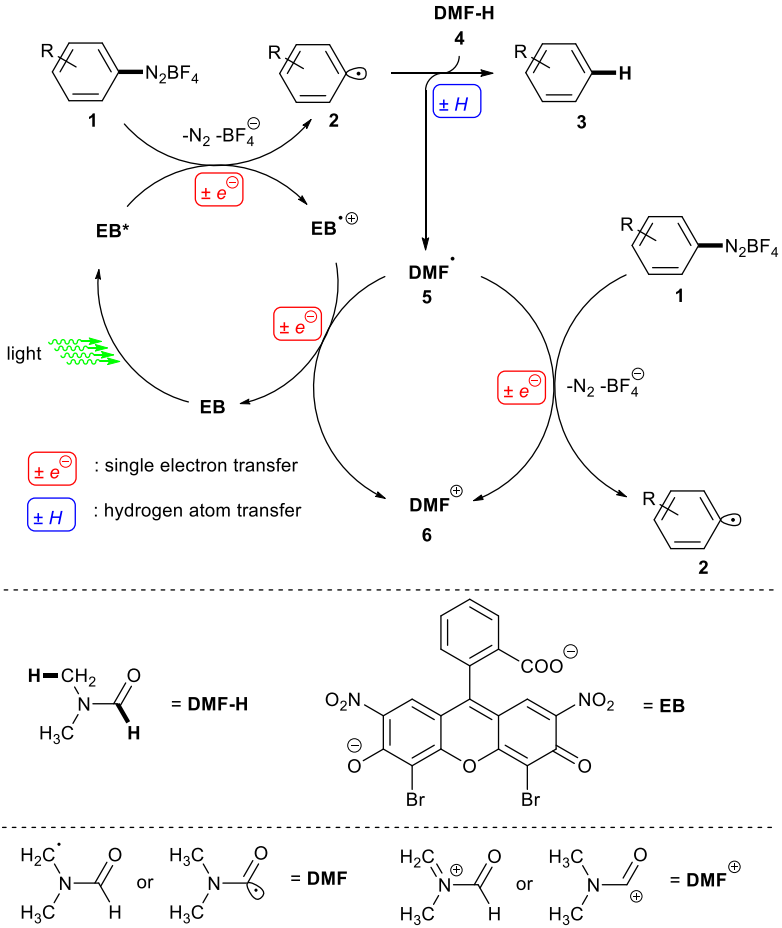

Scheme 4. Mechanism of the photocatalytic dediazonations.

The reduction potentials of most half-reactions were available from literature data.[24] However, the value of the **DMF$^{\bullet}$/DMF^{+}** redox couple is not known and cannot easily be derived from experiments. We have determined this potential from DFT calculations (Details on the calculations are given in the experimental and computational part). Both, the reduction of the arenediazonium salt by photo-excited eosin B and the oxidation of the **DMF$^{\bullet}$** radical by the radical cation **EB$^{+\bullet}$** are thermodynamically feasible processes ($\Delta G = -n \cdot F \cdot \Delta E$). On the other hand, reduction of

arenediazonium salts by **DMF•** is energetically neutral at best, but unfavorable by up to 750 mV for highly electron-rich substrates. While this finding renders a radical chain mechanism mediated by DMF rather unlikely, it is still possible to operate against a moderate potential gradient of appr. 500 mV if the onward- reaction following the electron transfer is rapid.[25] Such mechanism is facilitated by (i) the low uphill potential gradient (<500 mV) of SET reactions between **DMF•** and most arene-diazonium salts (except for 4-biphenyldiazonium tetrafluoro-borate), (ii) the rate and (iii) the irreversibility of the reductive cleavage of the C-N bond due to the gaseous leaving group N_2. Predicted unreactivity of 4-biphenyl salt correlates well with the published results on the hydro-dediazonation in DMF when using Fe(II) salts as electron donors.[18] In this case, most arenediazonium salts could be reduced with sub-stoichiometric amounts of Fe(II) which suggests the operation of a DMF-mediated radical chain process. Full conversion of 4-biphenyl-diazonium salt, however, required stoichiometric Fe(II) probably due to the thermodynamically disfavoured SET. We therefore cannot exclude the occurrence of DMF-mediated radical chain processes for most of the substrates studied here. Summary of the thermodynamic analysis is given below (Scheme 5).

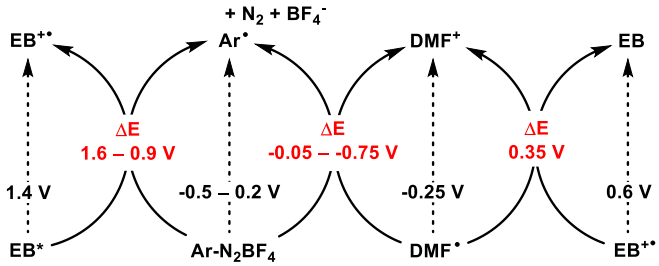

Scheme 5. Redox potentials of SET processes (vs. SCE). $\Delta G = -n \cdot F \cdot \Delta E$.

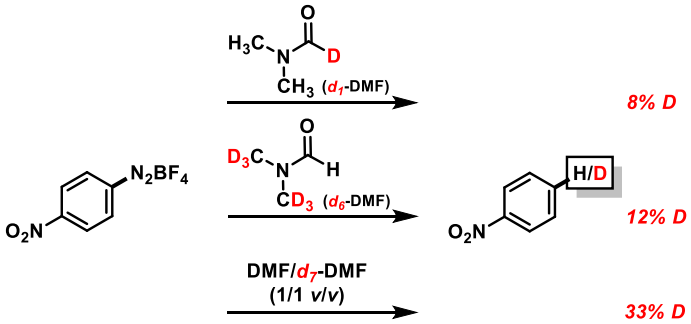

Scheme 6. Isotope labelling with *d*-DMF (1 mol% eosin B, green light, 18°C).

The DMF molecules contains seven potential H atoms which can be transferred to an intermediate aryl radical. In an effort to clarify the chemoselectivity of this process, we have performed isotopic labelling experiments and DFT calculations (further details are given in the experimental and computational part). Dediazonations of 4-nitrobenzenediazonium tetrafluoroborate were performed in partially deuterated DMF. With d_1-DMF (with the D atom in the formyl group, -C**D**O), 8% D incorporation were observed while d_6-DMF (with a perdeuterated -N(C**D**$_3$)$_2$ group) gave 12% D incorporation (Scheme 6). The H/D ratios of the product mirror the relative reactivities of the H donors in DMF. These values translate into a difference of transition state energies of the two competing pathways of $\Delta\Delta G^{\ddagger} = -1.6$ kJ/mol for d_1-DMF (i.e. in favor of N(C**H**$_3$)$_2$ abstraction) and $\Delta\Delta G^{\ddagger} = 9.4$ kJ/mol for d_6-DMF (in favor of C**H**O abstraction). Employment of an equimolar mixture of DMF and d_7-DMF afforded nitrobenzene with 33% incorporation of D into the 4-position from which an average reactivity ratio of 8/1 (DMF vs. d_7-DMF) can be derived.

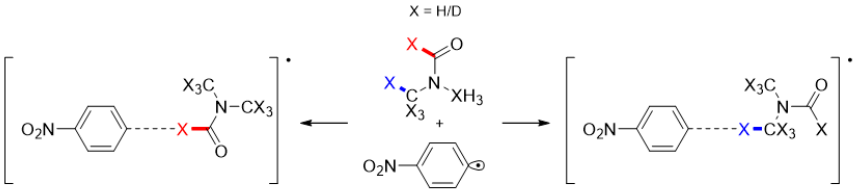

Preferrence of CXO abstraction: $\Delta\Delta G^{\ddagger}$(kJ/mol)

	DFT	experiment
d^1-DMF	- 2.5	- 1.6
d^6-DMF	6.2	9.4

Scheme 7. Transition states of competing formyl-H and methyl-H abstractions.

The relative energies of the transition states can also be deduced from DFT calculations (Scheme 7, details given in the experimental and computational part). In d_6-DMF, abstraction of the formyl-**H** is strongly favoured due to the much lower activation barrier of the corresponding transition state relative to abstraction from the $N(CD_3)_2$ moiety ($\Delta\Delta G^{\ddagger}$ = 6.2 kJ/mol). This selectivity is reversed in d_1-DMF where H donation from the N**Me**$_2$ groups is favoured ($\Delta\Delta G^{\ddagger}$ = 2.5 kJ/mol). This site selectivity is mainly determined by the kinetic isotope effect (KIE) rather than the stereoelectronic properties of both moieties in DMF. The relative transition state energies obtained from DFT calculations correlate very well with the relative reactivities derived from the H/D isotope labelling (see above and Scheme 6), with the H/D abstraction being rate-determining.

5.3: Conclusion

In summary, we have reported a new visible light-driven protocol that allows selective hydro and deutero dediazonations of arenediazonium salts as a key step of deamination strategies. In comparison with conventional processes, no metals or stoichiometric reducing agents are required. Both, electron-rich and electron-deficient aromatic substrates can be converted. The employment of the commercial solvent d_7-DMF allows the synthesis of deuterobenzenes with complete isotopic purity. Mechanistic studies involving chemical actinometry and DFT calculations showed that photocatalytic and radical chain processes are both operative. Isotope labelling experiments and DFT calculations exhibited strong kinetic isotope effects which support the feasibility of H and D donation from the dimethylamino and formyl moieties within DMF and *d*-DMF.

5.4: Experimental and computational part

General methods

Commercial chemicals were used as obtained from Sigma-Aldrich, TCI Europe or Fisher. Solvents were used without further purification. d_1-DMF, d_6-DMF and d_7-DMF were obtained from Deutero GmbH. TLC was performed on commercial silica gel coated aluminium plates (DC60 F254, Merck). Visualization was done with UV light or by staining with phosphomolybdenic acid for UV-inactive compounds. Column chromatography was performed using silica gel (60 Å pore size, Acros Organics) as the stationary phase. Product yields were determined by GC-FID (7820A Agilent) using *n*-pentadecane as internal standard. The purity and structure of isolated compounds were confirmed by ^{1}H NMR, ^{2}D NMR, ^{13}C NMR, and MS spectra and comparison with

authentic samples. NMR spectral data were collected on a Bruker Avance 400 (400 MHz for ^{1}H; 100 MHz for ^{13}C) or on a Bruker Avance 600 (92.1 MHz for ^{2}D) spectrometers at 25 °C. Chemical shifts are reported in δ/ppm, and coupling constants *J* are given in Hertz. Solvent residual peaks were used as internal reference for all NMR measurements. Abbreviations: s – singlet, d – doublet, t – triplet, q – quartet, m – multiplet, dd – doublet of doublet.

General procedure for the synthesis of arenediazonium tetrafluoroborates:

The aniline (4.5 mmol) was dissolved in glacial acetic acid (3 mL) and 48 % aqueous tetrafluoroboric acid (1.3 mL). Then, a solution of iso-amylnitrite (1 mL) in glacial acetic acid (2 mL) was added at room temperature over 5 min. Diethylether (15 mL) was added and the reaction mixture was cooled down to -30 °C in order to induce crystallization of the product. The crystals were filtered off in vacuo, washed with diethylether (2 x 10 mL) and dried on air.

General procedure for the hydrodediazonation:

The arenediazonium tetrafluoroborate (0.25 mmol) and eosin B, disodium salt (3.2 mg, 5 µmol, 2 mol%) were dissolved in DMF (2 mL) in the dark. Nitrogen was bubbled through the solution during vigorous stirring, and the reaction vessel was capped. The solution was subjected to irradiation with green light (LEDs, 3.8 W each, λ_{max} = 525 nm) for 30 min at ambient temperature (18 °C). The end point of the reaction was indicated by the cessation of gas evolution and/or TLC analysis. The reaction mixture was diluted with diethyl ether (5 mL) and washed with water (5 mL). The aqueous layer was extracted with diethyl ether (2 × 5 mL), the organic layers were combined, washed with brine (5 mL), and dried (Na_2SO_4). Products with high boiling points can easily be separated from the solvent DMF by distillation; non-polar arenes can be separated by liquid extraction with pentane. The residues were subjected to SiO_2 flash chromatography to isolate the pure benzenes or deuterobenzenes. For screening purposes, the internal GC standard *n*-pentadecane (20 µL) was added and the yield was determined by quantitative GC-FID.

General procedure for the deutero dediazonation:

The arenediazonium tetrafluoroborate (0.25 mmol) and eosin B, disodium salt (3.2 mg, 5 µmol, 2 mol%) were dissolved in d_7-DMF (0.8 mL) in the dark. Nitrogen was bubbled through the solution during vigorous stirring, and the reaction vessel was capped. The solution was subjected to irradiation with green light (LEDs, 3.8 W each, λ_{max} = 525 nm) for 7 h at ambient temperature (18 °C). The end point of the reaction was indicated by

the cessation of gas evolution and/or TLC analysis. The reaction mixture was diluted with diethyl ether (5 mL) and washed with water (5 mL). The aqueous layer was extracted with diethyl ether (2×5 ml), the organic layers were combined, washed with brine (5 mL), and dried (Na_2SO_4). The solvent was evaporated *in vacuo* and the residue purified by column chromatography (silica gel, eluent: pentane) to obtain the pure deuterated arene.

1,3,5-Trichloro[2-^{2}H]benzene

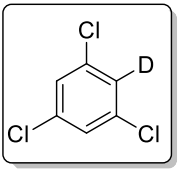

^{1}H NMR (400 MHz, $CDCl_3$, ppm): δ 7.27 (s, 2H); ^{13}C NMR (100 MHz, $CDCl_3$, ppm): δ 135.6 (C), 135.5 (C), 127.2 (CH), 126.9 (t, $^1J_{CD}$ = 26 Hz, CD); ^{2}H NMR (92.1 MHz, CH_3COCH_3, ppm): δ 7.55 (s, 1D); HRMS: calc'd: 180.9363; found: 180.93625, spectral data were consistent with literature.[22]

1-Methoxy-3-nitro[4-^{2}H]benzene

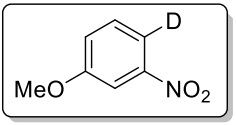

^{1}H NMR (400 MHz, $CDCl_3$, ppm): δ 7.68 (d, $^4J_{HH}$ = 2.5 Hz, 1H), 7.39 (d, $^3J_{HH}$ = 8.3 Hz, 1H), 7.18 (dd, $^3J_{HH}$ = 8.3 Hz, $^4J_{HH}$ = 2.5 Hz, 1H); ^{13}C NMR (100 MHz, $CDCl_3$, ppm): δ 160.2 (C), 149.2 (C), 129.9 (CH), 121.4 (CH), 115.6 (t, $^1J_{CD}$ = 26 Hz, CD) 108.1 (CH); ^{2}H NMR (92.1 MHz, CH_3COCH_3, ppm): δ 7.91 (s, 1D); HRMS: calc'd: 154.0489; found: 154.04864, spectral data were consistent with literature.[29]

Methyl [2-^{2}H]benzoate

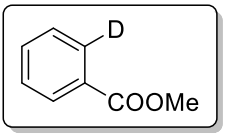

^{1}H NMR (400 MHz, $CDCl_3$, ppm): δ 8.04 (dd, $^3J(H\text{-}H)$ = 8.1 Hz, $^4J(H\text{-}H)$ = 1.2 Hz, 1H), 7.56 (dt, $J^3(H\text{-}H)$ = 7.5 Hz, $^3J_{HH}$ = 1.2 Hz, 1H), 7.45-7.42 (m, 2H), 3.92 (s, 3H); ^{13}C NMR (100 MHz, $CDCl_3$, ppm): δ 167.1 (CO), 132.9 (CH), 130.1 (C), 129.6 (CH),

129.3 (t, $^{1}J_{CD}$ = 25 Hz, CD), 128.4 (CH) 128.3 (CH), 52.1 (CH_3); ^{2}H NMR (92.1 MHz, CH_3COCH_3, ppm): δ 7.91 (s, 1D).

[4-^{2}H]Biphenyl:

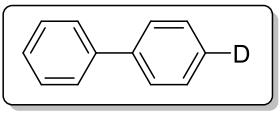

^{1}H NMR (400 MHz, $CDCl_3$, ppm): δ 7.62 (d, $^{3}J_{HH}$ = 8.2 Hz, 4H), 7.49-7.44 (m, 4H), 7.37 (tt, $^{3}J_{HH}$ = 7.4 Hz, $^{3}J_{HH}$ = 1.2 Hz, 1H); ^{13}C NMR (100 MHz, $CDCl_3$, ppm): δ 141.3 (2 C), 128.8 (2 CH), 128.7 (2 CH), 127.3 (CH), 127.2 (4 CH), 127.0 (t, $^{1}J_{CD}$ = 25 Hz, CD); ^{2}H NMR (92.1 MHz, CH_3COCH_3, ppm): δ 7.91 (s, 1D).

Calculation of redox potentials:

All reported values are referenced against SCE. The redox potential of eosin B in its excited state can be obtained from the literature values of the triplet state energy[24d] and from the ground state reduction potential.[24c]

$E_{red}(EB^{\cdot+}/EB(T_1)) = [E(EB(T_1)) - E(EB(S_1))] - E_{red}(EB^{\cdot+}/EB(S_1)) = -1.97 + 0.60\ V = -1.37\ V.$

Redox potentials of the **DMF^{+}/DMF$^{\bullet}$** couples (DMF-based cations **1A** or **1B**; radicals **2A** or **2B**) were not available but were obtained from DFT calculations (Gaussian G03)[26] following a well-precedented method[27] for the estimation of SET redox potentials. The geometries were optimized at the 6-31+G(d,p)/UB3LYP level, single point calculations with aug-cc-pVTZ/UB3LYP. The solvation was considered in both optimizations as well as single point calculations using the PCM model with universal force field radii to approximate the molecule surface. The following values were used to implement DMF as solvent into the PCM model: permittivity = 36.7; solvent radius = 5.04 Å; density = 0.00781 molecules per cubic Ångström. Both forms of DMF-based radical and cation (**1A**, **1B** and **2A**, **2B**) were taken into consideration.

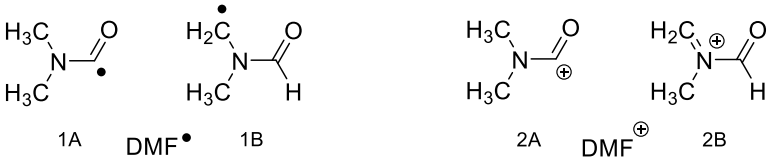

Scheme 8. Calculated structures of DMF-based intermediates

DFT: ΔE(**2A**/**1A**) = 4.44 V; ΔE(**2B**/**1B**) = 4.48 V.

These are absolute values referenced to infinity. Reference against SCE requires abstraction of 4.19 V from these values:[26]

E_{red}(**2A**/**1A**) = 0.25 V; E_{red} (**2B**/**1B**) = 0.29 V.

Calculation of transition state energies:

All DFT calculations were performed using the Gaussian G03 package.[25] Instead of the standard UB3LYP, the UMPW1K functional was used, which has been shown to perform better in cases of proton-coupled electron transfer processes.[27]

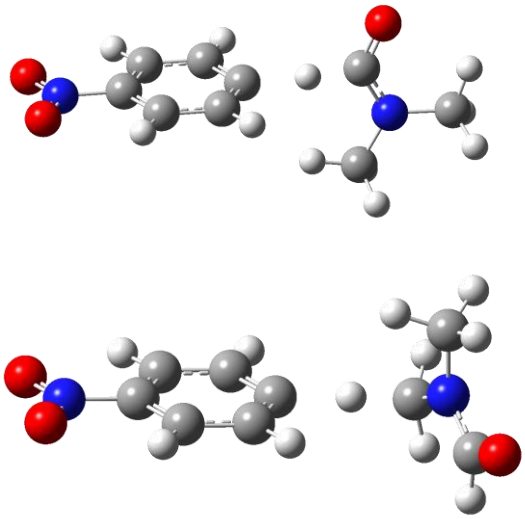

Figure 1. Transition states of CHO- and -NCH_3 hydrogen abstraction

Estimation of isotope incorporation:

For determination of H/D isotope incorporation, *p*-nitrobenzenediazonium tetrafluoroborate was chosen as model system. The H/D ratio was obtained from integration of ^{1}H NMR spectra by comparing signal intensities of the product mixture (nitrobenzene and 4-deuteronitrobenzene at ^{1}H signals at 8.25 ppm and 7.55 ppm, only H) with the resonance of the *para*-CH at 7.71 ppm (H or D). The selectivity of H/D abstraction from DMF were calculated from this ratio.

^{1}H, ^{13}C and ^{2}H NMR spectra of selected compounds

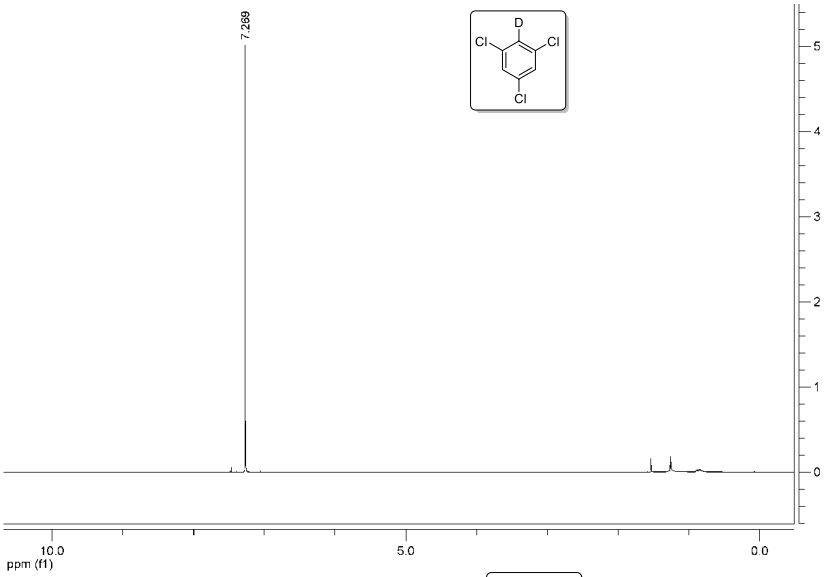

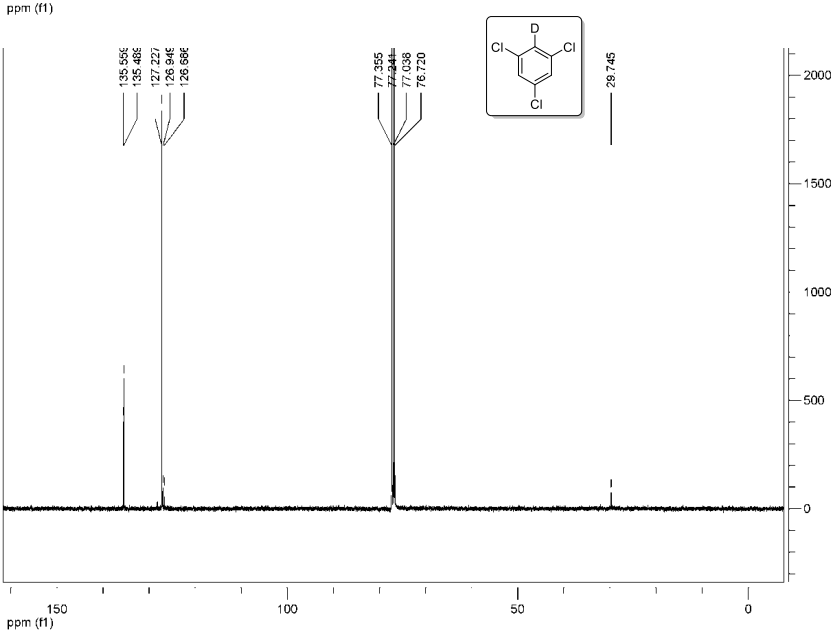

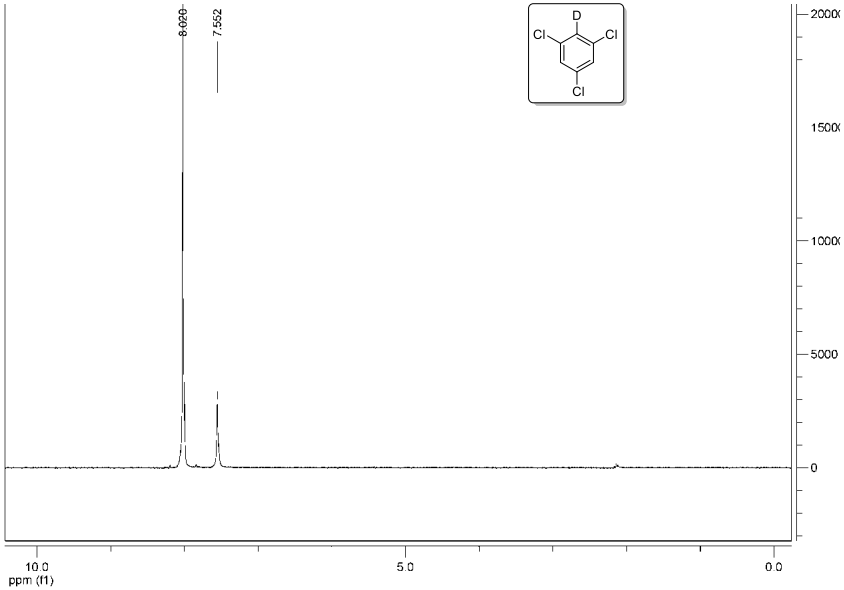
8.020
7.552
D
Cl
Cl
Cl
2000
1500
1000
5000
0
10.0
ppm (f1)
5.0
0.0

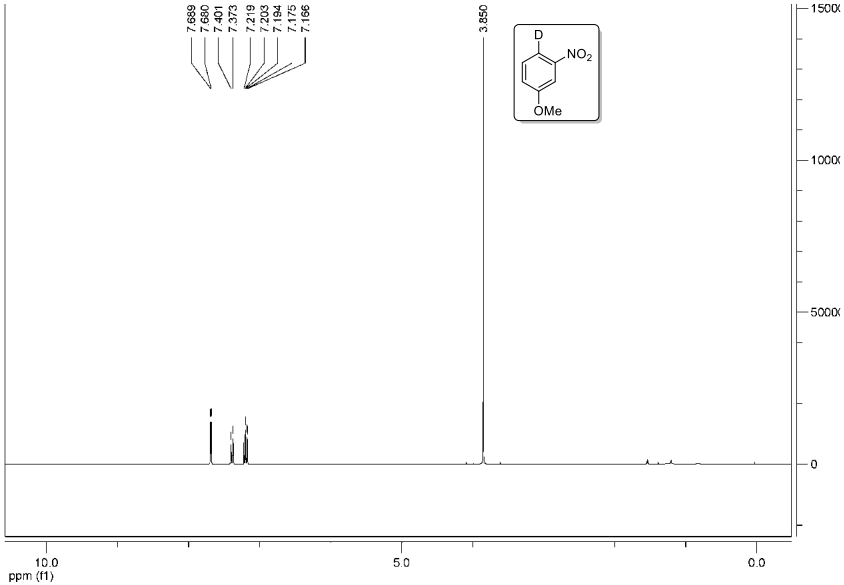
7.689
7.680
7.401
7.373
7.219
7.203
7.194
7.175
7.166
3.850
D
NO2
OMe
1500
1000
5000
0
10.0
ppm (f1)
5.0
0.0

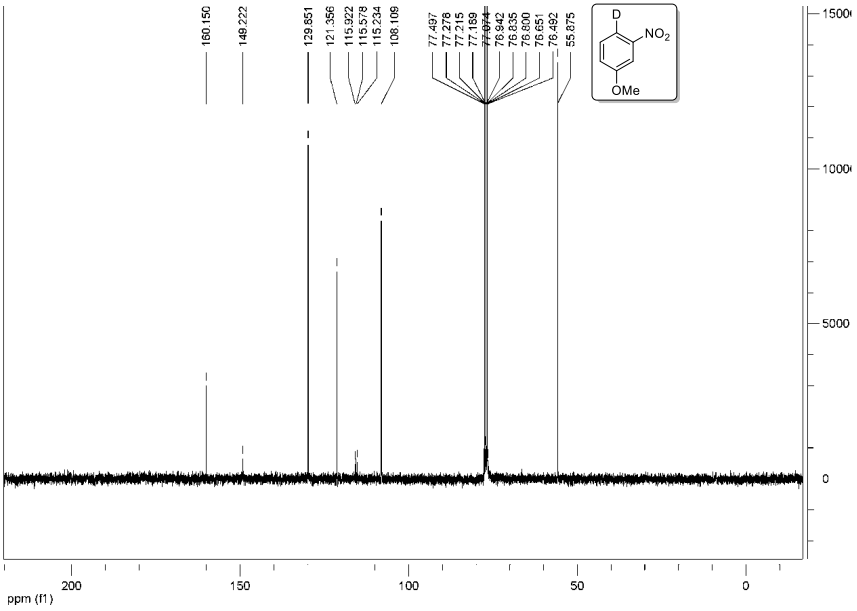
160.150
149.222
129.851
121.356
115.922
115.578
115.234
108.109
77.497
77.278
77.215
77.159
76.842
76.835
76.800
76.651
76.492
55.875
D
NO2
OMe
1500
1000
5000
0
200
150
100
50
0
ppm (f1)

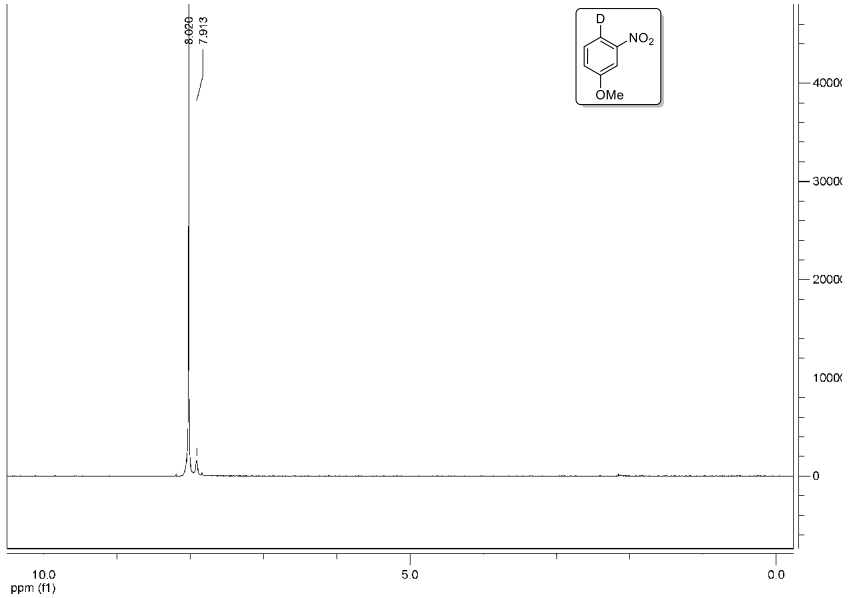
8.020
7.913
D
NO2
OMe
4000
3000
2000
1000
0
10.0
5.0
0.0
ppm (f1)

5.5: References

1. Vogt P. F., Gerulis J. J., in *Ullmann's Encyclopedia of Industrial Chemistry*, Vol. 2, Wiley-VCH, Weinheim, **2000**, pp. 699.
2. a) Gonzalez G. I., Zhu J., *J. Org. Chem.* **1999**, *64*, 914; b) Temal-Laib T., Chastanet J., Zhu J., *J. Am. Chem. Soc.* **2002**, *124*, 583; c) Abrous L., Hynes J., Friedrich S. R., Smith A. B., Hirschmann R., *Org. Lett.* **2001**, *3*, 1089.
3. a) Kubiczak G. A., Oesch F., Borlakoglu J. T., Kunz H., Robertson L. W., *J. Agric. Food Chem.* **1989**, *37*, 1160; b) Teclechiel D., Christiansson A., Bergman Å., Marsh G., *Environ. Sci. Technol.* **2007**, *41*, 7459.
4. a) Fournier J.-H., Maris T., Wuest J. D., *J. Org. Chem.* **2004**, *69*, 1762; b) Almáši M., Zeleňák V., R. Gyepes R., Zukal A., Čejka J., *Colloids Surf. A* **2013**, *437*, 101.
5. Renaud R. N., Kovachic D., Leitch L. C., *Can. J. Chem.* **1961**, *39*, 21.
6. Wassmundt F. W., Kiesman W. F., *J. Labelled Comp. Radiopharm.* **1995**, *36*, 281.
7. Kornblum N., Kelley A. E., Cooper G. D., *J. Am. Chem. Soc.* **1952**, *74*, 3074.
8. Geoffroy O. J., Morinelli T. A., Meier G. P., *Tetrahedron Lett.* **2001**, *42*, 5367.
9. Barbero M., Degani I., Dughera S., Fochi R., *Synthesis* **2004**, *15*, 2386.
10. Bunnett J. F., Takayama H., *J. Org. Chem.* **1968**, *33*, 1924.
11. Meerwein H., Allendörfer H., Beekmann P., Kunert F., Morschel H., Pawellek F., Wunderlich K., *Angew. Chem.* **1958**, *70*, 211.
12. Park K. H., Cho Y. H., *Synth. Commun.* **1996**, *26*, 1569.
13. Kutonova K. V., Trusova M. E., Postnikov P. S., Filimonov V. D., *Russ. Chem. Bull. Int. Ed.* **2012**, *61*, 206.
14. Tröndlin F., Rüchardt C., *Chem. Ber.* **1977**, *110*, 2494.
15. Threadgill M. D., Gledhill A. P., *J. Chem. Soc. Perkin Trans. 1* **1986**, 873.
16. Doyle M. P., Dellaria J. F., Sigfried B., Bishop S. W., *J. Org. Chem.* **1977**, *42*, 3494.
17. Markgraf J. H., Chang R., Cort J. R., Durant J. L., Finkelstein M., Gross A. W., Lavyne M. H., Moore W. M., Petersen R. C., Ross S. D., *Tetrahedron* **1997**, *53*, 10009.
18. Wassmundt F. W., Kiesman W. F., *J. Org. Chem.* **1995**, *60*, 1713.
19. For representative reviews on visible light photocatalysis, see:
    a) Schultz D. M., Yoon T. P., *Science* **2014**, *343*, 985; b) Ravelli D., Protti S., Fagnoni M., Albini A., *Curr. Org. Chem.* **2013**, *17*, 2366; c) Prier C. K., Rankic D. A., MacMillan D. W. C., *Chem. Rev.* **2013**, *113*, 5322; d) Tucker J. W., Stephenson C. R. J., *J. Org. Chem.* **2012**, *77*, 1617; e) Teplý F., *Collect. Czech.*

Chem. Commun. **2011**, *76*, 859; f) Zeitler K., *Angew. Chem. Int. Ed.* **2009**, *48*, 9785.

20. a) Hari D. P., Schroll P., König B., *J. Am. Chem. Soc.* **2012**, *134*, 2958; b) Hari, D. P., Hering T., König B., *Org. Lett.* **2012**, *14*, 5334; c) Hering T., Hari D. P., König B., *J. Org. Chem.* **2012**, *77*, 10347; d) Xiao T., Dong X., Tang Y., Zhou L., *Adv. Synth. Catal.* **2012**, *354*, 3195.
21. a) Májek M., Jacobi von Wangelin A., *Chem. Commun.* **2013**, *49*, 5507; b) Májek M., Jacobi von Wangelin A., *Angew. Chem. Int. Ed.* **2015**, *54*, 2270; c) Wang X., Cuny G. D., Noël T., *Angew. Chem. Int. Ed.* **2013**, *52*, 7860.
22. Rudzki M., Aragones-Alcade M., Dzik W. I., Rodriguez N., Gooßen L. J., *Synthesis* **2012**, *44*, 184.
23. Májek M., Filace F., Jacobi von Wangelin A., *Beilstein J. Org. Chem.* **2014**, *10*, 981.
24. Redox potentials of arenediazonium salts: a) McCreery R. L., Yang H.-H., *Anal. Chem.* **1999**, *71*, 4081; b) Allongue P., Delamar M., Desbat B., Fagebaume O., Hitmi R., Pinson J., Saveant J.-M., *J. Am. Chem. Soc.* **1997**, *119*, 201. Eosin B ground state reduction potential: c) McSkimming A., Colbran S. B., *Chem. Soc. Rev.* **2013**, *42*, 5439. Eosin B tripet energy: d) DeRosa M. C., Crutchley R. J., *Coord. Chem. Rev.* **2002**, *233-234*, 351.
25. a) Steckhan E., *Angew. Chem. Int. Ed.* **1986**, *25*, 683; b) Zhang N., Zeng C., Lam C. M., Gbur R. K., Little R. D., *J. Org. Chem.* **2013**, *78*, 2104.
26. Frisch M. J., Trucks G. W., Schlegel H. B., Scuseria G. E., Robb M. A., Cheeseman J. R., Montgomery Jr. J. A., Vreven T., Kudin K. N., Burant J. C., Millam J. M., Iyengar S. S., Tomasi J., Barone V., Mennucci B., Cossi M., Scalmani G., Rega N., Petersson G. A., Nakatsuji H., Hada M., Ehara M., Toyota K., Fukuda R., Hasegawa J., Ishida M., Nakajima T., Honda Y., Kitao O., Nakai H., Klene M., Li X., Knox J. E., Hratchian H. P., Cross J. B., Adamo C., Jaramillo J., Gomperts R., Stratmann R. E., Yazyev O., Austin A. J., Cammi R., Pomelli C., Ochterski J. W., Ayala P. Y., Morokuma K., Voth G. A., Salvador P., Dannenberg J. J., Zakrzewski V. G., Dapprich S., Daniels A. D., Strain M. C., Farkas O., Malick D. K., Rabuck A. D., Raghavachari K., Foresman J. B., Ortiz J. V., Cui Q., Baboul A. G., Clifford S., Cioslowski J., Stefanov B. B., Liu G., Liashenko A., Piskorz P., Komaromi I., Martin R. L., Fox D. J., Keith T., Al-Laham M. A., Peng C. Y., Nanayakkara A., Challacombe M., Gill P. M. W., Johnson B., Chen W., Wong M. W., Gonzalez C., Pople J. A., *Gaussian 03, Revision A.1*, Gaussian Inc., Pittsburgh, **2003**.
27. Baik M.-H., Friesner R. A., *J. Phys. Chem. A* **2002**, *106*, 7407.

28. a) Lingwood M., Hammond J. R., Hrovat D. A., Mayer J. M., Borden W. T., *J. Chem. Theory Comput.* **2006**, *2*, 740; b) Jing L., Nash J. J., Kenttämaa H. I., *J. Am. Chem. Soc.* **2008**, *130*, 17697-17709.
29. Vanderheiden S, Bulat B., Zevaco T., Jung N., Bräse S., *Chem. Commun*. **2011**, *47*, 9063.

Chapter 6:

Photocatalytic synthesis of pyrazoles

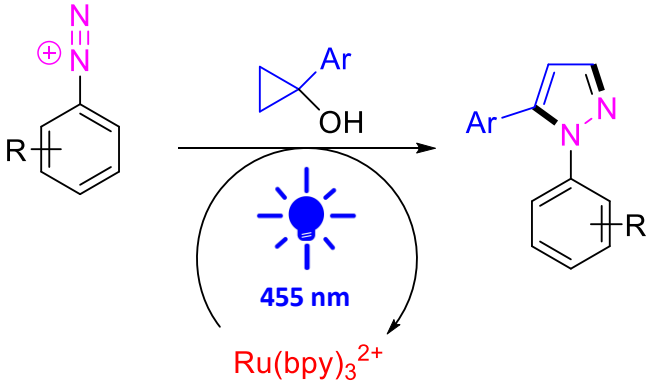

This chapter contains unpublished work

6.1: Introduction

β-Substituted ketones are interesting synthetic intermediates in the synthesis of pharmaceuticals and other fine chemicals, and are often synthesized by Michael-type 1,4-addition to unsaturated carbonyl compounds.[1] Recently, a cooperative photoredox-organocatalytic system was developed, which allows direct β-arylation of ketones.[2] Our aim was to develop a new photocatalytic method, which would not require the co-current organocatalytic steps, leading to β-arylated ketones, possibly by using a different starting material. Inspiration came from the work of Flowers *et al.*[3] In this paper, opening of cyclopropyl alcohols by radicals leads to formation of β-substituted ketones (Scheme 1). They propose a mechanism, where bromide anion is oxidized by superstoichiometric oxidant (CAN), generating bromine radical. Bromine radical attacks cyclopropyl alcohol, to yield stabilized benzylic radical that is again oxidized by the cerium reagent, leading to the desired β-substituted product.

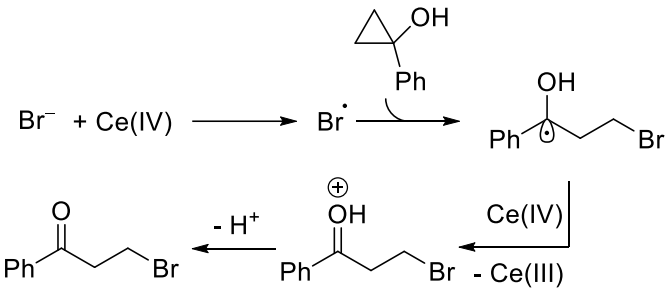

Scheme 1. Synthesis of β-substituted ketones from cyclopropanols.

This work was later followed up by expansion of substrate scope to cyclobutanol substrates, which gave γ-substituted ketones in a similar way.[4] The third, and so far the last publication on this topic was published very recently, and dealt with the expansion of the oxidative strained alcohols-to-ketones strategy to azide, as the anionic source of the attacking radicals, and offered improved oxidation system, using Mn(III) salts to carry on the oxidative steps.[5] Our idea was to replace the oxidation of anions as the source for the attacking radical with some photoredox process, which would deliver the aryl radicals, *e.g.* by reduction of diazonium salts. Oxidized photocatalyst would either oxidize the intermediate stabilized benzylic radical, or get reduced by sacrificial electron donor (SD, *e.g.* triethylamine) (Scheme 2). As the photocatalysts, eosin Y or $Ru(bpy)_3^{2+}$ could be used, as they were already demonstrated as competent catalysis for the generation of aryl radicals from diazonium salts.[6]

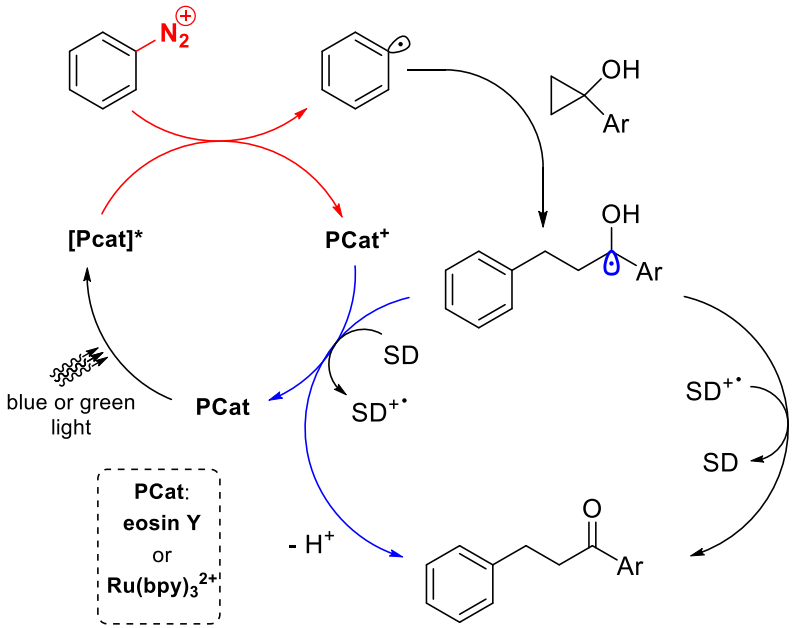

Scheme 2. Envisioned synthesis of β-arylated ketones from cyclopropanols.

In order to probe the viability of our approach, we needed to look for a straightforward route to substituted cyclopropanols. Traditional methods largely fail at the efficient synthesis of cyclopropanols, and their syntheses tended to be tedious multi-step processes.[7] More recently, elegant approaches using Simmons-Smith reagent were discovered, but they require complicated starting materials.[8] Probably the most straightforward method of synthesis of the substituted cyclopropyl alcohols, is the reaction discovered by Kulinkovich *et. al.* in 1989 (Scheme 3).[9] Reaction mechanism of this reaction is as follows:[10] By addition of ethyl-Grignard reagent, Ti(IV) alcoholate is converted to organotitanium compound (**I**). This compound is unstable even at lower temperatures and tends to eliminate ethylene gas, forming titanacycle (**II**). Cyclic compound is in equilibrium with a complex, where ethylene is coordinated to the titanium (**III**). Carboxylate can coordinate to the titanium, leading to the formation of 5-membered ring with titanium (**IV**). Alcoholate is transferred to the titanium center, forming the cyclopropyl ring. Driving force of these transformation is the high oxophilicity of titanium (Ti-O bond energy is 662 kJ/mol,[11] in comparison with the Ti-C bond energy of 435 kJ/mol). Ultimately, both of the alcoholate groups are displaced from titanium by the action of Grignard reagent. Driving force of this step is probably

the difference of pKa's between the Grignard reagent and the alcohol. Product, cyclopropyl alcohol, is obtained on acidic workup of the reaction mixture.

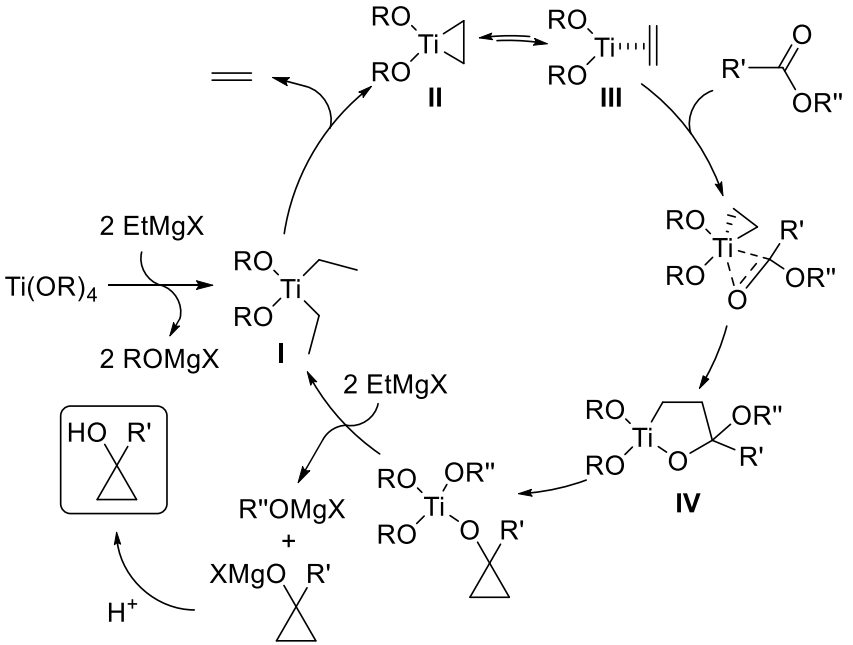

Scheme 3. Mechanism of the Kulinkovich reaction.

As can be inferred from the mechanism, catalytic amount of titanium reagent can be used in theory, and superstoichiometric amount of the Grignard reagent in necessary (at least 2 equivalents and additional amount needed to prepare the catalytically active species **I**). Indeed, the original protocols developed by Kulinkovich called for use of 5-15 mol% of titanium isopropoxide and appr. 2.2 equivalents of the ethyl-Grignard reagent.[9] Nevertheless, procedures where stoichiometric amount of titanium were used, and the active species **I** was preformed before the addition of the substrate (carboxylic ester), were successfully demonstrated as well.[12] When the traditional setup is used, and the catalytic species **I** is formed *in situ* in a reaction mixture already containing the ester R'COOR'', excess of ethyl-Grignard can react with the ester sooner, that the titanium reagent. This way leads to formation of ketones and tertiary alcohols by direct nucleophilic attack on the ester, diminishing the yield. Even worse, structure of the by-products resembles the structure of the desired product (cyclopropanol) so much, that isolation of by-products is often impossible. In order to circumvent this, an elegant modification was proposed recently.[13] In the modified version of the Kulinkovich reaction, methyl-Grignard reagent is added first, followed up

by the ethyl-Grignard reagent. While the methylmagnesium cannot react in the Kulinkovich-fashion, it is more reactive in the nucleophile then the ethylmagnesium, thus forming the by-products instead. Even though the amount of by-products is not diminished this way, they become more structurally different than the desired product, and thereby separable from it. Kulinkovich reaction allows us also to produce cyclopropanols with substitution in the positions 2 and 3 of the cyclopropyl ring. This is done by taking advantage of the equilibrium between **II** and **III**, where in the complex **III**, the ethylene is only loosely bound to the titanium center. Therefore if other alkene is present in the reaction mixture, it can exchange with ethylene as a ligand. Moreover, ethylene escapes the reaction mixture as a gas, pushing the equilibrium in the right direction. This way, further substitution on the cyclopropyl ling can be introduced.[14] Modified versions of Kulinkovich reaction also allow the synthesis of cyclopropyl amines.[15]

6.2: Results and discussion

We have first attempted to develop a reproducible synthesis of 1-arylcyclopropanols, based on the Kulinkovich synthesis. In order to probe the viability of our approach, we needed to look for a straightforward route to substituted cyclopropanols. Results of the optimization are summarized in the following table (Table 1). First attempts to preform the active titanium reagent and use the reagent stoichiometrically, as described in previous literature[12] failed in our hands completely, when no product was detected even on GC-MS, we suspected solubility issues, but product failed to materialize even in more dilute conditions (entry 1,2). Catalytic variant of Kulinkovich reaction was more successful, when under these conditions we could detect some product formation, albeit in an inseparable, complex mixture (entry 3). When the reaction temperature was kept at -78 °C over the whole time of the addition of the Grignard reagent, substantial amount of product was formed (entry 4). While its isolation was possible, significant amount of inseparable impurities were still present in the product. We have determined by GC-MS analysis, that these impurities are propiophenone and 3-phenylpentane-3-ol, products of the direct nucleophilic attack of the Grignard reagent on the ester (Scheme 4).

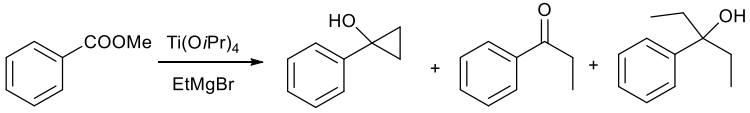

Scheme 4. Formation of impurities in the Kulinkovich reaction.

Table 1. Selected optimization experiments of Kulinkovich cyclopropanol synthesis.

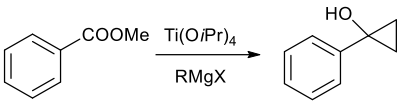

Entry	Ti(O*i*Pr)$_4$	Time/h	Grignard	Yield
1[a]	1.4 eq.	66	2.8 eq. EtMgBr 0 eq. MeMgCl	0
2[b]	1.4 eq.	66	2.8 eq. EtMgBr 0 eq. MeMgCl	0
3[c]	10 mol%	1	2.8 eq. EtMgBr 0 eq. MeMgCl	traces
4[d]	1.0 eq.	2	3.0 eq. EtMgBr 0 eq. MeMgCl	43
5[e]	1.0 eq.	**1.5**	**1.5 eq. EtMgBr** **1.5 eq. MeMgCl**	**46**

[a] Reaction conditions: 0 °C to RT, 4 ml of THF per mmol of substrate; [b] Same conditions as in [a], but 8 ml of THF per mmol of substrate; [c] addition of Grignard reagent and reaction at RT, 4 ml of THF per mmol of substrate.; [d] addition over 1 min at -78 °C, reaction at RT for 1 h, 4 ml of THF per mmol of substrate.; [e] Same conditions as in [d], but addition period shortened to 30 min.

Optimal procedure for the synthesis of cyclopropanols was found to be the modifieid Kulinkovich's protocol,[13] with the use of the sacrificial methylmagnesium (entry 5). This way, product was obtained at 46 % yield, and it could be easily purified by chromatography.

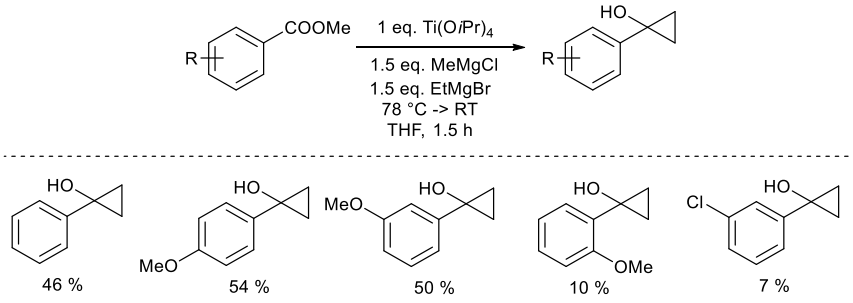

Scheme 5. Substrate scope of the synthesis of 1-arylcyclopropyl alcohols.

Various other substrates were subjected to the optimized conditions, in order to obtain a small library of starting cyclopropanols (Scheme 5). Similar yields as were obtained with the unsubstituted methyl benzoate were also obtained with 4-methoxybenzoate and 3-methoxybenzoate as the substrates. When 2-methoxybenzoate was used, yield drops significantly, supposedly due to the coordination of methoxy- group on the titanium reagent, which hampers the reactivity. Halogen substituents were only poorly tolerated, as we obtained just 7 % of product, when 4-chlorobenzoate was used as a substrate. Attempt to use its bromo-analogue failed completely, as a complex mixture was formed. The same behavior was observed with 4-nitro derivative. This is probably a manifestation of the ability of low-valent titanium reagents to induce SET. Interestingly, when we tried to react methyl propionate and methyl pivalate in our optimal conditions, the desired cyclopropyl product was not formed. In this case the analysis of products was made difficult by their volatility, and further investigations into the structure of the formed products are ongoing.

With the substrates for the photoredox reaction available, we have proceeded to probe them in the envisioned photocatalytic formation of β-arylketones. After 1 day of irradiation, large part of the starting material was converted, and the GC-MS showed its clean conversion to a new product, which we isolated. Much to our surprise, its spectra did not resemble the spectra of the anticipated β-arylketone at all. By using multiple analytical techniques, we were finally able to assign the structure of the unknown product to a substituted N-arylpyrazole (Scheme 6). Structure of the product was proven without doubt by comparing its spectra against its reported spectra.[16] As the such pyrazoles are an interesting synthetic target, and up to this date, there is no photocatalytic reaction for their preparation, we had not discounted the project at this stage, but we changed our target from synthesis of β-arylketones to N-arylpyrazoles.

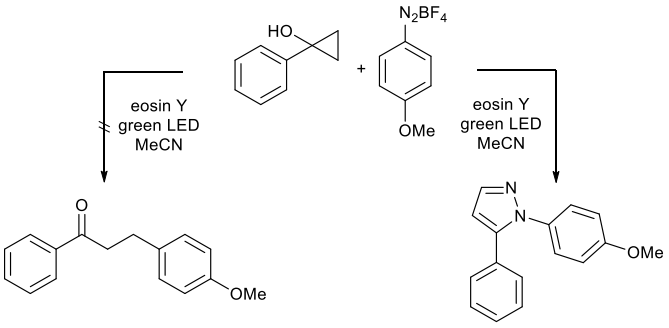

Scheme 6. Unexpected reactivity of 1-phenylcyclopropanol in the photoredox reaction

Table 2. Optimization of the photocatalytic pyrazole synthesis

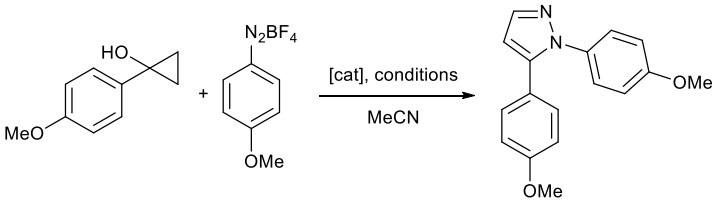

Entry	Catalyst loading	Time/h	Yield
1[a]	2.5 mol%	18	42
2	5 mol%	18	85
3	**5 mol%**	**0.33**	**92**
4	2.5 mol%	0.33	81
5	2.5 mol%	0.15	88
6	0 mol%	0.33	3
7[b]	2.5 mol%	0.33	0

Reaction conditions: cyclopropyl alcohol (0.37 mmol, 1 eq.), diazonium salt (0.56 mmol, 1.5 eq.), $Ru(bpy)_3Cl_2.6H_2O$ (as indicated), RT, blue LED irradiation. [a] eosin Y was used instead of $Ru(bpy)_3Cl_2.6H_2O$ as the photocatalyst, green LED irradiation was used instead of blue. T, 0 °C to RT, 4 ml of THF per mmol of substrate; [b] Reaction was performed in dark.

Short optimization of the reaction conditions was performed (Table 2). Significant increase of yield could be observed, if photoredox catalyst is switched from eosin Y to $Ru(bpy)_3^{2+}$ (entry 1,2). To our delight, this catalyst also allowed dramatic decrease of reaction time, from 18 h to 20 min (entry 3). Alas, lowered catalyst loading had negative impact on the yield (entry 4). Further decrease of reaction time was not possible, as the yields dropped (entry 5). We proceeded to the control experiments. If catalyst is omitted, only traces of product are formed (entry 6), and we have found that much longer reaction times in this case do not improve the yield any further. Traces of product are probably a result of some impurities, which form charge-transfer complex with the diazonium salt. Reaction fails to give any product if the light is omitted (entry 7), proving that the reaction is indeed initiated by light.

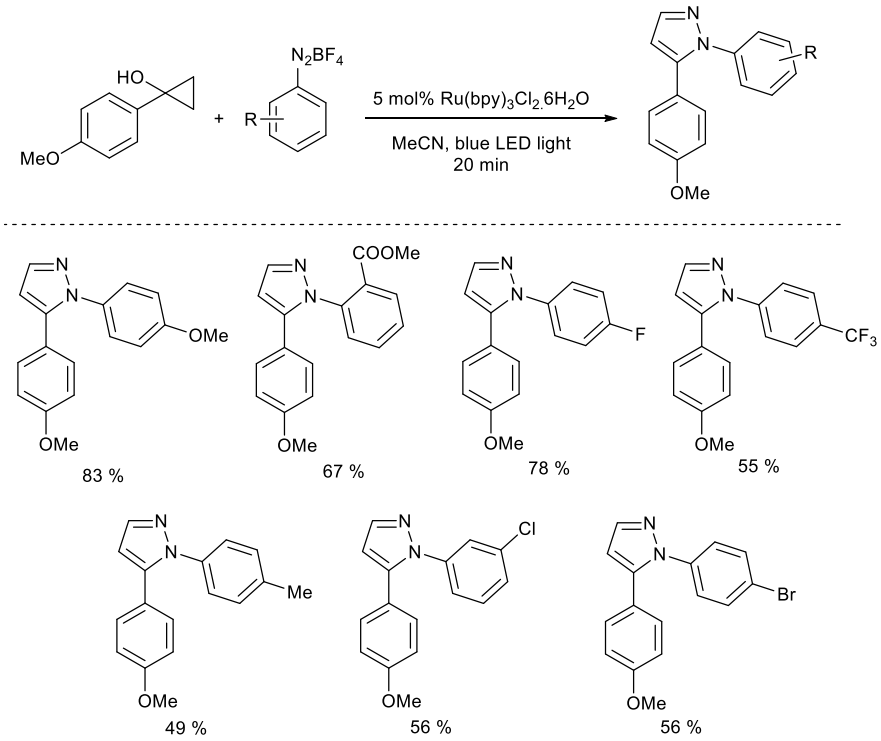

Scheme 6. Substrate scope of the photocatalytic pyrazole synthesis.

With the optimal reaction conditions at hand, substrate screening was performed (Scheme 6). Both electron-withdrawing and electron-accepting substituents on the diazonium salt were tolerated. Substituents could be on any of the positions *o*-, *m*-, *p*-. When we attempted to run the reaction with 1-naphthyldiazonium tetrafluoroborate and with 1-(methylthio)benzenediazonium tetrafluoroborate, products were obtained in poor yields (< 25 %), and they were part of complex mixtures. This is in line with our previous observations, as these two diazonium salts are prone to side reactions in radical conditions.[6c]

In the next step we proceeded to investigate the possible mechanism for this, so far unknown, transformation. The unique characteristic of this reaction is, that the diazo moiety from the diazonium salt is incorporated into the product. While this is not unheard of, it is surprising in photocatalytic conditions. Diazonium salts are oxidative quenchers of photocatalysts such as eosin Y or $Ru(bpy)_3^{2+}$, with quenching rates reaching the diffusion limit.[17] SET leads to formation of aryldiazenyl radical, which is by

no means stable, and readily and irreversibly expels molecule of nitrogen, leaving aryl radical.[18] This points to the fact, that catalyst must be very efficiently quenched by something else, before the diazonium salt would quench it. The only possible entity present in the reaction mixture which could quench the photocatalyst, other than diazonium salt, is the cyclopropyl alcohol. Taken this into account, we have proposed the following mechanism (Scheme 7):

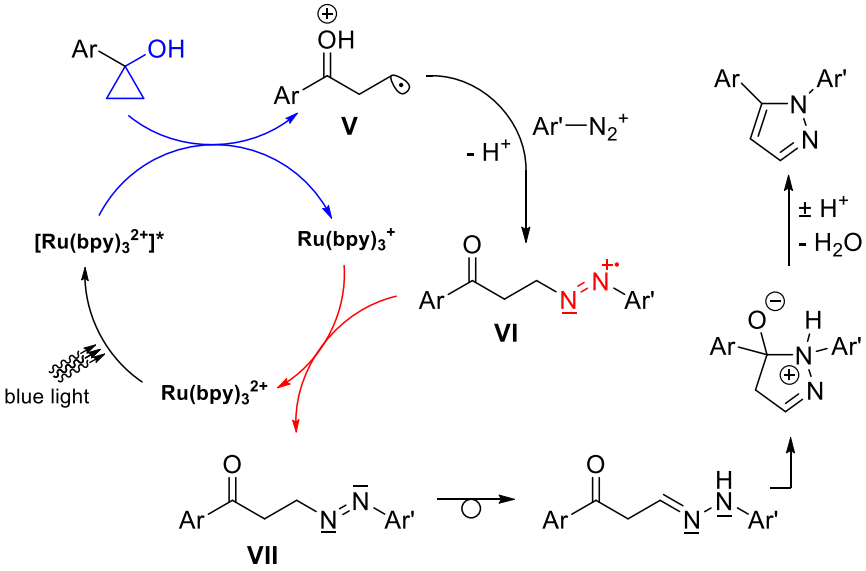

Scheme 7. Proposed mechanism for the photocatalytic pyrazole synthesis

In the first step, cyclopropyl alcohol is oxidized by the photocatalyst. Free alcohols are known to equilibrate with azo-alcohols (Ar-O-N=N-Ar') in presence of diazonium cations.[19] This may help to stabilize the intermediate radical cation **V**. Diazonium cation is electrophilic enough to react with this radical, forming stabilized radical cation **VI**.[20] Photocatalyst is regenerated by back electron transfer, to give azo compound **VII**. This undergoes tautomerization, and the resultant phenylhydrazone cyclizes in an allowed 5-exo-trig cyclization, to ultimately generate the observed pyrazole product.

Efforts to prove this mechanism are ongoing. Both fluorescence quenching and phosphorescence quenching of $Ru(bpy)_3^{2+}$ with reactants will be examined in combination with DFT calculations to clarify the kinetic and thermodynamic aspects of the steps in the proposed mechanism. CV measurements of model compounds will be also performed, in case they are easily available.

6.3: Conclusion

We have optimized conditions for the synthesis of 1-arylcyclopropane-1-oles from benzoates *via* Kulinkovich reaction, by using titanium isopropoxide and Grignard reagents. Small library of substituted cyclopropanols was produced by this method. Produced cyclopropanols were subjected to photoredox catalysis, with diazonium salts as reaction partners. Expected β-arylated propiophenones were not formed, but contrary to the expectations, 5-aryl-N-arylpyrazoles were obtained. Different diazonium salts could be used in this reaction, forming diverse 5-aryl-N-arylpyrazoles. We have proposed mechanism for this transformation, and the mechanistic investigations, both spectroscopic as well as computational, are ongoing. Our goal for the future is to broaden the scope of starting cyclopropanols, also by using ethylene-alkene exchange, to obtain other substituted cyclopropyl alcohols. All the cyclopropyl alcohols will be used in the pyrazole-forming photocatalytic reaction.

6.4: Experimental part

General methods

Commercial chemicals were used as obtained from Sigma-Aldrich, TCI Europe or Fisher. Dry THF was distilled from a ketyl sodium-benzophenone still. Other solvents were used without further purification. TLC was performed on commercial silica gel coated aluminum plates (DC60 F254, Merck). Visualization was done with UV light or by staining with phosphomolybdenic acid for UV-inactive compounds. Column chromatography was performed using silica gel (60 Å pore size, Acros Organics) as the stationary phase. Product yields, which were obtained by GC-FID (7820A Agilent), were referenced to *n*-pentadecane as internal standard. Purity and structure confirmation was done by ^{1}H NMR, ^{13}C NMR, GC-MS, and ^{19}F NMR (where appropriate). NMR spectral data were collected on a Bruker Avance 300 (300 MHz for ^{1}H spectra; 75 MHz for ^{13}C spectra) spectrometer and a Bruker Avance 400 (400 MHz for ^{1}H spectra; 100 MHz for ^{13}C spectra; 376 MHz for ^{19}F spectra) spectrometer at 25 °C. Chemical shifts are reported in δ/ppm, and coupling constant *J* given in Hertz. Solvent residual peak were used as internal reference for all NMR measurements. The number of protons was obtained by integration of appropriate signals. Abbreviations used in NMR spectra: s – singlet, d – doublet, t – triplet, q – quartet, m – multiplet, bs – broad singlet, dd – doublet of doublet, ddd – doublet of doublet of doublet.

General procedure for the synthesis of arenediazonium tetrafluoroborates:

The aniline (4.5 mmol) was dissolved in glacial acetic acid (3 mL) and 48 % aqueous tetrafluoroboric acid (1.3 mL). Then, a solution of iso-amylnitrite (1 mL) in glacial acetic acid (2 mL) was added at room temperature over 5 min. Diethylether (15 mL) was added and the reaction mixture was cooled down to -30 °C in order to induce crystallization of the product. The crystals were filtered off in vacuo, washed with diethylether (2 x 10 mL) and dried on air.

General procedure for the synthesis of 1-arylcyclopropane-1-ols.

$Ti(OiPr)_4$ (2.47 mL, 2.36 g, 8.33 mmol, 1.0 eq.) was added to THF (30 mL). The solution was cooled down to -78 °C and MeMgCl (4.81 mL, 12.5 mmol, 1.5 eq., 2.6 M in THF) was added over 5 min. Subsequently, EtMgBr (4.17 mL, 12.5 mmol, 1.5 eq., 3 M in Et_2O) was added over 20 min, and the now dark brown reaction mixture was stirred for 1 h. Afterwards, respective benzoate (8.33 mmol, 1.0 equiv.) was added to the mixture, again followed by 15 minutes of stirring. The cooling bath was removed, and the mixture was stirred for 1.5 h at room temperature. The mixture was then carefully quenched with cold (0 °C) aqueous H_2SO_4 (125 mL, 10 %) and extracted with Et_2O (3 × 30 mL). The combined organic phases were then washed with saturated aqueous $NaHCO_3$ (20 mL), water (20 mL), and brine (20 mL). Organic phase was separated and dried over $MgSO_4$. Solids were filtered off and volatiles were removed under reduced pressure to afford crude product. The crude product was further purified by flash column chromatography using ethyl acetate/pentane (from 1:20 to 1:6) on a 15 cm silica gel column to obtain pure product.

General procedure for the photocatalytic synthesis of pyrazoles:

A vial was charged with $Ru(bpy)_3Cl_2.6H_2O$ (18.5 µmol, 5 mol %), 1-(4-methoxyphenyl)cyclopropane-1-ol (0.37 mmol, 1 eq.) and the parent diazonium salt (0.56 mmol, 1.5 eq.). Vial was sealed, and subsequently MeCN (5 mL) was added, and the reaction mixture was degassed, by purging with nitrogen over 10 min. in dark. Light was switched on, and the reaction mixture was stirred at RT over 20 min. The reaction mixture was quenched with water (3 mL), extracted with ethyl acetate (3 × 3 mL), washed with water (3 mL), and brine (2 mL). Organic phase was separated, and dried over $MgSO_4$. Solids were filtered off, and the volatiles were removed under reduced pressure to afford viscous oil containing product. The crude product was further purified by column chromatography using ethyl acetate/pentane (1:4) on a silica gel column to afford pure product.

Analytical data of synthesized compounds:

1-Phenylcyclopropan-1-ol

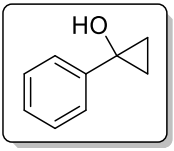

^{1}H NMR (400 MHz, $CDCl_3$, ppm) δ 7.19-7.39 (m, 5H), 2.68 (bs, 1H), 1.24-1.30 (m, 2H), 1.02-1.08 (m, 2H); GC-MS (EI) *m/z* (relative intensity): 134 (16) [M^+], 133 (52), 105 (96), 77 (100), 51 (79); spectral data were consistent with literature.[3]

1-(4-Methoxyphenyl)cyclopropan-1-ol

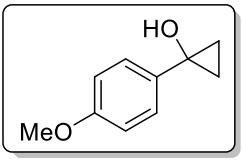

^{1}H NMR (400 MHz, $CDCl_3$, ppm): δ 7.23-7.25 (m, 2H), 6.87 (d, *J* = 9.0 Hz), 3.82 (s, 3H), 2.55 (bs, 1H), 1.20-1.29 (m, 2H), 0.85-0.91 (m, 2H); ^{13}C NMR (100 MHz, $CDCl_3$, ppm): δ 158.4 (C), 136.2 (C), 126.4(CH), 113.8(CH), 56.6 (C), 55.3 (CH_2), 16.7 (CH_2); GC-MS (EI) *m/z* (relative intensity): 164 (100) [M^+], 147 (46), 135 (42); spectral data were consistent with literature.[3]

1-(3-Chlorophenyl)cyclopropan-1-ol

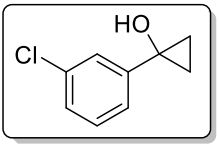

^{1}H NMR (400 MHz, $CDCl_3$, ppm): δ 7.25-7.22 (m, 1H), 7.19-7.14 (m, 2H), 7.06-7.00 (m, 1H), 4.18 (bs, 1H), 1.18-1.21 (m, 2H), 0.93-0.99 (m, 2H); ^{13}C NMR (100 MHz, $CDCl_3$, ppm): δ 146.7 (C), 134.2 (C), 129.6 (CH), 126.3 (CH), 124.6 (CH), 122.3 (CH), 55.8 (C), 18.3 (CH_2); GC-MS (EI) *m/z* (relative intensity): 167 (14) [M^+], 141 (28), 139 (69), 111 (65), 75 (100).

1-(3-Methoxyphenyl)cyclopropan-1-ol

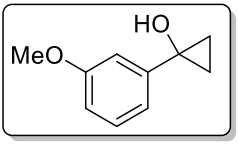

^{1}H NMR (400 MHz, $CDCl_3$, ppm): δ 7.21 (t, *J* = 7.7 Hz, 1H), 6.91 (t, *J* = 2.1 Hz, 1H), 6.78-6.82 (m, 1H), 6.75 (ddd, *J* = 8.2 Hz, *J* = 2.6 Hz, *J* = 0.8 Hz, 1H), 3.91 (bs, 1H), 3.75 (s, 3H), 1.20-1.24 (m, 2H), 0.98-1.01 (m, 2H); ^{13}C NMR (100 MHz, $CDCl_3$, ppm): δ 159.6 (C), 146.5 (C), 129.3 (CH), 116.7 (CH), 111.6 (CH), 110.6 (CH), 56.1 (C), 55.2 (CH_3), 18.1 (CH_2); GC-MS (EI) *m/z* (relative intensity): 164 (31) [M^+], 133 (98), 107 (33), 111 (65), 77 (100); spectral data were consistent with literature.[21]

1-(2-Methoxyphenyl)cyclopropan-1-ol

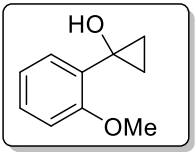

^{1}H NMR (400 MHz, $CDCl_3$, ppm): δ 7.21-7.31 (m, 2H), 6.90-6.95 (m, 2H), 3.92 (s, 3H), 3.56 (bs, 1H), 1.11-1.15 (m, 2H), 0.91-0.95 (m, 2H).; ^{13}C NMR (100 MHz, $CDCl_3$, ppm): δ 158.5 (C), 130.4 (C), 128.9 (CH), 127.5 (CH), 120.6 (CH), 110.6 (CH), 55.5 (CH), 55.3 (C), 13.6 (CH_2); GC-MS (EI) *m/z* (relative intensity): 164 (96) [M^+], 135 (100), 139 (69), 107 (27), 77 (87); spectral data were consistent with literature.[21]

1,5-Bis(4-methoxyphenyl)-1H-pyrazole

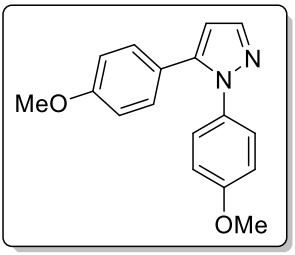

^{1}H NMR (400 MHz, $CDCl_3$, ppm): δ 7.67 (d, *J* = 1.6 Hz, 1H), 7.11-7.25 (m, 4H), 6.79-6.89 (m, 4H), 6.43 (d, *J* = 1.9 Hz, 1H), 3.80 (s, 3H), 3.79 (s, 3H); ^{13}C NMR (100 MHz, $CDCl_3$, ppm): δ 159.4 (C), 158.7 (C), 142.8 (C), 139.8 (CH), 133.4 (C), 130.0 (CH), 126.6 (CH), 123.0 (C), 114.0 (CH), 113.9 (CH), 106.8 (CH), 55.5 (CH_3), 55.3 (CH_3); GC-MS (EI) *m/z*

(relative intensity): 280 (100) [M+], 281 (73), 265 (36); spectral data were consistent with literature.[22]

5-(4-Methoxyphenyl)-1-(p-tolyl)-1H-pyrazole

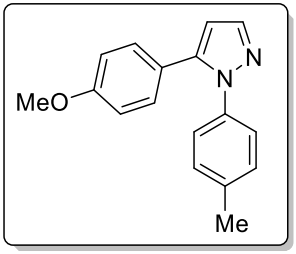

^{1}H NMR (400 MHz, $CDCl_3$, ppm): δ 7.68 (d, *J* = 1.8 Hz, 1H), 7.11-7.20 (m, 6H), 6.81 (d, *J* = 8.8 Hz, 4H), 6.43 (d, *J* = 1.9 Hz, 1H), 3.79 (s, 3H), 2.35 (s, 3H); ^{13}C NMR (100 MHz, $CDCl_3$, ppm): δ 159.5 (C), 142.8 (C), 140.0 (CH), 137.8 (C), 137.3 (C), 130.0 (CH), 129.5 (CH), 125.1 (CH), 123.1 (C), 113.9 (CH), 107.1 (CH), 55.3 (CH_3), 21.2 (CH_3); GC-MS (EI) *m/z* (relative intensity): 264 (100) [M+], 249 (36), 102 (36), 91 (71), 89 (56), 76 (43), 65 (92), 63 (45), 51 (30); spectral data were consistent with literature.[24]

5-(4-Methoxyphenyl)-1-(4-(trifluoromethyl)phenyl)-1H-pyrazole

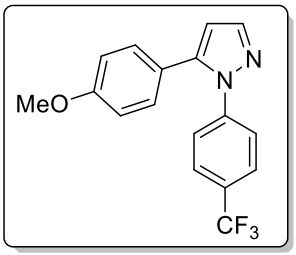

^{1}H NMR (400 MHz, $CDCl_3$, ppm): δ 7.73 (d, *J* = 1.8 Hz, 1H), 7.58 (d, *J* = 8.8 Hz, 2H), 7.43 (d, *J* = 8.8 Hz, 2H), 7.15 (d, *J* = 8.6 Hz, 2H), 6.87 (d, *J* = 8.8 Hz, 2H), 6.47 (d, *J* = 1.9 Hz, 1H), 3.82 (s, 3H); ^{13}C NMR (100 MHz, $CDCl_3$, ppm): δ 159.9 (s, C), 143.2 (s, C), 142.9 (q, *J* = 1.2Hz , C), 141.1 (s, CH), 130.2 (s, CH), 129.0 (q, *J* = 32.6 Hz ,CH), 126.1 (q, *J* = 3.8 Hz ,CH), 124.8 (s, CH), 123.9 (q, *J* = 273 Hz, C), 122.5 (s, C), 114.2 (s, CH), 108.4 (CH), 55.4 (s, CH_3); ^{19}F NMR (376 MHz, $CDCl_3$, ppm) δ -62.9 (s, 3F); GC-MS (EI) *m/z* (relative intensity): 318 (48) [M+], 145 (45), 102 (38), 69 (100), 63 (39); spectral data were consistent with literature.[23]

Methyl 2-(5-(4-methoxyphenyl)-1H-pyrazol-1-yl)benzoate

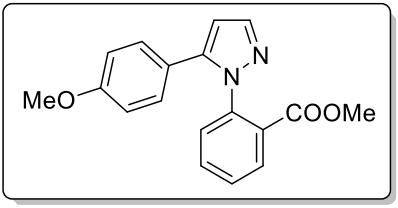

^{1}H NMR (400 MHz, $CDCl_3$, ppm): δ 7.85 (dd, *J* = 7.7 Hz, *J* = 1.6 Hz, 1H), 7.70 (d, *J* = 1.8 Hz, 1H), 7.50 (dt, *J* = 7.7 Hz, *J* = 1.7 Hz, 1H), 7.43 (dt, *J* = 7.6 Hz, *J* = 1.3 Hz, 1H), 7.30 (dd, *J* = 7.8 Hz, *J* = 1.2 Hz, 1H), 7.10 (d, *J* = 8.7 Hz, 2H), 6.77 (d, *J* = 8.7 Hz, 2H), 6.45 (d, *J* = 1.9 Hz, 1H), 3.76 (s, 3H), 3.63 (s, 3H); ^{13}C NMR (100 MHz, $CDCl_3$, ppm): δ 166.2 (CO), 159.5 (C), 144.1 (C), 140.2 (CH), 139.6 (C), 132.3 (CH), 130.7 (CH), 129.8 (CH), 129.2 (C), 128.7 (CH), 128.4 (CH), 122.5 (C), 113.9 (CH), 106.2 (CH), 55.2 (CH_3), 52.4 (CH_3).

1-(4-fluorophenyl)-5-(4-methoxyphenyl)-1H-pyrazole

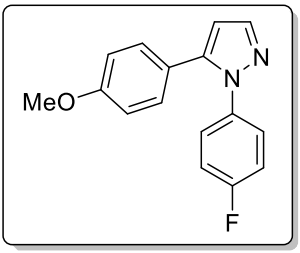

^{1}H NMR (400 MHz, $CDCl_3$, ppm): δ 7.68 (d, *J* = 1.8 Hz, 1H), 7.26-7.30 (m, 2H), 7.13 (d, *J* = 8.6 Hz, 2H), 7.02 (t, *J* = 8.6 Hz, 2H), 6.83 (d, *J* = 8.8 Hz, 2H), 6.44 (d, *J* = 1.8 Hz, 1H), 3.80 (s, 3H); ^{13}C NMR (100 MHz, $CDCl_3$, ppm): δ 161.6 (d, *J* = 248 Hz, C), 159.7 (s, C), 143.0 (s, C), 140.3 (s, CH), 136.4 (d, *J* = 3.0 Hz, C), 130.1 (s, CH), 126.9 (d, *J* = 8.7 Hz, CH), 122.7 (s, C), 115.8 (d, J= 23.0 Hz, CH), 114.0 (s, CH), 107.3 (s, CH), 55.3 (s, CH_3); ^{19}F NMR (376 MHz, $CDCl_3$, ppm) δ -114.2 (s, F); spectral data were consistent with literature.[22]

1-(3-Chlorophenyl)-5-(4-methoxyphenyl)-1H-pyrazole

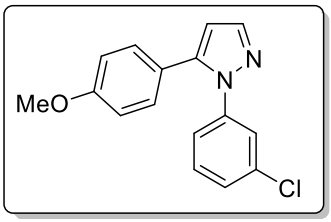

^{1}H NMR (400 MHz, $CDCl_3$, ppm): δ 7.70 (d, *J* = 1.8 Hz, 1H), 7.43 (t, *J* = 1.8 Hz, 1H), 7.08 - 7.28 (m, 4H), 6.85 (d, *J* = 8.9 Hz, 2H), 6.44 (d, *J* = 1.8 Hz, 1H), 3.81 (s, 3H), 2.35 (s, 3H); ^{13}C NMR (100 MHz, $CDCl_3$, ppm): δ 159.8 (C), 143.1 (C), 141.1 (C), 140.6 (CH), 134.6 (C), 130.1 (CH), 129.8 (CH), 127.5 (CH), 125.3 (CH), 123.2 (CH), 122.5 (C), 114.1 (CH), 107.9 (CH), 55.3 (CH_3); GC-MS (EI) *m/z* (relative intensity): 284 (53) [M+], 111 (53), 102 (45), 89 (40), 76 (41), 75 (100), 62 (55), 51 (30).

1-(4-bromophenyl)-5-(4-methoxyphenyl)-1H-pyrazole

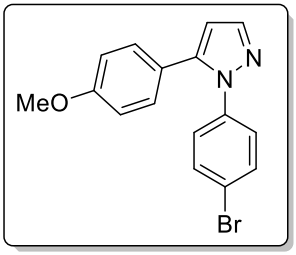

^{1}H NMR (400 MHz, $CDCl_3$, ppm): δ 7.70 (d, *J* = 1.8 Hz, 1H), 7.45 (d, *J* = 8.8 Hz, 2H), 7.18 (d, *J* = 8.8 Hz, 2H), 7.14 (d, *J* = 8.8 Hz, 2H), 6.86 (d, *J* = 8.8 Hz, 2H), 6.44 (d, *J* = 1.8 Hz, 1H), 3.81 (s, 3H); ^{13}C NMR (100 MHz, $CDCl_3$, ppm): δ 159.7 (C), 143.0 (C), 140.6 (CH), 139.2 (C), 132.0 (CH), 130.1 (CH), 126.6 (CH), 122.7 (C), 121.0 (C), 114.1 (CH), 107.8 (CH), 55.4 (CH_3); GC-MS (EI) *m/z* (relative intensity): 330 (28) [M+], 328 (46), 205 (21), 157 (23), 102 (75), 89 (62), 76 (95), 75 (100), 64 (83), 50 (78).

^{1}H, ^{13}C and ^{19}F NMR spectra of selected compounds

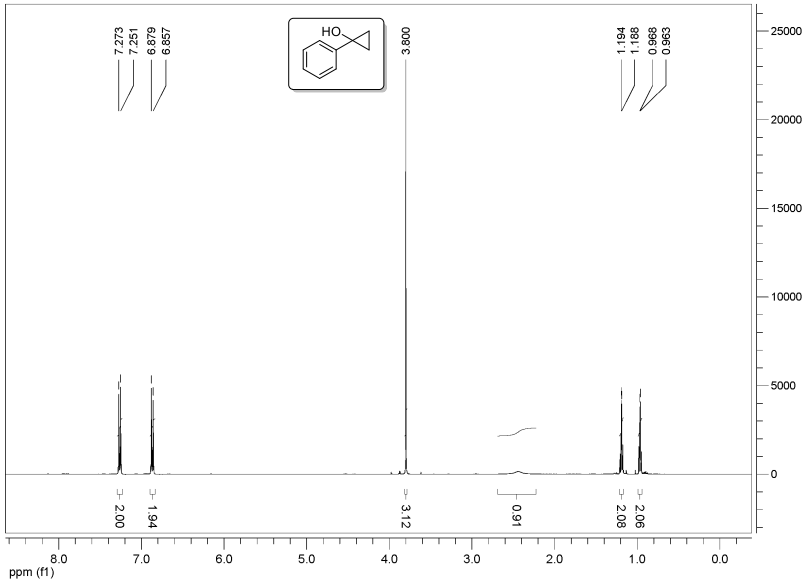

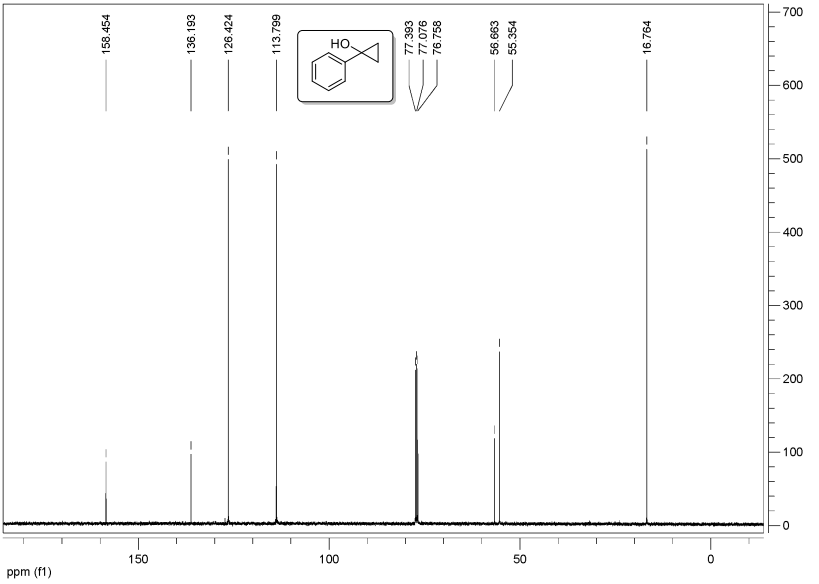

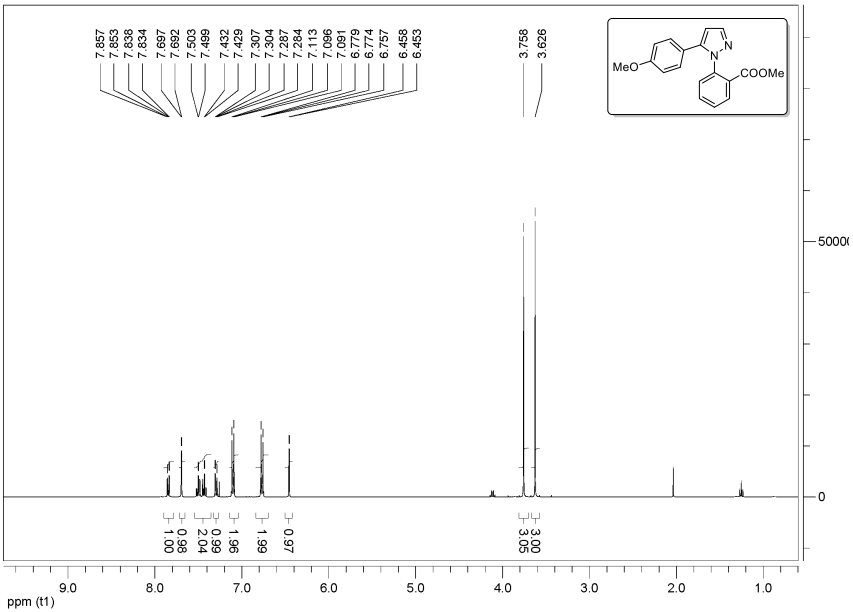
7.857
7.853
7.838
7.834
7.697
7.692
7.503
7.499
7.432
7.429
7.307
7.304
7.287
7.284
7.113
7.096
7.091
6.779
6.774
6.757
6.458
6.453
3.758
3.626
MeO
N
N
COOMe
5000
0
1.00
0.98
2.64
0.99
1.96
1.99
0.97
3.05
3.00
9.0
8.0
7.0
6.0
5.0
4.0
3.0
2.0
1.0
ppm (t1)

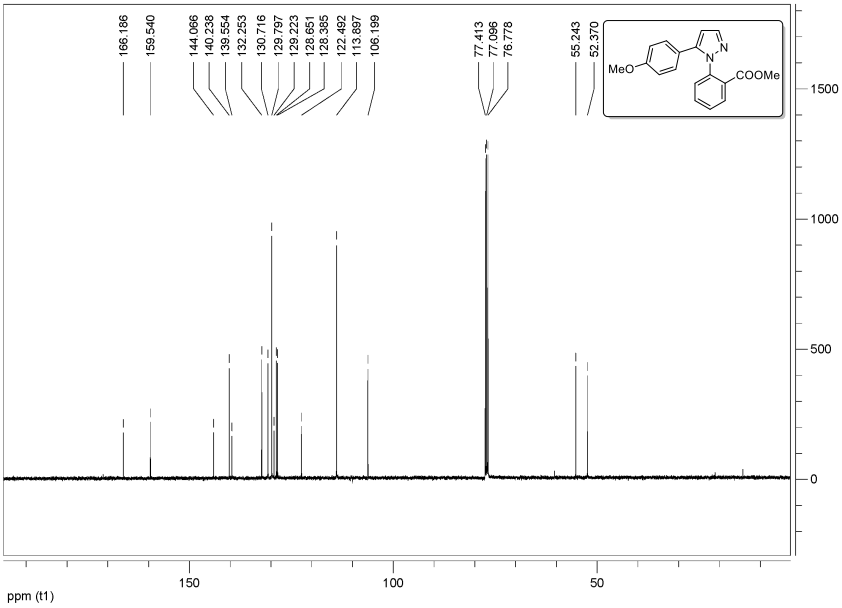
166.186
159.540
144.066
140.238
139.554
132.253
130.716
129.797
129.223
128.651
128.385
122.492
113.897
106.199
77.413
77.096
76.778
55.243
52.370
MeO
N
N
COOMe
1500
1000
500
0
150
100
50
ppm (t1)

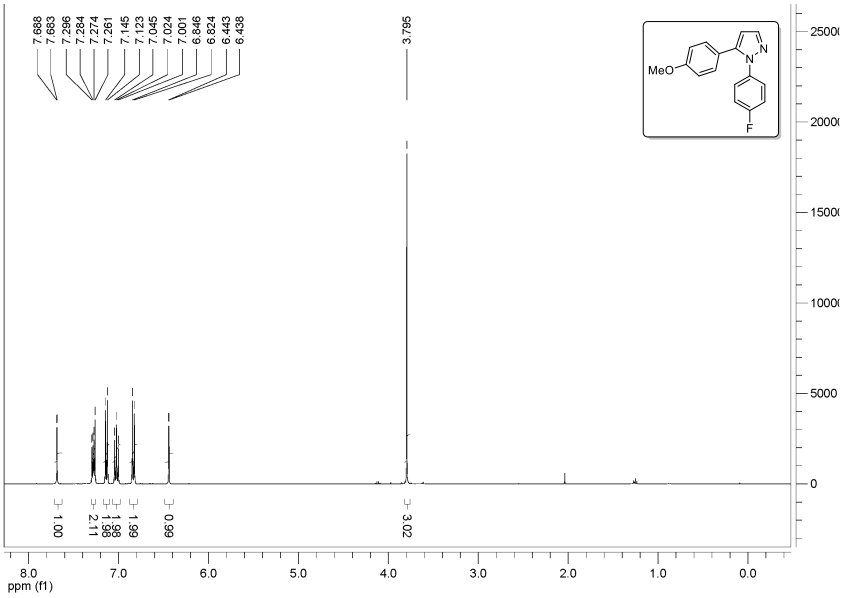
7.688
7.683
7.296
7.284
7.274
7.261
7.145
7.123
7.045
7.024
7.001
6.846
6.824
6.443
6.438
3.795
MeO
F
1.00
2.11
0.98
1.98
1.99
0.99
3.02
ppm (f1)

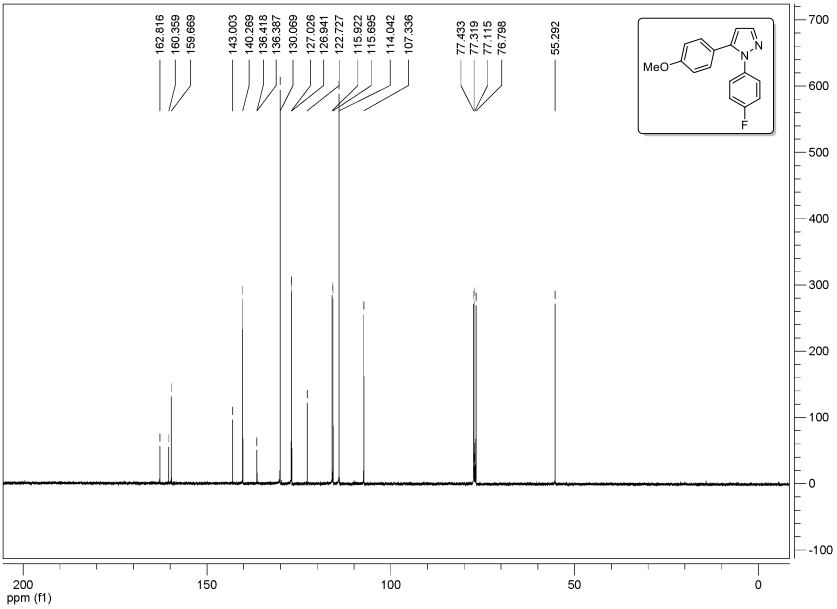
162.816
160.359
159.669
143.003
140.269
136.418
136.387
130.069
127.026
126.941
122.727
115.922
115.695
114.042
107.336
77.433
77.319
77.115
76.798
55.292
MeO
F
ppm (f1)

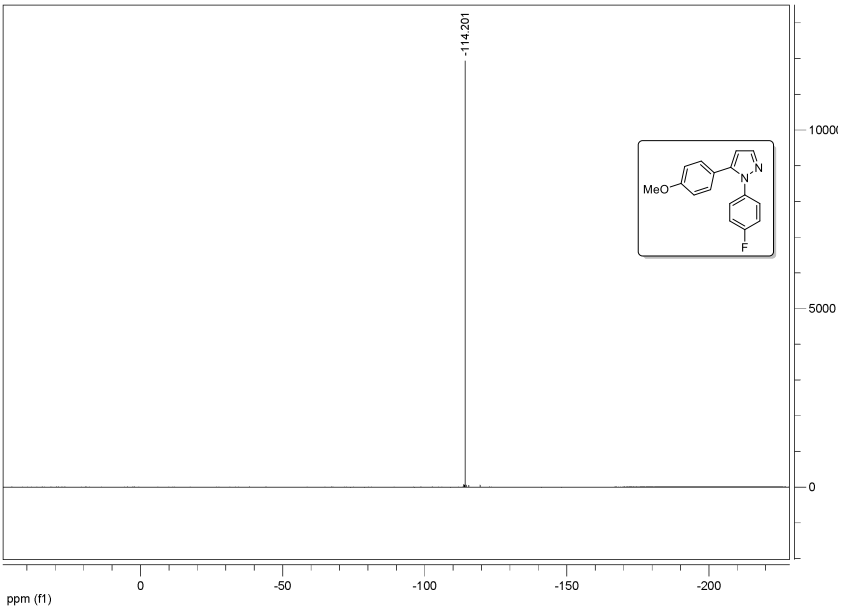

6.5: References

1. a) Robl J. A., Duncan L. A., Pluscec J., Karanewsky D. S., Gordon E. M., Ciosek C. P., Rich L. C., Dehmel V. C., Slusarchyk D. A., Harrity T. W., Obrien K. A., *J. Med. Chem.* **1991**, *34*, 2804; b) Cao X.-F., Hu M., Li F., Lu W.-C., Yo G.-A., Liu S.-H., *Helv. Chim. Act.* **2009**, *92*, 1007; c) Wei C.-H., Mannathan S., Cheng C.-H., *J. Am. Chem. Soc.* **2011**, *133*, 6942
2. Pirnot M. T., Rankic D. A., Martin D. B., MacMillan D. W., *Science* **2013**, *339*, 1593.
3. Jiao J., Nguyen L. X., Patterson D. R., Flowers III R. A., *Org. Lett.* **2007**, *9*, 1323.
4. Casey B. M., Eakin C. A., Flowers III R. A., *Tet. Lett.* **2009**, *50*, 1264.
5. Ren R., Zhao H., Huan L., Zhu C., *Angew. Chem. Int. Ed.* **2015**, *in press*; DOI: 10.1002/ange.201506578
6. a) Hari D. P., Schroll P., König B., *J. Am. Chem. Soc.* **2012**, *134*, 2958; b) Schroll P., Hari D. P., ., König B., *ChemistryOpen* **2012**, *1*, 130; c) Májek M., Jacobi von Wangelin A., *Chem. Commun.* **2013**, *49*, 5507.
7. Gibson D. H., DePuy C. H., *Chem. Rev.* **1974**, *74*, 605.

8. a) Nomura K., Oshima K., Matsubara S., *Angew. Chem. Int. Ed.* **2005**, *44*, 5860; b) Cheng K., Carroll P. J., Walsh P. J., *Org. Lett.* **2011**, *13*, 2346.
9. a) Kulinkovich O. G., Sviridov S. V., Vasilevsky D. A., Prityckaja T. S., *Zh. Org. Khim.* **1989**, *25*, 2245; b) Kulinkovich O. G., Sviridov S. V., Vasilevski D. A., *Synthesis* **1991**, *243*.
10. Wu Y.-D., Yu Z.-X., *J. Am. Chem. Soc.* **2001**, *123*, 5777.
11. McCrary P. D., Beasley P. A., Kelley S. P., Schneider S., Boatz J. A., Hawkins T. W., Perez J. P. L., McMahon B. W., Pfiel M., Son S. F., Anderson S. L., Rogers R. D., *Phys. Chem. Chem. Phys.* **2012**, *14*, 13194.
12. Ilangovan A., Saravanakumar S., Malayappasamy S., *Org. Lett.* **2013**, *15*, 4968.
13. Kulinkovich O. G., Kananovich D. G., *Eur. J. Org. Chem.* **2007**, *13*, 2121.
14. Kulinkovich O. G., Savchenko A. I., Sviridov S. V., Vasilevski D. A., *Mendeleev Comun.* **1993**, 231.
15. a) de Meijere, Williams C. M., Kourdiaoukov A., Sviridov S. V., Chaplinski V., Kordes M., Savchenko A. I., Straatmann C., Noltemeyer M., *Chem. Eur. J.* **2002**, *8*, 3789; b) Bertus P., Szymoniak J., *Chem. Commun.* **2001**, 1792.
16. Pellagatti L., Buchwald S. L., *Org. Process Res. Dev.* **2012**, *16*, 1442.
17. Macrae P. E., Wright T. R., *J. Chem. Soc., Chem. Commun.*, **1974**, 898.
18. Suehiro T., *Rev. Chem. Intermed.* **1988**, *10*, 101.
19. Bunnett J. F., Takayama H., *J. Org. Chem.* **1968**, *33*, 1924.
20. Matcha K., Antonchick A. P., *Angew. Chem. Int.* **2014**, *53*, 11960.
21. He X.-P., Shu Y.-J., Dai J.-J., Zhang W.-M., Feng Y.-S., Xu H.-J., *Org. Biomol. Chem.* **2015**, *13*, 7159.
22. Fuse S., Morita T., Johmoto K., Uekusa H., Tanaka H., *Chem. Eur. J.* **2015**, *21*, 14370.
23. Zora M., Kivrak A., *J. Org. Chem.* **2011**, *76*, 9379.
24. Zhang Z., Kang J., Niu P., Wu J., Yu W., Chang J., *J. Org. Chem.* **2014**, *79*, 10170.

Chapter 7:

Visible-to-UV Photon Upconversion for Photoredox Catalysis

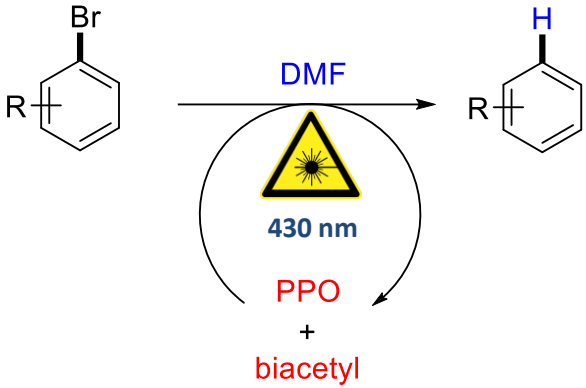

Data from this chapter were used in a publication:
Májek M., Feltmeier U., Dick B., Ruiz-Perez R., Jacobi von Wangelin A., *Chem. Eur. J.* **2015**, in press. Figure 2 and table 1 were used in the aforementioned publication, text of this chapter was writen anew.

Authors contribution:
MM did the quantum-chemical calculations, UF and RPR did photophysical and photochemical experimental work.

7.1: Introduction

Recent developments in the field of visible-light photocatalysis for selective bond formations are evidenced by booming amount of publications in this field, with some of them being the contents of the preceding chapters of this thesis. While the number of diverse classes of reactions enabled by photoredox catalysis seems limitless, there is one definitive constraint to these reactions – the limiting factor is the energy of the photon that we inject into the system. As we already demonstrated in this thesis, vast amount of the photoredox reactions operate on the principle of single electron transfer mediated by the photocatalyst, leading to bond cleavage to generate radical species. In this case, the energetic requirements of the reaction can be crudely approximated by the bond dissociation energy (BDE) of the bond of interest (Figure 1).

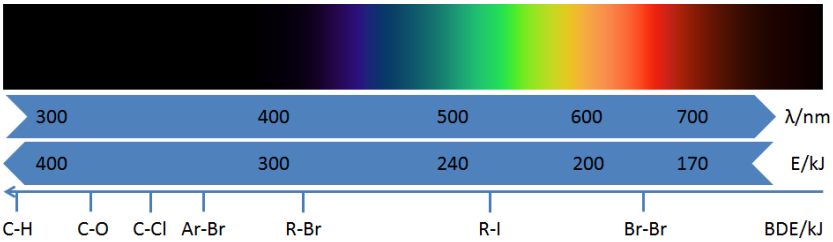

Figure 1. Bond dissociation energy vs. photon energy.

Development in the field of visible light photocatalysis was concentrated on the activation of π-bonds, which are weaker then σ- bonds, or the activation of relatively weak σ- bonds, such as An-N_2^+, C-I and C(sp^3)-Br.[1] It comes straightforward, that a large variety of interesting transformations are not in the range of visible light energies. In order to circumvent this problem a number of workarounds was already proposed in the literature, which we will discuss shortly.

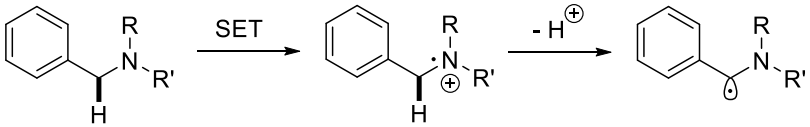

Scheme 1. Activation of hydrogen next to heteroatom.

C-H bonds next to heteroatom can be activated indirectly, by increasing its acidity *via* a redox process on the neighboring heteroatom. This strategy was broadly studied for the compounds containing nitrogen as the easily oxidizable center (Scheme 1).[2]

While efficient, this approach offers access to only to limited amount of compounds. Another approach for the C-H bond activation relies on the utilization of heavy metal catalyst for the C-H activation step, while the photoredox system is responsible for the generation of alkyl-/aryl- radical, that couples with the intermediate complex, as well as the oxidative regeneration of the heavy metal catalyst (Scheme 2).[3]

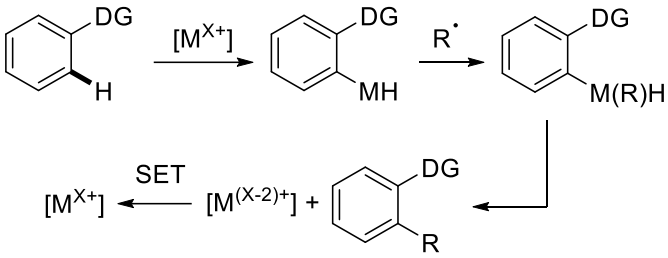

Scheme 2. Activation of hydrogen next to heteroatom.

C-H bond activation can be also performed by hydrogen atom transfer or proton coupled electron transfer. In this case, photocatalyst often bears a C=O double bond, which is weakened on absorption of photon, generating a formal biradical. In the next step, hydrogen is abstracted, with the resultant radical often being stabilized by neighboring group (Scheme 3).[4] Driving force of this process is the generating of more stable O-H bond (BDE = 530 kJ/mol) at the expense of the C-H bond (BDE = 480 kJ/mol).

In addition to these C-H bond activations, König *et. al*. has recently developed a photocatalytic process, where Ar-Br bonds can be activated at the expense of two visible-light photons and a sacrificial reductant (Scheme 3).[5] Derivative of perylenediimide (PDI) was used as the photocatalyst in this case. PDI is excited by blue light photon into excited state, which is reductively quenched by triethylamine. PDI radical anion is relatively stable in rigorously degassed solutions, and can be excited again, this time by green light photon, to obtain excited state of PDI radical anion – the high energy species, which reduces the aryl bromides. While this process needs a sacrificial electron donor, which may come as a drawback, the novelty of this approach comes in the utilization of two photons for the activation of a single bond. The substrate scope of this reaction is quite broad, but what comes as a problem for practical applications is the necessity of proper degassing of the reaction mixtures: Active form of catalyst is so reactive, that it will immediately get quenched by oxygen or other electron acceptors, which may be present in the reaction mixture as impurities.

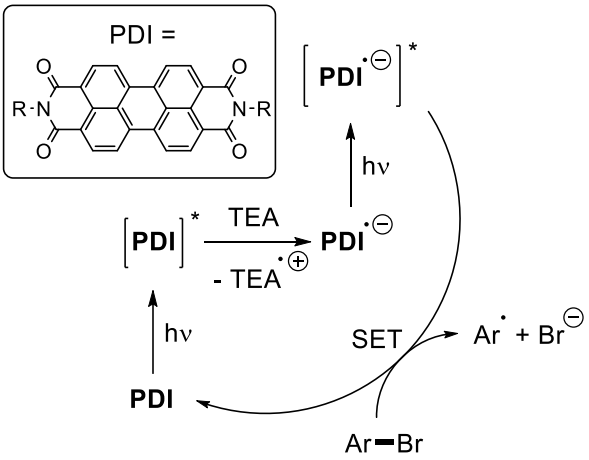

Scheme 3. Two-photon photocatalytic reduction of aryl bromides

We have decided to develop a catalyst system using similar philosophy – a system that would utilize two photons for activation of a single bond, but would not need a sacrificial electron donor as an additional driving force. A possible system, which would fulfill such criteria, is a system which would utilize photon upconversion.[6] Most photon upconversion processes require high energy density of light flux. Photon upconversion *via* triplet-triplet annihilation (TTA) comes as a viable mechanism for our purposes due to relatively low light power required for this process.[7] It operates as follows: sensitizer (donor) gets excited by visible light, first to singlet state $S(S_1)$, which then interconverts *via* ISC to the triplet state $S(T_1)$. Sensitizer then transfers energy to annihilator (acceptor), which gets into the triplet excited state $A(T_1)$. In the last step, two molecules of annihilator in its triplet state meet, and generate one molecule of annihilator in its singlet excited state $A(S_1)$ and one molecule of annihilator in its ground state $A(S_0)$ (Scheme 4 up). The largest variety of sensitizer-annihilator pairs were designed for photon upconversion from the infrared region to visible region, as this is interesting for the biological systems, where the infrared radiation has efficient penetration depth. Such couples are not useful for our purposes, as we require higher photon energies. A small overview of sensitizer-annihilator pairs, which operate in near UV region is given in the following scheme (Scheme 4 down). Last pair (SA4) looks the most promising, as the energy of upconverted photon is highest. Moreover, other pairs utilize complexes of expensive heavy-metal salts, while butadiene and 2,5-diphenyloxazole (**PPO**) are easily available and cheap organic compounds.

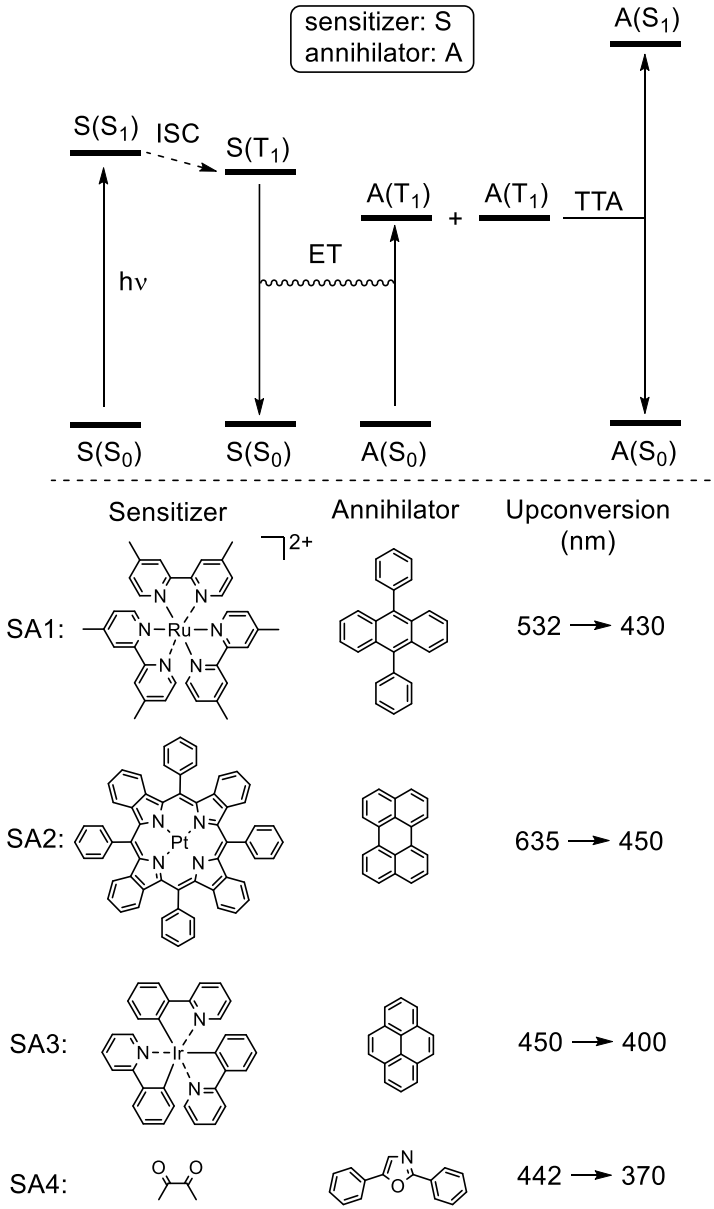

Scheme 4. Triplet-triplet annihilation mechanism and several sensitizer-annihilator pairs. Upconversion is defined by irradiation wavelength and fluorescence wavelength.

So far, most of the research on photon upconversion *via* TTA was concentrated on the studying of the photophysical properties of the sensitizer-annihilator systems. In case, that chemical applications of the system were studied, it was almost exclusively in the context of the production of singlet oxygen.[8] There is an isolated example, where the excited state of annihilator (anthracene) was used to perform a photochemical [4+4] cycloaddition (Scheme 5).[7q] In this case, triplet state of anthracene directly reacts with anthracene in its ground state in a thermally forbidden cycloaddition. This reaction can be viewed as stoichiometric with respect to the anthracene.

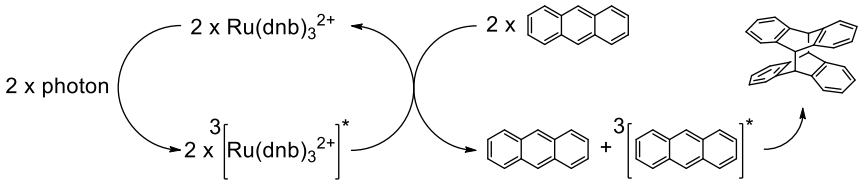

Scheme 5. Anthracene dimerization mediated by TTA process.

Our aim was to find a system, which would be catalytic with respect to both sensitizer as well as the annihilator, and use the annihilator as a photoredox catalyst. We have decided to start with the already introduced biacetyl/**PPO** system, due to the favorable spectral properties as well as easy handling.

7.2: Results and discussion

System, which we chose for our initial studies, consisting of the simple metal-free couple butane-2,3-dione (**BD**, sensitizer) and 2,5-diphenyloxazole (**PPO**, annihilator) was already reported to exhibit low power VIS-to-UV photon upconversion but has not been applied to a chemical reaction so far.[9] Energy is pumped into the system by selective excitation of **BD** (at 430 nm) in the presence of **PPO** by pulsed laser. The resultant formation of ^{1}**PPO*** was observed in degassed *N*,*N*-dimethylformamide (DMF) by its characteristic delayed fluorescence at 370 nm which corresponds to an excited singlet state energy of 3.35 eV (Figure 2). This, and other photophysical observations were consistent with already reported performance of this upconverting system.[9] Proving, that the delayed fluorescence of ^{1}**PPO*** can be produced by photon upconversion in our hands in the same way as was already reported, we have proceeded to probe its utility to induce chemical transformations.

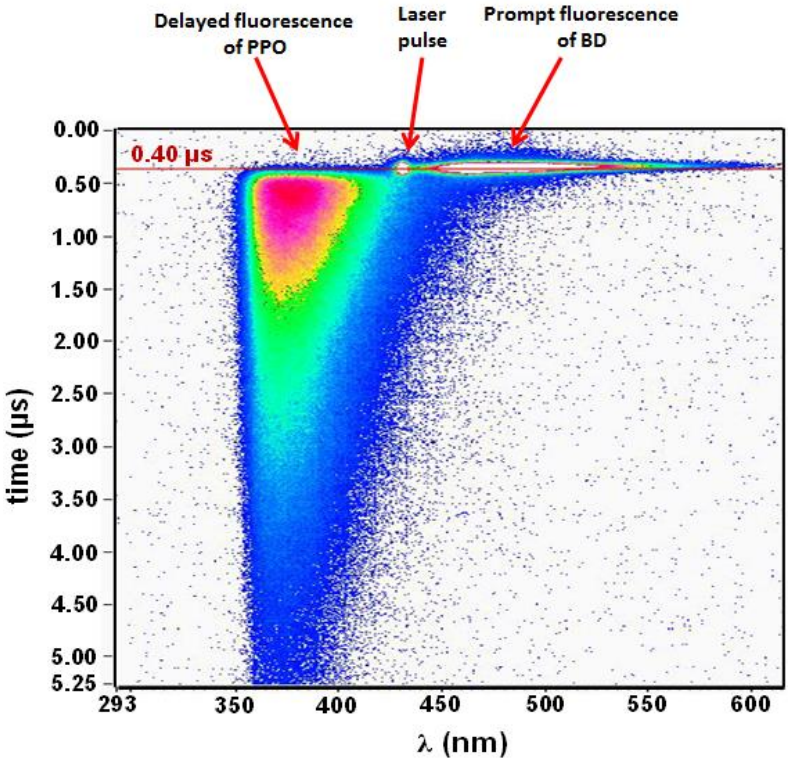

Figure 2. 2D transient fluorescence matrix of a mixture of **BD** (0.04 M) and **PPO** (0.013 M) in degassed DMF from laser excitation at 430 nm (at 0.4 µs after start of recording).

As a model system, reductive defunctionalization of three aryl bromides [4'-bromoacetophenone (**1**), 4'-bromobenzotrifluoride (**2**) and 4'-bromoanisole (**3**)] in DMF solution was chosen. Reactions were first performed by steady-state irradiation of the **BD**/**PPO** system. Alas, irradiation of a mixture of **1**, **BD** and **PPO** with a blue LED light (450 nm, 3.8 W) showed no conversion of **1** after 30 min on GC-FID analysis (Table 1, entry 1) which is mainly due to the low density of photon flux irradiated from the continuous LED source. Afterwards, steady-state irradiations were carried out by using a pulsed laser (10 s^{-1}, 15 mJ $pulse^{-1}$, pulse duration 8 ns). Such laser pulse translates into theoretical power of approx. 2 MW, in several orders of magnitude higher than in the case of continuous irradiation with LEDs. Indeed, low conversion of **1** and high selectivity was observed (Table 1, entry 3).

Table 1. Light-induced reduction of aryl bromides **1-3** under TTA conditions.[a]

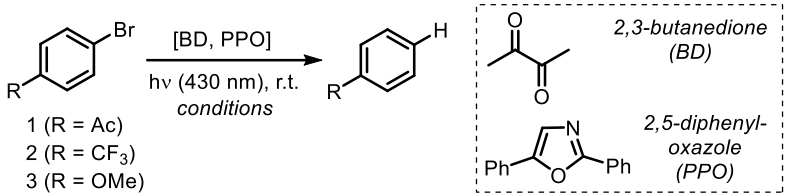

Entry	Substrate	Solvent	t [min]	Selectivity [%][b]
1[c]	**1**	DMF	30	0 (0)
2	**1**	DMF	10	48 (13)
3	**1**	DMF	30	88 (19)
4[d]	**1**	DMF	60	70 (26)
5	**1**	acetonitrile	30	41 (7)
6	**2**	DMF	30	71 (6)
7	**3**	DMF	30	0 (0)

[a] Conditions: 10 mM [**Substrate**], 40 mM [**BD**], 13 mM [**PPO**], under N_2; irradiation with a pulsed laser (10 s^{-1}, 15 mJ) at 430 nm; [b] conversion [%] in parentheses; calculated from quantitative GC-FID vs. internal *n*-pentadecane; [c] irradiation with blue LED (450 nm, 3.8 W); [d] after 30 min irradiation addition of another 40 mM **BD** and irradiation for 30 min.

The relatively low conversions can be attributed to the decomposition of catalyst over time of irradiation. Further addition of **BD** and irradiation resulted in higher conversions which can be a consequence of slow decomposition of **BD** (entry 4). This does not come as a surprise, as the **BD** is known to be an active photocatalyst in hydrogen atom transfer reactions.[10] When less electropositive substrates were used, conversion remained low (entry 6), and in the presence of electron donor on the substrate, no conversion was observed (entry 7).

Based on the known mechanism of photon upconversion by triplet-triplet annihilation[7] in combination with our recent findings of hydrodediazotations in DMF,[11] we propose a mechanism for the observed reaction (Scheme 6). It can be inferred from the photophysical measurements, that the singlet excited state of PPO is quenched by aryl bromides. What remains to be investigated is the reaction pathway of the aryl bromide (orange), the reaction pathway of DMF (blue), and the regeneration of the catalyst by SET reduction of cation radical **PPO**$^{+\bullet}$ to grond state **PPO**.

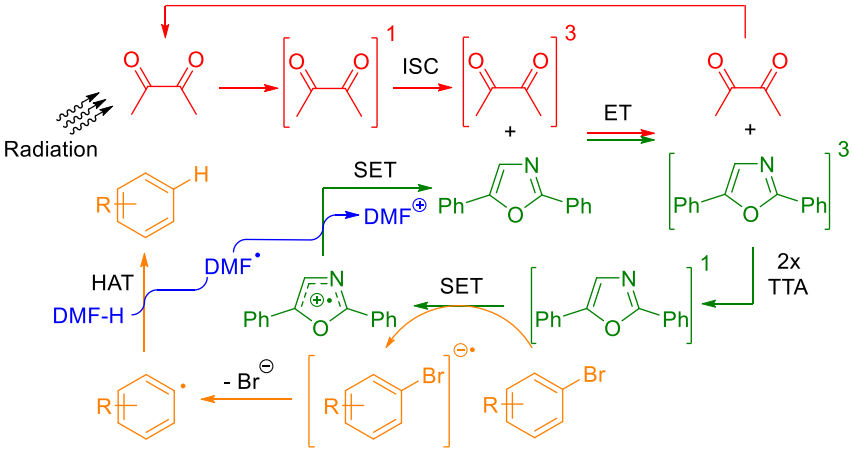

Scheme 6: Proposed mechanism of two-photon dehalogenation.

Hydrogen atom transfer from DMF to aryl radical should proceed smoothly, this process was already discussed in detail in previous chapter (Chapter 5). Regeneration of catalyst by reduction of **PPO**$^{+\bullet}$ by DMF radical had yet to be investigated. Redox potential of the **DMF**$^{+}$ -> **DMF**$^{\bullet}$ pair is 0.25 V (vs. SCE, see Chapter 5). The redox potential of the **PPO**$^{+\bullet}$ -> **PPO** pair was approximated by quantum-chemical calculations (see Computational part for details) to be 1.46 V (vs. SCE). This makes the reductive regeneration of **PPO** catalyst an exergonic process (ΔE = + 1.21 V), which should proceed smoothly under the reaction conditions. The most interesting step from the reaction mechanism is the SET reduction of aryl bromides, as we anticipate, that this is the step responsible for the selectivity of the reaction. Therefore we have studied this reaction step in detail. Energetics of reductive quenching was calculated by combination of DFT and TD-DFT calculations. Thermodynamical data obtained by this method were compared to the available experimental data from cyclic voltammetry to verify accuracy of the quantum-chemical calculations. Activation energies of electron transfer were obtained from Marcus theory (for details see Computational part).

Table 2. Calculated and experimental redox potentials.

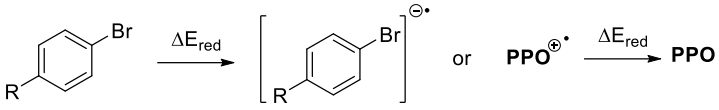

Compound	E_{red}(calc)	E_{red}(CV)
R = Ac	1.78	1.83
R = CF_3	2.45	2.42
R = OMe	3.04	2.84
PPO	1.46	1.65
^{1}PPO*	2.08	2.13

Redox potentials are given in Volt and are referenced against SCE in acetonitrile. Details on calculations are given in the computational part.

Experimental redox potentials match the redox potentials obtained by quantum-chemical calculations well, maximal error of calculation is 200 mV (Table 2). This proves, that even tough the method used for quantum-chemical calculations was not specifically suited for redox potential calculations, its accuracy is suitable for our purposes. As can be seen from the redox potentials, the largest difference is between the redox potential of the *p*-acetyl (**1**) and *p*-trifluoromethyl derivative (**2**) (+1.78 V vs. +2.45 V). Both of these substituents are strong electron acceptors, but while acetyl group can accept electron density from aromatic core by conjugation, trifluoromethyl group is not able to do so. This is a strong hint, that when electron is accepted by aryl bromide, it is first delocalized on the aromatic system, and the C-Br bond is cleaved afterwards – by other words the σ*(C-Br) orbital is not the primary electron acceptor. Standard Gibbs free energies were calculated from theoretical values as well as from the experimental (CV) values. By combining the calculations of the Gibbs free energies with DFT-calculated reorganization energies *λ,* one could obtain the activation energies for single electron reduction of aryl bromides by **^{1}PPO*** (SET), and the activation energies of back electron transfer (BET) (Table 3).

Table 3. Calculated electron transfer activation energies.

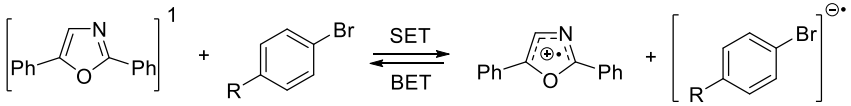

Compound	**R = Ac**	**R = CF_3**	**R = OMe**
ΔG^0(DFT)	-28.2	36.2	93.1
ΔG^0(CV)	-29.3	25.1	67
λ(calc)	34.7	56.1	30.4
$\Delta E^{\ddagger}$(SET)	**0.3**	**37.9**	125
$\Delta E^{\ddagger}$(BET)	**28.5**	**1.8**	32.4
$\Delta E^{\ddagger}$(BET-GS)	497	435	1138
Conversion	19	6	0

ΔG^0(DFT) and ΔG^0(CV) represent the standard free Gibbs energy of SET reaction obtained from DFT calculations and CV measurements, respectively. λ(calc) is the nuclear reorganization energy obtained from DFT. All energies are given in kJ/mol. Conversion is the experimentally obtained conversion of aryl bromide to corresponding arene (as in Table 1).

Activation energy for single electron reduction of *p*-acetyl derivative (**1**) is virtually non-existent, while activation energy of single electron reduction of *p*-trifluoromethyl derivative (**2**) is 37.9 kJ/mol. Such substantial activation energy is still not prohibitive at room temperature, especially if the follow-up reactions are fast. Cleavage of the Ar-Br bond of radical anions $[Ar\text{-}Br]^{\bullet-}$ was reported to be very fast and under the reaction conditions occurs at diffusion controlled rates.[12] Activation energies of SET therefore would not be enough to explain the selectivity difference between derivatives **1** and **2** (as measured by conversion, Table 3). Other factor which can be used to explain the selectivity is the back electron transfer (BET) – in this case, the barrier for BET is very low for the *p*-trifluoromethyl derivative, while being substantially higher for the *p*-acetyl derivative. It can be inferred from this data, that rapid electron transfer in to the *p*-acetyl derivative is followed by rapid bond Ar-Br cleavage, and the back electron transfer is not a serious competitor to the bromide cleavage as the kinetics of BET process are much slower. On the other hand, BET is very fast for the *p*-trifluoromethyl derivative, and therefore it is a serious competition to the bromide cleavage, leading to low conversions. Activation energy for the single electron reduction of *p*-methoxy

derivative (**3**) is too high to obtain any conversion of this staring material at room temperature. Interestingly, when the activation energies of the very endothermic back electron transfers to from the ground state of **PPO** (BET-GS) has much higher activation energies then the back electron transfer to form the singlet excited state of **^{1}PPO*** (Scheme 7). This is a manifestation of the so-called Marcus inverted region – prohibitively high activation energies of overly exothermic reactions, which is predicted by the Marcus theory of electron transfer.[13] Exothermicity of reaction can be lowered by generation of excited state species by electron transfer, leading to lower expected activation energies of electron transfer. This concept was predicted in early seventies,[14] but its experimental proof from was performed only recently by pump-probe time-resolved infrared spectroscopy.[15]

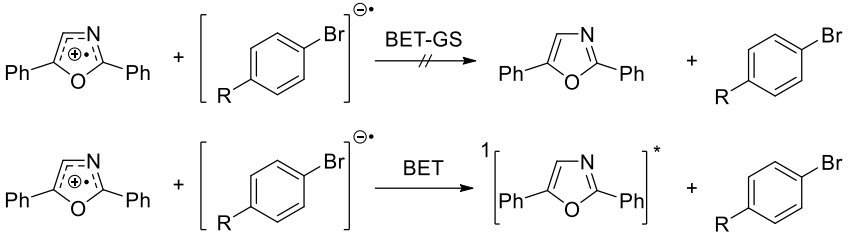

Scheme 7: Comparison of the two back electron transfer mechanisms.

7.3: Conclusion

In conclusion, we have demonstrated a novel application of visible-to-UV photon upconversion for the SET induced reductive activation of aryl bromides. Metal-free dyes **BD** (sensitizer) and **PPO** (triplet annihilator) were used for the TTA upconversion process. Photophysical studies were applied to prove the role of the PPO as the photocatalyst in this process. The main purpose of the theoretical work presented in this thesis was to provide theoretical backing for the proposed photocatalytic mechanism. DFT calculations were successfully used to show, that the single-electron transfer from ^{1}**PPO*** to the aryl bromides is rate-limiting and in combination with the corresponding back-electron transfer determines the overall substrate scope of the reaction. Optimizations considering selectivity and substrate are ongoing, with some improvements already accomplished.[16] Importance of this study is in the demonstration of viability of the concept of photon upconversion-photoredox catalysis, which was, to the best of our knowledge never applied so far. This strategy brings new promising method for selective bond activation, as even low energy photons can be used to activate otherwise non-active moieties.

7.4: Computational part

Photochemical and electrochemical experiments were carried out by Raul Ruiz-Perez and Uwe Faltmeier and they are explained in detail in the manuscript of our joint publication.[17] DFT and TD-DFT calculations were performed with the Gaussian G09 software package.[18] Geometry optimizations were carried out using the B3LYP functional and 6-31++G(2d,p) basis set. Geometry of the **^{1}PPO* (S_1)** excited state was optimized by TD-DFT, employing the unrestricted UB3LYP method and the 6-31++G(2d,p) basis set. All optimizations were carried out using a polarized continuum model to account for the solvent effects. Single point calculations were carried out using the CAM-B3LYP functional and 6-31++G(2d,p) basis set. CAM-B3LYP is expecially suited for the TD-DFT calculations where CT states have to be considered.[19] Redox potentials obtained from DFT are referenced against infinity, in order to obtain values referenced against SCE, 4.18 V had to be abstracted from the theoretical values.[20] The geometries of the radical cation and neutral species were optimized at the aug-cc-pVTZ basis set at UB3LYP level using the PCM model to account for the solvation. Vibrational analysis was performed on all optimized geometries in order to ascertain the types of minima obtained.

Activation energies of electron transfer were obtained via Marcus theory.[13] Short introduction into this theory, will be given here. Thermodynamics seem to be the driving force, when one considers electron transfer. While this is true, even the reactions which go energetically "uphill" can occur in case of a very fast subsequent reaction.[21] On the other hand, exothermicity is not the only necessary requirement for a rapid electron transfer, as was demonstrated on a series of intramolecular donor-acceptor systems.[22] Marcus theory gives a simplified explanation for these phenomena, as it allows to calculate the activation energy of electron transfer. According to Marcus, the main barrier of electron transfer is in the energy needed for reorganization of molecular geometry and molecular surroundings from starting materials to products, when the electron transfer occurs. This does not come as a surprise, when one considers Born-Oppenheimer approximation which asserts, that motion of electrons and nuclei can be separated – and in case that the timeframes of nuclear motion are considered, electronic motion can be approximated to occur instantly. Results of this approach can be drawn by potential curves of hypothetical single electron transfer between A and B^+ (brown potential curve) to form A^+ and B (blue potential curve) (Figure 3). If the electron transfer occurs instantaneously, we move from the minimum of the brown potential curve upwards to the blue potential curve of products. Energy needed for this transformation is called reorganization energy λ. Thermodynamics of

this electron transfer is defined by the reaction Gibbs free energy ΔG^0. Marcus theory derives the following expression for the reaction activation energy $\Delta E^{\ddagger}$:

$$\Delta E^{\ddagger} = \frac{(\Delta G^0 + \lambda)^2}{4\lambda}$$

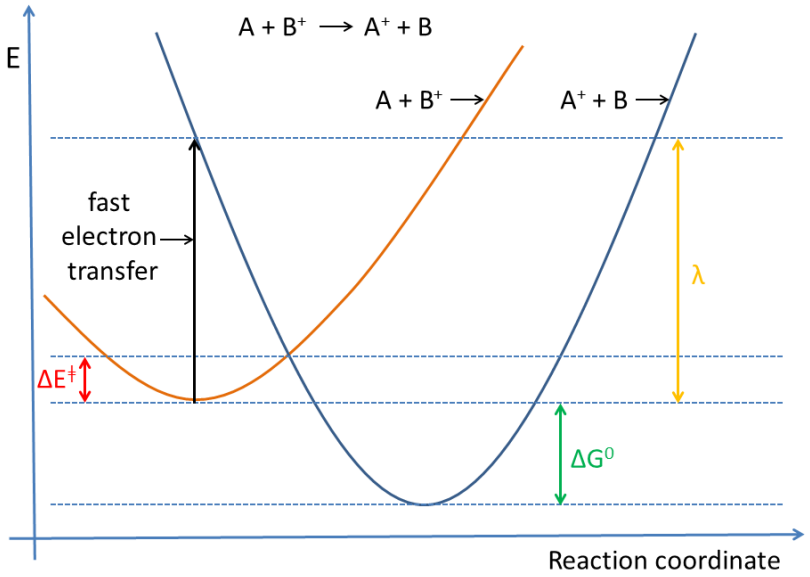

Figure 3. Marcus theory for reaction of two different reacting species.

Predictions of the Marcus theory can be demonstrated on four distinct cases (Figure 4). When a reaction has zero net Gibbs free energy, activation barrier equals to $\lambda/4$ (Figure 4, A). In reality, such situation occurs, when self-exchange of electron is considered, and is often used to directly experimentally obtain reorganization energies. When the reaction becomes more exothermic (Figure 4, B), activation energy drops. This is consistent with the prediction of Bell-Evans-Polanyi principle, and such situation occurs in the conventional reactions. When the reorganization energy equals to the negative Gibbs free energy of reaction (Figure 4, C), activationless electron transfer occurs. What comes contrary to the linear energy relationship predicted from the Bell-Evans-Polanyi principle is the case, when the reaction becomes even more exothermic (Figure 4, D), but the activation energy increases. This is called the Marcus inverted region.

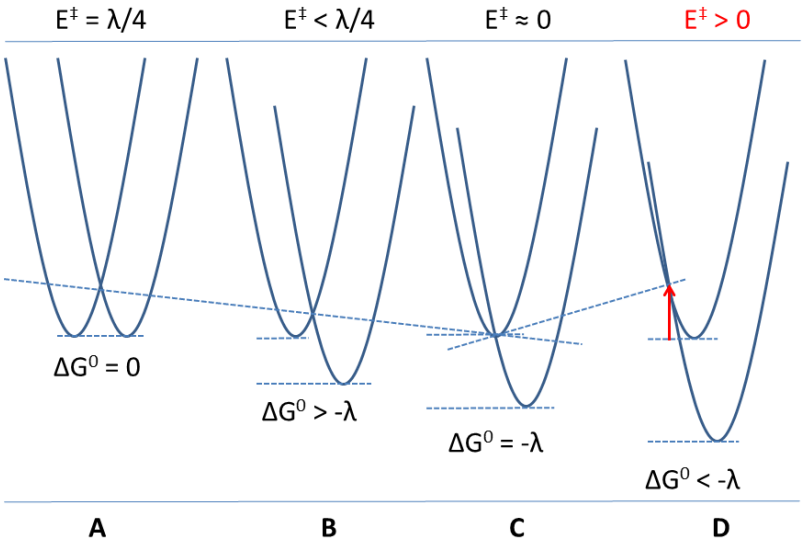

Figure 4. Predictions of Marcus theory for different thermodynamic situations.

Reorganization energy is composed from two parts: inner-sphere and outer-sphere reorganization energy. Inner-sphere reorganization energy comes directly from the different geometries of starting materials and products and is bound to the vibrational motion needed to deform geometries of starting materials to products. This energy can be obtained explicitly from DFT calculations, if the geometries of starting materials and products are known. Bigger problem is posed by the outer-sphere reorganization energy, which comes from the relaxation motion of the medium in which the electron transfer occurs. This accounts mainly to the solvent polarization and reorientation. Original approach suggested by Marcus treats the dissolved molecules as spheres immersed in linearly responding dielectric.[23] While such approach has its merits, when electron transfer from/to metallic ions is concerned, it suits organic molecules poorly for their geometries are seldom isotropic spheres. Within the framework of DFT calculations various approaches were proposed to obtain the explicit outer-sphere reorganization energy, most notably the constrained density functional theory.[24] Such calculations require more steps, and they are not embedded into available quantum-chemistry program packages. On the other hand, integral equation formalism polarizable continuum model (IEF-PCM) is readily available in the Gaussian G09, and can be integrated to the DFT and TD-DFT calculations easily.[25] By using this model, solvent reaction is coupled to the reactants, and total reorganization energy is obtained by the calculations. Outer-sphere reorganization energy can be obtained by

subtracting the conventionally obtained inner-sphere reorganization energy from this value, but this is not of interest to us, as we need the total reorganization energy to obtain activation energy from the Marcus theory.

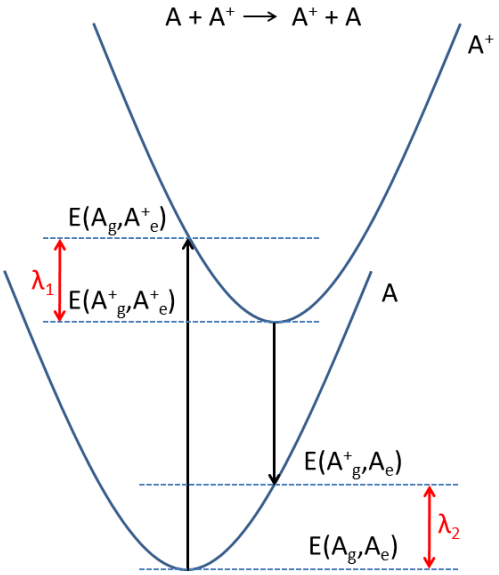

Figure 5. Diagram of Nelsen's four point method. $E(A^+_g,A_e)$ denotes energy of molecule with geometry of A^+ and electronic state of A.

We have used the Nelsen four-point approach to obtain the reorganization energy (Figure 5).[26] This method can be used for the calculation of the reorganization energy for self-exchange reaction. Let us consider electron self-exchange between A and A^+. In order to perform the calculation, two geometry optimizations need to be performed first to obtain optimum geometries of A and A^+. This is followed by four energy calculations to obtain the following energies: energy $E(A_g,A_e)$ of the molecule with geometry of A and electronic structure of A; energy $E(A_g,A^+_e)$ of the molecule with geometry of A and electronic structure of A^+; energy $E(A^+_g,A^+_e)$ of the molecule with geometry of A^+ and electronic structure of A^+ and energy $E(A^+_g,A_e)$ of the molecule with geometry of A^+ and electronic structure of A. Reorganization energy $\lambda_{A\text{-}A}$ is then obtained by the following equations:

$$\lambda_1 = E\left(A_g, A_e^+\right) - E\left(A_g^+, A_e^+\right)$$

$$\lambda_2 = E\left(A_g^+, A_e\right) - E(A_g, A_e)$$

$$\lambda_{A-A} = \lambda_1 + \lambda_2$$

Reorganization energy $\lambda_{A\text{-}B}$ for the reaction of two different reactants A and B can be obtained from Marcus cross-relation, where the self-exchange reorganization energies are simply averaged:[27]

$$\lambda_{A-B} = \frac{\lambda_{A-A} + \lambda_{B-B}}{2}$$

7.5: References

1. a) Schultz D. M., Yoon T. P., *Science* **2014**, *343*, 1239176; b) Ravelli D., Protti S., Fagnoni M., Albini A., *Curr. Org. Chem.* **2013**, *17*, 2366; c) Prier C. K., Rankic D. A., MacMillan D. W. C., *Chem. Rev.* **2013**, *113*, 5322; d) Reckenthäler M., Griesbeck A. G., *Adv. Synth. Catal.* **2013**, *355*, 2727; e) Tucker J. W., Stephenson C. R. J., *J. Org. Chem.* **2012**, *77*, 1617; f) Xuan J., Xiao W.-J., *Angew. Chem. Int. Ed.* **2012**, *51*, 6828; g) Teplý F., *Collect. Czech. Chem. Commun.* **2011**, *76*, 859.
2. a) Shi L., Xia W., *Chem. Soc. Rev.* **2012**, *41*, 7687; b) Hu J., Wang J., Nguyen T. H., Zheng N., *Beilstein J. Org. Chem.* **2013,** *9,* 1977.
3. a) Fabry D. C., Zoller J., Raja S., Rueping M., *Angew. Chem. Int. Ed.* **2014**, *53*, 10228; b) Kalyani D., McMurtrey K. B., Neufeldt S. R., Sanford M. S., *J. Am. Chem. Soc.* **2011**, *133*, 18566.
4. Protti S., Fagnoni M., Ravelli D., *ChemCatChem* **2015**, *7*, 1516.
5. Ghosh I., Ghosh T., Bardagi J. I., König B., *Science* **2014**, *346*, 725.
6. a) Schulze T. F., Schmidt T. W., *Energy Environ. Sci.* **2015**, *8*, 103; b) Chen G., Qiu H., Prasad P. N., Chen X., *Chem. Rev.* **2014**, *114*, 5161; c) Auzel F., *Chem. Rev.* **2004**, *104*, 139; d) Castellano F. N., Schmidt T. J., *Phys. Chem. Lett.* **2014**, *5*, 4062.
7. a) Recent review article: Singh-Rachford T. N., Castellano F. N., *Coord. Chem. Rev.* **2010**, *254*, 2560; b) Parker C. A., Hatchard C. G., *Proc. R. Soc. London A* **1962**, *269*, 574; c) Parker C. A., Hatchard C. G., *Proc. Chem. Soc. London* **1962**, *386*; d) Parker C. A., *Proc. R. Soc. London A* **1963**, *276*, 125. Selected recent examples: e) Adarsh N., Avirah R. R., Ramaiah D., *Org. Lett.* **2010**, *12*, 5720;

f) Gallavardin T., Armagnat C., Maury O., Baldeck P. L., Lindgren M., Monnereau C., Andraud C., *Chem. Commun.* **2012**, *48*, 1689; g) Wu W., Guo H., Wu W., Ji S., Zhao J. J., *J. Org. Chem.* **2011**, *76*, 7056; h) Yogo T., Urano Y., Ishitsuka Y., Maniwa F., Nagano T., *J. Am. Chem. Soc.* **2005**, *127*, 12162; i) Guo S., Wu W., Guo H., Zhao J., *J. Org. Chem.* **2012**, *77*, 3933; j) Kozlov D. V., Castellano F. N., *Chem. Commun.* **2004**, 2860; k) Islangulov R. R., Kozlov D. V., Castellano F. N., *Chem. Commun.*, **2005**, 3776; l) Singh-Rachford T. N., Islangulov R. R., Castellano F. N., *J. Phys. Chem. A* **2008**, *112*, 3906; m) Du P., Eisenberg R., *Chem. Sci.* **2010**, *1*, 502; n) Zhao W., Castellano F. N., *J. Phys. Chem. A* **2006**, *110*, 11440; o) McCusker C. E., Castellano F. N., *Chem. Commun.* **2013**, *49*, 3537; p) Zhao J., Ji S., Guo H., *RSC Adv.* **2011**, *1*, 937; q) Islangulov R. R., Castellano F. N., *Angew. Chem. Int. Ed.* **2006**, *45*, 5957; r) Khnayzer R. S., Blumhoff J., Harrington J. A., Haefele A., Denga F., Castellano F. N., *Chem. Commun.* **2012**, 209; s) Börjesson K., Dzebo D., Albinsson B., Moth-Poulsen K., *J. Mater. Chem. A* **2013**, *1*, 8521.

8. For recent examples see: a) Wu W., Zhao J., Guo S., *J. Org. Chem.* **2012**, *77*, 5305; b) Guo S., Wu W., Guo H., Zhao J., *J. Org. Chem.* **2012**, *77*, 3933; c) Zhang X-F., Yang X., *J. Phys. Chem. B* **2013**, *117*, 5533.
9. Singh-Rachford T. N., Castellano F. N., *J. Phys. Chem. A* **2009**, *113*, 5912.
10. Lakowicz J. R., *Principles of Fluorescence Spectroscopy*, 2nd ed., Kluwer/Plenum, New York, **1999**.
11. Májek M., Filace F., Jacobi von Wangelin A., *Chem. Eur. J.* **2015**, *21*, 4518.
12. Costentin C., Robert M., Savéant J.-M., *J. Am. Chem. Soc.* **2004**, *126*, 16051**.**
13. Marcus R. A., *Pure Appl. Chem.* **1997**, *69*, 13.
14. Mataga, N. *Bull. Chem. Soc. Jpn.* **1970**, *43*, 3623.
15. Koch M., Rosspeintner A., Adamczyk K., Land B., Dreyer J., Nibbering E. T. J., Vauthey E., *J. Am. Chem. Soc.* **2013**, *135*, 9843.
16. Häring M., Perez-Ruiz R., Jacobi von Wangelin A., Diaz-Diaz D., *Chem. Commun.* **2015**, *accepted*.
17. Májek M., Feltmeier U., Dick B., Ruiz-Perez R., Jacobi von Wangelin A., *Chem. Eur. J.* **2015**, *in press*, DOI: 10.1002/chem.201502698.
18. Frisch M. J., Trucks G. W., Schlegel H. B., Scuseria G. E., Robb M. A., Cheeseman J. R., Scalmani G., Barone V., Mennucci B., Petersson G. A., Nakatsuji H., Caricato M., Li X., Hratchian H. P., Izmaylov A. F., Bloino J., Zheng G., Sonnenberg J. L., Hada M., Ehara M., Toyota K., Fukuda R., Hasegawa J., Ishida M., Nakajima T., Honda Y., Kitao O., Nakai H., Vreven T., Montgomery Jr. J. A., Peralta J. E., Ogliaro F., Bearpark M., Heyd J. J., Brothers E., Kudin K. N., Staroverov V. N., Kobayashi R., Normand J., Raghavachari K., Rendell A., Burant J. C., Iyengar S. S., Tomasi J., Cossi M.,

Rega N., Millam J. M., Klene M., Knox J. E., Cross J. B., Bakken V., Adamo C., Jaramillo J., Gomperts R., Stratmann R. E., Yazyev O., Austin A. J., Cammi R., Pomelli C., Ochterski J. W., Martin R. L., Morokuma K., Zakrzewski V. G., Voth G. A., Salvador P., Dannenberg J. J., Dapprich S., Daniels A. D., Farkas Ö., Foresman J. B., Ortiz J. V., Cioslowski J., Fox D. J., *Gaussian 09, Revision D.01*, Gaussian, Inc., Wallingford CT, **2009**.

19. Yanai T., Tew D. P., Handy N. C., *Chem. Phys. Lett.*, **2004**, *393*, 51.
20. Baik M.-H., Friesner R. A., *J. Phys. Chem. A,* **2002**, *106*, 7407.
21. a) Steckhan E., *Angew. Chem. Int. Ed.* **1986**, *25*, 683; b) Zhang N., Zeng C., Lam C. M., Gbur R. K., Little R. D., *J. Org. Chem.* **2013**, *78*, 2104.
22. Closs G. L., Calcaterra L. T., Green N. J., Penfield K. W., Miller J. R., *J. Phys. Chem.* **1986**, *90*, 3673.
23. Marcus R. A., *J. Chem. Phys.*, **1956**, *24*, 966.
24. Ren H.-S., Ming M.-J., Ma J.-Y., Li X.-Y., *J. Phys. Chem. A*, **2013**, *117*, 8017.
25. Vaissier V., Barnes R., Kirkpatrick J., Nelson J., *Phys. Chem. Chem. Phys.* **2013**, *15*, 4804.
26. Nelsen S. F., Blackstock S. C., Kim Y., *J. Am. Chem. Soc.* **1987**, *109*, 677.
27. a) Marcus R. A., *J. Chem. Phys.* **1965**, 43, 679; for more recent example see: b) Jakobsen S. J., Mikkelsen K. V., Pedersen S. U., *J. Phys. Chem.* **1996**, *100*, 7411.

Chapter 8:

Appendix

8.1: List of abbreviations

Ac:	Acyl
appr.:	Approximately
Ar:	Aryl
ATRA:	Atom transfer radical addition
ATRP:	Atom transfer radical polymerization
BDE:	Bond dissociation energy
BET:	Back electron transfer
bpy:	2,2‘-bipyridine
CAN:	Ceric ammonium nitrate
CFL:	Compact fluorescent lightbulb
CIDNP:	Chemically induced dynamic nuclear polarization
CT:	Charge transfer
CV:	Cyclic voltammetry
dap:	2,9-dianisyl-1,10-phenanthroline
DCB:	1,4-dicyanobenzene
DCN:	1,4-dicyanonaphthalene
DFT:	Density functional theory
DMDS:	Dimethyldisulfide
DMF:	N,N-dimethylformamide
DMN:	1,4-dimethoxynaphthalene
DMSO:	Dimethylsulfoxide
dnb:	1,4-di(1,8-naphthyrudune-2-yl)benzene
DOI:	Digital object identifier
EDTA:	Etylenediamine tetraacetate
e.e.	Enantiomeric excess
EI:	Electron impact
eq.:	Equivalent
Et:	Ethyl
ET:	Energy transfer
eV:	Electronvolt
GC-FID:	Gas chromatrography coupled with flame ionization
GC-MS:	Gas chromatography detector coupled with mass spectroscopy
HAT:	Hydrogen atom transfer
HCH:	Hexachlorocyclohexane
HOMO:	Highest occupied molecular orbital
IEF-PCM:	Integral equation formalism of polarizable continuum model
*i*Pr:	*iso*-Propyl

ISC: Intersystem crossing
LED: Light emitting diode
LUMO: Lowest unoccupied molecular orbital
Me: Methyl
NMP: N-methylpyrollidine
NMR: Nuclear magnetic resonance
PCM: Polarizable continuum model
PDI: Perylene-diimide
PET: Photo-induced electron transfer
PGi: Prostaglandin
ppm: Parts per million
PPO: 2,5-diphenyloxazole
ppy: 2-phenylpyridine
R: Alkyl rest
RM: Reaction mixture
RT: Room temperature
SA: Sacrificial electron acceptor
SCE: Standard calomel electrode
SD: Sacrificial electron donor
SET: Single electron transfer
TBAOH: Tetrabutylammonium hydroxide
*t*Bu: *tert*-Butyl
TD-DFT: Time dependent density functional theory
TEA: Triethylamine
TEMPO: 2,2,6,6-tetramethylpiperidine N-oxide
THF: Tetrahydrofuran
TLC: Thin layer chromatography
TPP: 2,4,6-triphenylpyrylium
TTA: Triplet-triplet annihilation
UV: Ultraviolet radiation
VIS: Visible radiation

8.2: Summary

Aim of this thesis is the use of photo-redox catalysis for the activation of Ar-X bonds, and development of new synthetic methods based on this approach.

In the beginning, the evolution that led to the development of modern photo-redox catalysis is discussed. Explanation of basic theories and definitions, which are encountered in the field of photo-redox catalysis is given. This is followed by a short overview of common photocatalysts, and the most important photocatalytic reactions discovered so far.

Main part of the thesis deals with generation of aryl radical intermediates from diazonium salts by photoredox catalysis with eosin dyes. Intermediate aryl radicals were trapped by σ- and n-electron donors. New procedures for synthesis of aryl sulfides, benzoates and selectively deuterated aromates were developed, using this strategy. Mechanistic studies were performed, including spectroscopic and computational techniques and isotopic labeling, to prove the proposed mechanisms. Investigations on the effect of pH and light source on the eosin Y photocatalysis were performed, proving that pH and light spectral distribution are critical for the efficient photocatalysis.

In an attempt to develop a photocatalytic synthesis of β-aryl ketones from diazonium salts and cyclopropyl alcohols, we obtained unexpected products – N-aryl pyrazoles. We have proposed a mechanism of their formation, and synthesized a variety of N-aryl pyrazoles based on this method. Cyclopropyl alcohols, required for this synthesis were obtained by Kulinkovich reaction from benzoates.

In the last part of this thesis, a new strategy of activation of unreactive aryl-halide bonds is proposed, by using photon VIS-to-UV upconversion by triplet-triplet annihilation. We have successfully applied this strategy for photocatalytic dehalogenations of aryl bromides. We have explained the selectivity of this reaction by DFT calculation, using Marcus theory of electron transfer.

8.3: Zusammenfassung

Die Dissertation beschäftigt sich mit der Verwendung von Photo-Redox-Katalyse zur Aktivierung von Ar-X-Bindungen und die Entwicklung neuer synthetischer Methoden, die auf diesem Ansatz beruhen.

Zu Beginn werden die Umstände die zu der Entwicklung heutiger Photo-Redox Systeme geführt haben erläutert. Theoretische Grundlagen und Definitionen, welche häufig im Zusammenhang mit Photo-Redox-Katalyse stehen, werden aufgeführt. Anschließend folgt ein kurzer Überblick der heute gängigen Photokatalysatoren und der wichtigsten bis zum jetzigen Zeitpunkt entdeckten photokatalytischen Reaktionen.

Der Hauptteil die Dissertation beschäftigt sich mit der Generierung arylradikalischer Zwischenstufen ausgehend von Diazoniumsalzen durch Photoredoxkatalyse mit Eosin-Farbstoffen. Die Arylradikale wurden mit σ- und n- Elektrondonoren abgefangen. Mit Hilfe dieses Prinzips wurden neue Methoden für die Synthese von Arylsulfiden, Benzoesäureestern und selektiv deuterierten Aromaten entwickelt. Es wurden mechanistische Untersuchungen durchgeführt, welche spektroskopischen Techniken, rechnergestützte Modellierung und Isotopenmarkierung beinhalten, um den vorgeschlagene Mechanismus zu beweisen. Untersuchungen zu den Einflüssen des pH-Werts und der Lichtquelle auf die photokatalytischen Systeme mit Eosin Y zeigen, dass der pH-Wert und Spektralverteilung der Lichtquelle kritisch für eine effiziente Photokatalyse sind.

Bei dem Versuch, eine photokatalysierte Synthese von β-Arylketonen ausgehend von Diazoniumsalzen und Cyclopropyl-alkoholen zu entwickeln, haben wir unerwartete Produkte erhalten - N-Aryl-pyrazole. Wir haben einen Mechanismus postuliert und verschiedene N-Aryl-pyrazole nach dieser Methode synthetisiert. Cyclopropylalkohole die für diese Synthese benötigt wurden, wurden in einer Kulinkovich Reaktion aus Benzoesäureestern hergestellt.

Im letzten Teil dieser Dissertation, wird eine neue Strategie zur Aktivierung unkreativer Aryl-Halogen Bindungen vorgeschlagen, mit Hilfe von Photonen VIS-to-UV Upconversion durch Triplett-Triplett-Annihilation. Wir haben diese Strategie für die photokatalytische Dehalogenierungen von Arylbromiden erfolgreich angewendet. Wir haben die Selektivität dieser Reaktion durch DFT-Rechnungen auf Basis der Marcus-Theorie von Elektronentransfers erklärt.

8.4 Súhrn

Cieľom tejto dizertačnej práce je využitie foto-redoxnej katalýzy pre aktiváciu väzieb Ar-X a vývoj novej syntetickej metodológie, založenej na tomto prístupe.

Rozvoj v oblasti fotochémie, ktorý viedol k vývoju modernej foto-redoxnej katalýzy je naznačený v prvej časti. V tejto časti sú diskutované základné pojmy a definície s ktorými sa najčastejšie môžeme stretnúť v oblasti foto-redoxnej katalýzy. Úvodná časť je ukončená krátkym prehľadom najčastejšie užívaných fotokatalyzátorov a najvýznamnejších druhov fotokatalytických reakcií.

Hlavná časť tejto dizertačnej práce sa zaoberá prípravou nestálych arylových radikálov z diazóniových solí pomocou foto-redoxnej katalýzy farbivami z triedy eozínov. Takto pripravené aryl radikály boli zachytávané pomocou σ- a n- elektrónových donorov. Na základe tejto stratégie sme vyvinuli nové metódy pre prípravu aryl sulfidov, esterov kyseliny benzoovej a selektívne deuterovaných aromátov. Tieto nové reakčné systémy sme podrobili mechanistickým štúdiám, používajúc spektroskopické techniky, kvantovo-chemické výpočty a izotopové značenie, aby sme potvrdili navrhované mechanizmy nových reakcií. Preskúmali sme účínok zmeny pH reakčného prostredia a spektrálnej charakteristiky použitého žiarenia na účinnosť eozínu Y ako fotokatalyzátora.

Pokusy vyvinúť novú fotokatalytickú metódu na syntézu β-aryl ketónov z diazóniových solí a cyklopropylových alkoholov viedli k vzniku neočakávaných produktov – N-aryl pyrazolov. Navrhli sme mechanizmus ich vzniku a na základe tejto metódy sme pripravili sériu N-aryl pyrazolov. Východiskové cyclopropyl alkoholy, ktoré boli použité v týchto syntézach boli pripravené pomocou Kulinkovičovej reakcie z esterov kyseliny benzoovej.

V poslednej časti tejto dizertačnej práce je predstavená nova stratégia pre aktiváciu nereaktívnych väzieb aryl-halogén, na základe premeny viditeľných fotónov na fotóny v UV oblasti pomocou triplet-tripletovej anihilácie. Túto stratégiu sme úspešne využili pre fotokatalytickú dehalogenáciu aromatických bromidov. Na základe DFT výpočtov sme pomocou Marcusovej teórie elektrónového prenosu objasnili selektivitu tejto reakcie.

8.5: Acknowledgements

This section is devoted to all that helped me in the last three years during my PhD studies in Regensburg. Thank you – this thesis would not exist without you!

In the first place I want to thank Axel, for being such a great supervisor. I want to thank you for offering me the large freedom, which I had in the selection of my research projects, while also having the time to discuss my current problems. You always supported me in what I did, Axel, and I owe you a great deal for that.

I would also like to thank all the members – past or present – of the AJvW group for the nice and friendly atmosphere. It was great to work with you, guys! Namely I would like to thank to my labmate Josef, for his great attitude, and coping with me in the lab, to Dominik, who spent the most time with me together in the group, for sharing the moments of misfortune, when chemistry was not working, and to Raul, for his cheerful mood, and the cooperation on the TTA project. Thanks goes also to all the good students, who worked with me in the last 3 years, mainly to Fabiana, for doing so much of the synthetic effort during her time in Regensburg. Thanks go also to Michaela, for all the chemicals ordering which she done for me, and for being such a nice technician.

I am also thankful to the members of my thesis committee Olga and Robert – for finding the time to come to my defense and read this thesis. Especially I would like to thank Prof. Burkhard König, both as the member of my thesis committee, as well as the head of the GRK – you have been very helpful to me over the course of my studies.

I also want to thank all the people from other groups, who shared beers with me, over which we discussed chemical and non-chemical matters. Mainly I would like to thank to Ivana and Tomáš for all the great scientific input I got from them. My special thanks go to Mišo for surviving the last 8 years with me, as a labmate in Prague, and flatmate here in Regensburg.

Záverečná časť tohoto poďakovania patrí rodine. Ďakujem vám všetkým za to, že ste ma podporovali v tom, čo som robil počas posledných 27 rokov. Mami, oci, boli ste mi inšpiráciou a bez vás by som nebol tým, čím som. Ocino, ďakujem ti za to, že si ma naučil používať UNIX-ové systémy – veľká časť výpočtov v tejto dizertačke by tu bez teba nebola. Bráško, Evka, Zuzka, je fajn mať rodinu na ktorú človek môže byť hrdý. Ďakujem!

8.6: CV and list of publications

Michal Májek
Institute of Organic Chemistry, University of Regensburg, Universitätstr. 31, 93053 Regensburg, Germany
Personal No.: (+421)902112415 · Office No.: (+49)9419434620
E-Mail: majek.michal@ur.de

Research experience

SEP 2012 - present
Graduate student, GRK fellow, Universität Regensburg, Germany
Advisor: Prof. Axel Jacobi von Wangelin

SEP 2008 - JUL 2012
Researcher, J. Heyrovský Institute of Phys. Chem., CAS, Czech Republic

NOV 2006 - JUL 2012
Undergraduate student, UCT Prague, Czech Republic
Advisor: Prof. Jiří Svoboda

sep 2010 - JUN 2011
Visiting undergraduate student, University of Glasgow, UK
Advisor: Prof. Pavel Kočovský

JUN 2010 - AUG 2010
Visiting undergraduate student, University of St. Andrews, UK
Advisor: Prof. David O'Hagan

Education:

present
Doctor of Natural Sciences (Dr. rer. nat.); organic chemistry
Fellow of the GRK Chemical photocatalysis, University of Regensburg, Germany

JUN 2012
Master of Engineering (Ing.); organic chemistry
University of Chemistry and Technology in Prague, Czech Republic
Graduated with honors; Rector's prize for excellent work; GPA: 5.00/5.00

JUN 2009
Bachelor of Science (Bc.); chemistry
University of Chemistry and Technology in Prague, Czech Republic
Graduated with honors; Dean's prize for excellent work; GPA: 4.97/5.00

Teaching experience:

SEP 2012 - present
University of Regensburg, Germany
Teaching assistant; laboratory courses – 6 semesters
Mentoring and supervision of project, bachelor and master students (9 in total)

SEP 2012 - present
Slovak Committee of Chemical Olympiad, Slovakia
Author and reviewer of problems from organic chemistry

SEP 2010 - AUG 2014
Co-investigator, Slovak Research and Development Agency (APVV) grant
LPP-0277-09: Correspondence seminars from chemistry and biology for secondary schools and seminar of natural sciences for elementary schools;
total funding: 132 682 €

Awards and Scholarships:

2015 Bayhost scholarship
2013 Best talk in chemistry, Graduate Student Conference, Bratislava
2012-15 Scholarship from GRK Chemical Photocatalysis, DFG
2012 Rector's prize, the highest reward for academic excellence, ICT Prague
2012 Best talk in organic chemistry, Student Conference, Prague
2012 Best poster (organic and pharmaceutical chemistry section), Preveda 2012
2010 "Hlavička" scholarship, Slovak Gas Co., for St. Andrews placement
2010 Free movers scholarsip, for St. Andrews placement
2010 Erasmus/Socrates scholarship, for Glasgow placement
2010 Best poster (student section), Preveda 2010
2008 Lonza award for organic chemistry section, Student Conference, UCT Prague
2006 Scholarship from Nadace pro rozvoj vzdělání, Prague
2006 Saint Gorazd award, Slovak Ministry of Education
2006 Silver medal (31st), International Chemistry Olympiad in Gyeongsan, Korea
2005 Silver medal (68th), International Chemistry Olympiad in Taipei, Taiwan
2005 2nd place, AYPT, Austria, as captain of Slovak national team

List of Publications (as of 10/2015):

[1]: Májek M.; Jacobi von Wangelin A.; "Organocatalytic visible light mediated synthesis of aryl sulfides", Chem. Commun. 2013, 49, 5507

[2]: Májek M.; Jacobi von Wangelin A.; „Ambient-Light-Mediated Copper-Catalyzed C-C and C-N Bond Formation", Angew. Chem. Int. Ed. 2013, 52, 5919
- invited highlight

[3]: Májek M.*; Filace F.; Jacobi von Wangelin A.*; "On the mechanism of photocatalytic reactions with eosin Y", Beilstein J. Org. Chem. 2014, 10, 981
- invited article for special issue on photo-redox catalysis

[4]: Májek M., Jacobi von Wangelin A.; "Metal-Free Carbonylations by Photoredox Catalysis", Angew. Chem. Int. Ed. 2015, 54, 2270
- selected as a Hot paper by reviewers, featured in Synform 2015, 8, A102; featured in Synfacts 2015, 11(2), 0199; featured in Nachr. Chem. 2015, 63(6), 620

[5]: Májek M.; Filace F.; Jacobi von Wangelin A.; "Visible Light Driven Hydro-/Deutero-defunctionalization of Anilines", Chem. Eur. J. 2015, 21, 4518.

[6]: Májek M.; Faltermeier U.; Dick B.; Pérez-Ruiz R.; Jacobi von Wangelin A.; "Application of Visible-to-UV Photon Upconversion to Photoredox Catalysis: The Activation of Aryl Bromides", Chem. Eur. J. 2015, DOI: 10.1002/chem.201502698
- selected as a VIP paper by reviewers

Patent: Light-induced catalytic carbonylation of aromatic electrophiles; application pending.

Conference contributions: 7 poster contributions; 6 talks.

Professional references:

Prof. Dr. Axel Jacobi von Wangelin
University of Regensburg
Institute of Organic Chemistry
Universitätsstr. 31
D-93053 Regensburg
Germany
+49 (0)941 9434802
axel.jacobi@ur.de

Prof. Dr. Burkhard König
University of Regensburg
Institute of Organic Chemistry
Universitätsstr. 31
D-93053 Regensburg
Germany
+49 (0)941 9434575
burkhard.koenig@ur.de

Prof. Dr. Jiří Svoboda
UCT Prague
Institute of Organic Chemistry
Technická 5
166 28 Praha 6 – Dejvice
Czech Republic
+420 220 444182
jiri.svoboda@vscht.cz

8.7: List of figures

List of pictures created by other parties, or parts thereof, which are subject to licence, is given here.

Cover and Chapter 1, Preface.
Source: commons.wikimedia.org/wiki/File:Optical-dispersion.png
Licence: Creative Commons Attribution-Share Alike 3.0 Unported

Chapter 1, Figure 1. Giacomo Ciamician.
Source: upload.wikimedia.org/wikipedia/commons/3/3c/Ciamician.jpg
Licence: This work is in the public domain, author died more than 70 years ago.

Chapter 1, Figure 2. Spectral distribution of solar radiation.
Source: upload.wikimedia.org/wikipedia/commons/3/3c/Ciamician.jpg
Licence: Creative Commons Attribution-Share Alike 3.0 Unported

Chapter 1, Figure 3. BDE vs. photon energy.
Source: upload.wikimedia.org/wikipedia/commons/thumb/e/e7/
Solar_spectrum_en.svg/1200px-Solar_spectrum_en.svg.png
Licence: Creative Commons Attribution-Share Alike 3.0 Unported

Chapter 7, Figure 1. BDE vs. photon energy.
Source: upload.wikimedia.org/wikipedia/commons/thumb/e/e7/
Solar_spectrum_en.svg/1200px-Solar_spectrum_en.svg.png
Licence: Creative Commons Attribution-Share Alike 3.0 Unported

Chapter 8, Preface.
Source: upload.wikimedia.org/wikipedia/commons/f/f9/Phisicke_1599_Alchymya.jpg
Licence: This work is in the public domain, author died more than 70 years ago.

Other figures and schemes are either works of author, or they were used in previous authors publications (referenced in the beginning of respective chapter), and republished with the agreement of respective journals.

All figures and schemes in this thesis are protected by Creative Commons Licence: Attribution-ShareAlike 3.0 Unported